André Robert Flores Manrique

Precoding, Combining and Power Allocation Techniques for Rate-Splitting-Based Multiuser MIMO Systems

Tese de Doutorado

Thesis presented to the Programa de Pós–graduação em Engenharia Elétrica of PUC-Rio in partial fulfillment of the requirements for the degree of Doutor em Engenharia Elétrica.

Advisor: Prof. Rodrigo Caiado de Lamare

Rio de Janeiro
April 2021

PONTIFÍCIA UNIVERSIDADE CATÓLICA
DO RIO DE JANEIRO

André Robert Flores Manrique

Precoding, Combining and Power Allocation Techniques for Rate-Splitting-Based Multiuser MIMO Systems

Thesis presented to the Programa de Pós–graduação em Engenharia Elétrica of PUC-Rio in partial fulfillment of the requirements for the degree of Doutor em Engenharia Elétrica. Approved by the Examination Committee:

Prof. Rodrigo Caiado de Lamare
Advisor
Centro de Estudos em Telecomunicações – PUC-Rio

Prof. Lukas Tobias Nepomuk Landau
Centro de Estudos em Telecomunicações – PUC-Rio

Silvio Fernando Bernardes Pinto
Centro de Estudos em Telecomunicações – PUC-Rio

Prof. Paulo Sérgio Ramirez Diniz
Universidade Federal do Rio de Janeiro – UFRJ

Prof. Arsenia Chorti
Ecole Nationale Supérieure de l'Electronique et de ses
Applications – ENSEA

Prof. Tadeu Nagashima Ferreira
Universidade Federal Fluminense–UFF

Rio de Janeiro, April the 14th, 2021

André Robert Flores Manrique

The author graduated in Telecommunication Engineering from the San Pablo University, in Arequipa, Peru, 2014. In 2017, he obtained a Master's degree in Electrical Engineering Sciences from the Pontifical Catholic University of Rio de Janeiro (PUC-Rio), Rio de Janeiro, Brazil.

Acknowledgments

Abstract

Flores Manrique, André Robert; Caiado de Lamare, Rodrigo (Advisor). **Precoding, Combining and Power Allocation Techniques for Rate-Splitting-Based Multiuser MIMO Systems**. Rio de Janeiro, 2021. 139p. Tese de Doutorado – Departamento de Engenharia Elétrica, Pontifícia Universidade Católica do Rio de Janeiro.

Multiple-antenna systems employ different signal processing techniques at both ends of the communication to exploit the spatial dimensions and serve multiple users simultaneously in the same time-frequency domain. In this way, high spectral efficiency can be reached without the need of extra bandwidth. However, such gain depends on a highly accurate channel state information at the transmitter (CSIT). Perfect CSIT allows the system to suppress the multi user interference (MUI), which is the main responsible of the performance degradation. Nonetheless, assuming perfect CSIT is rather optimistic since the estimation procedure, quantization errors and delays of real system lead to CSIT uncertainties. In this context, rate splitting (RS) has arisen as a promising technique to deal with CSIT imperfections. Basically, RS splits the data into a common stream and private streams and then superimposes the common stream on top of the private streams. This thesis proposes several processing techniques which further enhance the benefits of RS systems.

We consider the downlink (DL) of a wireless communications system, where the transmitter sends independent messages to each receiver. The ergodic sum rate (ESR) is adopted as the main metric to evaluate the performance of the system. Different from conventional RS works, we consider that the users are equipped with multiple antennas. This allows us to implement stream combiners for the common stream at the receivers. The implementations of the stream combiners improves the common rate performance, which is a major problem of RS systems since the common rate is limited by the performance of the worst user and can be heavily degraded. In this work, three different stream combiners are proposed along with analytical expressions to compute their sum rate performance. Specifically, the combiners are derived employing the min-max, maximum ratio combining (MRC), and minimum mean square error (MMSE) criteria. The min-max criterion selects at each user the best receive antenna to decode the common symbol. The MRC criterion aims at maximizing the SNR when decoding the common symbol. Finally, the MMSE criterion minimizes the squared difference between the common symbol and the received signal.

So far, RS has been predominantly considered with channel inversion-type linear precoders. Therefore, this motivates us to investigate the performance of RS with non-linear precoders. For this purpose, we employ different architectures of the Tomlinson-Harashima precoder (THP) which are based on the zero-forcing (ZF) and MMSE precoders. We then propose a multi-branch (MB) algorithm for the proposed RS-THP, which creates several transmit patterns and selects the best for transmission. This pre-processing techniques further enhance the sum rate obtained since the performance of THP is dependent on the symbol ordering but also increases the computational complexity. Analytical expressions to calculate the sum rate of the proposed techniques are derived through statistical evaluation of key parameters.

Finally, we propose four different adaptive power allocation techniques, which are characterized by their low computational complexity. Two of them are designed for conventional SDMA systems whereas the other two are intended for RS systems. One major objective of the proposed algorithms is to perform robust power allocation capable of dealing with the detrimental effects of imperfect CSIT. It is important to mention that power allocation in RS systems is one of the critical tasks that should be carefully performed. If the power is not properly allocated the performance of RS systems is heavily degraded and conventional architectures such as SDMA and NOMA could perform better. However, RS rely on solving complex optimization problems to perform power allocation, increasing the time and effort dedicated to signal processing. The proposed adaptive power allocation algorithms reduce the computational complexity and are an attractive solution for practical applications with large-scale systems.

Keywords

Communication systems; Multiple-antenna systems; Precoding; Power allocation.

Resumo

Flores Manrique, André Robert; Caiado de Lamare, Rodrigo. **Técnicas de Pré-codificação, Combinação e Alocação de Potências para Sistemas MIMO Multiusuário com Múltiplo Acesso por Partição de Taxa**. Rio de Janeiro, 2021. 139p. Tese de Doutorado – Departamento de Engenharia Elétrica, Pontifícia Universidade Católica do Rio de Janeiro.

Os sistemas de múltiplas antenas empregam diferentes técnicas de processamento de sinais em ambos extremos do sistema de comunicações para se beneficiar das múltiplas dimensões espaciais e transmitir para diversos usuarios usando os mesmos recursos de tempo e frequência. Desta forma, uma alta eficiência espectral pode ser atingida sem precisar de largura de banda extra. No entanto, o desempenho depende de uma estimativa do canal altamente precisa do lado do transmissor, a qual é denominada "channel state information at the transmitter" (CSIT). Se o valor estimado do canal for perfeito, o sistema consegue suprimir a interferência multiusuário (MUI), que é a principal responsável pela degradação do desempenho do sistema. Porém, supor uma estimativa perfeita é bastante otimista pois sistemas reais introduzem incerteza devido ao processo de estimação, a erros de quantização e a retardos próprios dos sistemas. Nesse contexto, a técnica conhecida como divisão de taxas ou rate splitting (RS) surge como uma ferramenta promissora para lidar com as imperfeições na estimativa do canal. RS divide os dados em um fluxo comum e vários fluxos privados e então sobrepõe o fluxo comum no topo dos fluxos privados. Esta tese propõe várias técnicas de processamento que aumentam ainda mais os benefícios dos sistemas RS.

Neste trabalho, consideramos o downlink (DL) de um sistema de comunicações sem fio onde o transmissor envia mensagens independentes para cada usuário. A métrica usada para avaliar o desempenho do sistema é a soma das taxas ergódica (ESR). Diferente dos trabalhos convencionais em RS, consideramos que os terminais dos usuários estão equipados com múltiplas antenas. Isso nos permite implementar na recepção combinadores de fluxos que aumentem a taxa do fluxo comum. Aumentar esta taxa é um dos grandes problemas dos sistemas RS, uma vez que a taxa comum é limitada pelo pior usuário o que pode degradar fortemente o desempenho do sistema. Assim, três combinadores de fluxos diferentes são propostos e as expressões analíticas para calcular a soma das taxas são apresentadas. Os combinadores são derivados empregando-se os critérios Min-Max, MRC e MMSE. O critério Min-Max seleciona para cada

usuário a melhor antena para decodificar o símbolo comum. O MRC visa maximizar o SNR ao decodificar o símbolo comum. Finalmente, o critério MMSE minimiza o quadrado da diferença entre o símbolo comum e o sinal recebido.

Até o momento, RS foi considerado com precodificadores lineares. Devido a isto, neste trabalho investigamos o desempenho do RS com precodificadores não lineares. Para este fim, usamos diferentes tipos de precodificador Tomlinson-Harashima (THP) baseados nos precodificadores lineares ZF e MMSE. Em seguida, propomos um algoritmo multi-branch (MB) adequado para o RS-THP proposto. Este algoritmo cria vários padrões de transmissão e seleciona o melhor padrão para efetuar a transmissão. Esta técnica de pré-processamento aumentam ainda mais a soma das taxas obtida, uma vez que o desempenho do THP depende da ordem dos símbolos, porém também aumenta a complexidade computacional. Expressões analíticas para calcular a soma das taxas das técnicas propostas são derivadas por meio de análises estatísticas dos principais parâmetros.

Finalmente, propomos quatro técnicas adaptativas diferentes de alocação de potência, as quais se caracterizam por sua baixa complexidade computacional. Duas destas técnicas são projetadas para sistemas SDMA convencionais, enquanto as outras duas são projetadas para sistemas RS. Um dos principais objetivos dos algoritmos propostos é realizar uma alocação de potência robusta capaz de lidar com os efeitos prejudicias das imperfeições no CSIT. É importante mencionar que a alocação de potência em sistemas RS é uma das tarefas mais importantes e deve ser realizada com extremo cuidado. Se a potência não for alocada corretamente, o desempenho do sistema RS será bastante degradado e as arquiteturas convencionais, como SDMA e NOMA, poderão ter um desempenho melhor. No entanto, a alocação de potência em sistemas RS precisa da solução de problemas complexos de otimização, o que aumenta o tempo gasto no processamento do sinal. Os algoritmos adaptativos propostos reduzem a complexidade computacional e são uma solução atrativa para aplicações práticas em sistemas de grande porte.

Palavras-chave

Sistemas de comunicações; Sistemas de múltiplas antenas; Précodificação; Alocação de potências.

Table of contents

List of figures

List of tables

List of Abreviations

ASR	Average Sum Rate
AWGN	Additive White Gaussian Noise
BD	Block Diagonalization
BS	Base Station
CDMA	Code Division Multiple Access
CSIT	Channel State Information at the Transmitter
DoF	Degrees-of-Freedom
ESR	Ergodic Sum Rate
FDD	Frequency Division Duplex
FDMA	Frequency Division Multiple Access
MB	Multi-Branch
MF	Matched Filter
MIMO	Multiple-Input Multiple-Output
MMSE	Minimum Mean-Square Error
MRC	Maximum Ratio Combining
MSE	Mean-Square Error
MU-MIMO	Multiuser Multiple-Input Multiple-Output
MUI	Multiuser Interference
MUST	Multi-User Superposition Transmission
MSD	Mean-Square Deviation
NOMA	Non-Orthogonal Multiple Access
OFDMA	Orthogonal Frequency Division Multiple Access
OMA	Orthogonal Multiple Access
PN	Pseudo Noise

RBD	Regularized Block Diagonalization
RS	Rate Splitting
SC	Superposition Coding
SDMA	Space Division Multiple Access
SIC	Successive Interference Cancellation
SISO	Single-Input Single-Output
SNR	Signal-to-Noise Ratio
SR	Sum Rate
TDD	Time Division Duplex
TDMA	Time Division Multiple Access
THP	Tomlinson-Harashima Precoding
ZF	Zero Forcing

1
Introduction

Since its origins, radio techniques have been used in diverse areas such as wireless communications. The contributions to this area led to the development of mobile equipment. Thenceforth, each new generation of mobile technology provided a significant performance improvement. As a result, wireless networks have become a fundamental part of daily life by providing continuously new ways to establish communications between people and devices. Therefore, it is not surprising that the estimated number of devices by 2022 is 3.6 per person, which is a significant increase compared to the 2.4 devices per person reported in 2017 [1]. However, as the number of terminals and the quality of applications grow the demand for higher data rates increases as well. Therefore, it is not surprising that the monthly mobile traffic attained 38 Exabytes in 2019. Moreover, this traffic is expected to reach 160 Exabytes per month by 2025 [2, 3]. This scenario results in new challenges to develop efficient and robust wireless communications networks, which should provide enhanced mobile broadband (eMBB) and ultra-reliable and low latency communications (URLLC).

Multiple-Input Multiple-Output (MIMO) technology has arisen as a core physical layer technology to satisfy the continuously growing demands of wireless systems [4]. MIMO has evolved from the classical point-to-point channel to include multiuser deployments where the transmitter serves multiple receivers. In this context, multiuser MIMO (MU-MIMO) exploits spatial multiplexing, providing high data rates, improving the spectral efficiency without additional bandwidth and simultaneously serving several users, which are geographically distributed. However, multiuser setups have their own challenges. Given the broadcast nature of the wireless channels, all user equipments have access to all the components of the transmitted signal. Hence, each user receives an undesired part of the signal, which results in multiuser interference (MUI).

MUI can heavily degrade the overall performance of a MIMO system since it makes the recovery of the user data much harder. Therefore, several preprocessing techniques aimed at mitigating MUI have been reported in literature, as the receivers are usually decentralized and unable to cooperate

[5–7]. This techniques rely on the acquisition of a highly accurate channel state information at the transmitter (CSIT). Unfortunately, the ability to obtain an accurate and up-to-date CSIT remains questionable [8]. This calls for new methods to enhance the performance of MIMO systems under CSIT uncertainties.

1.1
MU-MIMO Challenges

The main problem found in wireless communications systems reside in the adverse environmental conditions. In this context, wireless communications have to deal with noise, fading and interference [9]. Usually, dealing with noise involves methods to maximize the signal-to-noise (SNR) ratio, such as matched filters. Equalization and diversity techniques are employed to counter fading effects. Preprocessing techniques such as precoders are commonly implemented at the transmitter in order to mitigate interference, which is harder to manage than noise since it scales with the SNR.

A precoder maps the information before transmission to the transmit antennas in such a way that the interference is cancelled or at least reduced to the noise level. However, precoding techniques rely on the knowledge of CSIT, which is characterized by the channel matrix $\mathbf{H}$. Such information is acquired through feedback links in frequency division duplex (FDD) systems and through training pilots in time division duplex (TDD) systems. Both methods are subject to errors which leads to an imperfect CSIT estimate. In such cases, precoders are no longer able to deal with MUI even when properly designed. As a result, the received signal still contains residual MUI. This means that the errors on CSIT estimates have a detrimental effect on the overall performance of the system since the residual MUI scales with the SNR. Furthermore, the wireless channel is expected to change constantly, bringing the need to update the CSIT in order to deal with the interference.

One extreme approach to deal with CSIT uncertainties is to assume that there is no CSIT available. In this context, several methods have been used to overcome the absence of CSIT. One possible option is to transmit the signal of different users in orthogonal slots. Suppose that the signal gets the entire channel for a small fraction of time. This technique, known as time division multiple access (TDMA) eliminates the MUI. Another option is frequency division multiple access (FDMA). However, in these methods each user gets only a fraction of the available time or frequency. Hence, both approaches limit the performance of the system.

The absence of CSIT is pessimistic, since modern communications sys-

tems obtain at least partial CSIT. As mentioned before, the errors in the CSIT originate residual MUI. Consequently, the development of approaches suitable for working under partial CSIT assumption is mandatory. The strategy adopted should bridge the transmission with perfect CSIT and with no CSIT. For this purpose, the transmitted data are split into two parts. One part should exploit the CSIT knowledge while the other should be adapted to the CSIT imperfections. Such strategy is known as rate splitting (RS) [10]. This thesis introduces several techniques based on RS to enhance the performance of a multiuser MIMO system under imperfect CSIT. The ergodic sum-rate (ESR) has been adopted as the main metric to evaluate the performance of the developed techniques. [1]

1.2
Contributions

Considering the problems discussed, the contributions of this work can be summarized as follows:

– A mathematical model for RS-MIMO systems has been developed, in contrast to previous works which mainly focus on RS-MISO schemes. Moreover, practical stream combining techniques have been proposed in order to enhance the common rate of the RS scheme and take advantage of the multiple antennas at the receivers. The computational complexity of the proposed combiners is analyzed. Simulation results show that the proposed technique greatly improves the common rate and better manages the MUI, enhancing the overall performance of the system.

– RS has been considered with the block diagonalization (BD) and the regularized block diagonalization (RBD) precoders, which are specifically designed for environments where the receivers are equipped with multiple antennas. A statistical analysis of both techniques has been carried out which led us to closed-form expressions to describe the sum-rate performance. Simulations results showed that the proposed scheme outperforms the conventional ZF and MMSE precoders under imperfect CSIT.

– Non-linear precoders have been developed along with RS to further improve the performance of RS-MIMO systems. Two different Tomlinson-Harashima precoders (THP), namely the centralized THP (cTHP) and decentralized THP (dTHP), have been employed with an RS scheme.

---

[1]The bit error rate (BER) is another widely used figure of merit, however, we assume that the BER performance required by most modern applications can be enforced by employing appropriate channel codes such as low-density parity-check and polar codes.

An analysis of the proposed schemes has been performed, along with the derivation of analytical expressions. Simulation results show that non-linear precoders outperform conventional linear precoders as expected.

– RS-THP with receivers with multiple antennas has been considered. Combiners for the common stream have been proposed with non-linear precoders. Closed form expressions to describe the sum-rate performance are derived and the computational complexity is analyzed. Numerical results show that this approach outperforms conventional techniques.

– A multibranch (MB) technique suitable for RS is proposed. This technique employs different transmit patterns to further enhance the performance of RS-MIMO systems. Not only the design is based on an RS system, but this approach also takes into account the imperfect CSIT when designing the patterns. Simulation results show that this technique has the potential to significantly increase the sum-rate performance.

– Robust adaptive power allocation techniques are derived in order to enhance the sum-rate performance under CSIT uncertainties. Conventional optimal power allocation techniques rely on complex optimization problems, which are not only difficult to solve but also computationally demanding. In contrast, the adaptive algorithms proposed only require the evaluation of simple sums and multiplications. Simulation results show that the proposed algorithms can increase the performance of wireless systems when compared to conventional strategies.

1.3 Publications

This work has resulted in a number of papers, which have been published or submitted.

Journal Papers

– A. Flores, R.C. de Lamare and B. Clerckx, "Linear Precoding and Stream Combining for Rate Splitting in Multiuser MIMO Systems," IEEE Communications Letters, vol. 24, no. 4, pp. 890-894, 2020.

– A. Flores, R.C. de Lamare and B. Clerckx, "Tomlinson-Harashima Precoded Rate-Splitting with Stream Combiners for MU-MIMO Systems," IEEE Transactions on Communications, to appear.

– A. Flores, R.C. de Lamare "Practical Iterative Power Allocation Techniques for RS Multi-Antenna Systems", under preparation.

Conference Papers

– A. Flores, R. C. de Lamare, "Linearly Precoded Rate-Splitting Techniques with Block Diagonalization for Multiuser MIMO Systems," 2019 IEEE International Conference on Communications Workshops (ICC Workshops), Shangai, China, 2019.

– A. Flores, B. Clerckx and R.C. de Lamare, "Tomlinson-Harashima Precoded Rate-Splitting for Multiuser Multiple-Antenna Systems," 2018 15th International Symposium on Wireless Communication Systems (ISWCS), Lisbon, 2018.

– A. Flores, R.C. de Lamare and B. Clerckx, "Multi-Branch Tomlinson-Harashima Precoding for Rate Splitting Based Systems with Multiple Antennas," IEEE International Conference on Acoustics, Speech and Signal Processing (ICASSP), (Accepted).

– A. Flores, R.C. de Lamare "Robust Adaptive Power Allocation for Multiuser MIMO Systems", under preparation.

1.4
Notation

Matrices and vectors are represented by upper and lowercase boldface letters, respectively. The conjugate transpose of a matrix is denoted by $(\cdot)^H$, whereas $(\cdot)^{\mathrm{T}}$ denotes the transpose. The complex conjugate is denoted by $(\cdot)^*$. The operators $\|\cdot\|$, $\odot$, and $\mathbb{E}_x[\cdot]$ stand for the Euclidean norm, the Hadamard product and the expectation operator w.r.t the random variable x. The trace of a matrix and the cardinality of a set are given by $\mathrm{tr}(\cdot)$, and $\mathrm{card}(\cdot)$. $\mathrm{diag}(\mathbf{c})$ is a diagonal matrix with the entries of $\mathbf{c}$ in the main diagonal. Let us consider a general matrix $\mathbf{C}_k$ with $k \in \mathbb{N}$. Then, $\mathbf{c}_i^{(k)}$ denotes the ith colum of matrix $\mathbf{C}_k$, whereas $\mathbf{c}_{i,*}^{(k)}$ represents the ith row of the matrix $\mathbf{C}_k$.

2
Fundamentals of MIMO and Multiple Access Systems

Over the last decades multiple-input multiple-output (MIMO) systems have been widely used due to their potential to dramatically increase the overall system performance. MIMO techniques employ multiple transmit and receive antennas to exploit multipath propagation and increase the throughput without increasing the required bandwidth. In [11], it has been proved that MIMO technology greatly improves the capacity of a radio link when compared to single-input single-output (SISO) systems. Furthermore, thanks to the spatial diversity, MIMO systems improve the reliability of a communications link since it mitigates detrimental effects inherent to the wireless communication channel. As a result of all these advantages, MIMO has become an essential element of several communications standards [12, 13] such as WiFi, WiMAX, LTE, and beyond [14]. In this chapter, we review the basic concepts behind MIMO systems and multiple access schemes. Moreover, we provide an overview of several precoding techniques that deal with key problems encountered in the downlink of MIMO systems such as multi-user interference (MUI) mitigation.

2.1
Multiple Access Schemes

Multiple access schemes play an essential role in wireless communications systems since they allow multiple users to access a network simultaneously by sharing the often limited spectrum available. As wireless technology evolves the demand for higher data rates increases. In order to satisfy these demands better spectrum and energy efficiencies are required which can be provided by efficient multiple access schemes.

In the first generation (1G) of wireless cellular technology, the data were multiplexed using frequency division multiple access (FDMA). FDMA divides the whole bandwidth into separated frequency bands. Each band is assigned to a different user, mitigating MUI. The second generation (2G) implements time division multiple access (TDMA) as a multiple access scheme. In TDMA, the available time resources are divided into time slots. The data of several users are transmitted in the same frequency band but in different time slots. To further increase the efficiency, code division multiple access (CDMA) was

adopted in the third generation (3G). This technology introduced a third dimension by using orthogonal Hadamard and pseudo-noise (PN) codes for different users. This allowed to transmit the messages of multiple users using the same band and time resources. Nonetheless, CDMA is susceptible to the near-far problem, i.e., a strong signal from a near source makes it harder for the receiver to detect the signal of distant source [15]. Another disadvantage is that the PN codes are almost orthogonal and the performance obtained by CDMA systems depends on the orthogonality between the PN codes generated. To overcome the drawbacks of CDMA, orthogonal frequency division multiple access (OFDMA) was implemented in the fourth generation (4G) of mobile networks. This technology separates the frequency band into multiple narrow and orthogonal subbands, which are also known as subcarriers. Subsets of subcarriers and time resources are assigned to different users based on demand.

Modern wireless networks employ devices which are usually equipped with multiple antennas. Such extra hardware feature allows the implementation of another multiple access scheme, known as space division multiple access (SDMA) and used in the fourth and fifth generation (4G,5G) of wireless standards. In SDMA, the users share the same time and frequency resources. The messages are separated by properly using the spatial dimensions. All of the multiple access schemes introduced so far are considered orthogonal multiple access (OMA) schemes due to the use of orthogonal dimensions to separate the users.

On the other hand, non-orthogonal multiple access (NOMA), also known as multi-user superposition transmission (MUST), superposes users in the same space-time-frequency resource [16]. The superposition of the transmissions over the same radio resource creates interference which is mitigated by signal processing techniques. Those techniques exploit different resource domains such as the power [17] or code [18] domains. Power domain NOMA employs superposition coding (SC) at the transmitter and successive Interference Cancellation (SIC) at the receiver. This is commonly known as superposition coding and successive interference cancellation (SC-SIC) [16, 19]. The performance obtained by employing SIC strongly depends on the symbol order. In this sense, NOMA comes with an increase in complexity at the transmitter and the receiver since multi-layer SIC is needed at the receivers and the decoding orders have to be optimized at the transmitter. One major drawback of this multiple access technique is that an increase in the number of users leads to an exponential increase in the number of possible decoding orders.

2.1.1
Rate Splitting

Rate splitting (RS) was originally developed in [20] for the 2-user SISO interferece channel. Recently, RS has been introduced for the design of MIMO wireless networks [8]. Basically, RS schemes splits the transmitted data into a common message and a private message. The common message must be decoded by all users, whereas the private message is decoded only by its corresponding user. The common stream is first decoded and all private messages are considered as interference and treated as noise. Then we use successive interference cancellation (SIC) to subtract the contribution of the common stream from the received signal, enhancing the detection of the private stream. At the end, the message sent via the private stream is decoded. When a user decodes its private stream, it treats the other private streams as noise.

Interestingly, RS constitutes a bridge between the two extremes of fully decoding the interference (NOMA) and treating the interference as noise (SDMA) [21,22]. The main benefit of this approach is its capability to partially decode interference and partially treat interference as noise. The strength of RS is its ability to adjust the content and the power of the common message to control how much interference should be decoded by all users (through the common message) and how much interference is treated as noise. As a consequence, RS provides room for rate and QoS enhancements in a wide range of network loads (underloaded and overloaded regimes) and user deployments (with a diversity of channel directions, channel strengths and qualities of CSIT) over standard schemes such as NOMA and SDMA [8, 21, 22].

RS has been considered with linear precoding using both perfect and imperfect CSIT assumptions [23, 24]. In [25], the problem of achieving max-min fairness amongst multiple co-channel multicast groups has been studied. RS has also been considered for robust transmissions under bounded CSIT errors in [26]. Studies of RS with massive MIMO have been reported in [27]. MISO networks using RS strategies have been considered in [28]. In [29], RS has been implemented to reduce the effects of the imperfect CSIT caused by finite feedback. An RS architecture has been proposed in [30] for millimetre waves using a ZF precoding.

Previous works have focused on multiple-input single-output (MISO) systems along with either optimized or closed-form zero-forcing (ZF) and minimum mean-squared error (MMSE) channel inversion-type precoders [5]. However, there is still a gap in the design of linear precoders for RS schemes where the receivers are equipped with multiple antennas. Furthermore, RS has not considered block diagonalization (BD) type linear precoders [6, 31],

which have the potential to significantly enhance the sum-rate performance of ZF and MMSE linear precoders when the receivers are equipped with multiple antennas. In addition, from a rate perspective, nonlinear precoding schemes can outperform linear precoding approaches Hence the combination of nonlinear precoding and RS is a promising avenue to improve the rate performance, especially in the imperfect CSIT setting. Interestingly, the potential benefits of RS using nonlinear precoding techniques remain unexplored in the literature. The objective of this thesis is to address these limitations in the current literature and develop innovative linear and nonlinear precoding techniques for RS schemes with MIMO.

2.2
System Model

Let us consider a broadcast channel (BC) of a multiple-input multiple-output (MIMO) system, where the communication is established between a single base station (BS) and K users. In addition, the kth user is provided with N_k antennas. Then, the total number of receive antennas is given by $N_r = \sum_{k=1}^{K} N_k$. On the other hand, the number of antennas at the transmitter is given by N_t. In this work we consider that $N_t \geq N_R$ [1]. Remark that each user may receive more than one data stream. The group of data streams intended for the kth user forms a set denoted by $\mathcal{M}_k$. The total number of transmitted data streams is $M = \sum_{k=1}^{K} M_k$ with $M_k = \text{card}(\mathcal{M}_k)$. In order to make the detection possible M_k should be less than or equal to N_k.

The information in the data streams is modulated and then gathered into the vector of symbols $\mathbf{s} \in \mathbb{C}^{M \times 1}$, where the vector $\mathbf{s}_k$ contains the information of the streams in $\mathcal{M}_k$ and the symbol $s_j^{(k)}$ corresponds to the information of the jth stream contained in the vector $\mathbf{s}_k$. For this work, we consider that the symbols are uncorrelated with zero mean and covariance matrix equal to $\mathbf{R_{ss}} = \sigma_s^2 \mathbf{I}$. [2] The BS employs preprocessing techniques to enhance the transmission of the data. These techniques transform the vector of symbols $\mathbf{s}$ into the transmit vector $\mathbf{x} \in \mathbb{C}^{N_t}$.

In general, the equipment sending information at the BS has limited power for transmission. This means that the transmit vector $\mathbf{x}$ should satisfy an average transmit power constraint. Mathematically, the total transmit power constraint is

$$\mathbb{E}\left[\|\mathbf{x}\|^2\right] \leq E_{tr}, \tag{2-1}$$

[1]Note that in practice we also find overloaded regimes where $N_t < N_r$. Such situations can be handled by employing an appropriate user scheduling scheme.

[2]A system employing nonzero mean symbols would require in most scenarios an increase in the transmit power which leads to an inefficient use of the resources. Therefore, the zero mean assumption holds also in practice.

where $E_t r$ denotes the available transmit power. When the information is ready for transmission it is sent to the receivers through a channel $\mathbf{H} = \hat{\mathbf{H}} + \tilde{\mathbf{H}} \in \mathbb{C}^{N_r \times N_t}$. The matrix $\hat{\mathbf{H}}$ represents the estimate of the channel and the matrix $\tilde{\mathbf{H}}$ models the quality of the channel estimate by adding the error of the estimation procedure. For simplicity, we consider a flat fading channel which remains fixed during a block transmission (coherence time). Each coefficient h_{ij} in the channel matrix $\mathbf{H}$ represents the link between the jth transmit antenna and the ith receive antenna. The channel matrix can be expressed by $\mathbf{H} = \left[\mathbf{H}_1^H, \mathbf{H}_2^H, \cdots, \mathbf{H}_K^H \right]^H$, where $\mathbf{H}_k$ denotes the channel connecting the BS to the kth user.

The received signal obtained following the model established is

$$\mathbf{y} = \mathbf{H}\mathbf{x} + \mathbf{n}, \tag{2-2}$$

where $\mathbf{n} \in \mathbb{C}^{N_r \times 1}$ is the additive noise modelled as a circularly symmetric complex Gaussian random vector, i.e., $\mathbf{n} \sim \mathcal{CN}\left(\mathbf{0}, \mathbf{R_{nn}}\right)$. The received signal at the kth user is given by

$$\mathbf{y}_k = \mathbf{H}_k \mathbf{x} + \mathbf{n}_k, \tag{2-3}$$

where the vector $\mathbf{n}_k \in \mathbb{C}^{N_k \times 1}$ represents the additive noise affecting the antennas of the kth user. Different channels may experience different SNR levels, for example $\sigma_{n,i}^2 \neq \sigma_{n,j}^2$, $\forall i \neq j$ with $i, j = 1, 2, \cdots, K$. Without loss of generality, we will consider that the noise is uncorrelated and has the same statistical properties at each antenna, i.e., $\sigma_{n,i}^2 = \sigma_{n,j}^2 = \sigma_n^2$, $\forall i, j$ unless the contrary is explicitly mentioned. In this case the covariance matrix of the noise is reduced to $\mathbf{R_{nn}} = \sigma_n^2 \mathbf{I}$.

2.3
Precoding

In this section, we review several precoding techniques, which will be used along with the techniques proposed in this work. Before sending the message, the transmitter processes the symbols using the precoding matrix $\mathbf{P} = [\mathbf{P}_1, \mathbf{P}_2, \cdots, \mathbf{P}_K] \in \mathbb{C}^{N_t \times M}$, also called precoder or transmit filter, where the matrix $\mathbf{P}_k \in \mathbb{C}^{N_t \times M_k}$ is the precoder of the kth user. Basically, the precoder maps the symbols to the transmit antennas. In transmit processing, the BS tries to find the optimal precoder which is going to send the symbols so that they reach the receiver in the best possible form. One of the main advantages of precoding is that the computational load is transferred to the BS. Keeping the equipment of the users as simple as possible has important benefits such as energy savings, smaller devices and more resources available [32]. The

transmit vector is given by the multiplication of the vector of symbols $\mathbf{s}$ and the precoding matrix $\mathbf{P}$, i.e.,

$$\mathbf{x} = \mathbf{P}\mathbf{s} = \sum_{k=1}^{K} \mathbf{P}_k \mathbf{s}_k, \tag{2-4}$$

which belongs to $\mathbb{C}^{N_t \times 1}$.

Precoding techniques can be grouped as linear precoders and nonlinear precoders. Although nonlinear precoders achieve a better performance, they also increase the computational load and demand more resources. On the other hand, linear precoders reduce significantly the computational complexity when compared to nonlinear precoders, but the performance is degraded by the high power loss introduced. The design of both kinds of precoders assumes perfect CSIT knowledge. Therefore, under imperfect CSIT, the precoder is unable to behave as expected, originating residual MUI, which can heavily degrade the overall performance of the system. In the following we review the most used precoding techniques.

2.3.1
Matched Filter

The Matched Filter (MF) precoder was introduced in [33], where the MF was moved from the receiver to the transmitter side. Later in [5] the mathematical derivation was established. The MF precoder is designed to maximize the desired signal portion at the receiver. This precoder can be found by solving the following constrained optimization problem:

$$\mathbf{P}^{(\mathrm{MF})} = \max_{\mathbf{P}} \frac{|\mathbb{E}\left[\mathbf{s}^H \mathbf{y}\right]|^2}{\mathbb{E}\left[\|\mathbf{n}\|^2\right]}$$
$$\text{s.t.} \quad \mathbb{E}\left[\|\mathbf{P}\mathbf{s}\|^2\right] = E_{tr}. \tag{2-5}$$

After applying the method of Lagrange multipliers over (2-5) we obtain

$$\mathbf{P}^{(\mathrm{MF})} = \beta^{(\mathrm{MF})} \mathbf{H}^H, \tag{2-6}$$

where $\beta^{(\mathrm{MF})}$ is a power scaling factor imposed to fulfil the transmit power constraint in (2-1) and is given by

$$\beta^{(\mathrm{MF})} = \sqrt{\frac{E_{tr}}{\mathrm{tr}\left(\mathbf{H}^H \mathbf{R_s} \mathbf{H}\right)}}, \tag{2-7}$$

where $\mathbf{R_s} = \mathbb{E}\left[\mathbf{s}\mathbf{s}^H\right]$

2.3.2
Linear Zero-Forcing Precoder

The linear Zero-Forcing (ZF) [5] precoder $\mathbf{P}$ originates a non-interfering received signal. In order to completely remove the interference we force the product $\mathbf{HP}$ to be reduced to the identity matrix. Unfortunately, this approach brings a high power loss, especially for ill conditioned matrices and does not take into account the effect of the noise. Thus, the performance of the ZF precoder at low SNR regime can be particularly poor.

The ZF precoder can be found by solving the following optimization problem:

$$\mathbf{P}^{(\text{ZF})} = \min_{\mathbf{P}} \mathbb{E}\left[\|\mathbf{Ps}\|^2\right]$$
$$\text{s.t.} \quad \mathbf{HP} = \mathbf{I}_M. \tag{2-8}$$

Using the method of Lagrange multipliers, setting the derivative of the Lagrangian to zero, and solving for $\mathbf{P}^{(\text{ZF})}$ we obtain

$$\mathbf{P}^{(\text{ZF})} = \mathbf{H}^H \left(\mathbf{HH}^H\right)^{-1}. \tag{2-9}$$

Let us remember that the transmit power is limited to E_{tr}. In order to satisfy the constraint we introduce a scaling factor $\beta \in \mathbb{R}$ to properly scale the transmit vector, such that

$$\mathbb{E}\left[\|\beta \mathbf{Ps}\|^2\right] = E_{tr}, \tag{2-10}$$

where we consider the equality since the best performance is achieved when all the available power is used. Solving with respect to β we get

$$\beta^{(\text{ZF})} = \sqrt{\frac{E_{tr}}{\text{tr}\left(\left(\mathbf{HH}^H\right)^{-1}\mathbf{R_{ss}}\right)}}. \tag{2-11}$$

2.3.3
Linear Minimum Mean-Square Error Precoder

The linear Minimum Mean-Square Error (MMSE) precoder [5] obtains a better performance than the Matched Filter (MF) and ZF precoders since it establishes an optimum tradeoff between the signal maximization obtained by the MF and the interference elimination performed by the ZF. However, the design of the MMSE precoder requires the noise covariance matrix as additional information. The MMSE precoder can be found through the following

optimization problem:

$$\mathbf{P}^{(\text{MMSE})} = \min_{\mathbf{P},\beta} \mathbb{E}\left[\|\mathbf{s} - \beta^{-1}\mathbf{y}\|^2\right]$$

$$\text{s.t.} \quad \mathbb{E}\left[\|\mathbf{P}\mathbf{s}\|^2\right] = E_{tr}, \tag{2-12}$$

where $\mathbf{y}$ is the received vector. This problem can be solved by constructing the Lagrangian function and setting the partial derivatives to zero. This procedure leads us to

$$\mathbf{P}^{(\text{MMSE})} = \beta^{(\text{MMSE})}\mathbf{D}^{-1}\mathbf{H}^H, \tag{2-13}$$

where the matrix $\mathbf{D}$ and the power scaling factor $\beta_{(\text{MMSE})}$ are given by

$$\mathbf{D} = \mathbf{H}^H\mathbf{H} + \frac{\text{tr}\left(\mathbf{R_n}\right)}{E_{tr}}\mathbf{I}_{N_t} \tag{2-14}$$

$$\beta_{(\text{MMSE})} = \sqrt{\frac{E_{tr}}{\text{tr}\left(\mathbf{D}^{-2}\mathbf{H}^H\mathbf{R_s}\mathbf{H}\right)}} \tag{2-15}$$

2.3.4
Block Diagonalization

The block diagonalization (BD) precoder was proposed in [6, 31, 34] as a generalization of the ZF technique for multiuser MIMO systems where the receivers are equipped with multiple antennas, and further studied in [35] due to its potential to increase the performance of the system. The design of the BD precoder involves two steps, therefore it is convenient to separate the precoder into two matrices, i.e.,

$$\mathbf{P}^{(\text{BD})} = \mathbf{P}_a^{(\text{BD})}\mathbf{P}_b^{(\text{BD})}. \tag{2-16}$$

The first matrix is employed to completely eliminate the interference between users. The second part of the precoder allows parallel symbol detection. The precoder of the kth user can be written as $\mathbf{P}_k^{(\text{BD})} = \mathbf{P}_{a,k}^{(\text{BD})}\mathbf{P}_{b,k}^{(\text{BD})}$.

In order to completely remove MUI, the following condition must hold:

$$\bar{\mathbf{H}}_k\mathbf{P}_{a,k}^{(\text{BD})} = \mathbf{0}, \tag{2-17}$$

where the matrix $\bar{\mathbf{H}}_k \in \mathbb{C}^{(N_r - N_k)\times N_t}$ is formed by excluding the channel of the kth user, i.e., $\bar{\mathbf{H}}_k = [\mathbf{H}_1, \cdots, \mathbf{H}_{k-1}, \mathbf{H}_{k+1}, \cdots, \mathbf{H}_K]$ and has a rank equal to $\bar{L}_k$. Performing a SVD over $\bar{\mathbf{H}}_k$ we get $\bar{\mathbf{H}}_k = \bar{\mathbf{U}}_k\bar{\boldsymbol{\Psi}}_k\left[\bar{\mathbf{V}}_{(1),k}\bar{\mathbf{V}}_{(0),k}\right]^H$. The matrix $\bar{\mathbf{V}}_{(0),k}$ contains the last $N_t - \bar{L}_k$ zero singular values, thus forming an orthogonal basis for the null space of $\bar{\mathbf{H}}_k$ and satisfying (2-17). It follows that the first precoder is given by

$$\mathbf{P}_{a,k}^{(\text{BD})} = \bar{\mathbf{V}}_{(0),k}. \tag{2-18}$$

The precoder in (2-18) separates the MU-MIMO channel into K parallel

independent channels. Consider the effective channel matrix defined as $\dot{\mathbf{H}}_k = \mathbf{H}_k \mathbf{P}_{a,k}^{(\mathrm{BD})}$. Let us perform a second SVD over the effective channel $\dot{\mathbf{H}}_k$, i.e., $\dot{\mathbf{H}}_k = \dot{\mathbf{U}}_k \boldsymbol{\Psi}_k \left[\mathbf{V}_{(1),k} \mathbf{V}_{(0),k} \right]^H$. Then, the second precoder is given by

$$\mathbf{P}_{b,k}^{(\mathrm{BD})} = \mathbf{V}_{(1),k}. \tag{2-19}$$

The receiver employs a filter equal to

$$\mathbf{G}_k^{(\mathrm{BD})} = \dot{\mathbf{U}}_k^H. \tag{2-20}$$

The matrices $\mathbf{P}_{b,k}^{(\mathrm{BD})}$ and $\mathbf{G}_k^{(\mathrm{BD})}$ allow us to perform symbol-by-symbol detection.

2.3.5
Regularized Block Diagonalization

In what follows we consider the regularized block diagonalization (RBD) precoding technique [36,37], which is not only designed to exploit receivers with multiple antennas, but also to better balance MUI supression and the effects of the power loss. Similar to BD, this technique separates the precoder into two matrices, i.e., $\mathbf{P}_k^{(\mathrm{RBD})} = \mathbf{P}_{a,k}^{(\mathrm{RBD})} \mathbf{P}_{b,k}^{(\mathrm{RBD})}$. In contrast to the BD precoding technique, the first precoder of the RBD technique partially removes MUI and is computed through the following optimization problem:

$$\mathbf{P}_{a,k}^{(\mathrm{RBD})} = \min_{\mathbf{P}_{a,k}^{(\mathrm{RBD})}} \mathbb{E} \left[\| \bar{\mathbf{H}}_k \mathbf{P}_{a,k}^{(\mathrm{RBD})} \|^2 + \frac{\| \mathbf{n}_k \|^2}{\beta^{(\mathrm{RBD})^2}} \right], \tag{2-21}$$

where the reduced matrix $\bar{\mathbf{H}}_k$ is the same from (2-17) and the parameter $\beta^{(\mathrm{RBD})}$ is the scaling factor imposed in order to fulfil the transmit power constraint. By applying SVD we get $\bar{\mathbf{H}}_k^{\mathrm{T}} = \bar{\mathbf{U}}_k \bar{\boldsymbol{\Psi}}_k \bar{\mathbf{V}}_k^H$. The solution to (2-21) is given by

$$\mathbf{P}_{a,k}^{(\mathrm{RBD})} = \bar{\mathbf{V}}_k \left(\bar{\boldsymbol{\Psi}}_{\mathbf{k}}^{\mathrm{T}} \bar{\boldsymbol{\Psi}}_k + \frac{N_r \sigma_n^2}{E_{tr}} \mathbf{I}_{N_t} \right)^{-1/2}. \tag{2-22}$$

The second filter $\mathbf{P}_{b,k}^{(\mathrm{RBD})}$ allows parallel symbol detection. Consider the effective channel matrix defined as $\dot{\mathbf{H}}_k = \mathbf{H}_k \mathbf{P}_{a,k}^{(\mathrm{RBD})}$. A second SVD is computed on the effective channel , i.e., $\dot{\mathbf{H}}_k = \dot{\mathbf{U}}_k \boldsymbol{\Psi}_k \dot{\mathbf{V}}_k^H$, in order to find the second precoder and the receive filter of the kth user as given by

$$\mathbf{P}_{b,k}^{(\mathrm{RBD})} = \dot{\mathbf{V}}_k, \tag{2-23}$$

and

$$\mathbf{G}_k^{(\mathrm{RBD})} = \dot{\mathbf{U}}_k^H. \tag{2-24}$$

2.3.6
Tomlinson-Harashima Precoding

Among the non-linear precoding techniques, we have Tomlinson-Harashima precoding (THP) [38, 39] which was originally proposed to deal with intersymbol interference (ISI) and then extended to spatial division multiple access (SDMA) in [40]. As mentioned in [41, 42], the THP implemented at the transmitter is the counterpart of the successive interference cancellation (SIC) technique used at the receiver.

A standard THP algorithm implements three filters, the feedback filter $\mathbf{B} \in \mathbb{C}^{N_t \times K}$, the feedforward filter $\mathbf{F} \in \mathbb{C}^{N_t \times N_t}$ and the scaling matrix $\mathbf{C} \in \mathbb{C}^{N_t \times N_t}$. The feedback filter deals with the MUI by successively subtracting the interference from the current symbol. The matrix $\mathbf{B}$ has a lower triangular structure, whereas the feedforward filter enforces the spatial causality. The scaling filter assigns a coefficient or weight to each stream of data, which means $\mathbf{C}$ is a diagonal matrix.

There are two general THP structures in the literature [7, 41, 43, 44], namely the centralized THP (cTHP) and the decentralized THP (dTHP). The main difference between these structures is that the scaling matrix $\mathbf{C}$ is placed at the transmitter for the cTHP, whereas for dTHP the same matrix is located at the receiver. Figure 2.1 ilustrates the cTHP deployment, whereas Figure 2.2 shows the dTHP.
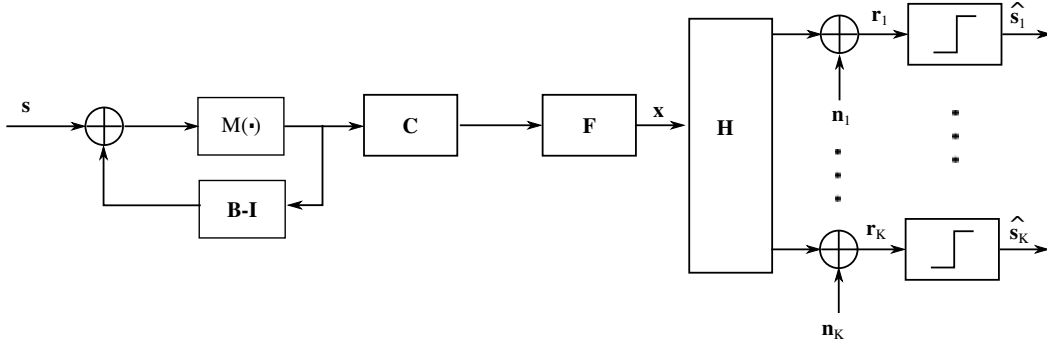
Figure 2.1: Block diagram of the cTHP.

Let us first consider the ZF version of the THP, which removes completely the MUI. This precoder is implemented by performing an LQ decomposition on the channel matrix, i.e., $\mathbf{H} = \mathbf{LQ}$. The THP filters are then defined as follows:

$$\mathbf{F} = \mathbf{Q}^H, \tag{2-25}$$

$$\mathbf{C} = \text{diag}\left(l_{11}, l_{22}, \ldots, l_{KK}\right)^{-1}, \tag{2-26}$$
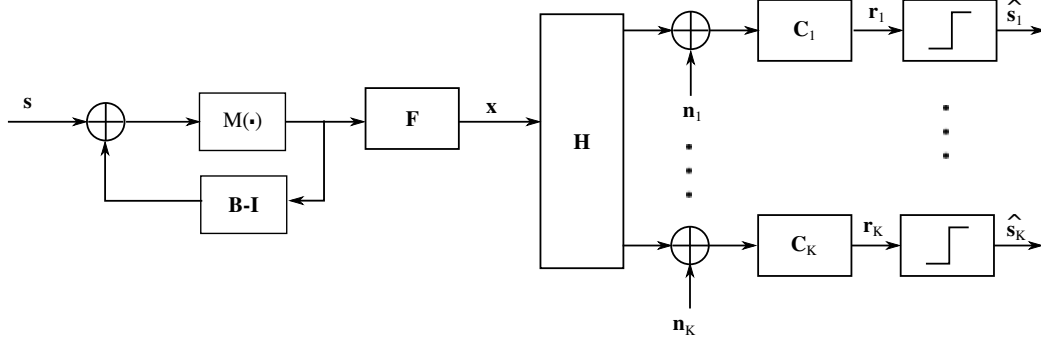
Figure 2.2: Block diagram of the dTHP.

$$\mathbf{B}^{(d)} = \mathbf{CL} \qquad \text{and} \qquad \mathbf{B}^{(c)} = \mathbf{LC}, \tag{2-27}$$

where $\mathbf{B}^{(d)}$ and $\mathbf{B}^{(c)}$ correspond to the feedback filter for dTHP and cTHP, respectively.

The transmitted symbol $\breve{s}_k$ is successively generated as

$$\breve{s}_k = s_k - \sum_{i=1}^{k-1} b_{k,i}\breve{s}_i. \tag{2-28}$$

However, this process increases the amplitude of the transmitted symbols originating a power loss. In other words, the power loss comes from the energy difference between the original constellation and the transmitted symbols after precoding. A modulo operation is therefore applied in order to reduce the amplitude of the symbol to the boundary of the modulation. This modulo operation is defined element-wise as follows:

$$M\left(\breve{s}_k\right) = \breve{s}_k - \left\lfloor \frac{\mathrm{Re}\left(\breve{s}_k\right)}{\tau} + \frac{1}{2} \right\rfloor \tau - j \left\lfloor \frac{\mathrm{Im}\left(\breve{s}_k\right)}{\tau} + \frac{1}{2} \right\rfloor \tau, \tag{2-29}$$

where the coefficient τ defines the periodic extension of the constellation and depends on the modulation alphabet and the power allocation scheme[3].

The modulo processing is equivalent to adding a perturbation vector $\mathbf{d}_p$ to the transmit data $\mathbf{s}$, i.e., $\breve{\mathbf{s}} = \mathbf{s} + \mathbf{d}_p$. Mathematically, the feedback processing is equivalent to an inversion operation over the matrix $\mathbf{B}$. Then, we have

$$\breve{\mathbf{s}}^{(d)} = \mathbf{B}^{(d)^{-1}}\breve{\mathbf{s}} = \mathbf{B}^{(d)^{-1}}\left(\mathbf{s} + \mathbf{d}_p^{(d)}\right), \tag{2-30}$$

$$\breve{\mathbf{s}}^{(c)} = \mathbf{B}^{(c)^{-1}}\breve{\mathbf{s}} = \mathbf{B}^{(c)^{-1}}\left(\mathbf{s} + \mathbf{d}_p^{(c)}\right). \tag{2-31}$$

The received signal vector for each structure is obtained by stacking up

---

[3]Some common values of τ when the symbol variance is equal to one are $\tau = 2\sqrt{2}$ and $\tau = 4\sqrt{10}/5$ for QPSK and 16-QAM, respectively.

the received signal $\mathbf{r}_k$ of each user, where $\mathbf{r}_k$ is a scaled version of $\mathbf{y}_k$ in (2-3) that corrects the amplitude for detection purposes[4]. It follows that

$$\mathbf{r}^{(\mathrm{d})} = \frac{1}{\beta^{(\mathrm{d})}} \mathbf{C} \left(\mathbf{H} \beta^{(\mathrm{d})} \mathbf{F} \breve{\mathbf{s}}^{(\mathrm{d})} + \mathbf{n} \right), \tag{2-32}$$

$$\mathbf{r}^{(\mathrm{c})} = \frac{1}{\beta^{(\mathrm{c})}} \left(\mathbf{H} \beta^{(\mathrm{c})} \mathbf{F} \mathbf{C} \breve{\mathbf{s}}^{(\mathrm{c})} + \mathbf{n} \right), \tag{2-33}$$

where $\beta^{(\mathrm{d})} \approx \sqrt{\frac{E_{tr}}{K}}$ and $\beta^{(\mathrm{c})} \approx \sqrt{\frac{E_{tr}}{\sum_{k=1}^{K} \left(1/l_{k,k}^2 \right)}}$ are the scaling factors used to fulfil the transmit power constraint. We can simplify the received signal using the expressions of the filters, which leads us to

$$\mathbf{r}^{(\mathrm{d})} = \breve{\mathbf{s}} + \frac{1}{\beta^{(\mathrm{d})}} \mathbf{C} \mathbf{n} \tag{2-34}$$

$$\mathbf{r}^{(\mathrm{c})} = \breve{\mathbf{s}} + \frac{1}{\beta^{(\mathrm{c})}} \mathbf{n} \tag{2-35}$$

At the receiver, another modulo operation is performed to recover the symbol. This incurs in a modulo loss since the detected symbols may be mistaken by other symbol in the opposite boundary[5]. We remark that the covariance matrices of the error $\mathbf{\Phi}^{(\mathrm{d})} = \mathbb{E}\left[\left(\mathbf{r}^{(\mathrm{d})} - \breve{\mathbf{s}} \right) \left(\mathbf{r}^{(\mathrm{d})} - \breve{\mathbf{s}} \right)^H \right]$ and $\mathbf{\Phi}^{(\mathrm{c})} = \mathbb{E}\left[\left(\mathbf{r}^{(\mathrm{c})} - \breve{\mathbf{s}} \right) \left(\mathbf{r}^{(\mathrm{c})} - \breve{\mathbf{s}} \right)^H \right]$ directly affect the performance of the precoders. Since $\Phi_{k,k}^{(\mathrm{c})} > \Phi_{k,k}^{(\mathrm{d})}$ [7], dTHP outperforms cTHP. However, cTHP requires less complex receivers than dTHP.

Let us now consider the MMSE-THP and define the extended channel matrix $\check{\mathbf{H}} = \left[\hat{\mathbf{H}}, \sqrt{\frac{N_r \sigma_n^2}{E_{tr}}} \mathbf{I} \right] \in \mathbb{C}^{N_r \times (N_r + N_t)}$. Computing an LQ decomposition on $\check{\mathbf{H}}$ leads to

$$\check{\mathbf{H}} = \check{\mathbf{L}} \check{\mathbf{Q}} = \check{\mathbf{L}} \left[\mathbf{Q}_1, \mathbf{Q}_2 \right], \tag{2-36}$$

where the unitary matrix $\check{\mathbf{Q}}$ has been split into the matrix $\mathbf{Q}_1 \in \mathbb{C}^{N_r \times N_t}$ and the matrix $\mathbf{Q}_2 \in \mathbb{C}^{N_r \times N_r}$. It follows that the filters for the MMSE-THP are given by $\check{\mathbf{F}} = \check{\mathbf{Q}}^H$, $\check{\mathbf{C}} = \mathrm{diag}\left(\check{l}_{1,1}, \cdots, \check{l}_{N_t, N_t} \right)^{-1}$, $\check{\mathbf{B}}^{(\mathrm{d})} = \check{\mathbf{C}} \check{\mathbf{L}}$ for the decentralized structure and $\check{\mathbf{B}}^{(\mathrm{c})} = \check{\mathbf{L}} \check{\mathbf{C}}$ for the centralized one. Then, the received signal is given by

$$\mathbf{y}^{(\mathrm{d})} = \beta^{(\mathrm{d})} \mathbf{H} \mathbf{D} \check{\mathbf{F}} \breve{\mathbf{s}} + \mathbf{n} \tag{2-37}$$

$$\mathbf{y}^{(\mathrm{c})} = \beta^{(\mathrm{c})} \mathbf{H} \mathbf{D} \check{\mathbf{F}} \check{\mathbf{C}} \breve{\mathbf{s}} + \mathbf{n}, \tag{2-38}$$

---

[4]Note that the parameter β scales the symbols. Thus, the receiver must compensate this effect before the detection.

[5]The power loss and the modulo loss can be neglected for analysis purposes especially for moderate and large modulation constellations where its effects are minimal. In such cases, the power of $\breve{\mathbf{s}}$ is approximated by that of $\mathbf{s}$ [7].

where $\mathbf{D} = [\mathbf{I}_{N_t}, \mathbf{0}_{N_t,N_r}]$. Note that in this case $\check{\mathbf{s}} = \check{\mathbf{B}}^{-1}(\mathbf{s} + \mathbf{d}_p)$. The power scaling constants are given by

$$\beta^{(\mathrm{d})} = \sqrt{\frac{E_{tr}}{\operatorname{tr}\left(\mathbf{Q}_1\mathbf{Q}_1^H\right)}}, \tag{2-39}$$

$$\beta^{(\mathrm{c})} = \sqrt{\frac{E_{tr}}{\operatorname{tr}\left(\mathbf{Q}_1\check{\mathbf{C}}\check{\mathbf{C}}^H\mathbf{Q}_1^H\right)}}. \tag{2-40}$$

2.4
Power Allocation

Power loading schemes may be applied to enhance the performance of the system. Assuming we have uncorrelated symbols, a power loading matrix $\mathbf{A}$ may be included into the system model presented. In general, the power loading matrix is a diagonal matrix i.e., $\mathbf{A} = \operatorname{diag}\left(\left[\mathbf{a}_1^{\mathrm{T}}, \mathbf{a}_2^{\mathrm{T}}, \cdots, \mathbf{a}_K^{\mathrm{T}}\right]^{\mathrm{T}}\right)$. The vector $\mathbf{a}_k$ allocates the power to the M_k streams intended for the kth user. The coefficient $a_i^{(k)}$ represents the square root of the power allocated to the ith stream of the kth user. Then, the transmit signal turns into:

$$\mathbf{x} = \mathbf{PAs}. \tag{2-41}$$

It is convenient to separate the transmitted signal to have a detailed description of the MUI. For the kth user we have

$$\mathbf{x} = \overbrace{\mathbf{P}_k\operatorname{diag}\left(\mathbf{a}_k\right)\mathbf{s}_k}^{\text{User Data}} + \overbrace{\sum_{\substack{i=1\\i\neq k}}^{K}\mathbf{P}_i\operatorname{diag}\left(\mathbf{a}_i\right)\mathbf{s}_i}^{\text{Multi-User Interference}}. \tag{2-42}$$

In a MISO system, since the receivers are equipped with a single antenna, equation (2-42) is reduced to

$$\mathbf{x} = \overbrace{a_k s_k \mathbf{p}_k}^{\text{User Data}} + \overbrace{\sum_{\substack{i=1\\i\neq k}}^{K}a_i s_i \mathbf{p}_i}^{\text{MUI}}. \tag{2-43}$$

The transmitted signal must satisfy the transmit power constraint leading to:

$$\begin{aligned}
E_{tr} &= \mathbb{E}\left[\|\mathbf{P}\operatorname{diag}\left(\mathbf{a}\right)\mathbf{s}\|^2\right]\\
&= \sigma_s^2\operatorname{tr}\left(\mathbf{P}\operatorname{diag}\left(\mathbf{a}\odot\mathbf{a}\right)\mathbf{P}^H\right).
\end{aligned} \tag{2-44}$$

The design of matrix $\mathbf{A}$ depends on the performance metric adopted. One commonly used strategy is the water-filling algorithm [45] used to maximize the sum-rate performance. Water-filling allocates powers according to the

effective channel gain, assigning more power to stronger channels. However this approach is not suitable for other objective functions, such as balancing the power over all users [46], or assigning power to achieve a target SINR [47]. For this kind of problems the algorithms are designed based on optimization theory [48, 49].

Another popular approach is the uniform power allocation (UPA). UPA is a suboptimal strategy that simplifies the evaluation of **A** by allocating equal power to all streams. UPA also allows a more tractable system performance analysis in certain scenarios, yielding closed form expressions. This strategy is especially useful when perfect CSI is available. Otherwise, when partial CSIT is available, numerical methods are usually employed [32].

2.5
Detection Techniques

In this section we address the most commonly used detection techniques for MIMO systems. In contrast to precoding, detection techniques are implemented at the receiver[6]. These classical detection methods rely on an accurate CSI at the receiver.

2.5.1
Zero-Forcing

This technique implements a linear filter at the receiver to completely remove the interference between symbols and is expressed as

$$\mathbf{G}^{(\mathrm{ZF})} = \left(\mathbf{H}^H \mathbf{H}\right)^{-1} \mathbf{H}^H. \tag{2-45}$$

The ZF detection technique yields the following equation:

$$\hat{\mathbf{s}}^{(\mathrm{ZF})} = \mathbf{s} + \left(\mathbf{H}^H \mathbf{H}\right)^{-1} \mathbf{H}^H \mathbf{n}. \tag{2-46}$$

From (2-46), we can see that the power of the noise can be greatly increased, especially if the channel is ill conditioned, which reduces the overall performance of the system.

The final decision is obtained element by element as follows:

$$\hat{\mathbf{s}} = Q\left(\hat{\mathbf{s}}^{(\mathrm{ZF})}\right), \tag{2-47}$$

where $Q(s)$ returns the closest point to s in the constellation.

---

[6]In a MU-MIMO BC scenario, the receive filter has block diagonal structure, since no jointly processing is allowed between users (user k does not have access to the information that arrive to the antennas of user i). Precoding techniques are then employed to make detection possible.

2.5.2
Minimum Mean Square Error Detector

The MMSE detector reduces the noise effect compared to the ZF. The MMSE filter can be obtained by minimizing the MSE and is given by

$$\mathbf{G}^{(\mathrm{MMSE})} = \min_{\mathbf{G}} \mathbb{E} \left[\|\mathbf{s} - \mathbf{G}\mathbf{y}\|^2 \right]$$
$$= \left(\mathbf{H}^H \mathbf{H} + \frac{\sigma_n^2}{\sigma_s^2} \mathbf{I} \right)^{-1} \mathbf{H}^H. \tag{2-48}$$

The estimate of the symbols obtained using the MMSE technique is

$$\hat{\mathbf{s}}^{(\mathrm{MMSE})} = \mathbf{G}^{(\mathrm{MMSE})} \mathbf{H}\mathbf{s} + \mathbf{G}^{(\mathrm{MMSE})} \mathbf{n}. \tag{2-49}$$

Finally, the decision is obtained by

$$\hat{\mathbf{s}} = Q \left(\left(\mathrm{diag} \left(\mathbf{G}^{\mathrm{MMSE}} \mathbf{H} \right) \right)^{-1} \hat{\mathbf{s}}^{(\mathrm{MMSE})} \right) \tag{2-50}$$

The ZF and MMSE linear detectors offer a reduced computational complexity compared to nonlinear detectors.

2.5.3
Maximum Likehood Detection

The maximum likehood (ML) detector minimizes the error probability, defined as

$$\left(P_e \triangleq \mathrm{P} \left(\mathbf{s} \neq \hat{\mathbf{s}} \right) \right), \tag{2-51}$$

by estimating the transmitted symbols based on the knowledge of the received vector $\mathbf{y}$ and the channel matrix $\mathbf{H}$. Note that minimizing the probability of error is equivalent to maximize the probability of detecting $\mathbf{s}$ correctly. Considering that the inputs are independent and identically distributed and that uniform signaling is used, i.e., the symbols in the constellation are equally likely, the ML and the maximum *a posteriori* (MAP) detectors are equivalent. Then, the estimate leading to the highest *a posteriori* probability is given by

$$\hat{\mathbf{s}}^{(\mathrm{MAP})} = \max_{\hat{\mathbf{s}}} \frac{\mathrm{P} \left(\mathbf{s} = \hat{\mathbf{s}} \right) p_{\mathbf{y}|\mathbf{s}} \left(\mathbf{y}|\mathbf{s} = \hat{\mathbf{s}} \right)}{p_{\mathbf{y}} \left(\mathbf{y} \right)} \tag{2-52}$$

Equation (2-52) is reduced to

$$\hat{\mathbf{s}}^{(\mathrm{ML})} = \max_{\hat{\mathbf{s}}} p_{\mathbf{y}|\mathbf{s}} \left(\mathbf{y}|\mathbf{s} = \hat{\mathbf{s}} \right), \tag{2-53}$$

since $p_{\mathbf{y}} \left(\mathbf{y} \right)$ does not depend on $\hat{\mathbf{s}}$ and the symbols have the same *a priori* probability. The probability density function of $\mathbf{y}$ given $\mathbf{s}$ and Gaussian noise is

$$p_{\mathbf{y}|\mathbf{s}} \left(\mathbf{y}|\mathbf{s} = \hat{\mathbf{s}} \right) = \frac{1}{(\pi \sigma_n^2)^{N_r}} \exp \left(-\frac{\|\mathbf{y} - \mathbf{H}\hat{\mathbf{s}}\|^2}{\sigma_n^2} \right). \tag{2-54}$$

Maximizing (2-54) is equivalent to minimize $\|\mathbf{y} - \mathbf{H}\hat{\mathbf{s}}\|^2$. Then, the ML detector selects the vector with the smallest Euclidean distance between the received vector $\mathbf{y}$ and $\mathbf{H}\hat{\mathbf{s}}$. This requires to solve a discrete optimization problem over $\text{card}\,(\mathcal{S})^M$ candidates. It follows that the computational complexity of the ML detector increases exponentially with the modulation order M_o and the dimensions of $\mathbf{s}$, since it requires an exhaustive search of the M_o^M possible vectors, resulting in a computational expensive detector.

2.5.4
Successive Interference Cancellation

In contrast to the ML detection, the successive interference cancellation (SIC) technique [50] performs the detection task in a sequential form. At each step the detected symbol is subtracted from the received signal. The remaining signal is used to perform the detection of the following symbols. It follows that the interference is reduced at each step as the symbols are detected, improving the bit error rate performance. This procedure can be summarized as follows:

$$
\begin{aligned}
\mathbf{y}^{(i)} &= \mathbf{y} & i = 1 \\
\mathbf{y}^{(i)} &= \mathbf{y} - \sum_{j=1}^{i-1} \mathbf{h}_j \hat{s}_j & i \geq 2
\end{aligned}
\tag{2-55}
$$

At each step the remaining signal $\mathbf{y}^{(i)}$ is processed using a filter (usually an MMSE or ZF filters) to estimate the following symbol. It is important to note that the order of the symbols detected directly affects the performance of the SIC. In this sense, several ordering criteria have been proposed such as the SINR ordering, the SNR ordering and the channel norm ordering in order to enhance the performance of the SIC detector [51,52]. In addition, many SIC-type strategies [53–58] have been developed in the last decades in order to mitigate error propagation and improve performance.

2.6
Channel Estimation

In order to acquire knowledge of the channel we can resort to channel estimation techniques. As mentioned in [59], the most commonly used approach to estimate the channel parameters is based on training sequences also known as pilot signals. This technique estimates the channel based on the received signal and the knowledge of the training symbols. There are two main methods to structure the training techniques. The first one is the preamble technique which adds a packet of pilot symbols. The second technique is the pilot

structure, in which the packet consists of pilot and information symbols. The preamble technique is effective in slow fading channels while the other method allows to track a fast moving channel but with less accuracy.

Let us consider the training vectors $\boldsymbol{\pi}_i$ with $i \in [1, 2, ..., N]$, which are transmitted to estimate the channel matrix $\mathbf{H}$. The matrix $\mathbf{Y} = [\mathbf{y}_1, \cdots, \mathbf{y}_N]$ $\in \mathbb{C}^{N_r \times N}$ contains the N received signals and can be expressed as follows:

$$\mathbf{Y} = \mathbf{H}\boldsymbol{\Pi} + \mathbf{N}, \tag{2-56}$$

where $\mathbf{N} \in \mathbb{C}^{N_r \times N}$ represents the additive noise matrix and $\boldsymbol{\Pi} \in \mathbb{C}^{N_t \times N}$ is a matrix containing in its columns the vectors $\boldsymbol{\pi}_i$.

2.6.1
Least Squares Estimation

The least squares (LS) channel estimation technique has been widely used due to its simplicity. This method finds the channel estimate through the following equation:

$$\hat{\mathbf{H}}^{(\text{LS})} = \mathbf{Y}\boldsymbol{\Pi}^H \left(\boldsymbol{\Pi}\boldsymbol{\Pi}^H\right)^{-1}. \tag{2-57}$$

The mean-square error obtained by employing the LS channel estimator is given by

$$\mathbb{E}\left[\|\mathbf{H} - \hat{\mathbf{H}}^{(\text{LS})}\|_{\mathcal{F}}^2\right] = \sigma_n^2 N_r \text{tr}\left(\left(\boldsymbol{\Pi}\boldsymbol{\Pi}^H\right)^{-1}\right). \tag{2-58}$$

The training sequence must satisfy the power constraint, i.e., $\text{tr}\left(\boldsymbol{\Pi}\boldsymbol{\Pi}^H\right) = E_{tr}$. It turns out that the MSE of the LS channel estimation technique is inversely proportional to the SNR.

2.6.2
Minimum Mean Square Error Estimation

This estimation technique minimizes the MSE between $\mathbf{H}$ and $\hat{\mathbf{H}}^{(\text{MMSE})}$, where the estimate of the channel has the following form [59, 60]:

$$\hat{\mathbf{H}}^{(\text{MMSE})} = \mathbf{Y}\mathbf{D}^{(o)}, \tag{2-59}$$

where $\mathbf{D}^{(o)}$ is the matrix that minimizes the optimization problem given by

$$\mathbf{D}^{(o)} = \min_{\mathbf{D}} \mathbb{E}\left[\|\mathbf{H} - \hat{\mathbf{H}}^{(\text{MMSE})}\|_{\mathcal{F}}^2\right]. \tag{2-60}$$

After evaluating the expected value of (2-60) we can obtain the optimal matrix $\mathbf{D}^{(o)}$ by computing the derivative and equating the result to zero. Thus, we get

$$\mathbf{D}^{(o)} = \left(\boldsymbol{\Pi}^H \mathbf{R_{HH}} \boldsymbol{\Pi} + \sigma_n^2 N_r \mathbf{I}\right)^{-1} \boldsymbol{\Pi}^H \mathbf{R_{HH}}, \tag{2-61}$$

where $\mathbf{R_{HH}} = \mathbb{E}\left[\mathbf{H}\mathbf{H}^H\right]$. This technique leads us to the following MSE:

$$\mathbb{E}\left[\|\mathbf{H} - \hat{\mathbf{H}}^{(\mathrm{MMSE})}\|^2\right] = \mathrm{tr}\left(\left(\mathbf{R}_{\mathbf{HH}}^{-1} + \frac{1}{\sigma_n^2 N_r}\mathbf{\Pi\Pi}^H\right)^{-1}\right). \tag{2-62}$$

The MSE obtained by this method is lower than the MSE obtained by the LS technique. However, this approach requires the knowledge of the channel autocorrelation matrix and the statistical properties of the noise.

2.7
General Received Signal

Considering the transmit and receive processing techniques reviewed in the previous sections, from equation (2-2) we can obtain a general receive vector for each user as follows:

$$\mathbf{r}_k = \mathbf{G}_k\left(\mathbf{H}_k\mathbf{P}\mathrm{diag}\left(\mathbf{a}\right)\mathbf{s} + \mathbf{n}_k\right)$$

$$= \underbrace{\mathbf{G}_k\mathbf{H}_k\mathbf{P}_k\mathrm{diag}\left(\mathbf{a}_k\right)\mathbf{s}_k}_{\text{User Data}} + \overbrace{\mathbf{G}_k\mathbf{H}_k\sum_{\substack{i=1\\i\neq k}}^{K}\mathbf{P}_i\mathrm{diag}\left(\mathbf{a}_i\right)\mathbf{s}_i}^{\text{MUI}} + \underbrace{\mathbf{G}_k\mathbf{n}_k}_{\text{noise}} \tag{2-63}$$

The receive vector $\mathbf{r}_k \in \mathbb{C}^{M_k}$ contains the M_k streams intended to user k. Remark that $\mathbf{r}_k$ represents the signal after receive processing and $\mathbf{y}_k$ denotes the signal at the receive antennas. The expression for the receive signal can be further simplified when considering a MISO system, i.e., when each user device is provided by just one receive antenna. For a MISO system we get

$$r_k = g_k\left(\mathbf{h}_{k,*}\sum_{i=1}^{K}a_i s_i \mathbf{p}_i + n_k\right),$$

$$= g_k a_k s_k \mathbf{h}_{k,*}\mathbf{p}_k + g_k \mathbf{h}_{k,*}\sum_{\substack{i=1\\i\neq k}}^{K}a_i s_i \mathbf{p}_i + g_k n_k \tag{2-64}$$

Table 2.1 summarizes the expressions of the received signal for the MIMO and MISO systems.

Table 2.1: Received signal per user

System	Received Signal
MIMO	$\mathbf{r}_k = \mathbf{G}_k\left(\mathbf{H}_k\mathbf{P}_k\mathrm{diag}\left(\mathbf{a}_k\right)\mathbf{s}_k + \mathbf{H}_k\sum_{\substack{i=1\\i\neq k}}^{K}\mathbf{P}_i\mathrm{diag}\left(\mathbf{a}_i\right)\mathbf{s}_i + \mathbf{n}_k\right)$
MISO	$r_k = g_k\left(a_k s_k \mathbf{h}_{k,*}\mathbf{p}_k + \sum_{\substack{i=1\\i\neq k}}^{K}a_i s_i \mathbf{h}_{k,*}\mathbf{p}_i + n_k\right)$

2.8
Sum-rate Performance

The sum-rate (SR) performance of a MIMO system with power constraint E_{tr} depends on the mutual information $I(\mathbf{x};\mathbf{r})$, which is given by

$$I(\mathbf{x};\mathbf{r}) = h(\mathbf{r}) - h(\mathbf{n}). \tag{2-65}$$

The following theorem is employed to obtain the sum-rate performance of a Gaussian channel.

Theorem 2.1 *Let the random vector $\mathbf{z} \in \mathbb{R}^n$ have mean $\boldsymbol{\mu}$ and covariance matrix $\mathbf{R_{zz}} = \mathbb{E}\left[(\mathbf{z} - \boldsymbol{\mu})(\mathbf{z} - \boldsymbol{\mu})^T\right]$. Then,*

$$h(\mathbf{z}) = \frac{1}{2}\log_2\left(\det\left[2\pi e \mathbf{R_{zz}}\right]\right) \quad bits. \tag{2-66}$$

Let us consider zero mean i.i.d. symbols drawn from a Gaussian distribution. Suppose also that the symbols and the noise are uncorrelated . From equation (2-63) we can get the covariance matrix for user k as follows:

$$\mathbf{R}_{\mathbf{r}_k\mathbf{r}_k} = \sigma_s^2 \mathbf{G}_k \mathbf{H}_k \mathbf{P}_k \mathrm{diag}\left(\mathbf{a}_k \odot \mathbf{a}_k\right) \mathbf{P}_k^H \mathbf{H}_k^H \mathbf{G}_k^H$$
$$+ \sigma_s^2 \sum_{\substack{i=1 \\ i \neq k}}^{K} \mathbf{G}_k \mathbf{H}_k \mathbf{P}_i \mathrm{diag}\left(\mathbf{a}_i \odot \mathbf{a}_i\right) \mathbf{P}_i^H \mathbf{H}_k^H \mathbf{G}_k^H + \sigma_n^2 \mathbf{G}_k \mathbf{G}_k^H \tag{2-67}$$

We can consider that the precoder reduces the interference to noise level. In such case, the effective noise is composed by the information of other users and the noise, i.e.,

$$\mathbf{z}_k = \mathbf{G}_k \mathbf{H}_k \sum_{\substack{i=1 \\ i \neq k}}^{K} \mathbf{P}_i \mathrm{diag}\left(\mathbf{a}_i\right) \mathbf{s}_i + \mathbf{G}_k \mathbf{n}_k \tag{2-68}$$

The covariance matrix of the effective noise is

$$\mathbf{R}_{\mathbf{z}_k\mathbf{z}_k} = \sigma_s^2 \sum_{\substack{i=1 \\ i \neq k}}^{K} \mathbf{G}_k \mathbf{H}_k \mathbf{P}_i \mathrm{diag}\left(\mathbf{a}_i \odot \mathbf{a}_i\right) \mathbf{P}_i^H \mathbf{H}_k^H \mathbf{G}_k^H + \sigma_n^2 \mathbf{G}_k \mathbf{G}_k^H \tag{2-69}$$

The achievable rate for the kth user is

$$R_k = I(\mathbf{x}_k;\mathbf{y}_k) = h(\mathbf{y}_k) - h(\mathbf{z}_k)$$
$$= \log_2\left(\det\left[\mathbf{I} + \sigma_s^2 \mathbf{G}_k \mathbf{H}_k \mathbf{P}_k \mathrm{diag}\left(\mathbf{a}_k \odot \mathbf{a}_k\right) \mathbf{P}_k^H \mathbf{H}_k^H \mathbf{G}_k^H \mathbf{R}_{\mathbf{z}_k\mathbf{z}_k}^{-1}\right]\right) \tag{2-70}$$

Finally, the sum-rate of the system given a channel realization can be defined by the following equation:

$$S_I = \sum_{k=1}^{K} R_k \tag{2-71}$$

The ergodic sum-rate across multiple channel realizations is given by

$$S_r = \mathbb{E} \left[\sum_{k=1}^{K} R_k \right] \tag{2-72}$$

In a MISO environment equation (2-70) is simplified to

$$R_k = \log_2 \left(1 + \frac{\sigma_s^2 a_k^2 |g_k \mathbf{h}_k^{\mathrm{T}} \mathbf{p}_k|^2}{\sigma_s^2 \sum_{\substack{i=1 \\ i \neq k}}^{K} a_i^2 |g_k \mathbf{h}_k^{\mathrm{T}} \mathbf{p}_i|^2 + \sigma_n^2 |g_k|^2} \right)$$
$$= \log_2 \left(1 + \gamma_k \right) \tag{2-73}$$

where γ_k represents the SINR of the kth user. The instantaneous SR of the system is given by (2-71) and the ergodic sum-rate can be computed with equation (2-72).

Example 1: Fig. 2.3 shows the performance of different precoding techniques when perfect CSIT is available. For this simulation, we consider a BC channel where the BS has eight transmit antennas. We consider $K = 4$ users each equipped with 2 receive antennas. A total of 10 000 channels have been averaged to obtain the final curves. The best performance is achieved by the nonlinear precoders as expected. From Fig. 2.3 we can see that the ESR increases as the SNR increases. This means that transmitting with more power enhances the performance since the level of the noise remains the same. The performance obtained by the MF precoder saturates because the MUI is not removed. This affects the performance at high SNR values, where the MUI is the predominant factor. From the curves in Fig. 2.3 we can see that as the SNR increases the performance of the MMSE precoder gets closer to the performance obtained by the ZF precoder. Similarly, the performance of the RBD gets closer to the performance of the BD precoder at high SNR. This occurs because the precoder tries to remove completely the MUI at high SNR values to avoid the saturation of the performance.

Example 2: In this example we show the detrimental effect caused by the channel uncertainties. We consider that each coefficient of $\tilde{\mathbf{H}}$ follows a Gaussian distribution with zero mean and $\mathbb{E} \left[\tilde{\mathbf{h}}_{i,*} \tilde{\mathbf{h}}_i \right] = 0.05$. Other parameters remain as set in the first example. We can see from Figure 2.4 that not only the achievable rate is reduced, but also that it saturates around 25 dB. The saturation is produced by the residual MUI, which was a result of the imperfect
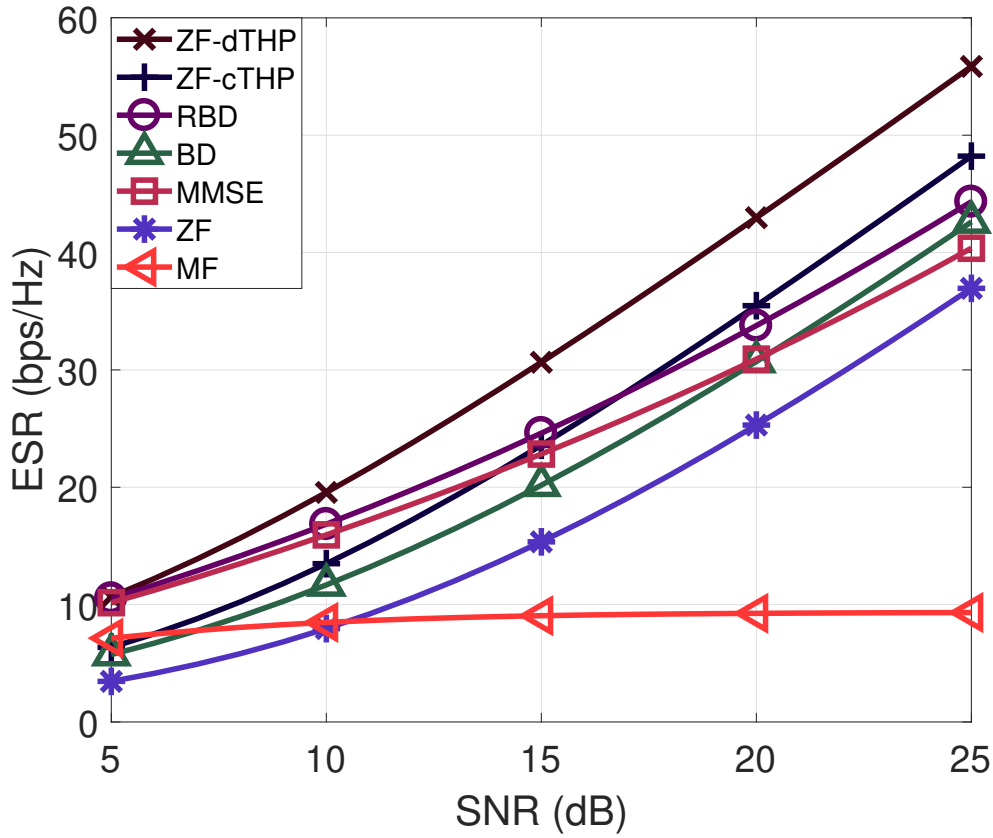
Figure 2.3: Sum-rate performance of conventional precoding techniques. $N_t = 8, K = 4$, and $N_k = 2$.

CSIT. Contrary to the noise, the residual MUI scales with the transmitted power .This constitutes a huge disadvantage since increasing the power of the transmitted signal will not produce any further gain

2.9
Summary

In this chapter, a review of the key aspects of MIMO systems has been carried out. The different multiple access schemes, which allow multiple users to access the network, have been described. A mathematical model of multiuser MIMO systems has also been established. Moreover, an overview of several signal processing techniques for MIMO systems, such as precoding techniques, detection techniques and power allocation schemes has been made. In general, MIMO systems have shown the capability of increasing the performance of wireless systems dramatically. However, dealing with MUI and CSI imperfections remain a challenging task to solve. Promising strategies to better handle these problems include novel precoding approaches for RS-based multiple access schemes which could further enhance the system performance.
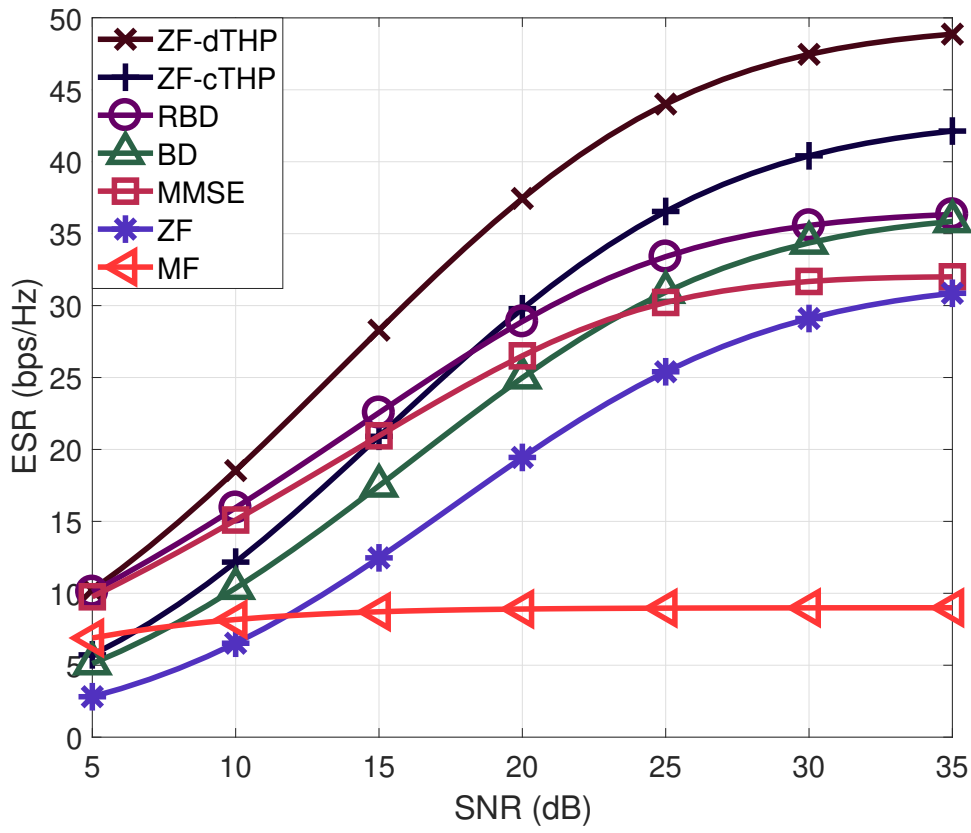
Figure 2.4: Sum-rate performance of conventional precoding techniques. $N_t = 8$, $K = 4$, $N_k = 2$, and $\sigma_e^2 = 0.05$

3
Stream Combining for Rate Splitting in Linearly Precoded MU-MIMO Systems

In this chapter we develop a mathematical model for rate splitting (RS) in MIMO systems. In contrast to previous RS works, we consider a multiuser MIMO (MU-MIMO) system where the receivers are possibly equipped with multiple antennas. This allows us to establish a general RS MU-MIMO model and consider scenarios which are more likely to be encountered in 5G networks. It turns out that conventional MU-MIMO can be seen as a particular case of the model established. The linear BD and RBD precoders are incorporated into the RS scheme to exploit the multiple antennas at the user equipments (UEs). Furthermore, we develop stream combining techniques to enhance the performance of the common rate. Closed-form expressions to describe the SINR and the sum-rate of the proposed techniques are also derived. Simulation results show that the proposed linearly precoded RS schemes and combiners have the pontential to increase the common rate over previously reported techniques.

In Section 3.1 a general RS model considering receivers equipped with multiple antennas is defined. Then, the RS-BD techniques are presented in Section 3.2. In Section 3.3 common stream combiners are derived in order to enhance the common rate of the proposed techniques. A sum-rate analysis of the proposed techniques is presented in Section 3.4. Simulations results are given in Section 3.5, where it is shown that the proposed techniques outperform conventional precoding strategies. Finally, Section 3.6 draws the conclusions from this chapter.

3.1
System Model

Let us consider the downlink of a MU-MIMO system where the communication is established between a single base station (BS) and K users, as depicted in Fig. 3.1. The kth user equipment (UE) is equipped with N_k antennas i.e., the total number of receive antennas is $Nr = \sum_{k=1}^{K} N_k$. The transmitter has N_t antennas where $N_t \geq K \geq 2$. We consider an RS scheme where the BS wants to deliver M messages to the users, and, for simplicity splits only one

message into a common part and a private part, e.g., message m$^{(\text{RS})}$ as in Fig. 3.1[1]. The BS then encodes 1 commmon part and M private parts (the private part from m$^{(\text{RS})}$, namely m$_k$ and the remaining $M-1$ messages that have not been split). Then, the number of data streams transmitted is equal to $M+1$. The set $\mathcal{M}_k$ contains the index of all the data streams intended to the kth user. It follows that $M = \sum_{k=1}^{K} M_k$ with $M_k = \text{card}\,(\mathcal{M}_k)$.
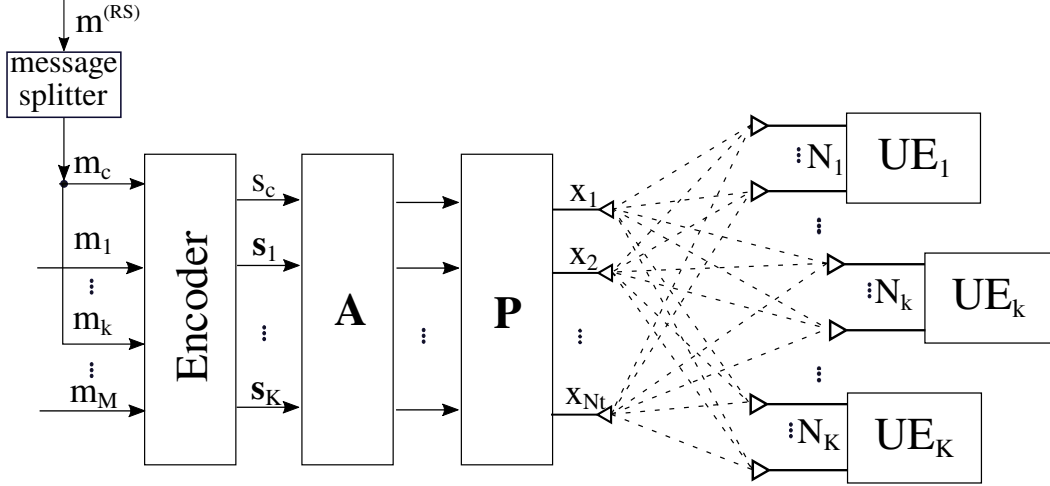
Figure 3.1: System model

The data stream m$^{(\text{RS})}$ is split, modulated and superimposed to the transmitted signal, resulting in a vector of symbols $\mathbf{s}^{(\text{RS})} = [s_c, \mathbf{s}_1^{\text{T}}, \mathbf{s}_2^{\text{T}}, \cdots, \mathbf{s}_K^{\text{T}}]^{\text{T}} \in \mathbb{C}^{M+1}$. The common symbol is denoted by s_c, whereas the vector $\mathbf{s}_k$ contains the M_k private streams of the kth user. For the rest of this work we assume that the entries of $\mathbf{s}^{(\text{RS})}$ are i.i.d with zero mean and covariance matrix equal to the identity matrix. The common stream should be decoded by all users, whereas the private streams should be decoded only by its respective user. After the detection of the common symbol, the UE performs successive interference cancellation (SIC) in order to decode the private streams.

At the transmitter, a common precoder is included to the model, i.e., $\mathbf{P}^{(\text{RS})} = [\mathbf{p}_c, \mathbf{P}] \in \mathbb{C}^{N_t} \times (M+1)$. In particular, $\mathbf{p}_c \in \mathbb{C}^{N_t}$ performs the mapping of the common symbol to the transmit antennas. The private precoder is given by $\mathbf{P} = [\mathbf{P}_1, \mathbf{P}_2, \cdots, \mathbf{P}_K]$, where $\mathbf{P}_k \in \mathbb{C}^{N_t \times M_k}$ denotes the precoder of the kth user and the vector $\mathbf{p}_k$ denotes the kth column of $\mathbf{P}$. The vector $\mathbf{p}_j^{(k)}$ represents the jth column of the matrix $\mathbf{P}_k$.

---

[1]The metric employed in this work to evaluate the performance of the system is the ergodic sum-rate. For this purpose splitting the message of a single user is sufficient as explained in [24].

The transmit vector is given by

$$
\begin{aligned}
\mathbf{x}^{(\mathrm{RS})} &= \mathbf{P}^{(\mathrm{RS})}\mathbf{A}^{(\mathrm{RS})}\mathbf{s}^{(\mathrm{RS})} \\
&= a_c s_c \mathbf{p}_c + \sum_{k=1}^{K} \mathbf{P}_k \mathrm{diag}\left(\mathbf{a}_k\right)\mathbf{s}_k,
\end{aligned}
\tag{3-1}
$$

where $\mathbf{A}^{(\mathrm{RS})} = \mathrm{diag}\left(\mathbf{a}^{(\mathrm{RS})}\right) = \mathrm{diag}\left(\left[a_c, \mathbf{a}_1^{\mathrm{T}}, \cdots, \mathbf{a}_k^{\mathrm{T}}\right]^{\mathrm{T}}\right) \in \mathbb{R}^{(M+1)\times(M+1)}$ represents a general power loading matrix. The vector $\mathbf{a}_k$ allocates power to the M_k symbols in $\mathcal{M}_k$ and the coefficient a_c distributes the power to the common message. In general, power loading schemes are jointly applied with precoding techniques to enhance the performance of the system.

The model satisfies the transmit power constraint which for the RS system is rewritten as

$$
\begin{aligned}
E_{tr} &= \mathbb{E}\left[\|\mathbf{P}^{(\mathrm{RS})}\mathrm{diag}\left(\mathbf{a}^{(\mathrm{RS})}\right)\mathbf{s}^{(\mathrm{RS})}\|^2\right] \\
&= \mathbb{E}\left[\mathrm{tr}\left(\mathbf{s}^{(\mathrm{RS})^H}\mathrm{diag}\left(\mathbf{a}^{(\mathrm{RS})}\right)\mathbf{P}^{(\mathrm{RS})^H}\mathbf{P}^{(\mathrm{RS})}\mathrm{diag}\left(\mathbf{a}^{(\mathrm{RS})}\right)\mathbf{s}^{(\mathrm{RS})}\right)\right] \\
&= \mathrm{tr}\left(\mathbf{P}^{(\mathrm{RS})}\mathrm{diag}\left(\mathbf{a}^{(\mathrm{RS})}\right)\mathbb{E}\left[\mathbf{s}^{(\mathrm{RS})}\mathbf{s}^{(\mathrm{RS})^H}\right]\mathrm{diag}\left(\mathbf{a}^{(\mathrm{RS})}\right)\mathbf{P}^{(\mathrm{RS})^H}\right) \\
&= \mathrm{tr}\left(\mathbf{P}^{(\mathrm{RS})}\mathrm{diag}\left(\mathbf{a}^{(\mathrm{RS})}\right)\mathbf{R_{ss}}\mathrm{diag}\left(\mathbf{a}^{(\mathrm{RS})}\right)\mathbf{P}^{(\mathrm{RS})^H}\right) \\
&= \sigma_s^2 \mathrm{tr}\left(\mathbf{P}^{(\mathrm{RS})}\mathrm{diag}\left(\mathbf{a}^{(\mathrm{RS})} \odot \mathbf{a}^{(\mathrm{RS})}\right)\mathbf{P}^{(\mathrm{RS})^H}\right) \\
&= a_c^2 \sigma_s^2 \|\mathbf{p}_c\|^2 + \sigma_s^2 \sum_{k=1}^{K} \mathrm{tr}\left(\mathbf{P}_k \mathrm{diag}\left(\mathbf{a}_k \odot \mathbf{a}_k\right)\mathbf{P}_k^H\right),
\end{aligned}
\tag{3-2}
$$

where we consider the transmit power constraint as an equality since the best performance of the system is achieved when all the available power is used. Then, expanding the terms of equation (3-2) lead us to

$$
E_{tr} = a_c^2 \sigma_s^2 \|\mathbf{p}_c\|^2 + \sigma_s^2 \sum_{m=1}^{M} a_m^2 \|\mathbf{p}_m\|^2.
\tag{3-3}
$$

Note that the first term in (3-3) represents the power allocated to the common stream, which results in the reduction of the power allocated to the private streams. It turns out that the conventional non-RS MIMO system represents a particular case where no power is distributed to the common message, i.e., $a_c = 0$ (and therefore no split of the message is conducted), resulting in

$$
E_{tr} = \sigma_s^2 \sum_{m=1}^{M} a_m^2 \|\mathbf{p}_m\|^2.
\tag{3-4}
$$

Assuming a precoder $\bar{\mathbf{P}}^{(\mathrm{RS})}$ with normalized columns, i.e., $\bar{\mathbf{p}}_c = \frac{\mathbf{p}_c}{\|\mathbf{p}_c\|}$ and $\bar{\mathbf{p}}_m = \frac{\mathbf{p}_m}{\|\mathbf{p}_m\|}$ for $m = 1, \cdots, M$, the transmit power constraint is reduced to

$$
E_{tr} = \sigma_s^2 \left(a_c^2 + \sum_{m=1}^{M} a_m^2\right).
\tag{3-5}
$$

At the kth UE, the received signal can be expressed as follows:

$$\mathbf{y}_k = \mathbf{H}_k \mathbf{P}^{(\mathrm{RS})} \mathrm{diag}\left(\mathbf{a}^{(\mathrm{RS})}\right) \mathbf{s}^{(\mathrm{RS})} + \mathbf{n}_k$$

$$= a_c s_c \mathbf{H}_k \mathbf{p}_c + \sum_{j=1}^{K} \mathbf{H}_k \mathbf{P}_j \mathrm{diag}\left(\mathbf{a}_j\right) \mathbf{s}_j + \mathbf{n}_k$$

$$= \overbrace{a_c s_c \mathbf{H}_k \mathbf{p}_c}^{\text{Common stream}} + \overbrace{\sum_{i \in \mathcal{M}_k} a_i s_i \mathbf{H}_k \mathbf{p}_i}^{\text{User-k private streams}} + \overbrace{\sum_{\substack{j=1 \\ j \notin \mathcal{M}_k}}^{M} a_j s_j \mathbf{H}_k \mathbf{p}_j}^{\text{Multi-User Interference}} + \mathbf{n}_k, \quad (3\text{-}6)$$

where the vector $\mathbf{n}_k \in \mathbb{C}^{N_k}$ represents the additive noise affecting the kth UE. In a MISO scenario the previous equation is reduced to

$$y_k = a_c s_c \mathbf{h}_{k,*} \mathbf{p}_c + a_k s_k \mathbf{h}_{k,*} \mathbf{p}_k + \sum_{\substack{j=1 \\ j \neq k}}^{K} a_j s_j \mathbf{h}_{k,*} \mathbf{p}_j + n_k \quad (3\text{-}7)$$

Table 3.1 summarizes the expressions of the received signal for the RS-MIMO and RS-MISO systems when no particular receive filter $\mathbf{G}_k$ is employed.

3.2
Proposed RS-BD Techniques

Employing a BD-type precoder in (3-6) lead us to the following received vector at the kth user:

$$\mathbf{y}_k = a_c s_c \mathbf{H}_k \mathbf{p}_c + \left(\hat{\mathbf{H}}_k + \tilde{\mathbf{H}}_k\right) \mathbf{P}_{a,k} \mathbf{P}_{b,k} \mathrm{diag}\left(\mathbf{a}_k\right) \mathbf{s}_k$$
$$+ \sum_{\substack{j=1 \\ j \neq k}}^{K} \left(\hat{\mathbf{H}}_k + \tilde{\mathbf{H}}_k\right) \mathbf{P}_{a,j} \mathbf{P}_{b,j} \mathrm{diag}\left(\mathbf{a}_j\right) \mathbf{s}_j + \mathbf{n}_k. \quad (3\text{-}8)$$

Using a BD precoder in (3-8) we obtain

$$\mathbf{y}_k = a_c s_c \mathbf{H}_k \mathbf{p}_c + \left(\hat{\mathbf{\underline{H}}}_k + \tilde{\mathbf{\underline{H}}}_k\right) \mathbf{P}_{b,k}^{(\mathrm{BD})} \mathrm{diag}\left(\mathbf{a}_k\right) \mathbf{s}_k$$
$$+ \sum_{\substack{j=1 \\ j \neq k}}^{K} \left(\hat{\mathbf{\underline{H}}}^{(k,j)} + \tilde{\mathbf{\underline{H}}}^{(k,j)}\right) \mathbf{P}_{b,j}^{(\mathrm{BD})} \mathrm{diag}\left(\mathbf{a}_j\right) \mathbf{s}_j + \mathbf{n}_k, \quad (3\text{-}9)$$

where $\hat{\mathbf{\underline{H}}}^{(k,j)} = \hat{\mathbf{H}}_k \mathbf{P}_{a,j}^{(\mathrm{BD})}$, $\tilde{\mathbf{\underline{H}}}^{(k,j)} = \tilde{\mathbf{H}}_k \mathbf{P}_{a,j}^{(\mathrm{BD})}$, and $\tilde{\mathbf{\underline{H}}}_k = \tilde{\mathbf{H}}_k \mathbf{P}_{a,k}^{(\mathrm{BD})}$. Considering the restriction of zero interference between users imposed by the BD precoder

Table 3.1: Received signal per user

System	Received Signal
MIMO	$\mathbf{y}_k = a_c s_c \mathbf{H}_k \mathbf{p}_c + \mathbf{H}_k \mathbf{P}_k \mathrm{diag}\left(\mathbf{a}_k\right) \mathbf{s}_k + \mathbf{H}_k \sum\limits_{\substack{i=1 \\ i\neq k}}^{K} \mathbf{P}_i \mathrm{diag}\left(\mathbf{a}_i\right) \mathbf{s}_i + \mathbf{n}_k$
MISO	$y_k = a_c s_c \mathbf{h}_{k,*} \mathbf{p}_c + a_k s_k \mathbf{h}_{k,*} \mathbf{p}_k + \sum\limits_{\substack{i=1 \\ i\neq k}}^{K} a_i s_i \mathbf{h}_{k,*} \mathbf{p}_i + n_k$

in (2-17), equation (3-9) can be simplified to

$$\mathbf{y}_k = a_c s_c \mathbf{H}_k \mathbf{p}_c + \left(\hat{\mathbf{H}}_k + \tilde{\mathbf{H}}_k\right) \mathbf{P}_{b,k}^{(\mathrm{BD})} \mathrm{diag}\left(\mathbf{a}_k\right) \mathbf{s}_k + \sum_{\substack{j=1 \\ j\neq k}}^{K} \tilde{\mathbf{H}}_k^{(k,j)} \mathbf{P}_{b,j}^{(\mathrm{BD})} \mathrm{diag}\left(\mathbf{a}_j\right) \mathbf{s}_j + \mathbf{n}_k. \tag{3-10}$$

On the other hand, employing an RBD over (3-8) we get

$$\begin{aligned}
\mathbf{y}_k =\, & a_c s_c \mathbf{H}_k \mathbf{p}_c + \left(\hat{\mathbf{H}}_k + \tilde{\mathbf{H}}_k\right) \mathbf{P}_{b,k}^{(\mathrm{RBD})} \mathrm{diag}\left(\mathbf{a}_k\right) \mathbf{s}_k \\
& + \sum_{\substack{j=1 \\ j\neq k}}^{K} \left(\hat{\mathbf{H}}^{(k,j)} + \tilde{\mathbf{H}}^{(k,j)}\right) \mathbf{P}_{b,j}^{(\mathrm{RBD})} \mathrm{diag}\left(\mathbf{a}_j\right) \mathbf{s}_j + \mathbf{n}_k, \tag{3-11}
\end{aligned}$$

where $\hat{\mathbf{H}}^{(k,j)} = \hat{\mathbf{H}}_k \mathbf{P}_{a,j}^{(\mathrm{RBD})}$, $\tilde{\mathbf{H}}^{(k,j)} = \tilde{\mathbf{H}}_k \mathbf{P}_{a,j}^{(\mathrm{RBD})}$, and $\tilde{\mathbf{H}}_k = \tilde{\mathbf{H}}_k \mathbf{P}_{a,k}^{(\mathrm{BD})}$. From (3-10) we get the received signal of the RS-BD scheme at each antenna which is given by

$$y_i^{(k)} = a_c s_c \mathbf{h}_{i,*}^{(k)} \mathbf{p}_c + \left(\hat{\mathbf{h}}_{i,*}^{(k)} + \tilde{\mathbf{h}}_{i,*}^{(k)}\right) \sum_{j\in\mathcal{M}_k} a_j s_j \mathbf{p}_j^{(b,k)^{(\mathrm{BD})}} + \sum_{l\notin\mathcal{M}_k} a_l s_l \tilde{\mathbf{h}}_{i,*}^{(k,l)} \mathbf{p}_l^{(b,k)^{(\mathrm{BD})}} + n_i^{(k)}. \tag{3-12}$$

Similarly, using (3-11) for the RS-RBD scheme we obtain

$$\begin{aligned}
y_i^{(k)} =\, & a_c s_c \mathbf{h}_{i,*}^{(k)} \mathbf{p}_c + \left(\hat{\mathbf{h}}_{i,*}^{(k)} + \tilde{\mathbf{h}}_{i,*}^{(k)}\right) \sum_{j\in\mathcal{M}_k} a_j s_j \mathbf{p}_j^{(b,k)^{(\mathrm{RBD})}} \\
& + \sum_{l\notin\mathcal{M}_k} a_l s_l \left(\hat{\mathbf{h}}_{i,*}^{(k,l)} + \tilde{\mathbf{h}}_{i,*}^{(k,l)}\right) \mathbf{p}_l^{(b,k)^{(\mathrm{RBD})}} + n_i^{(k)}. \tag{3-13}
\end{aligned}$$

In the following, we dropped the terms RBD and BD to simplify the notation. By squaring and taking the expected value over equations (3-12) and (3-13) we arrive at

$$\mathbb{E}\left[|y_i^{(k)}|^2\right] = a_c^2|\mathbf{h}_{i,*}^{(k)}\mathbf{p}_c|^2 + \sum_{j\in\mathcal{M}_k} a_j^2|\left(\hat{\mathbf{h}}_{i,*}^{(k)} + \tilde{\mathbf{h}}_{i,*}^{(k)}\right)\mathbf{p}_j^{(b,k)}|^2 + \sum_{\substack{l=1\\l\neq k}}^{K}\sum_{q\notin\mathcal{M}_l} a_q^2|\tilde{\mathbf{h}}_{i,*}^{(k,l)}\mathbf{p}_q^{(b,l)}|^2 + \sigma_n^2,$$

$$(3\text{-}14)$$

$$\mathbb{E}\left[|y_i^{(k)}|^2\right] = a_c^2|\mathbf{h}_{i,*}^{(k)}\mathbf{p}_c|^2 + \sum_{j\in\mathcal{M}_k} a_j^2|\left(\hat{\mathbf{h}}_{i,*}^{(k)} + \tilde{\mathbf{h}}_{i,*}^{(k)}\right)\mathbf{p}_j^{(b,k)}|^2$$
$$+ \sum_{\substack{l=1\\l\neq k}}^{K}\sum_{q\notin\mathcal{M}_l} a_q^2|\left(\hat{\mathbf{h}}_{i,*}^{(k,l)} + \tilde{\mathbf{h}}_{i,*}^{(k,l)}\right)\mathbf{p}_q^{(b,k)}|^2 + \sigma_n^2. \qquad (3\text{-}15)$$

Thus, the SINR at the ith antenna of the kth user when decoding the common message is given by

$$\gamma_{c,k,i}^{(\text{BD})} = \frac{a_c^2|\mathbf{h}_{i,*}^{(k)}\mathbf{p}_c|^2}{\sum\limits_{j\in\mathcal{M}_k} a_j^2|\left(\hat{\mathbf{h}}_{i,*}^{(k)} + \tilde{\mathbf{h}}_{i,*}^{(k)}\right)\mathbf{p}_j^{(b,k)}|^2 + \sum\limits_{\substack{l=1\\l\neq k}}^{K}\sum\limits_{q\notin\mathcal{M}_l} a_q^2|\tilde{\mathbf{h}}_{i,*}^{(k,l)}\mathbf{p}_q^{(b,l)}|^2 + \sigma_n^2} \qquad (3\text{-}16)$$

$$\gamma_{c,k,i}^{(\text{RBD})} = \frac{a_c^2|\mathbf{h}_{i,*}^{(k)}\mathbf{p}_c|^2}{\sum\limits_{j\in\mathcal{M}_k} a_j^2|\left(\hat{\mathbf{h}}_{i,*}^{(k)} + \tilde{\mathbf{h}}_{i,*}^{(k)}\right)\mathbf{p}_j^{(b,k)}|^2 + \sum\limits_{\substack{l=1\\l\neq k}}^{K}\sum\limits_{q\notin\mathcal{M}_l} a_q^2|\left(\hat{\mathbf{h}}_{i,*}^{(k,l)} + \tilde{\mathbf{h}}_{i,*}^{(k,l)}\right)\mathbf{p}_q^{(b,k)}|^2 + \sigma_n^2}$$

$$(3\text{-}17)$$

Under perfect CSIT equations (3-16) and (3-17) are reduced to

$$\gamma_{c,k,i}^{(\text{BD})} = \frac{a_c^2|\mathbf{h}_{i,*}^{(k)}\mathbf{p}_c|^2}{\sum\limits_{j\in\mathcal{M}_k} a_j^2|\hat{\mathbf{h}}_{i,*}^{(k)}\mathbf{p}_j^{(b,k)}|^2 + \sigma_n^2} \qquad (3\text{-}18)$$

$$\gamma_{c,k,i}^{(\text{RBD})} = \frac{a_c^2|\mathbf{h}_{i,*}^{(k)}\mathbf{p}_c|^2}{\sum\limits_{j\in\mathcal{M}_k} a_j^2|\hat{\mathbf{h}}_{i,*}^{(k)}\mathbf{p}_j^{(b,k)}|^2 + \sum\limits_{\substack{l=1\\l\neq k}}^{K}\sum\limits_{q\notin\mathcal{M}_l} a_q^2|\hat{\mathbf{h}}_{i,*}^{(k,l)}\mathbf{p}_q^{(b,k)}|^2 + \sigma_n^2} \qquad (3\text{-}19)$$

Let us now consider that the proposed RS-BD techniques employ Gaussian signalling. In this circumstances the instantaneous sum-rate is achievable. Then, the instantaneous common rate at user k is defined as

$$R_{c,k} = \log_2\left(1 + \gamma_{c,k}\right), \qquad (3\text{-}20)$$

where $\gamma_{c,k}$ SINR of the kth user when decoding the common message.

In order to evaluate the performance under imperfect CSIT, we consider the ergodic sum-rate (ESR) over a long sequence of fading channel states to ensure that the rates are achievable, as detailed in [23]. For the established RS-BD scheme, the total ESR of the system consists of the sum of the ergodic common rate and the ergodic sum-private rate and is given by

$$S_r^{(\mathrm{RS})} = \min_{k \in [1,K]} \mathbb{E}_{\hat{\mathbf{H}}}\left[\bar{R}_{c,k}\right] + \mathbb{E}_{\hat{\mathbf{H}}}\left[\bar{R}_p\right]. \tag{3-21}$$

The term $\mathbb{E}_{\hat{\mathbf{H}}}\left[\bar{R}_{c,k}\right]$ represents the ergodic common rate of the kth user. In (3-21), the ergodic common rate of the overall system is set to the minimum ergodic common rate found across the users in order to guarantee that all users decode the common message successfully [2]. Additionally, the term $\bar{R}_{c,k} = \mathbb{E}_{\mathbf{H}|\hat{\mathbf{H}}}\left[R_{c,k}|\hat{\mathbf{H}}\right]$ stands for the average common rate, which is a short-term measure that characterizes the expected performance over the error distribution given a channel estimate, and $R_{c,k}$ is the instantaneous common rate at the kth user. On the other hand, the term $\mathbb{E}_{\hat{\mathbf{H}}}\left[\bar{R}_p\right]$ denotes the ergodic sum-private rate, where $\bar{R}_p = \mathbb{E}_{\mathbf{H}|\hat{\mathbf{H}}}\left[R_p|\hat{\mathbf{H}}\right]$ represents the average sum-private rate and R_p the instantaneous sum-private rate. R_p corresponds to the sum of all private rates, i.e., $R_p = \sum_{k=1}^{K} R_k$, where R_k denotes the instantaneous private rate of the kth user. Then, the ESR of the proposed RS-BD framework can be computed by employing (2-70), (3-16), (3-17), and (3-21).

3.3
Proposed Stream Combining Techniques

Unlike receivers in RS MISO systems, the kth receiver in a MIMO system has access to N_k copies of the common symbol. Therefore, the performance of the system can be improved by implementing a common combiner at the receivers. Let us consider (3-6), where the vector $\mathbf{y}_k$ has N_k components, i.e., $\mathbf{y}_k = \begin{bmatrix} y_1^{(k)} & y_2^{(k)} & \cdots & y_{N_k}^{(k)} \end{bmatrix}^{\mathrm{T}}$, and define the combined signal $\tilde{y}_k = \mathbf{w}_k^H \mathbf{y}_k$, where the vector $\mathbf{w}_k = \begin{bmatrix} \mathrm{w}_1^{(k)} & \mathrm{w}_2^{(k)} & \cdots & \mathrm{w}_{N_k}^{(k)} \end{bmatrix}^{\mathrm{T}}$ represents the combining filter used to enhance the sum-rate performance. Expanding terms, we have

$$\tilde{y}_k = \mathbf{w}_k^H \left(a_c s_c \mathbf{H}_k \mathbf{p}_c + \sum_{j=1}^{K} \mathbf{H}_k \mathbf{P}_j \mathrm{diag}\left(\mathbf{a}_j\right) \mathbf{s}_j + \mathbf{n}_k \right). \tag{3-22}$$

Let us consider the following quantity:

$$\mathbb{E}\left[|\mathbf{w}_k^H \mathbf{n}_k|^2\right] = \mathbb{E}\left[\left(\mathrm{w}_1^{(k)} n_1^{(k)} + \cdots + \mathrm{w}_{N_k}^{(k)} n_{N_k}^{(k)}\right)^* \left(\mathrm{w}_1^{(k)} n_1^{(k)} + \cdots + \mathrm{w}_{N_k}^{(k)} n_{N_k}^{(k)}\right)\right], \tag{3-23}$$

which is reduced to

$$\begin{aligned} \mathbb{E}\left[|\mathbf{w}_k^H \mathbf{n}_k|^2\right] &= |\mathrm{w}_1^{(k)}|^2 \sigma_n^2 + |\mathrm{w}_2^{(k)}|^2 \sigma_n^2 + \cdots + |\mathrm{w}_{N_k}^{(k)}|^2 \sigma_n^2 \\ &= \|\mathbf{w}_k\|^2 \sigma_n^2 \end{aligned} \tag{3-24}$$

---

[2]Note that the achievable common rate is limited by the performance of the worst user. Hence, selecting a general user k is sufficient to evaluate the total ESR.

since the components of the noise are uncorrelated. Then, the average power of $\tilde{y}_k$ is

$$\mathbb{E}\left[|\tilde{y}_k|^2\right] = a_c^2|\mathbf{w}_k^H\mathbf{t}_{k,c}|^2 + \sum_{j=1}^{M} a_j^2|\mathbf{w}_k^H\mathbf{t}_{k,j}|^2 + \|\mathbf{w}_k\|^2\sigma_n^2, \qquad (3\text{-}25)$$

where the vectors $\mathbf{t}_{k,c} = \mathbf{H}_k\mathbf{p}_c$ and $\mathbf{t}_{k,i} = \mathbf{H}_k\mathbf{p}_i$ have been introduced to simplify the notation. From (3-25) we obtain the SINR when decoding the common message, which is given by

$$\gamma_{c,k} = \frac{a_c^2|\mathbf{w}_k^H\mathbf{t}_{k,c}|^2}{\sum\limits_{i\in\mathcal{M}_k} a_i^2|\mathbf{w}_k^H\mathbf{t}_{k,i}|^2 + \sum\limits_{\substack{j=1\\j\notin\mathcal{M}_k}}^{M} a_j^2|\mathbf{w}_k^H\mathbf{t}_{k,j}|^2 + \|\mathbf{w}_k\|^2\sigma_n^2}. \qquad (3\text{-}26)$$

The structure of the kth receiver is shown in Fig. 3.2. In what follows, we propose combining strategies to compute $\mathbf{w}_k$ and enhance the common rate performance.
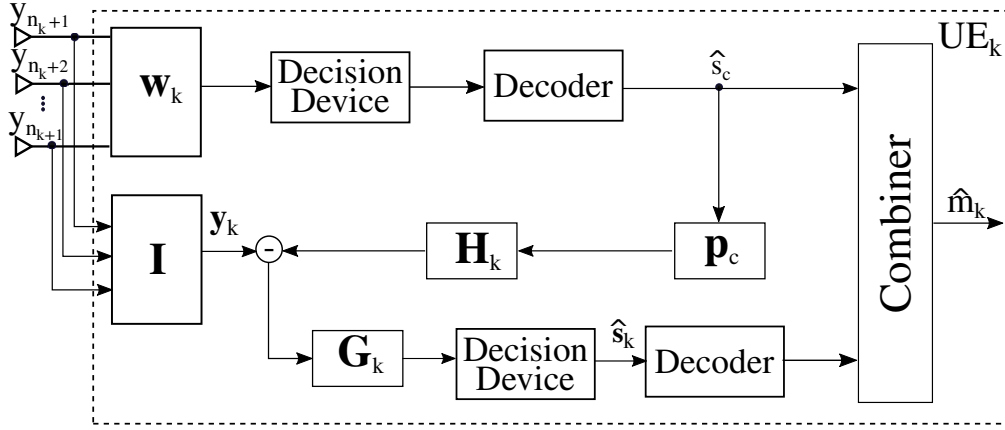
Figure 3.2: Receiver structure.

3.3.1
Min-Max Criterion

The min-max criterion selects at each receiver the antenna i_{opt}, which leads to the highest ergodic common rate. It follows that $i_{opt} = \max\limits_{i} \mathbb{E}_{\hat{\mathbf{H}}}\left[\bar{R}_{c,k,i}\right]$, where $\bar{R}_{c,k,i} = \mathbb{E}_{\mathbf{H}|\hat{\mathbf{H}}}\left[R_{c,k,i}|\hat{\mathbf{H}}\right]$ is the average common rate obtained at the ith antenna and $R_{c,k,i}$ is the instantaneous common rate given by

$$R_{c,k,i} = \log_2\left(1 + \frac{a_c^2|\mathbf{h}_{i,*}^{(k)}\mathbf{p}_c|^2}{\sum_{j=1}^{M} a_j^2|\mathbf{h}_{i,*}^{(k)}\mathbf{p}_j|^2 + \sigma_n^2}\right). \qquad (3\text{-}27)$$

The entry $\mathrm{w}_{i_{opt}}$ of the combiner $\mathbf{w}_k$ is set to one and all the other entries are set to zero. Finally, the common rate performance is

$$R_c = \min_{k\in[1,K]}\left(\max_i \mathbb{E}_{\hat{\mathbf{H}}}\left[\bar{R}_{c,k,i}\right]\right). \qquad (3\text{-}28)$$

The rate is still limited by the user attaining the worst ergodic common rate. However, the common rate improves as the number of antennas in the UE increases.

Another possible option is to choose the best antenna for each channel realization. In this case the common rate performance is given by

$$R_c = \min_{k \in [1,K]} \mathbb{E}_{\hat{\mathbf{H}}} \left[\max_i \bar{R}_{c,k,i} \right]. \tag{3-29}$$

Remark that this approximation would increase the computational complexity and would also require extra signalling.

3.3.2
Maximum Ratio Combining

Another possibility to enhance the common rate is to use maximum ratio combining (MRC). This combiner maximizes the SNR at the receiver. The maximum value of the SNR is achieved when the combiner $\mathbf{w}_k$ and the vector $\mathbf{t}_{k,c} = \mathbf{H}_k \mathbf{p}_c$ are parallel. Thus, we can set $\mathbf{w}_k^{(\text{MRC})} = \frac{\mathbf{t}_{k,c}}{\|\mathbf{t}_{k,c}\|}$ in order to maximize the SNR. Expanding the dot product and simplifying terms in (3-26), the SINR can be expressed as follows:

$$\gamma_{c,k}^{(\text{MRC})} = \frac{a_c^2 \|\mathbf{w}_k\|^2 \|\mathbf{t}_{k,c}\|^2}{\|\mathbf{w}_k\|^2 \sum\limits_{i \in \mathcal{M}_k} a_i^2 \|\mathbf{t}_{k,i}\|^2 \cos^2 \theta_i + \|\mathbf{w}_k\|^2 \sum\limits_{\substack{j=1 \\ j \notin \mathcal{M}_k}}^{M} a_j^2 \|\mathbf{t}_{k,j}\|^2 \cos^2 \theta_j + \|\mathbf{w}_k\|^2 \sigma_n^2}$$

$$= \frac{a_c^2 \|\mathbf{t}_{k,c}\|^2}{\sum\limits_{i \in \mathcal{M}_k} a_i^2 \|\mathbf{t}_{k,i}\|^2 \cos^2 \theta_{k,i} + \sum\limits_{\substack{j=1 \\ j \notin \mathcal{M}_k}}^{M} a_j^2 \|\mathbf{t}_{k,j}\|^2 \cos^2 \theta_{k,j} + \sigma_n^2}, \tag{3-30}$$

where $\theta_{k,j}$ is the Hermitian angle between $\mathbf{w}_k$ and $\mathbf{t}_{k,j}$. The sum-rate performance can be found by using (3-30) in (3-20) and then substituting the result in (3-21).

3.3.3
Minimum Mean-Square Error Combining

The proposed MMSE combiner (MMSEc) considers the optimization problem given by

$$\mathbf{w}_k^{(\text{MMSE})} = \min_{\mathbf{w}_k} \mathbb{E} \left[|s_c - \mathbf{w}_k^H \mathbf{y}_k|^2 \right]. \tag{3-31}$$

Evaluating the expected value on the right-hand side of (3-31), we have

$$
\begin{aligned}
\mathbb{E}\left[|s_c - \mathbf{w}_k^H \mathbf{y}_k|^2\right] =& \mathbb{E}\left[\left(s_c - \mathbf{w}_k^H \mathbf{y}_k\right)^* \left(s_c - \mathbf{w}_k^H \mathbf{y}_k\right)\right] \\
=& 1 - \mathbf{w}_k^H \mathbf{H}_k \mathbf{p}_c - \mathbf{p}_c^H \mathbf{H}_k^H \mathbf{w}_k + \\
& \mathbf{w}_k^H \mathbf{R}_{\mathbf{y}_k \mathbf{y}_k} \mathbf{w}_k,
\end{aligned}
\tag{3-32}
$$

where $\mathbf{R}_{\mathbf{y}_k \mathbf{y}_k} = \mathbb{E}\left[\mathbf{y}_k \mathbf{y}_k^H\right]$. Taking the derivative with respect to $\mathbf{w}_k^H$ and equating the result to zero we obtain

$$
\frac{\partial \mathbb{E}\left[|s_c - \mathbf{w}_k^H \mathbf{y}_k|^2\right]}{\partial \mathbf{w}_k^H} = -\mathbf{H}_k \mathbf{p}_c + \mathbf{R}_{\mathbf{y}_k \mathbf{y}_k} \mathbf{w}_k = 0.
\tag{3-33}
$$

Solving (3-33) with respect to $\mathbf{w}_k$ we get the MMSEc expression, which is given by

$$
\mathbf{w}_k^{\text{(MMSE)}} = \mathbf{R}_{\mathbf{y}_k \mathbf{y}_k}^{-1} \mathbf{H}_k \mathbf{p}_c.
\tag{3-34}
$$

Let us consider the quantities:

$$
\begin{aligned}
\|\mathbf{w}_k\|^2 \sigma_n^2 =& \text{tr}\left(\mathbf{R}_{\mathbf{y}_k \mathbf{y}_k}^{-2} \mathbf{H}_k \mathbf{p}_c \mathbf{p}_c^H \mathbf{H}_k^H\right) \sigma_n^2, \\
=& \text{tr}\left(\mathbf{R}_{\mathbf{y}_k \mathbf{y}_k}^{-2} \mathbf{t}_{k,c} \mathbf{t}_{k,c}^H\right) \sigma_n^2
\end{aligned}
\tag{3-35}
$$

$$
\begin{aligned}
|\mathbf{w}_k^H \mathbf{t}_{k,i}|^2 =& \mathbf{p}_i^H \mathbf{H}_k^H \mathbf{R}_{\mathbf{y}_k \mathbf{y}_k}^{-1} \mathbf{H}_k \mathbf{p}_c \mathbf{p}_c^H \mathbf{H}_k^H \mathbf{R}_{\mathbf{y}_k \mathbf{y}_k}^{-1} \mathbf{H}_k \mathbf{p}_i, \\
=& \mathbf{t}_{k,i}^H \mathbf{R}_{\mathbf{y}_k \mathbf{y}_k}^{-1} \mathbf{t}_{k,c} \mathbf{t}_{k,c}^H \mathbf{R}_{\mathbf{y}_k \mathbf{y}_k}^{-1} \mathbf{t}_{k,i}
\end{aligned}
\tag{3-36}
$$

$$
\begin{aligned}
|\mathbf{w}_k^H \mathbf{t}_{k,c}|^2 =& \mathbf{p}_c^H \mathbf{H}_k^H \mathbf{R}_{\mathbf{y}_k \mathbf{y}_k}^{-1} \mathbf{H}_k \mathbf{p}_c \mathbf{p}_c^H \mathbf{H}_k^H \mathbf{R}_{\mathbf{y}_k \mathbf{y}_k}^{-1} \mathbf{H}_k \mathbf{p}_c, \\
=& \mathbf{t}_{k,c}^H \mathbf{R}_{\mathbf{y}_k \mathbf{y}_k}^{-1} \mathbf{t}_{k,c} \mathbf{t}_{k,c}^H \mathbf{R}_{\mathbf{y}_k \mathbf{y}_k}^{-1} \mathbf{t}_{k,c}
\end{aligned}
\tag{3-37}
$$

Substituting (3-35),(3-36), and (3-37) into (3-26) we obtain the SINR of MMSEc, which is given by

$$
\gamma_{k,c}^{\text{(MMSEc)}} = \frac{a_c^2 |\mathbf{t}_{k,c}^H \mathbf{R}_{\mathbf{y}_k \mathbf{y}_k}^{-1} \mathbf{t}_{k,c}|^2}{\sum\limits_{j=1}^{M} a_j^2 |\mathbf{t}_{k,c}^H \mathbf{R}_{\mathbf{y}_k \mathbf{y}_k}^{-1} \mathbf{t}_{k,j}|^2 + \text{tr}\left(\mathbf{R}_{\mathbf{y}_k \mathbf{y}_k}^{-2} \mathbf{t}_{k,c} \mathbf{t}_{k,c}^H\right) \sigma_n^2}.
\tag{3-38}
$$

By substituting (4-100) in (3-20) we get the common rate of the MMSEc technique.

3.3.4
Rate analysis

In this section, we carry out the sum-rate analysis of the proposed combining strategies along with the ZF precoder. This analysis is extended to

the proposed RS-BD and RS-RBD techniques with common stream combiners. The received vector signal for the RS-ZF can be found with

$$\mathbf{y}_k = a_c s_c \mathbf{H}_k \mathbf{p}_c + \mathrm{diag}\left(\mathbf{a}_k\right) \mathbf{s}_k + \sum_{j=1}^{M} a_j s_j \tilde{\mathbf{H}}_k \hat{\mathbf{H}}^H \mathbf{z}_j + \mathbf{n}_k, \qquad (3\text{-}39)$$

where $\mathbf{z}_j$ is the jth column of the matrix $\mathbf{Z} = \left(\hat{\mathbf{H}}\hat{\mathbf{H}}^H\right)^{-1}$. Then, the received signal at each antenna is given by

$$y_i^{(k)} = a_c s_c \mathbf{h}_{i,*}^{(k)} \mathbf{p}_c + a_i^{(k)} s_i^{(k)} + \sum_{j=1}^{N_r}\sum_{q=1}^{N_r}\sum_{l=1}^{N_r} a_j s_j \tilde{h}_{i,l}^{(k)} \hat{h}_{q,l}^* z_{q,j} + n_i^{(k)}. \qquad (3\text{-}40)$$

The mean power at each antenna is given by

$$\mathbb{E}\left[|y_i^{(k)}|^2\right] = a_c^2 |\mathbf{h}_{i,*}^{(k)} \mathbf{p}_c|^2 + a_i^{(k)^2}\left|1 + \sum_{q_1}^{N_r}\sum_{l_1}^{N_r} \tilde{h}_{i,l_1}^{(k)} \hat{h}_{q_1,l_1}^* z_{q_1,i}\right|^2$$

$$+ \sum_{\substack{j=1 \\ j \neq i}}^{N_r} a_j^2 \left|\sum_{q_2=1}^{N_r}\sum_{l_2=1}^{N_r} \tilde{h}_{i,l_2}^{(k)} \hat{h}_{q_2,l_2}^* z_{q_2,j}\right|^2 + \sigma_n^2. \qquad (3\text{-}41)$$

Hence, the instantaneous common rate at the ith antenna is

$$R_{c,k,i}^{(\mathrm{ZF})} = \log_2\left(1 + \gamma_{c,k,i}^{(\mathrm{ZF})}\right), \qquad (3\text{-}42)$$

where

$$\gamma_{c,k,i}^{(\mathrm{ZF})} = \frac{a_c^2 |\mathbf{h}_{i,*}^{(k)} \mathbf{p}_c|^2}{a_i^{(k)^2}\left|1 + \sum_{q_1}^{N_r}\sum_{l_1}^{N_r} \tilde{h}_{i,l_1}^{(k)} \hat{h}_{q_1,l_1}^* z_{q_1,i}\right|^2 + \sum_{\substack{j=1 \\ j \neq i}}^{N_r} a_j^2 \left|\sum_{q_2=1}^{N_r}\sum_{l_2=1}^{N_r} \tilde{h}_{i,l_2}^{(k)} \hat{h}_{q_2,l_2}^* z_{q_2,j}\right|^2 + \sigma_n^2}. $$

$$(3\text{-}43)$$

Employing (3-42) we can compute the average rate $\bar{R}_{c,k,i} = \mathbb{E}_{\mathbf{H}|\hat{\mathbf{H}}}\left[R_{c,k,i}|\hat{\mathbf{H}}\right]$ and the ergodic rate $\mathbb{E}_{\hat{\mathbf{H}}}\left[\bar{R}_{c,k,i}\right]$. Then, for the min-max criterion, the antenna leading to the best performance is selected at each user. Under perfect CSIT, the instantaneous rate is achievable and is given by

$$R_{c,k,i}^{(\mathrm{ZF})} = \log_2\left(1 + \frac{a_c^2 |\mathbf{h}_{i,*}^{(k)} \mathbf{p}_c|^2}{a_i^{(k)^2} + \sigma_n^2}\right) \qquad (3\text{-}44)$$

For the MRC combiner we compute the norm of $\mathbf{t}_{k,j}$. Let us suppose that $j \in \mathcal{M}_k$. We obtain

$$\|\mathbf{t}_{k,j}^{(\mathrm{ZF})}\|^2 = \|\mathbf{e}_j + \tilde{\mathbf{H}}_k \hat{\mathbf{H}}^H \mathbf{z}_j\|^2, \qquad (3\text{-}45)$$

where the entries of $\mathbf{e}_j$ are equal to zero except at the jth position where its value is equal to one. On the other hand, if $j \notin \mathcal{M}_k$ we get

$$\|\mathbf{t}_{k,j}^{(\mathrm{ZF})}\|^2 = \sum_{i=1}^{N_k}|\sum_{q=1}^{N_r}\sum_{l=1}^{N_r} \tilde{h}_{i,l}^{(k)} \hat{h}_{q,l} z_{q,j}|^2. \qquad (3\text{-}46)$$

Next, we consider the MMSEc. Assuming that $j \in \mathcal{M}_k$, we have

$$\sum_{i \in \mathcal{M}_k} a_j^2 |\mathbf{w}_k^H \mathbf{t}_{k,j}|^2 = \sum_{i=1}^{M_k} a_j^{(k)^2} |\mathbf{p}_c^H \mathbf{H}_k^H \mathbf{R}_{\mathbf{y}_k \mathbf{y}_k}^{-1} \left(\mathbf{e}_j + \tilde{\mathbf{H}}_k \hat{\mathbf{H}}^H \mathbf{z}_j \right)|^2, \qquad (3\text{-}47)$$

whereas if $j \notin \mathcal{M}_k$ we get

$$\sum_{i \in \mathcal{M}_k} a_j^2 |\mathbf{w}_k^H \mathbf{t}_{k,j}|^2 = \sum_{i=1}^{M_k} a_j^{(k)^2} |\mathbf{p}_c^H \mathbf{H}_k^H \mathbf{R}_{\mathbf{y}_k \mathbf{y}_k}^{-1} \tilde{\mathbf{H}}_k \hat{\mathbf{H}}^H \mathbf{z}_j|^2. \qquad (3\text{-}48)$$

In what follows, we carried out the sum-rate analysis of the proposed combiners with BD-type precoding algorithms. For this purpose, it is convenient to simplify the matrix $\mathbf{P}_{a,k}^{(\mathrm{RBD})}$ of the RBD precoder first. Let us evaluate the matrix given by

$$\mathbf{\Lambda}_k = \left(\bar{\mathbf{\Psi}}_k^{\mathrm{T}} \bar{\mathbf{\Psi}}_k + \frac{N_r \sigma_n^2}{E_{tr}} \mathbf{I}_{N_t} \right)^{-1/2}. \qquad (3\text{-}49)$$

The matrix $\mathbf{\Psi}_k$ is a diagonal matrix. Hence, the matrix $\mathbf{\Lambda}_k$ is also diagonal, and can be represented by

$$\mathbf{\Lambda}_k = \left[\begin{array}{cccc|ccc} \bar{\psi}_1^{(k)^2} + \frac{N_r \sigma_n^2}{E_{tr}} & 0 & \cdots & 0 & 0 & \cdots & 0 \\ 0 & \bar{\psi}_2^{(k)^2} + \frac{N_r \sigma_n^2}{E_{tr}} & \cdots & 0 & 0 & \cdots & 0 \\ \vdots & \vdots & \ddots & \vdots & \vdots & \vdots & \vdots \\ 0 & 0 & \cdots & \bar{\psi}_{\bar{L}_k}^{(k)^2} + \frac{N_r \sigma_n^2}{E_{tr}} & 0 & \cdots & 0 \\ \hline 0 & 0 & \cdots & 0 & \frac{N r \sigma_n^2}{E_{tr}} & \cdots & 0 \\ \vdots & \vdots & \ddots & \vdots & \vdots & \ddots & \vdots \\ 0 & 0 & \cdots & 0 & 0 & \cdots & \frac{N r \sigma_n^2}{E_{tr}} \end{array} \right]^{-1/2}$$

$$
= E_{tr}
\begin{bmatrix}
\frac{1}{\sqrt{E_{tr}\bar{\psi}_1^{(k)^2}+N_r\sigma_n^2}} & \cdots & 0 & 0 & \cdots & 0 \\
0 & \cdots & 0 & 0 & \cdots & 0 \\
\vdots & \ddots & \vdots & \vdots & \vdots & \vdots \\
0 & \cdots & \frac{1}{\sqrt{E_{tr}\bar{\psi}_{\bar{L}_k}^{(k)^2}+N_r\sigma_n^2}} & 0 & \cdots & 0 \\
\hline
0 & \cdots & 0 & \frac{1}{\sqrt{N_r\sigma_n^2}} & \cdots & 0 \\
\vdots & \ddots & \vdots & \vdots & \ddots & \vdots \\
0 & \cdots & 0 & 0 & \cdots & \frac{1}{\sqrt{N_r\sigma_n^2}}
\end{bmatrix},
\tag{3-50}
$$

where $\bar{L}_k$ is the rank of the matrix $\bar{\mathbf{H}}_k$, as defined in Chapter 2. Using the previous result, the matrix $\mathbf{P}_{a,k}^{(\text{RBD})}$ of the RBD precoder can be rewritten as

$$
\mathbf{P}_{a,k}^{(\text{RBD})} = E_{tr}
\left[
\frac{1}{\lambda_1^{(k)}}\bar{\mathbf{v}}_1^{(k)},
\frac{1}{\lambda_2^{(k)}}\bar{\mathbf{v}}_2^{(k)},
\cdots,
\frac{1}{\lambda_{l_k}^{(k)}}\bar{\mathbf{v}}_{l_k}^{(k)},
\frac{1}{\sqrt{N_r\sigma_n^2}}\bar{\mathbf{v}}_{l_k+1}^{(k)},
\cdots,
\frac{1}{\sqrt{N_r\sigma_n^2}}\bar{\mathbf{v}}_{N_t}^{(k)}
\right],
\tag{3-51}
$$

where $\lambda_q^{(k)} = \left(\sqrt{E_{tr}\bar{\psi}_q^{(k)}} + N_r\sigma_n^2\right)^{-1}$.

Using a BD precoder in (3-8) we obtain

$$
\begin{aligned}
\mathbf{y}_k =& a_c s_c \mathbf{H}_k \mathbf{p}_c + \hat{\mathbf{H}}_k \hat{\mathbf{V}}_{(1),k}\text{diag}\,(\mathbf{a}_k)\,\mathbf{s}_k + \tilde{\mathbf{H}}_k \hat{\mathbf{V}}_{(1),k}\text{diag}\,(\mathbf{a}_k)\,\mathbf{s}_k \\
&+ \sum_{\substack{j=1 \\ j\neq k}}^{K} \tilde{\mathbf{H}}^{(k,j)}\hat{\mathbf{V}}_{(1),j}\text{diag}\,(\mathbf{a}_j)\,\mathbf{s}_j + \mathbf{n}_k \\
=& a_c s_c \mathbf{H}_k \mathbf{p}_c + \left(\hat{\mathbf{U}}_k \hat{\boldsymbol{\Psi}}_k + \tilde{\mathbf{H}}_k \hat{\mathbf{V}}_{(1),k}\right)\text{diag}\,(\mathbf{a}_k)\,\mathbf{s}_k \\
&+ \sum_{\substack{j=1 \\ j\neq k}}^{K} \tilde{\mathbf{H}}^{(k,j)}\hat{\mathbf{V}}_{(1),j}\text{diag}\,(\mathbf{a}_j)\,\mathbf{s}_j + \mathbf{n}_k.
\end{aligned}
\tag{3-52}
$$

On the other hand, the RBD precoder in (3-8) lead us to

$$
\begin{aligned}
\mathbf{y}_k =& a_c s_c \mathbf{H}_k \mathbf{p}_c + \hat{\mathbf{H}}_k \hat{\mathbf{V}}_k\text{diag}\,(\mathbf{a}_k)\,\mathbf{s}_k + \tilde{\mathbf{H}}_k \hat{\mathbf{V}}_k\text{diag}\,(\mathbf{a}_k)\,\mathbf{s}_k \\
&+ \sum_{\substack{j=1 \\ j\neq k}}^{K} \mathbf{H}^{(k,j)}\hat{\mathbf{V}}_j\text{diag}\,(\mathbf{a}_j)\,\mathbf{s}_j + \mathbf{n}_k \\
=& a_c s_c \mathbf{H}_k \mathbf{p}_c + \left(\hat{\mathbf{U}}_k \hat{\boldsymbol{\Psi}}_k + \tilde{\mathbf{H}}_k \hat{\mathbf{V}}_k\right)\text{diag}\,(\mathbf{a}_k)\,\mathbf{s}_k + \sum_{\substack{j=1 \\ j\neq k}}^{K} \mathbf{H}^{(k,j)}\hat{\mathbf{V}}_j\text{diag}\,(\mathbf{a}_j)\,\mathbf{s}_j + \mathbf{n}_k,
\end{aligned}
\tag{3-53}
$$

with $\underline{\ddot{\mathbf{H}}}^{(k,j)} = \mathbf{H}_k \mathbf{P}_{a,j}^{(\mathrm{RBD})}$.

Let us introduce the matrices $\tilde{\ddot{\mathbf{\Upsilon}}}^{(k,j)} = \tilde{\ddot{\mathbf{H}}}^{(k,j)} \mathbf{V}_{(1),j}$, $\ddot{\mathbf{\Upsilon}}^{(k,j)} = \underline{\ddot{\mathbf{H}}}^{(k,j)} \underline{\mathbf{V}}_j$, and $\tilde{\mathbf{\Upsilon}}^{(k,j)} = \tilde{\mathbf{H}}^{(k,j)} \mathbf{V}_j$ to simplify the notation. Then, (3-52) can be rewritten as follows:

$$\mathbf{y}_k = a_c s_c \mathbf{H}_k \mathbf{p}_c + \left(\mathbf{U}_k \mathbf{\Psi}_k + \tilde{\ddot{\mathbf{\Upsilon}}}^{(k,k)} \right) \mathrm{diag}\left(\mathbf{a}_k\right) \mathbf{s}_k + \sum_{\substack{j=1 \\ j \neq k}}^{K} \tilde{\ddot{\mathbf{\Upsilon}}}^{(k,j)} \mathrm{diag}\left(\mathbf{a}_j\right) \mathbf{s}_j + \mathbf{n}_k.$$

$$(3\text{-}54)$$

Equation (3-53) turns into

$$\mathbf{y}_k = a_c s_c \mathbf{H}_k \mathbf{p}_c + \left(\underline{\mathbf{U}}_k \underline{\mathbf{\Psi}}_k + \tilde{\mathbf{\Upsilon}}^{(k,k)} \right) \mathrm{diag}\left(\mathbf{a}_k\right) \mathbf{s}_k + \sum_{\substack{j=1 \\ j \neq k}}^{K} \mathbf{\Upsilon}^{(k,j)} \mathrm{diag}\left(\mathbf{a}_j\right) \mathbf{s}_j + \mathbf{n}_k$$

$$(3\text{-}55)$$

We obtain the received signal at the ith antenna for the BD and RBD precoders from (3-54) and (3-55), which are given by

$$y_{i_{(\mathrm{RBD})}}^{(k)} = a_c s_c \mathbf{h}_{i,*}^{(k)} \mathbf{p}_c + \sum_{j=1}^{M_k} a_j^{(k)} s_j^{(k)} \left(\hat{\ddot{\psi}}_j^{(k)} \hat{\ddot{u}}_{i,j}^{(k)} + \tilde{\ddot{v}}_{i,j}^{(k,k)} \right) + \sum_{\substack{q=1 \\ q \neq k}}^{K} \sum_{l}^{M_l} \ddot{v}_{q,l}^{(k,q)} a_l^{(q)} s_l^{(q)} + n_q^{(k)}$$

$$(3\text{-}56)$$

$$y_{i_{(\mathrm{BD})}}^{(k)} = a_c s_c \mathbf{h}_{i,*}^{(k)} \mathbf{p}_c + \sum_{j=1}^{M_k} a_j^{(k)} s_j^{(k)} \left(\hat{\psi}_j^{(k)} \hat{u}_{i,j}^{(k)} + \tilde{v}_{i,j}^{(k,k)} \right) + \sum_{\substack{q=1 \\ q \neq k}}^{K} \sum_{l}^{M_l} \tilde{v}_{q,l}^{(k,q)} a_l^{(q)} s_l^{(q)} + n_q^{(k)}$$

$$(3\text{-}57)$$

Squaring the absolute value of (3-56), (3-57) and taking the expected value we get

$$\mathbb{E}\left[|y_{i_{(\mathrm{RBD})}}^{(k)}|^2 \right] = a_c^2 |\mathbf{h}_{i,*}^{(k)} \mathbf{p}_c|^2 + \sum_{j=1}^{M_k} a_j^{(k)^2} |\hat{\ddot{\psi}}_j^{(k)} \hat{\ddot{u}}_{i,j}^{(k)} + \tilde{\ddot{v}}_{i,j}^{(k,k)}|^2 + \sum_{\substack{q=1 \\ q \neq k}}^{K} \sum_{l}^{M_l} a_l^{(q)^2} |\ddot{v}_{q,l}^{(k,q)}|^2 + \sigma_n^2.$$

$$(3\text{-}58)$$

$$\mathbb{E}\left[|y_{i_{(\mathrm{BD})}}^{(k)}|^2 \right] = a_c^2 |\mathbf{h}_{i,*}^{(k)} \mathbf{p}_c|^2 + \sum_{j=1}^{M_k} a_j^{(k)^2} |\hat{\psi}_j^{(k)} \hat{u}_{i,j}^{(k)} + \tilde{v}_{i,j}^{(k,k)}|^2 + \sum_{\substack{q=1 \\ q \neq k}}^{K} \sum_{l}^{M_l} a_l^{(q)^2} |\tilde{v}_{q,l}^{(k,q)}|^2 + \sigma_n^2.$$

$$(3\text{-}59)$$

Thus, the rate at the ith antenna is

$$R_{c,k,i}^{(\mathrm{RBD})} = \log_2\left(1 + \frac{a_c^2|\mathbf{h}_{i,*}^{(k)}\mathbf{p}_c|^2}{\sum_{j=1}^{M_k}a_j^{(k)^2}|\hat{\psi}_j^{(k)}\hat{u}_{i,j}^{(k)} + \tilde{v}_{i,j}^{(k,k)}|^2 + \sum_{\substack{q=1\\q\neq k}}^{K}\sum_l^{M_l}a_l^{(q)^2}|v_{q,l}^{(k,q)}|^2 + \sigma_n^2}\right), .$$
$$(3\text{-}60)$$

$$R_{c,k,i}^{(\mathrm{BD})} = \log_2\left(1 + \frac{a_c^2|\mathbf{h}_{i,*}^{(k)}\mathbf{p}_c|^2}{\sum_{j=1}^{M_k}a_j^{(k)^2}|\hat{\psi}_j^{(k)}\hat{u}_{i,j}^{(k)} + \tilde{v}_{i,j}^{(k,k)}|^2 + \sum_{\substack{q=1\\q\neq k}}^{K}\sum_l^{M_l}a_l^{(q)^2}|\tilde{v}_{q,l}^{(k,q)}|^2 + \sigma_n^2}\right)$$
$$(3\text{-}61)$$

Then we compute the average common rate $\bar{R}_{c,k,i} = \mathbb{E}_{\mathbf{H}|\hat{\mathbf{H}}}\left[R_{c,k,i}|\hat{\mathbf{H}}\right]$ and select the antenna leading to the best performance. Finally, the common rate and the total sum-rate performance can be found using (3-28) and (3-21) respectively.

Let us now consider the MRC criterion for the kth user and evaluate the vector $\mathbf{t}_{k,j}$ with $j \in \mathcal{M}_k$. In this case, the squared norm of vector $\mathbf{t}_{k,j}$ is reduced to:

$$\|\mathbf{t}_{k,j}^{(\mathrm{RBD})}\|^2 = \|\psi_j^{(k)}\mathbf{u}_j^{(k)} + \tilde{\mathbf{H}}_k\mathbf{v}_j^{(k)}\|^2. \qquad (3\text{-}62)$$

$$\|\mathbf{t}_{k,j}^{(\mathrm{BD})}\|^2 = \|\psi_j^{(k)}\mathbf{u}_j^{(k)} + \tilde{\mathbf{H}}_k\mathbf{v}_{(1),j}^{(k)}\|^2. \qquad (3\text{-}63)$$

Under perfect CSIT assumption, (3-63) is reduced to $\|\mathbf{t}_{k,j}\|^2 = |\psi_j^{(k)}|^2$. When $j \in \mathcal{M}_q$, with $q \neq k$ the squared norm of $\mathbf{t}_{k,j}$ is given by

$$\|\mathbf{t}_{k,j}^{(\mathrm{RBD})}\|^2 = E_{tr}\sum_{i=1}^{N_k}\left(\left|\sum_{l=1}^{N_t}\sum_{n=1}^{N_t}h_{i,l}^{(k)}\lambda_n^{(q)}\bar{v}_{l,n}^{(q)}v_{n,j}^{(q)}\right|^2\right), \qquad (3\text{-}64)$$

$$\|\mathbf{t}_{k,j}^{(\mathrm{BD})}\|^2 = \sum_{i=1}^{N_k}\left(\left|\sum_{l=1}^{N_t}\sum_{n=1}^{N_t}\tilde{h}_{i,l}^{(k)}\bar{v}_{l,n}^{(q)(0)}v_{n,j}^{(q)(1)}\right|^2\right), \qquad (3\text{-}65)$$

Substituting (3-63) and (3-65) in (4-98) we get the SINR of the MRC criterion, which can be used in (3-20) and (3-21) to obtain the achievable sum-rate.

Finally, we consider MMSEc and define $\mathbf{D}_k = \mathbf{U}_k\mathbf{\Psi}_k + \tilde{\mathbf{\Upsilon}}^{(k,k)}$. In this case we have

$$\sum_{i\in\mathcal{M}_k}a_i^2|\mathbf{w}_k^H\mathbf{t}_{k,i}|^2 = \mathrm{tr}\left(\mathbf{t}_{k,c}^H\mathbf{R}_{\mathbf{y}_k\mathbf{y}_k}^{-1}\mathbf{D}_k\mathbf{A}_k^2\mathbf{D}_k^H\mathbf{R}_{\mathbf{y}_k\mathbf{y}_k}^{-1}\mathbf{r}_{k,c}\right)$$

$$= \sum_{i=1}^{M_k}a_i^{(k)^2}\left|\mathbf{p}_c\hat{\mathbf{H}}_k^H\mathbf{R}_{\mathbf{y}_k\mathbf{y}_k}^{-1}\left(\hat{\psi}_i^{(k)}\mathbf{u}_i^{(k)} + \tilde{v}_i^{(k,k)}\right)\right|^2, \qquad (3\text{-}66)$$

and

$$\sum_{\substack{j=1 \\ j \notin \mathcal{M}_k}}^{M} a_j^2 |\mathbf{w}_k^H \mathbf{t}_{k,j}|^2 = \sum_{\substack{j=1 \\ j \neq k}}^{K} \mathrm{tr} \left(\mathbf{t}_{k,c}^H \mathbf{R}_{\mathbf{y}_k \mathbf{y}_k}^{-1} \tilde{\boldsymbol{\Upsilon}}^{(k,j)} \mathbf{A}_k^2 \tilde{\boldsymbol{\Upsilon}}^{(k,j)^H} \mathbf{R}_{\mathbf{y}_k \mathbf{y}_k}^{-1} \mathbf{t}_{k,c} \right)$$

$$= \sum_{i=1}^{M_k} a_i^{(k)^2} \left| \mathbf{p}_c \hat{\mathbf{H}}_k^H \mathbf{R}_{\mathbf{y}_k \mathbf{y}_k}^{-1} \boldsymbol{\upsilon}_j^{(k,j)} \right|^2, \tag{3-67}$$

Substituting (3-66) and (3-67) in (3-26) we obtain the SINR, which can be used in (3-20) and (3-21) to obtain the total sum-rate performance.

3.4
Simulations

In this section several simulations in a RS-based MIMO system were carried out to assess the performance of the proposed combiners along with different linear precoders. As reported in the literature [5, 36] the MMSE and RBD precoders outperform their ZF and BD counterparts by allowing small MUI to significantly reduce the power penalty associated with linear precoding. On the other hand, the BD and RBD precoders outperform the ZF and MMSE precoders, respectively, since they take advantage of the multiple antennas at the receivers. We set $\mathbf{G}_k = \mathbf{I}$ for the MMSE precoder, whereas the RBD precoder uses the receiver defined in (2-24) since we focus on evaluating the common combiners. We consider $N_t = 12$ and $K = 6$ for all simulations. Each user is equipped with 2 receive antennas. The inputs are Gaussian distributed with zero mean and unit variance. Each coefficient of $\tilde{\mathbf{H}}$ follows a Gaussian distribution, i.e., $\sim \mathcal{CN}(0, \sigma_{e_i}^2)$ and $\mathbb{E}\left[\mathbf{h}_{i,*} \mathbf{h}_{i,*}^H\right] = \sigma_e^2$. We consider additive white Gaussian noise and define SNR $\triangleq E_{tr}/\sigma_n^2$ with $\sigma_n^2 = 1$. The ESR was computed averaging 1000 independent channel realizations. For each channel realization we obtained $\bar{R}_c$ and $\bar{R}_p$ employing 100 error matrices. Note that $\bar{R}_p = \mathbb{E}_{\mathbf{H}|\hat{\mathbf{H}}}\left[\sum_{k=1}^{K} R_k | \hat{\mathbf{H}}\right]$, where R_k can be found by employing (2-70). We use SVD over the channel ($\mathbf{H} = \mathbf{U}\boldsymbol{\Psi}\mathbf{V}$) and then set $\mathbf{p}_c = \mathbf{v}_1$.[3]

In the first example, we fixed the variance of the channel error to $\sigma_e^2 = 0.1$. Fig. 3.3 shows the sum-rate performance obtained by the proposed combiners with the ZF and BD precoders, whereas Fig. 3.4 shows the sum-rate performance of the MMSE and RBD precoders. The conventional precoders are denoted by ZF, MMSE, BD and RBD. The terms RS-ZF, RS-BD, RS-MMSE and RS-BD denote the use of the RS scheme without the common

---

[3]Note that the optimization of the common precoder would further increase the sum-rate performance. However, finding the optimum is a non convex problem that does not lend itself easily to practical implementation, in contrast to the closed-form precoding/combining techniques developed in this work.

Figure 3.3: Sum-rate performance of the proposed stream combiners with ZF-type precoders under imperfect CSIT. $N_t = 12$, $K = 6$, $N_k = 2$, and $\sigma_e^2 = 0.1$.

combiner. The proposed combiners exploit the multiple antennas at the receiver, enhancing the common stream, which leads to a better performance as shown in both figures. The BD and RBD precoders allow not only the enhancement of the common stream but also of the private stream obtaining an overall gain in terms of sum-rate. The best performance is achieved by the RS-RBD-MMSEc due to the use and combination of all available signals at the receive antennas. The curves obtained exhibit saturation because of the imperfect CSIT assumption, which originates MUI that scales with the SNR.

Fig. 3.5 and Fig. 3.6 show the performance of the proposed schemes as the estimation error increases. The proposed RS-BD outperforms the conventional RS-ZF strategy, whereas the RS-RBD outperforms the RS-MMSE scheme. For this simulation we set the SNR to 20 dB. The robustness of the system increases across all error variances when a common combiner is employed as shown in Fig. 3.5 and Fig. 3.6. In other words, the imperfect CSIT has a lower impact when a common combiner is employed even when the variance of the error of the channel estimate is high. In contrast, the performance of conventional schemes is heavily degraded. In general, schemes employing an RS approach are more robust to CSIT imperfections than conventional precoding techniques.

Figure 3.4: Sum-rate performance of the proposed stream combiners with MMSE-type precoders under imperfect CSIT. $N_t = 12$, $K = 6$, $N_k = 2$, and $\sigma_e^2 = 0.1$.

The proposed MIMO RS-RBD-MMSEc scheme attains a sum-rate performance up to 11% higher than conventional RBD at $\sigma_e^2 = 0.2$. Moreover, MMSEc achieves the best performance among the combiners for all error variances.

In the next example, we consider a high error in the channel estimate which is reduced as the SNR increases, i.e. $\sigma_e^2 = \xi \left(E_{tr}/\sigma_n^2 \right)^{-\alpha}$ with $\xi = 0.631$ and $\alpha = 0.4$. The parameters ξ and α where chosen so that $\sigma_e^2 = 0.1$ at an SNR of 20 dB. Figs. 3.7 and 3.8 show that the use of combiners results in a higher sum-rate than that of conventional schemes. Note that the curves do not show saturation since the quality in the CSIT estimate improves with the SNR. The schemes employing RS outperform the conventional precoding. Moreover, including a common combiner at the receiver improves even more the performance obtained by all precoders. The RS-BD and RS-RBD obtain a better performance than the RS-ZF and the RS-MMSE, respectively. The proposed MIMO RS-RBD-MMSEc obtains the best performance, which is up to 6% as compared to conventional RBD precoding.

In the last example we include the optimal power allocation across all streams. The coefficients of matrix $\mathbf{A}^{(\mathrm{RS})}$ were found through exhaustive search
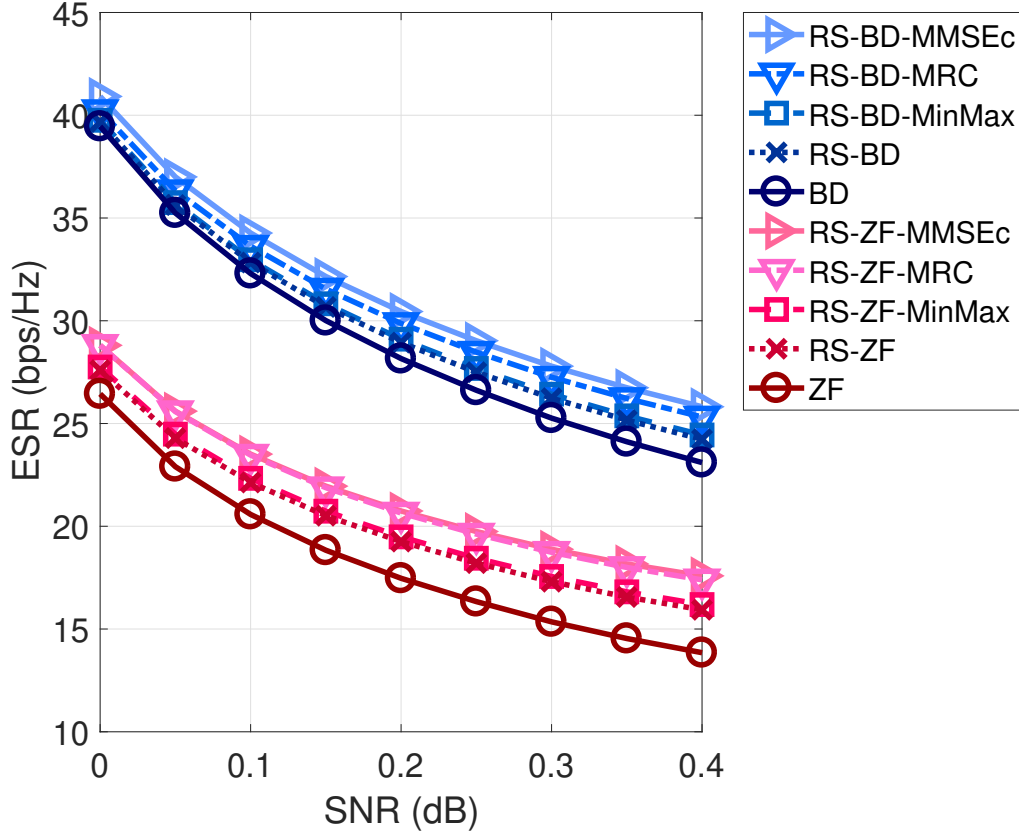
Figure 3.5: Error variance VS Sum-rate performance of the proposed stream combiners at a SNR of 20 dB with ZF-type precoders, $N_t = 12$, $K = 6$, $N_k = 2$.

with a grid step of 0.01 for all simulations in order to maximize the sum-rate. Alternatively, designers can resort to convex optimization techniques to optimize the precoders/power allocation for RS as done in [21, 23, 26]. Fig. 3.9 shows that the power allocation scheme further enhance the performance of the proposed combiners. In this case, the proposed MIMO RS-RBD-MMSEc scheme attains a sum-rate performance up to 11% higher than conventional RBD.

3.5
Summary

In this chapter we have developed a mathematical model for the RS MU-MIMO BC. The structure of the receivers has been proposed along with three common stream combiners techniques. The proposed stream combiners exploit the channel propagation and the multiple antennas at the receiver to further enhance the performance of the common rate as shown by the simulations. The RBD-RS-MMSEc shows the best performance among the proposed strategies. Finally, simulations have shown that the proposed stream combiners increase
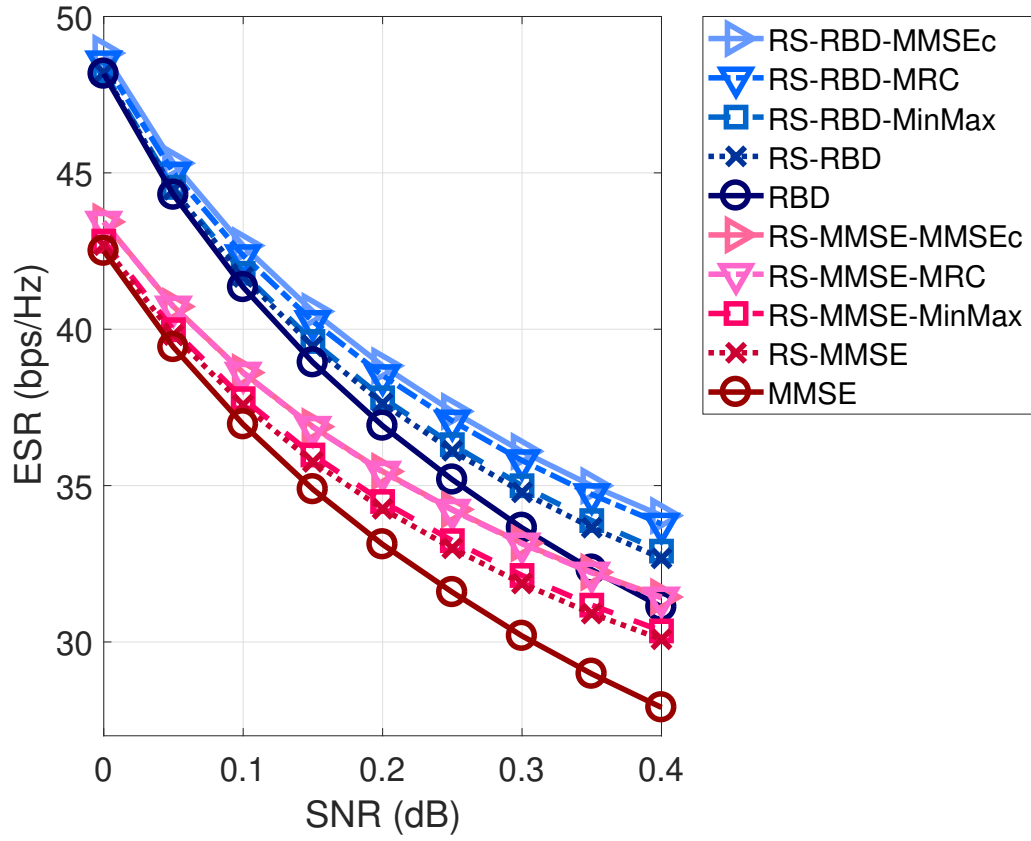
Figure 3.6: Error variance VS Sum-rate performance of the proposed stream combiners at a SNR of 20 with MMSE-type precoders, $N_t = 12$, $K = 6$, $N_k = 2$.
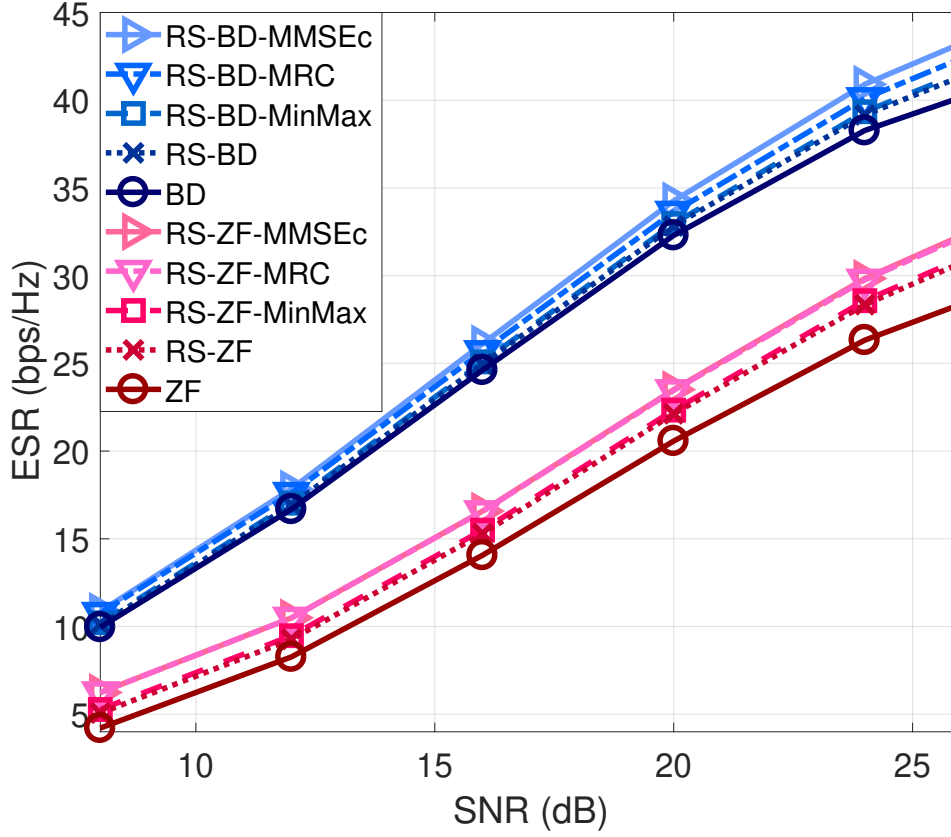
the robustness of the system under imperfect CSIT.
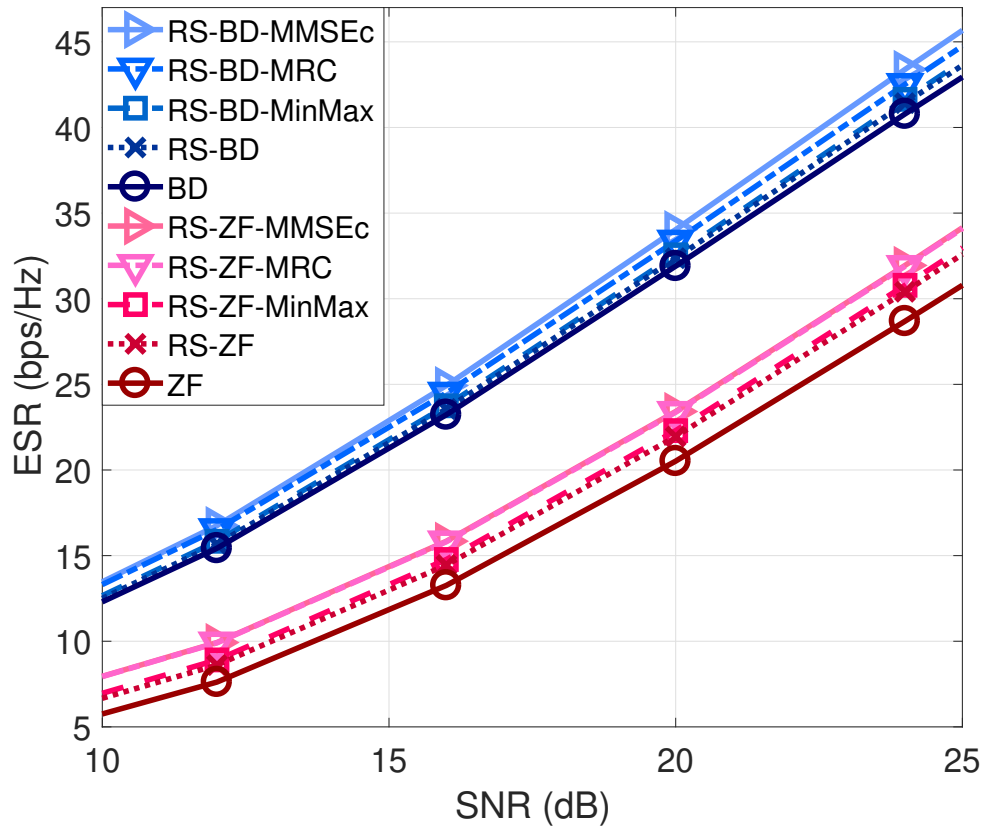
Figure 3.7: Sum-rate performance of the proposed stream combiners with ZF-type precoders under imperfect CSIT, $N_t = 12$, $K = 6$, $N_k = 2$ and $\sigma_e^2 = 0.631 E_{tr}^{-0.4}$.
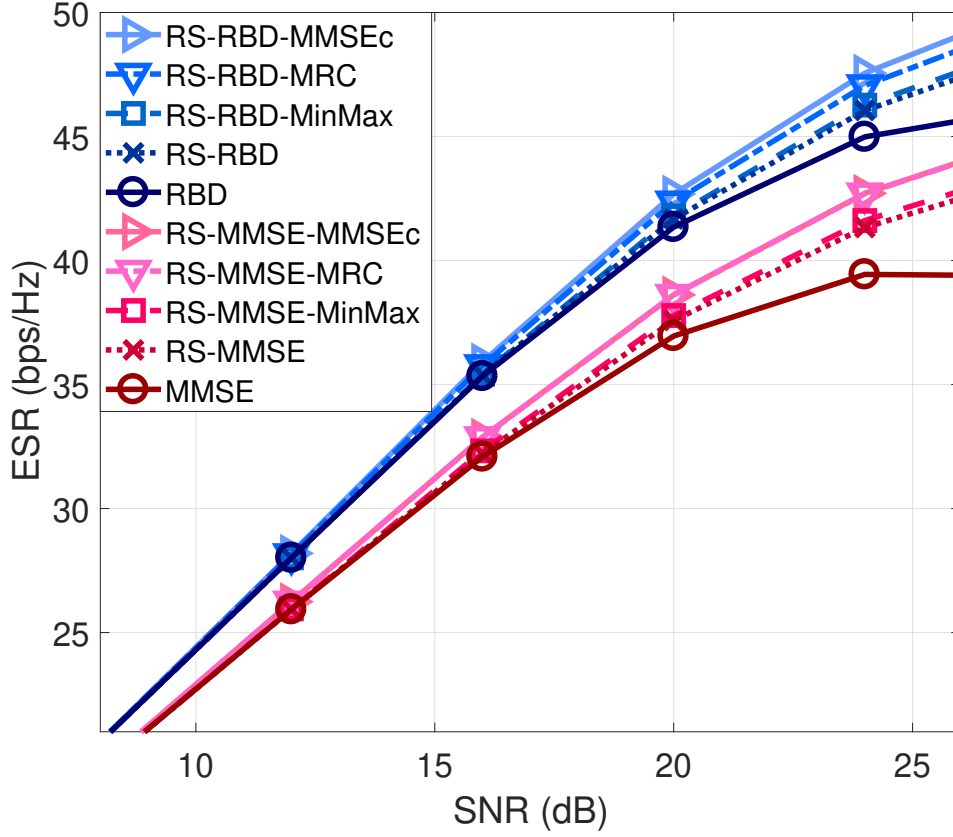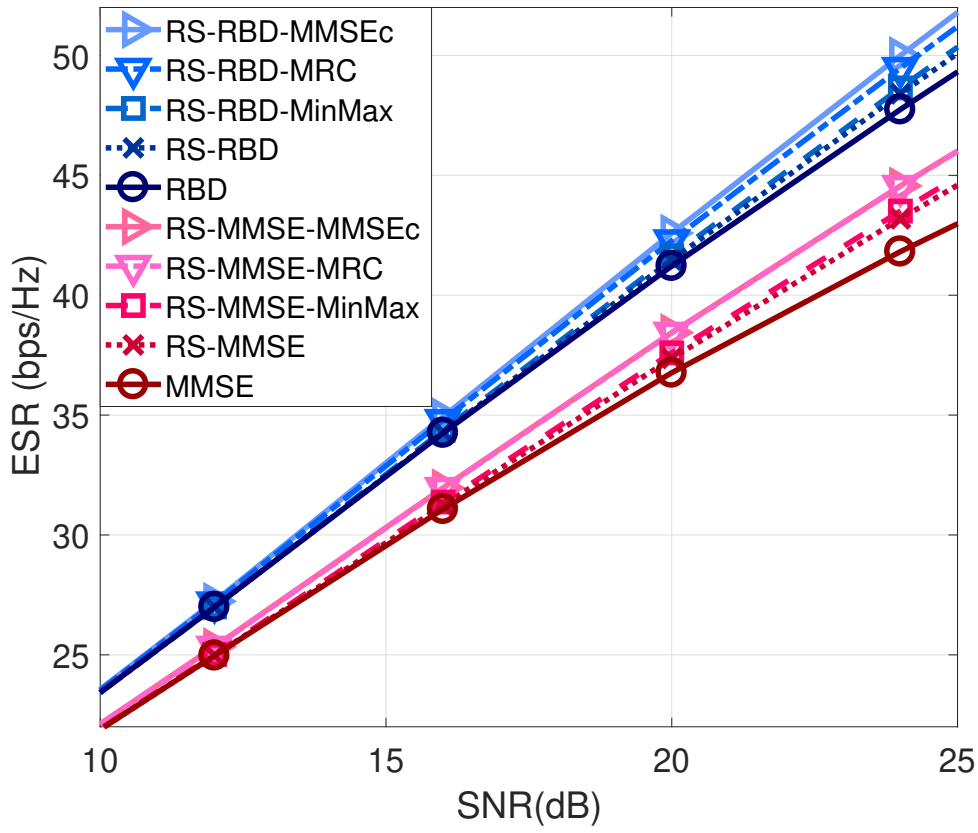
Figure 3.8: Sum-rate performance of the proposed stream combiners with MMSE-type precoders under imperfect CSIT, $N_t = 12$, $K = 6$, $N_k = 2$ and $\sigma_e^2 = 0.631 E_{tr}^{-0.4}$.
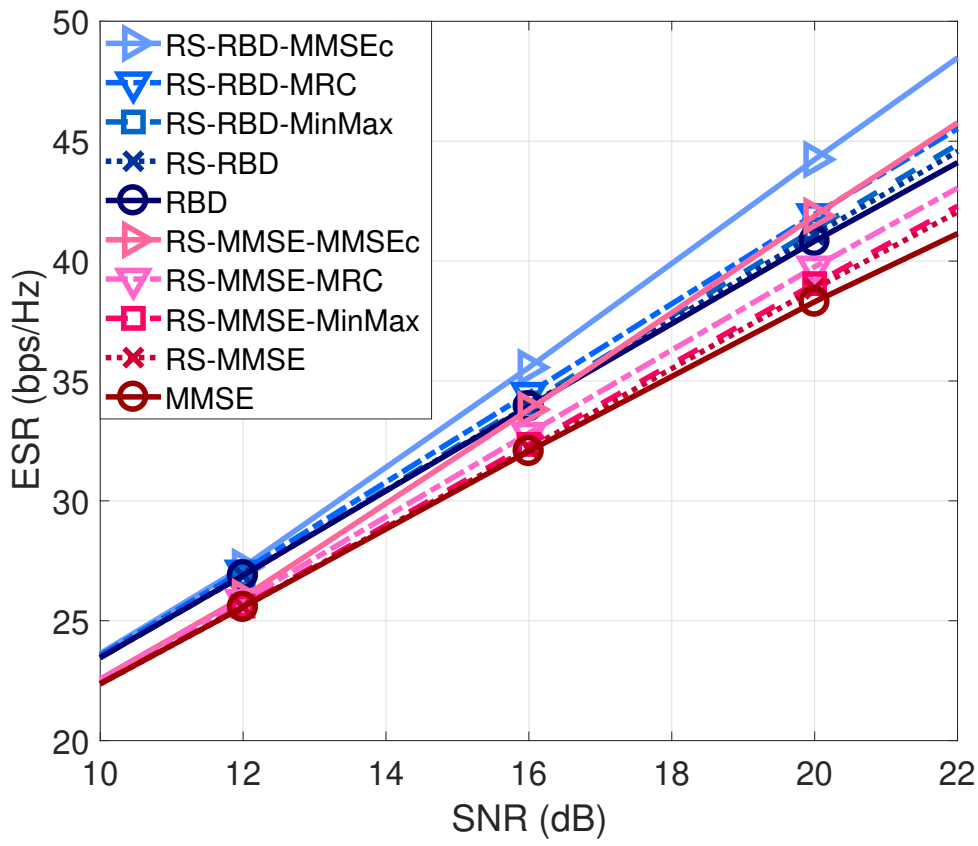
Figure 3.9: Sum-rate performance with optimal power allocation under imperfect CSIT, $N_t = 12$, $K = 6$, $N_k = 2$ and $\sigma_e^2 = 0.0631 E_{tr}^{-0.4}$.

4
Nonlinear Precoding for RS MU-MIMO Systems

In this chapter, we present and analyze RS schemes with non-linear precoders based on Tomlinson-Harashima Precoding (THP). Specifically, the broadcast channel of RS-MIMO and RS-MISO systems with non-linear precoders is analyzed under perfect and imperfect CSIT assumption. Two different THP designs are considered, one based on the ZF precoder and the other on the MMSE precoder. Furthermore, two THP schemes along with the RS technique are devised, namely the RS centralized THP (RS-cTHP) and the RS decentralized THP (RS-dTHP). Expressions to describe the SINR ratio and the sum rates associated with these schemes are developed. Simulations show that RS with THP outperforms existing standard THP and RS with linear precoding techniques.

Furthermore, we consider common stream combiners with the proposed RS-cTHP and RS-dTHP schemes to further enhance the common rate. In particular, we devise common stream combiners based on the same criteria adopted for the combiners proposed for linear precoders in the previous chapter. Moreover, based on the fact that the symbol ordering directly affects the performance of systems employing THP, a multibranch technique (MB) is proposed for the RS-THP schemes. The MB technique creates several transmit patterns and selects the one that achieves the highest performance. The computational complexity and the SINR of these techniques is analyzed. Simulations show that the common stream combiners and the MB techniques greatly increase the overall performance of the proposed RS-THP MIMO systems.

This chapter is structured as follows. In Section 4.1 the system model is presented. The RS-THP precoding strategies are detailed in Section 4.2. The sum-rate analysis is presented in Section 4.3. In Section 4.4 the RS-MB-THP, which enhances the sum-rate performance by creating several transmit patterns, is presented. In Section 4.5 the common combiners are incorporated into the RS-THP structure to further improve the common rate when the UE is equipped with multiple antennas. The complexity and the sum-rate performance are analyzed in Section 4.6. Simulations results are depicted in Section 4.7. Finally, Section 4.8 gives the conclusions of this chapter.

4.1
System Model

Let us consider the downlink of a MU-MIMO system where the BS, which is equipped with N_t antennas, transmits M messages to K users. Each User Equipment (UE) may have multiple antennas, where N_k denotes the number of receive antennas at the kth user and $N_r = \sum_{k=1}^{K} N_k$ denotes the total number of receive antennas. It follows that $M \leq N_r$. Moreover, the number of transmit antennas N_t is larger than N_r.

As illustrated on the left hand side of Fig. 4.1, the system employs an RS scheme that for simplicity splits the message of a single user, namely the kth user. The message $m^{(\mathrm{RS})}$ intended for the kth user is therefore split into a common message m_c and a private message m_k. At this point it is important to highlight that selecting a different user to split its message does not affect the overall performance of the system since the system performance is bounded by the worst user. The messages m_i of the other users, with $i \neq k$, are not split into common and private parts[1]. After the splitting process, the messages are encoded, modulated and gathered into a vector of symbols $\mathbf{s} \in \mathbb{C}^{N_r+1}$ where the common stream is superimposed to the private streams, i.e., $\mathbf{s} = \left[s_c, \mathbf{s}_p^{\mathrm{T}}\right]^{\mathrm{T}}$. Remark that the system employs SIC at the receiver, which allows the decoding of the common symbol s_c. The vector $\mathbf{s}_p \in \mathbb{C}^{N_r}$ contains the private streams of all users and is given by $\mathbf{s}_p = \left[\mathbf{s}_1^{\mathrm{T}}, \cdots, \mathbf{s}_K^{\mathrm{T}}\right]^{\mathrm{T}}$, where the vector $\mathbf{s}_k \in \mathbb{C}^{N_k}$ contains the N_k private streams intended for the kth user. The set $\mathcal{M}_k$ contains the private streams intended for the kth user. It follows that $\mathrm{card}\left(\mathcal{M}_k\right) = N_k$.

The precoder $\mathbf{P} = \left[\mathbf{p}_c, \mathbf{P}_1, \cdots, \mathbf{P}_K\right] \in \mathbb{C}^{N_t \times (N_r+1)}$ maps the symbols to the transmit antennas. Specifically, the common precoder $\mathbf{p}_c \in \mathbb{C}^{N_t}$ maps the common symbol to the transmit antennas. In contrast, the private precoder $\mathbf{P}_k \in \mathbb{C}^{N_t \times N_k}$ maps the N_k private symbols intended for the kth user to the transmit antennas. This model employs non-linear precoders which modify the data vector $\mathbf{s}$ through non-linear processing before mapping the data streams to the transmit antennas, originating the random vector $\breve{\mathbf{s}}^{(\mathrm{RS})} = \left[s_c, \breve{\mathbf{s}}_p^{\mathrm{T}}\right]^{\mathrm{T}} \in \mathbb{C}^{M+1}$. The vector $\breve{\mathbf{s}}_p = \left[\breve{\mathbf{s}}_1^{\mathrm{T}}, \cdots, \breve{\mathbf{s}}_K^{\mathrm{T}}\right]^{\mathrm{T}} \in \mathbb{C}^{N_r}$ represents the private data after the non-linear processing, where $\breve{\mathbf{s}}_k$ contains the private symbols intended for user k. A modulo operation is applied on the private symbols, which leads to

---

[1]In a general RS scheme the messages of multiple users may be split. Assuming that the common message is entirely composed by the message of a single user constitutes an special case that achieves a common rate given by R_{c_o}. The proposed schemes, however, aim at maximizing the total ergodic sum-rate (ESR). For this purpose, splitting the message of a single user is sufficient as mentioned in [24], since we can also achieve the common rate R_{c_o} obtained when splitting the message of a single user by splitting properly the messages of several users.

$\mathbb{E}\left[\|\mathbf{s}^{(\mathrm{RS})}\|^2\right] \approx \mathbb{E}\left[\|\breve{\mathbf{s}}^{(\mathrm{RS})}\|^2\right]$ in order to diminish the effects of the power loss. In this case, the transmit vector is then given by

$$\mathbf{x}^{(\mathrm{RS})} = \mathbf{P}\breve{\mathbf{s}}^{(\mathrm{RS})}, \tag{4-1}$$

where the vector $\mathbf{x}^{(\mathrm{RS})} \in \mathbb{C}^{N_t}$. The system satisfies a transmit power constraint given by $\mathbb{E}\left[\|\mathbf{x}^{(\mathrm{RS})}\|^2\right] \leq E_{tr}$, where E_{tr} represents the available power.

The transmit signal reaches the UE's through the flat fading channel given by $\mathbf{H} = \left[\mathbf{H}_1^{\mathrm{T}}, \cdots, \mathbf{H}_K^{\mathrm{T}}\right]^{\mathrm{T}} \in \mathbb{C}^{N_r \times N_t}$. The matrix $\mathbf{H}_k \in \mathbb{C}^{N_k \times N_t}$ represents the channel between the BS and the kth user. Then, the received signal of the RS-THP in a given channel use is given by

$$\mathbf{y} = \mathbf{H}\mathbf{P}\breve{\mathbf{s}}^{(\mathrm{RS})} + \mathbf{n}, \tag{4-2}$$

where $\mathbf{n} \in \mathbb{C}^{N_k}$ represents the additive noise, which follows a circularly symmetric complex Gaussian distribution, i.e., $\mathbf{n} \sim \mathcal{CN}\left(\mathbf{0}, \sigma_n^2 \mathbf{I}\right)$. The signal obtained at the kth user is given by

$$\mathbf{y}_k = s_c \mathbf{H}_k \mathbf{p}_c + \sum_{i \in \mathcal{M}_k} \breve{s}_i \mathbf{H}_k \mathbf{p}_i + \sum_{j \notin \mathcal{M}_k} \breve{s}_j \mathbf{H}_k \mathbf{p}_j + \mathbf{n}_k. \tag{4-3}$$

From (4-3) we can compute the power at the ith receive antenna of the kth UE, which is expressed by

$$\mathbb{E}\left[|\mathbf{y}_i^{(k)}|^2\right] = |\mathbf{h}_{i,*}^{(k)}\mathbf{p}_c|^2 + \sum_{j=1}^{M}|\mathbf{h}_{i,*}^{(k)}\mathbf{p}_j|^2 + \sigma_n^2, \tag{4-4}$$

where we consider symbols with unitary variance. Remark that the scalar $\mathbf{y}_i^{(k)}$ stands for the ith element of the vector $\mathbf{y}_k$ and $\mathbf{h}_{i,*}^{(k)}$ denotes the ith row of the matrix $\mathbf{H}_k$.

Considering a MISO system we have $N_i = 1, \forall\, i \in \{1, \cdots, K\}$. Then the received signal in (4-3) at the kth user is reduced to

$$y_k = s_c \mathbf{h}_{k,*}\mathbf{p}_c + \breve{s}_k \mathbf{h}_{k,*}\mathbf{p}_k + \sum_{j \neq k}^{K} \breve{s}_j \mathbf{h}_{k,*}\mathbf{p}_j + n_k. \tag{4-5}$$

Hence, the power of the received signal at the kth user in a MISO system is described by

$$\mathbb{E}\left[|y_k|^2\right] = |\mathbf{h}_{k,*}\mathbf{p}_c|^2 + \sum_{j=1}^{K}|\mathbf{h}_{k,*}\mathbf{p}_j|^2 + \sigma_n^2. \tag{4-6}$$

4.1.1
Imperfect CSIT model

In general, the BS has only access to imperfect CSI. The imperfect CSIT is modeled through the error channel matrix $\tilde{\mathbf{H}} = \left[\tilde{\mathbf{H}}_1^{\mathrm{T}}, \cdots, \tilde{\mathbf{H}}_K^{\mathrm{T}}\right]^{\mathrm{T}} \in \mathbb{C}^{N_r \times N_t}$,

which is introduced by the estimation procedure. It follows that $\mathbf{H} = \hat{\mathbf{H}} + \tilde{\mathbf{H}}$, where the channel estimate is given by $\hat{\mathbf{H}}$.

The model presented considers that the CSIT error may scale with the SNR as $O\left(E_{tr}^{-\alpha}\right)$, i.e. $\sigma_{e,i}^2 = O\left(E_{tr}^{-\alpha}\right)$, where α is the scaling factor that quantifies the CSIT quality as the SNR increases [10]. We approach perfect CSIT as $\alpha \to +\infty$, which results in $\sigma_{e,1}^2, \sigma_{e,2}^2, \cdots, \sigma_{e,N_r}^2 \to 0$. On the other hand, $\alpha = 0$ leads to a fixed CSIT quality across all values of SNR. Other finite values of α imply that the quality of CSIT improves with the SNR. The value $\alpha = 1$ is equivalent to perfect CSIT in the degrees-of-freedom (DoF) sense [8, 10]. Therefore, we employ $\alpha \in [0, 1]$.

4.1.2
Sum-Rate Performance

At the receiver, SIC is performed to subtract the common symbol from the received signal that contains the private and common streams.[2] This means that the instantaneous sum-rate of an RS MIMO system consists of two parts, the instantaneous common rate R_c, which is related to the common stream, and the instantaneous sum private rate, which is related to the private streams and is given by $R_p = \sum_{k=1}^{K} R_k$, where R_k denotes the private rate of the kth user. Remark that R_k is also the sum of multiple rates, since multiple streams are transmitted to the kth user. Assuming Gaussian signalling we have that $R_{c,k} = \log_2\left(1 + \gamma_{c,k}\right)$ where $\gamma_{c,k}$ is the SINR obtained by the kth user when decoding the common message. Considering perfect CSIT, where the instantaneous sum-rate is achievable, we can set $R_c = \min_k R_{c,k}$. This ensure that all users decode the common message.

As mentioned in the previous sections the model established considers imperfect CSIT where the error is fixed or decays as $O\left(E_{tr}^{-\alpha}\right)$. Because of the imperfect CSIT residual MUI is originated and the instantaneous rate is not achievable. Therefore, we adopt the ESR as the metric to assess the performance of the system as done in [61]. Once a channel estimate $\hat{\mathbf{H}}$ is obtained, the precoders are updated accordingly, obtaining an average sum-rate (ASR) per channel estimate. The ASR represents the average performance with respect to the channel errors given a channel estimate. The BS computes the ASR using imperfect instantaneous knowledge. Specifically we have that the average common rate is given by $\bar{R}_{c,k} = \mathbb{E}_{\mathbf{H}|\hat{\mathbf{H}}}\left[R_{c,k}|\hat{\mathbf{H}}\right]$. Equivalently we have that the average sum private rate is equal to $\bar{R}_p = \mathbb{E}_{\mathbf{H}|\hat{\mathbf{H}}}\left[R_p|\hat{\mathbf{H}}\right]$. The ergodic common rate at the kth user is given by $\mathbb{E}_{\hat{\mathbf{H}}}\left[\bar{R}_{c,k}\right]$. On the other hand,

---

[2]It is important to note that the SIC implemented at the receiver allows the simultaneous transmission of $M + 1$ symbols .
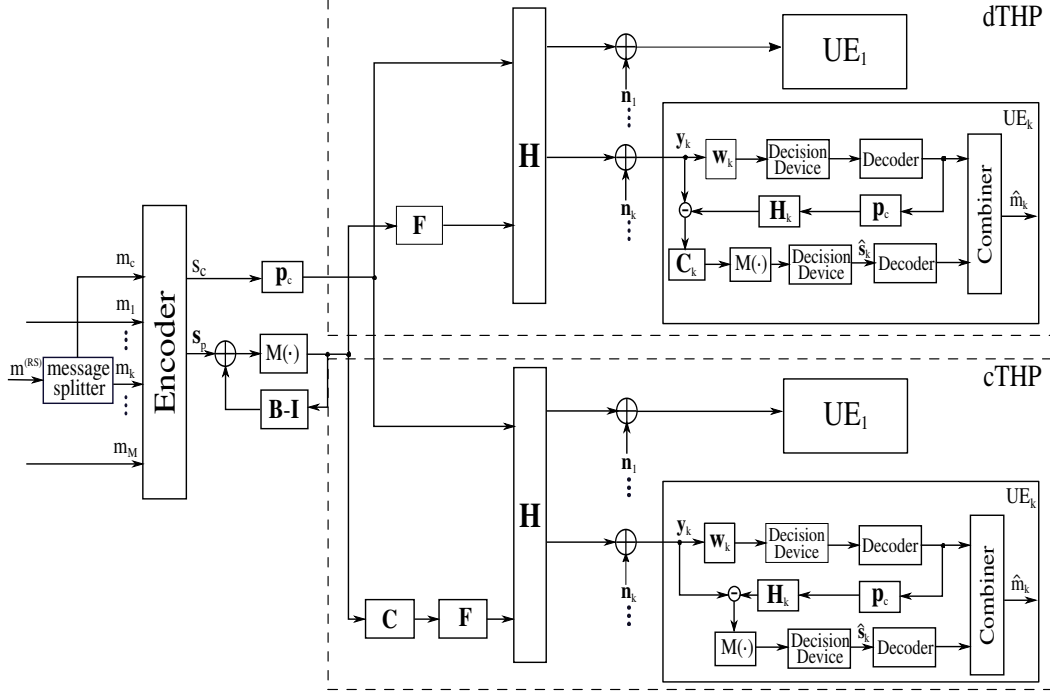
Figure 4.1: Proposed RS-THP structures

the ergodic sum private rate is equal to $\mathbb{E}_{\hat{\mathbf{H}}}\left[\bar{R}_p\right]$. Finally, the ESR of the system is given by

$$S_r = \min_{k \in [1,K]} \mathbb{E}_{\hat{\mathbf{H}}}\left[\bar{R}_{c,k}\right] + \mathbb{E}_{\hat{\mathbf{H}}}\left[\bar{R}_p\right]. \tag{4-7}$$

Remark that in (4-7) the common rate is limited by the performance of the worst user. Then, from the ESR perspective splitting the message of any user k, with $k \in [1, K]$, does not affect the overall system performance.

4.2
Proposed Rate-Splitting Tomlinson-Harashima Precoding (RS-THP)

In this section, we propose RS-THP structures, motivated by the fact that non-linear precoding techniques outperform their linear counterparts. In the proposed scheme, THP acts as the private precoder of the matrix **P**. We consider two different THP designs, one based on the ZF precoder and the other on the MMSE precoder. Both designs have been reported in literature in [62,63] for conventional SDMA. In general, the MMSE-THP design achieves a better performance than the ZF-THP design at the expense of extra computational complexity.

We consider that transmission takes place over a channel whose parameters remain fixed during a data packet. The SNR is defined as $\text{SNR} \triangleq E_{tr}/\sigma_n^2$, where E_{tr} denotes the total transmitted power. We also consider that σ_n^2 remains fixed, is available to the receiver and has a non-zero value in order to avoid indetermination. This means that a modification of the SNR depends

only on the parameter E_{tr}.

4.2.1
Power Allocation

The proposed RS-THP schemes transmit a common stream and multiple private streams. Therefore, the available power must be allocated to both the private streams and the common stream. The power allocated to the common stream is given by $\|\mathbf{p}_c\| = \delta\sqrt{E_{tr}}$, where delta denotes the percentage of E_{tr} that is designated to s_c and is chosen to maximize the performance of a specific metric. It follows that the power available for the private streams is given by $E_{tr} - \|\mathbf{p_c}\|^2$ and, for simplicity, is uniformly allocated across streams. In this work, we select δ that maximizes the ESR of the system which can be mathematically expressed by

$$
\begin{aligned}
\delta_o &= \max_{\delta} S_r\left(\delta\right) \\
&= \max_{\delta}\left(\min_{k\in[1,K]}\mathbb{E}_{\hat{\mathbf{H}}}\left[\bar{R}_{c,k}\left(\delta\right)\right] + \mathbb{E}_{\hat{\mathbf{H}}}\left[\bar{R}_p\left(\delta\right)\right]\right).
\end{aligned}
\tag{4-8}
$$

We remark that the power constraint must be satisfied. In this sense, the design of the private precoder must fulfill the transmit power restriction, i.e., the power of the private streams should be equal to $E_{tr} - \|\mathbf{p_c}\|^2$.

4.3
Private Precoder Design

Regardless of which design is considered, THP generally implements three filters. The first one is a feedback filter denoted by $\mathbf{B}$, which is a lower triangular matrix. This matrix cancels succesively the interference caused by the previous symbols. The second filter is the feedforward filter $\mathbf{F}$, which partially removes the MUI. The last one is a diagonal scaling matrix given by $\mathbf{C}$ and contains the weighted coefficients assigned to each stream. The position of the scaling matrix defines two different THP structures. The centralized THP (cTHP) implements the matrix $\mathbf{C}$ at the transmitter. In contrast, the decentralized THP (dTHP) places the scaling matrix at the receiver. Fig. 4.1 shows both structures considering an RS-ZF-THP scheme.

Mathematically, the transmitted signal can be expressed as $\mathbf{x}^{(\mathrm{RS})} = \left[\mathbf{p}_c, \mathbf{P}^{(\mathrm{THP})}\right]\left[s_c, \breve{\mathbf{s}}_p^{\mathrm{T}}\right]^{\mathrm{T}}$. Let us first consider an MMSE-THP private precoder.

Then, for the cTHP and dTHP deployments we have

$$\mathbf{P}_p^{(\text{rs-d})} = \beta^{(\text{rs-d})} \mathbf{D} \check{\mathbf{F}}, \tag{4-9}$$

$$\mathbf{P}_p^{(\text{rs-c})} = \beta^{(\text{rs-c})} \mathbf{D} \check{\mathbf{F}} \check{\mathbf{C}}, \tag{4-10}$$

where the power scaling factors $\beta^{(\text{rs-d})}$ and $\beta^{(\text{rs-c})}$ are imposed in order to fulfil the transmit power constraint. We split the message of one user, linearly precode the common stream and use THP from (4-9) and (4-10) to precode the private streams. Then, the transmitted signal is rewritten as

$$\mathbf{x}^{(\text{rs-d})} = \mathbf{p}_c s_c + \sum_{i=1}^{K} \mathbf{P}_i^{(\text{rs-d})} \check{\mathbf{s}}_i, \tag{4-11}$$

$$\mathbf{x}^{(\text{rs-c})} = \mathbf{p}_c s_c + \sum_{i=1}^{K} \mathbf{P}_i^{(\text{rs-c})} \check{\mathbf{s}}_i, \tag{4-12}$$

where $\mathbf{P}_i$ corresponds to the precoder of the ith user and can be found using (4-9) or (4-10), depending on the architecture adopted. Note that no power allocation scheme was employed for the private streams, i.e., $\mathbf{A} = \mathbf{I}$ and the power assigned to the common stream is embedded in $\mathbf{p}_c$.

Since the power constraint must be fulfilled, it follows that

$$\mathbb{E}\left[\|\beta^{(\text{rs-d})} \mathbf{D} \check{\mathbf{F}} \check{\mathbf{s}}_p\|^2\right] = E_{tr} - \|\mathbf{p}_c\|^2, \tag{4-13}$$

$$\mathbb{E}\left[\|\beta^{(\text{rs-c})} \mathbf{D} \check{\mathbf{F}} \check{\mathbf{C}} \check{\mathbf{s}}_p\|^2\right] = E_{tr} - \|\mathbf{p}_c\|^2. \tag{4-14}$$

Let us consider that the power loss is measured by the factor $1/\lambda > 1$, i.e., $\mathbf{R}_{\check{\mathbf{s}}} = E[\check{\mathbf{s}} \check{\mathbf{s}}^H] = \lambda^{-1} \mathbf{I}$ [64]. Then, expanding terms and evaluating the expected value, we obtain

$$\beta^{(\text{rs-d})^2} \lambda^{-1} \text{tr}\left(\mathbf{Q}_1 \mathbf{Q}_1^H\right) = E_{tr} - \|\mathbf{p}_c\|^2, \tag{4-15}$$

$$\beta^{(\text{rs-c})^2} \lambda^{-1} \text{tr}\left(\mathbf{Q}_1 \check{\mathbf{C}} \check{\mathbf{C}}^H \mathbf{Q}_1^H\right) = E_{tr} - \|\mathbf{p}_c\|^2, \tag{4-16}$$

where the matrix $\mathbf{Q}_1$ was defined in (2-36). Then, the power scaling factors of the MMSE-THP structure are given by

$$\beta^{(\text{rs-d})} = \sqrt{\frac{\lambda \left(E_{tr} - \|\mathbf{p}_c\|^2\right)}{\text{tr}\left(\mathbf{Q}_1 \mathbf{Q}_1^H\right)}}, \tag{4-17}$$

$$\beta^{(\text{rs-c})} = \sqrt{\frac{\lambda \left(E_{tr} - \|\mathbf{p}_c\|^2\right)}{\text{tr}\left(\mathbf{Q}_1 \check{\mathbf{C}} \check{\mathbf{C}}^H \mathbf{Q}_1^H\right)}}. \tag{4-18}$$

Considering that a fraction of the power given by δE_{tr} has been allocated to

the common stream, we have

$$\beta^{(\text{cTHP})} = \sqrt{\frac{\lambda\left(1-\delta\right)E_{tr}}{\text{tr}\left(\mathbf{Q}_1\check{\mathbf{C}}\check{\mathbf{C}}^H\mathbf{Q}_1^H\right)}}, \tag{4-19}$$

$$\beta^{(\text{dTHP})} = \sqrt{\frac{\lambda\left(1-\delta\right)E_{tr}}{\text{tr}\left(\mathbf{Q}_1\mathbf{Q}_1^H\right)}}. \tag{4-20}$$

Let us now consider the THP using a ZF approach, which can be obtained by directly applying the LQ decomposition over the channel matrix $\hat{\mathbf{H}}$, i.e., $\hat{\mathbf{H}} = \mathbf{LQ}$. The precoder can be obtained with

$$\mathbf{P}_p^{(\text{rs-d})} = \beta^{(\text{rs-d})}\mathbf{F}, \tag{4-21}$$

$$\mathbf{P}_p^{(\text{rs-c})} = \beta^{(\text{rs-c})}\mathbf{FC}. \tag{4-22}$$

The transmitted vector has the form of equations (4-11) and (4-12), but employs (4-21) and (4-22) to compute the precoder. The power constraint of each structure is given by

$$\mathbb{E}\left[\|\beta^{(\text{rs-d})}\mathbf{F}\check{\mathbf{s}}\|^2\right] = E_{tr} - \|\mathbf{p}_c\|^2, \tag{4-23}$$

$$\mathbb{E}\left[\|\beta^{(\text{rs-c})}\mathbf{FC}\check{\mathbf{s}}\|^2\right] = E_{tr} - \|\mathbf{p}_c\|^2. \tag{4-24}$$

Once again, let us introduce the parameter λ to quantify the power loss. Then, we have

$$\beta^{(\text{rs-d})^2}\lambda^{-1}\text{tr}\left(\mathbf{FF}^H\right) = E_{tr} - \|\mathbf{p}_c\|^2. \tag{4-25}$$

$$\beta^{(\text{rs-c})^2}\lambda^{-1}\text{tr}\left(\mathbf{FCC}^H\mathbf{F}^H\right) = E_{tr} - \|\mathbf{p}_c\|^2. \tag{4-26}$$

The matrix $\mathbf{F}$ is a unitary matrix, i.e., $\mathbf{FF}^H = \mathbf{F}^H\mathbf{F} = \mathbf{I}$ and the scaling matrix $\mathbf{C}$ is a diagonal matrix. Thus, equations (4-27) and (4-28) are reduced to:

$$\beta^{(\text{rs-d})^2}\lambda^{-1}K = E_{tr} - \|\mathbf{p}_c\|^2, \tag{4-27}$$

$$\beta^{(\text{rs-c})^2}\lambda^{-1}\sum_{i=1}^{K}l_{i,i}^{-2} = E_{tr} - \|\mathbf{p}_c\|^2. \tag{4-28}$$

Solving for β we get

$$\beta^{(\text{rs-d})} = \sqrt{\frac{\lambda\left(E_{tr}-\|\mathbf{p}_c\|^2\right)}{M}}, \tag{4-29}$$

$$\beta^{(\text{rs-c})} = \sqrt{\frac{\lambda\left(E_{tr}-\|\mathbf{p}_c\|^2\right)}{\sum_{i=1}^{K}\left(1/l_{i,i}^2\right)}}. \tag{4-30}$$

Considering that $\|\mathbf{p}_c\|^2 = \delta E_{tr}$ the ZF-THP power scaling parameters take the value of

$$\beta^{(\text{rs-d})} = \sqrt{\frac{\lambda\,(1-\delta)\,E_{tr}}{K}}, \tag{4-31}$$

$$\beta^{(\text{rs-c})} = \sqrt{\frac{\lambda\,(1-\delta)\,E_{tr}}{\sum_{i=1}^{K}\left(1/l_{i,i}^{2}\right)}}. \tag{4-32}$$

Note that all the scaling factors β are reduced due the power assigned to the common precoder and the power loss.

After precoding, the transmit vector is sent to the receivers through the channel $\mathbf{H}$. The signal obtained at the receiver by the proposed RS-MMSE-THP scheme before the SIC of the common message is described by

$$\mathbf{y}^{(\text{rs-d})} = s_c \mathbf{H} \mathbf{p}_c + \beta^{(\text{rs-d})} \mathbf{H} \mathbf{D} \check{\mathbf{F}} \breve{\mathbf{s}}_p + \mathbf{n} \tag{4-33}$$

$$\mathbf{y}^{(\text{rs-c})} = s_c \mathbf{H} \mathbf{p}_c + \beta^{(\text{rs-c})} \mathbf{H} \mathbf{D} \check{\mathbf{F}} \check{\mathbf{C}} \breve{\mathbf{s}}_p + \mathbf{n}, \tag{4-34}$$

whereas the received signal for the RS-ZF-THP is given by

$$\mathbf{y}^{(\text{rs-d})} = s_c \mathbf{H} \mathbf{p}_c + \beta^{(\text{rs-d})} \mathbf{H} \mathbf{F} \breve{\mathbf{s}}_p + \mathbf{n}, \tag{4-35}$$

$$\mathbf{y}^{(\text{rs-c})} = s_c \mathbf{H} \mathbf{p}_c + \beta^{(\text{rs-c})} \mathbf{H} \mathbf{F} \mathbf{C} \breve{\mathbf{s}}_p + \mathbf{n}. \tag{4-36}$$

At the receiver, the common symbol is detected and then removed from (4-33) or (4-34) by performing SIC. The RS-MMSE-THP received signal after SIC is described by

$$\mathbf{r}^{(\text{rs-d})} = \check{\mathbf{C}}\left(\beta^{(\text{rs-d})} \mathbf{H} \mathbf{D} \check{\mathbf{F}} \breve{\mathbf{s}}_p + \mathbf{n}\right) \tag{4-37}$$

$$\mathbf{r}^{(\text{rs-c})} = \beta^{(\text{rs-c})} \mathbf{H} \mathbf{D} \check{\mathbf{F}} \check{\mathbf{C}} \breve{\mathbf{s}}_p + \mathbf{n}. \tag{4-38}$$

On the other hand, the received signal for the RS-ZF-THP strategy after removing the common message can be written as follows:

$$\mathbf{r}^{(\text{rs-d})} = \beta^{(\text{rs-d})} \mathbf{C}\left(\mathbf{H} \mathbf{F} \breve{\mathbf{s}}_p + \mathbf{n}\right), \tag{4-39}$$

$$\mathbf{r}^{(\text{rs-c})} = \beta^{(\text{rs-c})} \mathbf{H} \mathbf{F} \mathbf{C} \breve{\mathbf{s}}_p + \mathbf{n}. \tag{4-40}$$

Once the common message is removed from the received signal, another modulo operation is performed in order to eliminate the effects of the first modulo operation applied over the private streams. This last operation incurs in a performance penalty due the periodic extension of the constellation. In other words, some symbols at the boundary of the constellation may be mistaken by the opposite symbol. This performance degradation is known as the modulo loss.

For a MISO system, equations (4-33) and (4-34) are simplified, leading

to

$$y_k^{(\text{rs-d})} = s_c \mathbf{h}_{k,*}\mathbf{p}_c + \beta^{(\text{rs-d})}\mathbf{h}_{k,*}\mathbf{D}\check{\mathbf{F}}\check{\mathbf{s}}_p + n_k \tag{4-41}$$

$$y_k^{(\text{rs-c})} = s_c \mathbf{h}_{k,*}\mathbf{p}_c + \beta^{(\text{rs-c})}\mathbf{h}_{k,*}\mathbf{D}\check{\mathbf{F}}\check{\mathbf{C}}\check{\mathbf{s}}_p + n_k, \tag{4-42}$$

whereas (4-35) and (4-36) are reduced to

$$y_k^{(\text{rs-d})} = s_c \mathbf{h}_{k,*}\mathbf{p}_c + \beta^{(\text{rs-d})}\mathbf{h}_{k,*}\mathbf{F}\check{\mathbf{s}}_p + n_k, \tag{4-43}$$

$$y_k^{(\text{rs-c})} = s_c \mathbf{h}_{k,*}\mathbf{p}_c + \beta^{(\text{rs-c})}\mathbf{h}_{k,*}\mathbf{F}\mathbf{C}\check{\mathbf{s}}_p + n_k. \tag{4-44}$$

After decoding the common symbol, equations (4-41) and (4-42) turn into

$$y_k^{(\text{rs-d})} = \beta^{(\text{rs-d})}\mathbf{h}_{k,*}\mathbf{D}\check{\mathbf{F}}\check{\mathbf{s}}_p + n_k \tag{4-45}$$

$$y_k^{(\text{rs-c})} = \beta^{(\text{rs-c})}\mathbf{h}_{k,*}\mathbf{D}\check{\mathbf{F}}\check{\mathbf{C}}\check{\mathbf{s}}_p + n_k. \tag{4-46}$$

On the other hand, equations (4-43) and (4-44) are reduced to

$$y_k^{(\text{rs-d})} = \beta^{(\text{rs-d})}\mathbf{h}_{k,*}\mathbf{F}\check{\mathbf{s}}_p + n_k, \tag{4-47}$$

$$y_k^{(\text{rs-c})} = \beta^{(\text{rs-c})}\mathbf{h}_{k,*}\mathbf{F}\mathbf{C}\check{\mathbf{s}}_p + n_k. \tag{4-48}$$

4.4
Proposed RS-THP Sum-Rate

Let us consider the RS-MMSE-THP architecture and define the quantities $\mathbf{Q}_1\mathbf{Q}_1^H = \mathbf{I} + \mathbf{Q}_e$, $\underline{\mathbf{B}} = \check{\mathbf{B}}^{-1}$ and $\mathbf{H}_{eff} = \check{\mathbf{L}}\mathbf{Q}_e$. Then, we have

$$\mathbf{y}^{(\text{rs-d})} = s_c\mathbf{H}\mathbf{p}_c + \beta^{(\text{rs-d})}\mathbf{C}^{-1}\check{\mathbf{s}} + \beta^{(\text{rs-d})}\check{\mathbf{L}}\mathbf{Q}_e\mathbf{B}^{-1}\check{\mathbf{s}} + \beta^{(\text{rs-d})}\tilde{\mathbf{H}}\mathbf{Q}_1^H\check{\mathbf{B}}^{-1}\check{\mathbf{s}} + \mathbf{n}, \tag{4-49}$$

$$\mathbf{y}^{(\text{rs-c})} = s_c\mathbf{H}\mathbf{p}_c + \beta^{(\text{rs-c})}\check{\mathbf{s}} + \beta^{(\text{rs-c})}\check{\mathbf{L}}\mathbf{Q}_e\check{\mathbf{L}}^{-1}\check{\mathbf{s}} + \beta^{(\text{rs-c})}\tilde{\mathbf{H}}\mathbf{Q}_1^H\check{\mathbf{L}}^{-1}\check{\mathbf{s}} + \mathbf{n}. \tag{4-50}$$

Then, the receive signal at each user equipment is given by

$$y_k^{(\text{rs-d})} = s_c\mathbf{h}_{k,*}\mathbf{p}_c + \beta^{(\text{rs-d})}\left(\check{l}_{k,k}^{-1}\check{s}_k + \check{\mathbf{l}}_{k,*}\mathbf{Q}_e\sum_{i=1}^{K}\underline{\mathbf{b}}_i\check{s}_i + \tilde{\mathbf{h}}_{k,*}\mathbf{Q}_1^H\sum_{j=1}^{K}\underline{\mathbf{b}}_j\check{s}_j\right) + n_k \tag{4-51}$$

$$y_k^{(\text{rs-c})} = s_c\mathbf{h}_{k,*}\mathbf{p}_c + \beta^{(\text{rs-c})}\left(\check{s}_k + \check{\mathbf{l}}_{k,*}\mathbf{Q}_e\sum_{i=1}^{K}\underline{\mathbf{l}}_i\check{s}_i + \tilde{\mathbf{h}}_{k,*}\mathbf{Q}_1\sum_{j=1}^{K}\underline{\mathbf{l}}_j\check{s}_j\right) + n_k \tag{4-52}$$

The average power of the received signal can be computed with the following expression:

$$\mathbb{E}\left[|y_k^{\text{(rs-d)}}|^2\right] = |\mathbf{h}_{k,*}\mathbf{p}_c|^2 + \beta^{\text{(rs-d)}^2}|\check{l}_{k,k}^{-1} + \check{\mathbf{l}}_{k,*}\mathbf{Q}_e\underline{\mathbf{b}}_k + \tilde{\mathbf{h}}_{k,*}\mathbf{Q}_1^H\underline{\mathbf{b}}_k|^2$$

$$+ \beta^{\text{(rs-d)}^2}|\check{\mathbf{l}}_{k,*}\mathbf{Q}_e\sum_{\substack{i=1\\i\neq k}}^{K}\underline{\mathbf{b}}_i + \tilde{\mathbf{h}}_{k,*}\mathbf{Q}_1^H\sum_{\substack{j=1\\j\neq k}}^{K}\underline{\mathbf{b}}_j|^2 + \sigma_n^2, \qquad (4\text{-}53)$$

$$\mathbb{E}\left[|y_k^{\text{(rs-c)}}|^2\right] = |\mathbf{h}_{k,*}\mathbf{p}_c|^2 + \beta^{\text{(rs-c)}^2}|1 + \check{\mathbf{l}}_{k,*}\mathbf{Q}_e\underline{\mathbf{l}}_k + \tilde{\mathbf{h}}_{k,*}\mathbf{Q}_1^H\underline{\mathbf{l}}_k|^2$$

$$+ \beta^{\text{(rs-c)}^2}|\check{\mathbf{l}}_{k,*}\mathbf{Q}_e\sum_{\substack{i=1\\i\neq k}}^{K}\underline{\mathbf{l}}_i + \tilde{\mathbf{h}}_{k,*}\mathbf{Q}_1^H\sum_{\substack{j=1\\j\neq k}}^{K}\underline{\mathbf{l}}_j|^2 + \sigma_n^2. \qquad (4\text{-}54)$$

Thus, the SINR is given by

$$\gamma_{c,k}^{\text{(rs-d)}} = \frac{|\mathbf{h}_{k,*}\mathbf{p}_c|^2/\beta^{\text{(rs-d)}^2}}{|\check{l}_{k,k}^{-1} + \left(\check{\mathbf{l}}_{k,*}\mathbf{Q}_e + \tilde{\mathbf{h}}_{k,*}\mathbf{Q}_1^H\right)\underline{\mathbf{b}}_k|^2 + |\left(\check{\mathbf{l}}_{k,*}\mathbf{Q}_e + \tilde{\mathbf{h}}_{k,*}\mathbf{Q}_1^H\right)\sum_{\substack{i=i\\i\neq k}}^{K}\underline{\mathbf{b}}_i|^2 + \frac{\sigma_n^2}{\beta^{\text{(rs-d)}^2}}}.$$

$$(4\text{-}55)$$

$$\gamma_{c,k}^{\text{(rs-c)}} = \frac{|\mathbf{h}_{k,*}\mathbf{p}_c|^2/\beta^{\text{(rs-c)}^2}}{|1 + \left(\check{\mathbf{l}}_{k,*}\mathbf{Q}_e + \tilde{\mathbf{h}}_{k,*}\mathbf{Q}_1^H\right)\underline{\mathbf{l}}_k|^2 + |\left(\check{\mathbf{l}}_{k,*}\mathbf{Q}_e + \tilde{\mathbf{h}}_{k,*}\right)\mathbf{Q}_1^H\sum_{\substack{i=1\\i\neq k}}^{K}\underline{\mathbf{l}}_i|^2 + \frac{\sigma_n^2}{\beta^{\text{(rs-c)}^2}}}.$$

$$(4\text{-}56)$$

On the other hand, we can express the received signal of the proposed RS-ZF-THP as follows:

$$\mathbf{y}^{\text{(rs-d)}} = \frac{1}{\beta^{\text{(rs-d)}}}\mathbf{CHp}_c s_c + \check{\mathbf{s}} + \mathbf{C\tilde{H}FB}^{-1}\check{\mathbf{s}} + \frac{1}{\beta^{\text{(rs-d)}}}\mathbf{Cn}, \qquad (4\text{-}57)$$

$$\mathbf{y}^{\text{(rs-c)}} = \frac{1}{\beta^{\text{(rs-c)}}}\mathbf{Hp}_c s_c + \check{\mathbf{s}} + \mathbf{\tilde{H}FCB}^{-1}\check{\mathbf{s}} + \frac{1}{\beta^{\text{(rs-c)}}}\mathbf{n}. \qquad (4\text{-}58)$$

From the last equation we can obtain the received signal at each user equipment, which is given by

$$y_k^{\text{(rs-d)}} = \frac{\beta^{\text{(rs-d)}^{-1}}}{l_{k,k}}\mathbf{h}_k^H\mathbf{p}_c s_c + \check{s}_k + \frac{1}{l_{k,k}}\tilde{\mathbf{h}}_k^H\sum_{i=1}^{K}\mathbf{p}_i^{\text{(rs-d)}}\check{s}_i + \frac{\beta^{\text{(rs-d)}^{-1}}n_k}{l_{k,k}}, \qquad (4\text{-}59)$$

$$y_k^{\text{(rs-c)}} = \frac{1}{\beta^{\text{(rs-c)}}}\mathbf{h}_k^H\mathbf{p}_c s_c + \check{s}_k + \tilde{\mathbf{h}}_k^H\sum_{i=1}^{K}\mathbf{p}_i^{\text{(rs-c)}}\check{s}_i + \frac{n_k}{\beta^{\text{(rs-c)}}}. \qquad (4\text{-}60)$$

Squaring and taking the expected value from (4-59) and (4-60), we obtain

$$\mathbb{E}\left[|r_k^{\text{(rs-d)}}|^2\right] = \frac{|\mathbf{h}_k \mathbf{p}_c|^2}{\beta^{\text{(rs-d)}^2} l_{k,k}^2} + \frac{|l_{k,k} + \tilde{\mathbf{h}}_k^H \mathbf{p}_k^{\text{(rs-d)}}|^2}{l_{k,k}^2} + \frac{\sum_{\substack{i=1 \\ i \neq k}}^{K} |\tilde{\mathbf{h}}_k^H \mathbf{p}_i^{\text{(rs-d)}}|^2}{l_{k,k}^2} + \frac{\sigma_n^2}{\beta^{\text{(rs-d)}^2} l_{k,k}^2}$$

(4-61)

$$\mathbb{E}\left[|r_k^{\text{(rs-c)}}|^2\right] = \frac{|\mathbf{h}_k \mathbf{p}_c|^2}{\beta^{\text{(rs-c)}^2}} + |1 + \tilde{\mathbf{h}}_k^H \mathbf{p}_k^{\text{(rs-c)}}|^2 + \sum_{\substack{i=1 \\ i \neq k}}^{K} |\tilde{\mathbf{h}}_k^H \mathbf{p}_i^{\text{(rs-c)}}|^2 + \frac{\sigma_n^2}{\beta^{\text{(rs-c)}^2}}.$$

(4-62)

Thus, the SINR for the common message can be computed by the following equations:

$$\gamma_{c,k}^{(d)} = \frac{|\mathbf{h}_k^H \mathbf{p}_c|^2/\beta^{\text{(rs-d)}^2}}{|l_{k,k} + \tilde{\mathbf{h}}_k^H \mathbf{p}_k^{\text{(rs-d)}}|^2 + \sum\limits_{\substack{i=1 \\ i \neq k}}^{K} |\tilde{\mathbf{h}}_k^H \mathbf{p}_i^{(d)}|^2 + \sigma_n^2/\beta^{\text{(rs-d)}^2}},$$

(4-63)

$$\gamma_{c,k}^{(c)} = \frac{|\mathbf{h}_k^H \mathbf{p}_c|^2/\beta^{\text{(rs-c)}}}{|1 + \tilde{\mathbf{h}}_k^H \mathbf{p}_k^{\text{(rs-c)}}|^2 + \sum\limits_{\substack{i=1 \\ i \neq k}}^{K} |\tilde{\mathbf{h}}_k^H \mathbf{p}_i^{\text{(rs-c)}}|^2 + \sigma_n^2/\beta^{\text{(rs-c)}^2}}.$$

(4-64)

The instantaneous rate of the private messages can be calculated with equation (2-73). However, the transmit power for the private streams is reduced to $E_{tr} - \|\mathbf{p}_c\|^2$ to take into account the power assigned to the common stream. The rates for ZF-DPC-RS approximation based on [65] with imperfect CSIT can be obtained by using the previous expressions and by neglecting the power loss and the modulo loss.

Let us now consider a perfect CSIT scenario. The received signal of the proposed scheme is reduced to

$$\mathbf{y}^{\text{(rs-d)}} = \frac{1}{\beta^{\text{(rs-d)}}} \mathbf{C} \mathbf{H} \mathbf{p}_c s_c + \check{\mathbf{s}} + \frac{1}{\beta^{\text{(rs-d)}}} \mathbf{C} \mathbf{n},$$

(4-65)

$$\mathbf{y}^{\text{(rs-c)}} = \frac{1}{\beta^{\text{(rs-c)}}} \mathbf{H} \mathbf{p}_c s_c + \check{\mathbf{s}} + \frac{1}{\beta^{\text{(rs-c)}}} \mathbf{n}.$$

(4-66)

At the kth user we have

$$y_k^{\text{(rs-d)}} = \frac{\beta^{\text{(rs-d)}^{-1}}}{l_{k,k}} \mathbf{h}_k^H \mathbf{p}_c s_c + \check{s}_k + \frac{\beta^{\text{(rs-d)}^{-1}} n_k}{l_{k,k}},$$

(4-67)

$$y_k^{\text{(rs-c)}} = \frac{1}{\beta^{\text{(rs-c)}}} \mathbf{h}_k^H \mathbf{p}_c s_c + \check{s}_k + \frac{n_k}{\beta^{\text{(rs-c)}}}.$$

(4-68)

It follows that the power of the received signals is given by

$$\mathbb{E}\left[|y_k^{(\text{rs-d})}|^2\right] = \frac{|\mathbf{h}_k\mathbf{p}_c|^2}{\beta^{(\text{rs-d})^2}l_{k,k}^2} + 1 + \frac{\sigma_n^2}{\beta^{(\text{rs-d})^2}l_{k,k}^2}, \tag{4-69}$$

$$\mathbb{E}\left[|y_k^{(\text{rs-c})}|^2\right] = \frac{|\mathbf{h}_k\mathbf{p}_c|^2}{\beta^{(\text{rs-c})^2}} + 1 + \frac{\sigma_n^2}{\beta^{(\text{rs-c})^2}}. \tag{4-70}$$

From the last equation we obtain the SINR for the common message of the kth user:

$$\gamma_{c,k}^{(\text{rs-d})} = \frac{K|\mathbf{h}_k^H\mathbf{p}_c|^2}{\lambda l_{k,k}^2\left(E_{tr} - \|\mathbf{p}_c\|^2\right) + K\sigma_n^2}, \tag{4-71}$$

$$\gamma_{c,k}^{(\text{rs-c})} = \frac{\sum\limits_{i=1}^{K}\left(1/l_{i,i}^2\right)|\mathbf{h}_k^H\mathbf{p}_c|^2}{\lambda E_{tr} + \sigma_n^2\sum\limits_{i=1}^{K}\left(1/l_{i,i}^2\right)}. \tag{4-72}$$

The instantaneous rates for user k can be obtained by $R_{c,k}^{(\text{rs-d})} = \log_2\left(1 + \gamma_{c,k}^{(\text{rs-d})}\right)$ and $R_{c,k}^{(\text{rs-c})} = \log_2\left(1 + \gamma_{c,k}^{(\text{rs-c})}\right)$ for dTHP and cTHP, respectively. In order to ensure that all users can decode the message, the common rates are set to

$$R_c^{(\text{rs-d})} = \min_k R_{c,k}^{(\text{rs-d})}, \tag{4-73}$$

$$R_c^{(\text{rs-c})} = \min_k R_{c,k}^{(\text{rs-c})}. \tag{4-74}$$

After decoding the common message, the receiver subtracts it from the received signal. The SINR expressions for the private messages are

$$\gamma_{p,k}^{(\text{rs-d})} = \frac{\lambda l_{k,k}^2\left(E_{tr} - \|\mathbf{p}_c\|^2\right)}{K\sigma_n^2}, \tag{4-75}$$

$$\gamma_{p,k}^{(\text{rs-c})} = \frac{\lambda\left(E_{tr} - \|\mathbf{p}_c\|^2\right)}{\sigma_n^2\sum\limits_{i=1}^{K}\left(1/l_{i,i}^2\right)}. \tag{4-76}$$

The value of γ_k is reduced due to the power assigned to the common message. The instantaneous private rates for user k can be obtained by $R_{p,k}^{(\text{rs-d})} = \log_2\left(1 + \gamma_{p,k}^{(\text{rs-d})}\right)$ and $R_{p,k}^{(\text{rs-c})} = \log_2\left(1 + \gamma_{p,k}^{(\text{rs-c})}\right)$. At the end, the instantaneous sum-rates for the proposed RS system can be expressed as

$$R^{(\text{rs-d})} = R_c^{(\text{rs-d})} + \sum_{k=1}^{K} R_{p,k}^{(\text{rs-d})}, \tag{4-77}$$

$$R^{(\text{rs-c})} = R_c^{(\text{rs-c})} + \sum_{k=1}^{K} R_{p,k}^{(\text{rs-c})}. \tag{4-78}$$

To calculate the ESR, we first calculate the average SR (ASR), which is the average performance computed for a given channel estimate with respect to

the errors [23]. The ASRs are given by

$$\bar{R}_{p,k}^{(\text{rs-d})} = \mathbb{E}\left[R_{p,k}^{(\text{rs-d})}|\hat{\mathbf{H}}\right] \qquad\qquad \bar{R}_{c,k}^{(\text{rs-d})} = \mathbb{E}\left[R_{c,k}^{(\text{rs-d})}|\hat{\mathbf{H}}\right], \qquad (4\text{-}79)$$

$$\bar{R}_{p,k}^{(\text{rs-c})} = \mathbb{E}\left[R_{p,k}^{(\text{rs-c})}|\hat{\mathbf{H}}\right] \qquad\qquad \bar{R}_{c,k}^{(\text{rs-c})} = \mathbb{E}\left[R_{c,k}^{(\text{rs-c})}|\hat{\mathbf{H}}\right]. \qquad (4\text{-}80)$$

Finally, the ESRs can be calculated as follows:

$$S_{p,r}^{(\text{rs-d})} = \mathbb{E}\left[\sum_{k=1}^{K} \bar{R}_{p,k}^{(\text{rs-d})}\right], \qquad\qquad S_{c,k}^{(\text{rs-d})} = \mathbb{E}\left[\bar{R}_{c,k}^{(\text{rs-d})}\right], \qquad (4\text{-}81)$$

$$S_{p,r}^{(\text{rs-c})} = \mathbb{E}\left[\sum_{k=1}^{K} \bar{R}_{p,k}^{(\text{rs-c})}\right], \qquad\qquad S_{c,k}^{(\text{rs-c})} = \mathbb{E}\left[\bar{R}_{c,k}^{(\text{rs-c})}\right], \qquad (4\text{-}82)$$

where $S_{p,r}$ denotes the ergodic sum-private rate and $S_{c,k}$ represents the ergodic common rate.

4.4.1
Multi-Branch THP

Similar to the conventional THP for SDMA, the order of the symbols affects the performance of the proposed RS-THP. In this sense, incorporating a symbol ordering scheme to the proposed RS-THP structures can further improve the performance. To this end we employ a modified multi-branch (MB) processing technique. The conventional multi-branch (MB) processing was first proposed in [54] for decision feedback receivers and further extended to THP in SDMA scenarios [63]. MB-THP employs multiple parallel branches to find the best symbol ordering and enhance the performance of the THP structure. This technique generates L_o different symbol ordering patterns to generate L_o transmit vectors candidates. Let us consider the matrix $\mathbf{T}_l^{i,j}$ with $l \in 1, \cdots, L_o$, which stores one possible transmit pattern. These patterns are pre-stored at both the transmitter and the receivers. The transmitter selects, among the stored patterns, the one that leads to the highest sum-rate performance. It is important to mention that other metrics to select the optimal branch may be used.

In the MU-MIMO scenario, the patterns are designed in three steps. In the first phase, users are arranged according to several ordering patterns, which

are described as follows:

$$\mathbf{T}_{u,1} = \mathbf{I}_K \tag{4-83}$$

$$\mathbf{T}_{u,i} = \begin{bmatrix} \mathbf{I}_{i-2} & \mathbf{0}_{i-2,K-i+2} \\ \mathbf{0}_{K-i+2,i-2} & \mathbf{\Pi}_i^{(u)} \end{bmatrix}, 2 \leq i \leq K. \tag{4-84}$$

The matrix $\mathbf{T}_{u,i}$ in (4-84) denotes the ith ordering pattern between users. The matrix $\mathbf{\Pi}_i^{(u)} \in \mathbb{C}^{(K-i+2)\times(K-i+2)}$ exchange the order of the users and its entries are equal to zero except on the reverse diagonal, which is filled with ones. Afterwards, for each user the streams are rearranged in a similar way, i.e.

$$\mathbf{T}_{\mathbf{s}_k,1} = \mathbf{I}_{N_k} \tag{4-85}$$

$$\mathbf{T}_{\mathbf{s}_k,j} = \begin{bmatrix} \mathbf{I}_{j-2} & \mathbf{0}_{j-2,N_k-j+2} \\ \mathbf{0}_{N_k-j+2,j-2} & \mathbf{\Pi}_j^{(\mathbf{s}_k)}, \end{bmatrix}, 2 \leq j \leq N_k \tag{4-86}$$

where $\mathbf{T}_{\mathbf{s}_k,j}$ stands for the jth symbol ordering pattern of the kth user. In this case, the matrix $\mathbf{\Pi}_j^{(\mathbf{s}_k)} \in \mathbb{C}^{(N_k-j+2)\times(N_k-j+2)}$ exchanges the order of the symbols of the kth user. It is important to highlight that the matrices in (4-86) ensure that the data streams of a specific user will not be allocated to another user. We then employ both patterns $\mathbf{T}_{u,i}$ and $\mathbf{T}_{\mathbf{s}_k,j}$ together to create multiple patterns given by $\mathbf{T}_l^{(i,j)}$ with $l \in 1, \cdots, L_o$. If the users are equipped with the same number of antennas the matrix $\mathbf{T}_l^{(i,j)}$ can be found by computing the Kronecker product between $\mathbf{T}_{u,i}$ and $\mathbf{T}_{\mathbf{s}_k,j}$, as is given by

$$\mathbf{T}_l^{(i,j)} = \mathbf{T}_{u,i} \otimes \mathbf{T}_{\mathbf{s}_k,j}. \tag{4-87}$$

In contrast to conventional MU-MIMO, RS schemes employs a common precoder in addition to the private precoders. Then, the best pattern is selected according to the following criterion:

$$\mathbf{T}_{(o)} = \max_l \left(\min_{k \in [1,K]} \mathbb{E}_{\mathbf{H}|\hat{\mathbf{H}}} \left[\bar{R}_{c,k} | \hat{\mathbf{H}}\left(\mathbf{T}_l\right) \right] + \mathbb{E}_{\mathbf{H}|\hat{\mathbf{H}}} \left[\bar{R}_p | \hat{\mathbf{H}}\left(\mathbf{T}_l\right) \right] \right). \tag{4-88}$$

Once the best branch is selected, the channel estimate is rearranged accordingly, i.e., $\hat{\mathbf{H}}_{(o)}^{\mathrm{T}} = \mathbf{T}_{(o)}\hat{\mathbf{H}}^T$. Remark that decoding the common message, the private symbols are treated as additional noise. It follows that the symbol ordering also affects the common rate and omitting the common rate in the selection criterion may lead to the selection of the wrong candidate. Moreover, setting the precoders requires $\hat{\mathbf{H}}_{(o)}^{\mathrm{T}}$. In this sense, the computation of the common precoder should be performed by taking into account the pattern used to order the symbols.

The proposed Multi-Branch RS-THP algorithm is summarized in Algorithm 1. The algorithm employs equation (4-88) at step 4. This criterion calculates the ASR given by $\bar{R}_{c,k}$ and $\bar{R}_p$ in order to average out the effects of the imperfect CSIT. Note that under perfect CSIT assumption the instantaneous sum-rate is achievable. In such cases the criterion given in (4-88) should use $R_{c,k}$ and R_p instead of $\bar{R}_{c,k}$ and $\bar{R}_p$.

Algorithm 1: Multi-Branch RS-THP algorithm

---

1 **for** $l = 1$ **to** L_o **do**

2 $\qquad$ Form the channel matrix $\hat{\mathbf{H}}^{(l)}$ for the lth branch;

3 $\qquad$ Perform an LQ decomposition, $\mathbf{H}^{(l)} = \mathbf{L}^{(l)}\mathbf{Q}^{(l)}$;

4 $\qquad$ Get the feedforward filter, $\mathbf{F}^{(l)} = \mathbf{Q}^{(l)^H}$;

5 $\qquad$ Compute the scaling matrix, $\mathbf{C}^{(l)} = \mathrm{diag}\left(l_{1,1}, \cdots, l_{N_t,N_t}\right)^{-1}$;

6 $\qquad$ Get the filter $\mathbf{B}^{(\mathrm{cTHP},l)} = \mathbf{L}^{(l)}\mathbf{C}^{(l)}$ or $\mathbf{B}^{(\mathrm{dTHP},l)} = \mathbf{C}^{(l)}\mathbf{L}^{(l)}$;

7 **end**

8 Choose $\mathbf{T}_{(o)} = \max_l \left(\min_{k \in [1,K]} \mathbb{E}_{\mathbf{H}|\hat{\mathbf{H}}}\left[R_{c,k}|\hat{\mathbf{H}}^{(l)} \right] + \mathbb{E}_{\mathbf{H}|\hat{\mathbf{H}}}\left[R_p|\hat{\mathbf{H}}^{(l)} \right] \right)$;

9 $\breve{s}_1 = s_1$;

10 **for** $i = 1$ **to** M **do**

11 $\qquad$ $\breve{s}_i^{(o)} = s_i - \sum_{j=1}^{i-1} b_{i,j}^{(o)} \breve{s}_j^{(o)}$;

12 $\qquad$ $\breve{s}_i^{(o)} = \mathrm{M}\left(\breve{s}_i^{(o)} \right)$;

13 **end**

14 Compute the transmit vector, $\mathbf{x}^{(o)} = \mathbf{P}^{(o)}\breve{\mathbf{s}}^{(o)}$;

15 Get the receive vector, $\mathbf{y}^{(o)} = \mathbf{H}^{(o)}\mathbf{x}^{(o)} + \mathbf{n}$

4.5
Stream Combining

The proposed scheme employs RS at the transmitter to enhance the ESR. Additionally, receive processing techniques may be employed to further enhance the performance. In [66] a MIMO cloud setting for RS with multiantenna receivers has been studied and optimized. In [30] the precoder and the receiver of multiuser millimeter-wave system with RS are jointly optimized to maximize the sum-rate. However, both approaches require an optimization performed for each frame, which is computationally expensive. Therefore, in [67] practical stream combiners have been proposed to enhance the common rate by taking advantage of the diversity provided by the multiple antennas. These combiners improve the performance by employing the multiple antennas at the UEs. Each receiver obtains multiple copies of the common symbol leading to a better performance a system robustness. In this work, we devise

stream combining techniques to support non-linear processing.

The stream combiner $\mathbf{w}_k$ is implemented at the kth receiver in order to take advantage of the multiple copies of the common symbol and improve the performance of the common rate. The combined signal is defined as $\tilde{y}_k = \mathbf{w}_k^H \mathbf{y}_k$. The average power of the combined signal is given by

$$\mathbb{E}\left[|\tilde{y}_k|^2\right] = |\mathbf{w}_k^H \mathbf{H}_k^{\mathrm{T}} \mathbf{p}_c|^2 + \sum_{j=1}^{M} |\mathbf{w}_k^H \mathbf{H}_k^{\mathrm{T}} \mathbf{q}_{b_j}|^2 + \|\mathbf{w}_k\|^2 \sigma_n^2, \qquad (4\text{-}89)$$

where $\mathbf{q}_{b_j}$ depends on the THP structure employed. Let us define the matrices $\underline{\mathbf{B}} = \mathbf{B}^{-1}$ and $\underline{\check{\mathbf{B}}} = \check{\mathbf{B}}^{-1}$. Then, the ZF-THP algorithms lead to

$$\mathbf{q}_{b_j}^{(c)} = \mathbf{Q}^H \left(\underline{\mathbf{b}}_j \odot [\mathrm{diag}\,(\mathbf{L})]^{-1}\right), \qquad (4\text{-}90)$$

$$\mathbf{q}_{b_j}^{(d)} = \mathbf{Q}^H \underline{\mathbf{b}}_j. \qquad (4\text{-}91)$$

On the other hand, for the MMSE-THP precoders we have

$$\mathbf{q}_{b_j}^{(c)} = \mathbf{Q}_1^H \left(\underline{\check{\mathbf{b}}}_j \odot [\mathrm{diag}\,(\mathbf{L})]^{-1}\right), \qquad (4\text{-}92)$$

$$\mathbf{q}_{b_j}^{(d)} = \mathbf{Q}_1^H \underline{\check{\mathbf{b}}}_j. \qquad (4\text{-}93)$$

The SINR of (4-89) when decoding the common message is expressed by

$$\gamma_{k,c} = \frac{|\mathbf{w}_k^H \mathbf{H}_k^{\mathrm{T}} \mathbf{p}_c|^2}{\sum\limits_{j=1}^{M} |\mathbf{w}_k^H \mathbf{H}_k^{\mathrm{T}} \mathbf{q}_{b_j}|^2 + \|\mathbf{w}_k\|^2 \sigma_n^2}. \qquad (4\text{-}94)$$

Assuming Gaussian signalling the instantaneous common rate at the kth user is obtained by

$$R_{c,k} = \log_2\left(1 + \gamma_{c,k}\right). \qquad (4\text{-}95)$$

In the literature, several criteria to define the combiner $\mathbf{w}_k$ have been proposed, such as the Min-Max, the MRC, and the MMSE criteria. Considering the Min-Max criterion, the common rate at the ith antenna of the kth user is given by

$$R_{c,k,i} = \log_2\left(1 + \frac{|[\mathbf{H}_k]_i^{\mathrm{T}} \mathbf{p}_c|^2}{\sum\limits_{j=1}^{M} |[\mathbf{H}_k]_i^{\mathrm{T}} \mathbf{q}_{b_j}|^2 + \sigma_n^2}\right). \qquad (4\text{-}96)$$

At each receiver, we select the antennas that achieve the highest ergodic common rate according to the Min-Max criterion:

$$R_c = \min_{k \in [0,K]} \max_{i \in \mathcal{M}_k} \mathbb{E}_{\hat{\mathbf{H}}}\left[\mathbb{E}_{\mathbf{H}|\hat{\mathbf{H}}}\left[R_{c,k,i}|\hat{\mathbf{H}}\right]\right] \qquad (4\text{-}97)$$

The MRC combiner is defined as $\mathbf{w}_k^{(\mathrm{MRC})} = \frac{\mathbf{H}_k^{\mathrm{T}} \mathbf{p}_c}{\|\mathbf{H}_k^{\mathrm{T}} \mathbf{p}_c\|^2}$. The SINR of this technique is computed by

$$\gamma_{c,k}^{(\text{MRC})} = \frac{\|\mathbf{H}_k^{\mathrm{T}}\mathbf{p}_c\|^2}{\sum\limits_{j=1}^{M} \|\mathbf{H}_k^{\mathrm{T}}\mathbf{q}_{b_j}\|^2 \cos^2\theta_j + \sigma_n^2}, \tag{4-98}$$

where θ_j denotes the angle between $\mathbf{w}_k$ and the vector $\mathbf{H}_k^{\mathrm{T}}\mathbf{q}_{b_j}$. The instantaneous common rate can be found using (4-98) in (4-95).

Finally, we consider the MMSE combiner (MMSEc), which is given by

$$\mathbf{w}_k^{(\text{MMSEc})} = \mathbf{R}_{\mathbf{y}_k\mathbf{y}_k}^{-1}\mathbf{H}_k^{\mathrm{T}}\mathbf{p}_c, \tag{4-99}$$

and the SINR obtained with this technique is

$$\gamma_{c,k}^{(\text{MMSEc})} = \frac{|\mathbf{p}_c^H\mathbf{H}_k^H\mathbf{R}_{\mathbf{y}_k\mathbf{y}_k}^{-1}\mathbf{H}_k\mathbf{p}_c|}{\sum\limits_{j=1}^{M} |\mathbf{p}_c^H\mathbf{H}_k^H\mathbf{R}_{\mathbf{y}_k\mathbf{y}_k}^{-1}\mathbf{H}_k\mathbf{q}_{b_j}|^2 + \text{tr}\left(\mathbf{R}_{\mathbf{y}_k\mathbf{y}_k}^{-2}\mathbf{H}_k\mathbf{p}_c\mathbf{p}_c^H\mathbf{H}_k^H\right)\sigma_n^2}. \tag{4-100}$$

The common rate can be computed by substituting (4-100) into (4-95).

4.6
Complexity and Rate Analysis

Wireless communications system possess limited processing and hardware resources. In this sense, the computational complexity of the algorithms implemented play an essential role. Therefore, in this section, we analyze the computational complexity of the proposed and existing precoding and combining techniques. Furthermore, we derive equations that describe the achievable rates of the proposed techniques.

4.6.1
Complexity Analysis

In this section, we calculate the number of floating point operations (FLOPS) to describe the computational complexity of the proposed algorithms. Let us consider the matrices $\mathbf{Z}_1 \in \mathbb{C}^{m \times n}$ with $m < n$ and $\mathbf{Z}_2 \in \mathbb{C}^{n \times p}$. Then, the following results hold:

- $\mathbf{Z}_1$ multiplied by $\mathbf{Z}_2$ requires $8mnp - 2mp$ FLOPS.
- The LQ decomposition of $\mathbf{Z}_1$ requires $8m^2\left(n - \frac{1}{3}m\right)$ FLOPS.

We consider that the LQ factorization is carried out with the Householder transformation as described in [68]. Considering the special case where $m = n = p$ results in $8m^3 - 2m^2$ FLOPS for the multiplication of two complex matrices and $\frac{16}{3}m^3$ FLOPS for the LQ decomposition. Table 4.1 shows the complexity of the conventional ZF-THP scheme, where we consider that $N_t = N_r = n$. Note that the computational complexity of the MMSE-THP

algorithms is dominated by the LQ decomposition of the extended channel matrix, which results in $\frac{40}{3}n^3$ FLOPS.

Table 4.1: Conventional ZF-THP

Steps	Operations	FLOPS
1	LQ($\mathbf{H}$)	$\frac{16}{3}n^3$
2	$\mathbf{B} = \mathbf{LC}$	n^2
3	$\mathbf{v}$	$4n^2 + 4n - 8$
4	$\mathbf{F}\,(\mathbf{C'v})$	$8n^2 + 4n$

The proposed techniques include a common stream combiner which increases the performance of the system at the expense of a higher computational complexity. Table 4.3 summarizes the computational complexity of the proposed techniques with the use of different combiners and SIC. The required number of FLOPS of the proposed RS-THP algorithms with stream combiners for different system dimensions is presented in Fig. 4.2.

Table 4.2: Computational complexity of the stream combiners

Technique	FLOPS
Min-Max	$8n - 2K$
MRC	$8n^2 + 6n + 6K$
MMSEc	$\frac{4}{3K^2}n^3 + \frac{8}{K}n^2 + 8n^2 + 4n - 2K$

Table 4.3: Computational complexity of the proposed schemes

Technique	FLOPS
ZF-THP	$\frac{16}{3}n^3 + 13n^2 + 8n - 8$
RS-ZF-THP-MinMax MinMax	$\frac{16}{3}n^3 + 21n^2 + 22n - 2K - 8$
RS-ZF-THP MRC	$\frac{16}{3}n^3 + 29n^2 + 20n + 6K - 8$
RS-ZF-THP MMSEc	$\frac{16}{3}n^3 + \frac{4}{3K^2}n^3 + 29n^2 + \frac{8}{K}n^2 + 34n - 2K - 8$
MMSE-THP	$\frac{40}{3}n^3 + 13n^2 + 8n - 8$
RS-MMSE-THP MinMax	$\frac{40}{3}n^3 + 21n^2 + 22n - 2K - 8$
RS-MMSE-THP MRC	$\frac{40}{3}n^3 + 29n^2 + 20n + 6K - 8$
RS-MMSE-THP MMSEc	$\frac{40}{3}n^3 + \frac{4}{3K^2}n^3 + 29n^2 + \frac{8}{K}n^2 + 34n - 2K - 8$

4.6.2
Rate Analysis

In this section, we carry out the sum-rate analysis of the proposed strategies. Furthermore, we derive expressions that describe the SINR of the proposed techniques. Assuming that the BS employs a ZF-THP with RS, the received signal at the kth user is given by

$$\mathbf{y}_k^{(c)} = s_c\mathbf{H}_k^{\mathrm{T}}\mathbf{p}_c + \check{\mathbf{s}}_k^{(c)} + \tilde{\mathbf{H}}_k^{\mathrm{T}}\mathbf{Q}^H\mathrm{diag}\,(\mathbf{l})^{-1}\,\mathbf{B}^{(c)^{-1}}\left(\mathbf{s} + \mathbf{d}^{(c)}\right) \qquad (4\text{-}101)$$

$$\mathbf{y}_k^{(d)} = s_c\mathbf{H}_k^{\mathrm{T}}\mathbf{p}_c + \mathbf{L}_k\mathbf{B}^{(d)^{-1}}\check{\mathbf{s}}_k^{(d)} + \tilde{\mathbf{H}}_k^{\mathrm{T}}\mathbf{Q}^H\mathbf{B}^{(d)^{-1}}\left(\mathbf{s} + \mathbf{d}^{(d)}\right). \qquad (4\text{-}102)$$

From (4-102) we can obtain the average power of the received signal at the ith antenna, which is given by

$$\mathbb{E}\left[\left|y_i^{(c)}\right|^2\right] = \left|\left(\hat{\mathbf{h}}_i^{\mathrm{T}} + \tilde{\mathbf{h}}_i^{\mathrm{T}}\right)\mathbf{p}_c\right|^2 + \sigma_{s_i}^2 + \sum_{j=1}^{N_r}\frac{1}{|l_{j,j}|^2}\left|\tilde{\mathbf{h}}_i^{\mathrm{T}}\mathbf{q}_{j,*}^H\right|^2 + \sigma_n^2, \qquad (4\text{-}103)$$
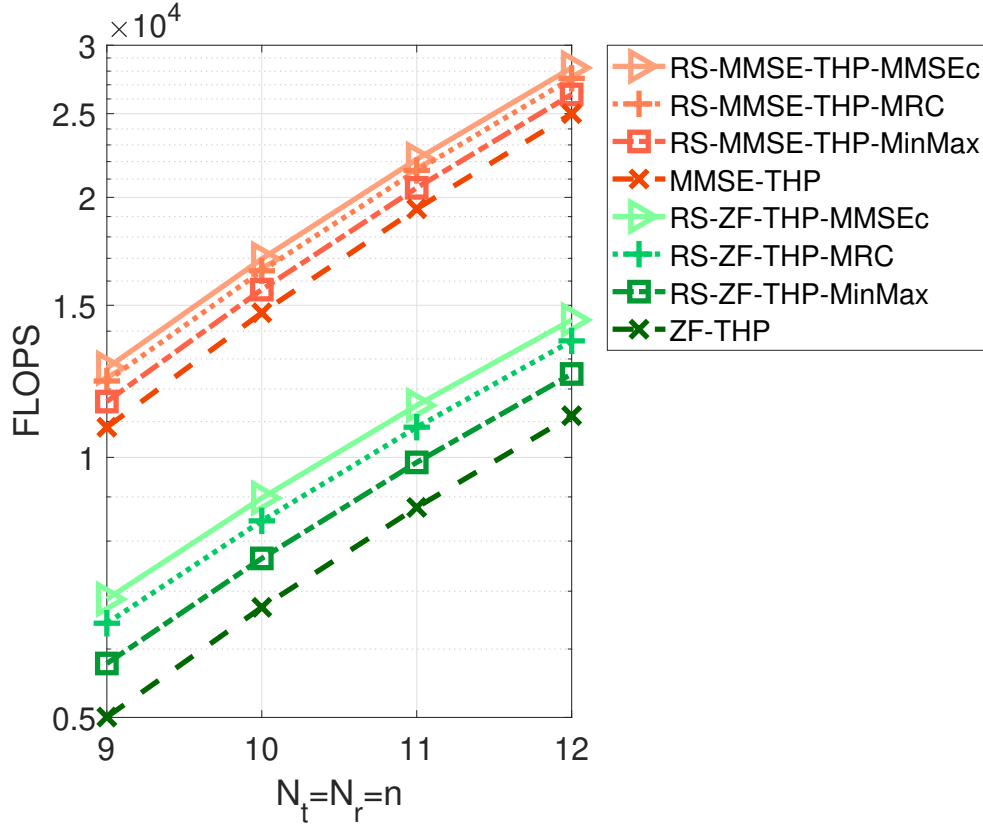
Figure 4.2: Complexity analysis

$$\mathbb{E}\left[\left|y_i^{(d)}\right|^2\right] = \left|\left(\hat{\mathbf{h}}_i^{\mathrm{T}} + \tilde{\mathbf{h}}_i^{\mathrm{T}}\right)\mathbf{p}_c\right|^2 + \left\|\left[\mathbf{L}^{\mathrm{T}}\right]_i\right\|^2 + \sum_{j=1}^{N_r}\left|\tilde{\mathbf{h}}_i^{\mathrm{T}}\mathbf{q}_{j,*}^H\right|^2 + \sigma_n^2. \qquad (4\text{-}104)$$

The SINR of the proposed techniques can be computed with (4-104) and (4-103), which lead us to

$$\gamma_{c,k,i}^{(c)} = \frac{|\hat{\mathbf{h}}_i^{\mathrm{T}}\mathbf{p}_c|^2}{|\tilde{\mathbf{h}}_i^{\mathrm{T}}\mathbf{p}_c|^2 + \sigma_{s_i}^2 + \sum\limits_{j=1}^{N_r}\frac{1}{|l_{j,j}|^2}|\tilde{\mathbf{h}}_i^{\mathrm{T}}\mathbf{q}_{j,*}^H|^2 + \sigma_n^2} \qquad (4\text{-}105)$$

$$\gamma_{c,k,i}^{(d)} = \frac{|\hat{\mathbf{h}}_i^{\mathrm{T}}\mathbf{p}_c|^2}{|\tilde{\mathbf{h}}_i^{\mathrm{T}}\mathbf{p}_c|^2 + \left\|\left[\mathbf{L}^{\mathrm{T}}\right]_i\right\|^2 + \sum\limits_{j=1}^{N_r}|\tilde{\mathbf{h}}_i^{\mathrm{T}}\mathbf{q}_{j,*}^H|^2 + \sigma_n^2} \qquad (4\text{-}106)$$

We can get the common rate of the RS-ZF-cTHP and RS-ZF-dTHP structures by using (4-105) and (4-106), respectively. First, we compute the ASR, given by $\mathbb{E}\left[\log_2\left(1 + \gamma_{c,k,i}\right)|\hat{\mathbf{H}}\right]$, to select at the kth user the antenna that leads to the best performance, i.e., $i_k^{(o)} = \max\limits_{i \in \mathcal{M}_k} \mathbb{E}\left[\log_2\left(1 + \gamma_{c,k,i}\right)|\hat{\mathbf{H}}\right]$. Finally, for the Min-Max criterion, we set $\mathbf{w}_k = \mathbf{e}_{i_k^{(o)}}$, where $\mathbf{e}_i$ is the column index vector,

which contains an entry equal to one at the ith position and zeros at any other position.

For the MRC combiner we need to find the value of $\|\mathbf{H}_k^{\mathrm{T}}\mathbf{q}_{b_i}\|^2$ with $i = 1, 2, \cdots, M$, which corresponds to the multiplication of the kth user channel with the private precoders. In order to find this value, we need to expand the terms of the products given by $\mathbf{H}_k^{\mathrm{T}}\mathbf{Q}^H\left(\mathrm{diag}\left(\mathbf{l}\right)\right)^{-1}\mathbf{B}^{(\mathrm{c})^{-1}}$ and $\mathbf{H}_k^{\mathrm{T}}\mathbf{Q}^H\mathbf{B}^{(\mathrm{d})^{-1}}$. Then, we have

$$\mathbf{H}_k^{\mathrm{T}}\mathbf{Q}^H\left(\mathrm{diag}\left(\mathbf{l}\right)\right)^{-1}\mathbf{B}^{(\mathrm{c})^{-1}} = \mathbf{H}_k^{\mathrm{T}}\left[\frac{1}{l_{1,1}}\mathbf{q}_{1,*}^H \quad \frac{1}{l_{2,2}}\mathbf{q}_{2,*}^H \quad \cdots \quad \frac{1}{l_{M,M}}\mathbf{q}_{M,*}^H\right]\mathbf{B}^{(\mathrm{c})^{-1}}, \tag{4-107}$$

$$\mathbf{H}_k^{\mathrm{T}}\mathbf{Q}^H\mathbf{B}^{(\mathrm{d})^{-1}} = \mathbf{H}_k^{\mathrm{T}}\left[\mathbf{q}_{1,*}^H \quad \mathbf{q}_{2,*}^H \quad \cdots \quad \mathbf{q}_{M,*}^H\right]\mathbf{B}^{(\mathrm{d})^{-1}}. \tag{4-108}$$

Using (4-107) and (4-108) we can obtain the vector $\mathbf{H}_k^{\mathrm{T}}\mathbf{q}_{b_i}$, which is given by

$$\mathbf{H}_k^{\mathrm{T}}\mathbf{q}_{b_i}^{(\mathrm{c})} = \begin{bmatrix} h_{1,1}^{(k)}\sum_{j=1}^{M}\frac{1}{l_{jj}}q_{j,1}\underline{b}_{j,i}^{(\mathrm{c})} + \cdots + h_{1,M}^{(k)}\sum_{j=1}^{M}\frac{1}{l_{jj}}q_{j,M}\underline{b}_{j,i}^{(\mathrm{c})} \\ h_{2,1}^{(k)}\sum_{j=1}^{M}\frac{1}{l_{jj}}q_{j,1}\underline{b}_{j,i}^{(\mathrm{c})} + \cdots + h_{2,M}^{(k)}\sum_{j=1}^{M}\frac{1}{l_{jj}}q_{j,M}\underline{b}_{j,i}^{(\mathrm{c})} \\ \vdots \\ h_{N_k,1}^{(k)}\sum_{j=1}^{M}\frac{1}{l_{jj}}q_{j,1}\underline{b}_{j,i}^{(\mathrm{c})} + \cdots + h_{N_k,M}^{(k)}\sum_{j=1}^{M}\frac{1}{l_{jj}}q_{j,M}\underline{b}_{j,i}^{(\mathrm{c})} \end{bmatrix}, \tag{4-109}$$

$$\mathbf{H}_k^{\mathrm{T}}\mathbf{q}_{b_i}^{(\mathrm{d})} = \begin{bmatrix} h_{1,1}^{(k)}\sum_{j=1}^{M}q_{j,1}\underline{b}_{j,i}^{(\mathrm{d})} + \cdots + h_{1,M}^{(k)}\sum_{j=1}^{M}q_{j,M}\underline{b}_{j,i}^{(\mathrm{d})} \\ h_{2,1}^{(k)}\sum_{j=1}^{M}q_{j,1}\underline{b}_{j,i}^{(\mathrm{d})} + \cdots + h_{2,M}^{(k)}\sum_{j=1}^{M}q_{j,M}\underline{b}_{j,i}^{(\mathrm{d})} \\ \vdots \\ h_{N_k,1}^{(k)}\sum_{j=1}^{M}q_{j,1}b_{j,i}^{(\mathrm{d})} + \cdots + h_{N_k,M}^{(k)}\sum_{j=1}^{M}q_{j,M}\underline{b}_{j,i}^{(\mathrm{d})} \end{bmatrix}. \tag{4-110}$$

Finally, we calculate the value of $\|\mathbf{H}_k\mathbf{p}_i\|^2$ as follows

$$\|\mathbf{H}_k^{\mathrm{T}}\mathbf{q}_{b_i}^{(\mathrm{c})}\|^2 = \sum_{p=1}^{N_k}\left|\sum_{n=1}^{M}\sum_{j=1}^{M}\frac{1}{l_{j,j}}h_{p,n}^{(k)}q_{j,n}\underline{b}_{j,i}^{(\mathrm{c})}\right|^2, \tag{4-111}$$

$$\|\mathbf{H}_k^{\mathrm{T}}\mathbf{q}_{b_i}^{(\mathrm{d})}\|^2 = \sum_{p=1}^{N_k}\left|\sum_{n=1}^{M}\sum_{j=1}^{M}h_{p,n}^{(k)}q_{j,n}\underline{b}_{j,i}^{(\mathrm{d})}\right|^2 \tag{4-112}$$

By substituting (4-111) and (4-112) in (4-98) we obtain the SINR of the RS-THP-MRC technique.

Note that the power loss, which depends on the modulation, was neglected in this analysis. To include the power loss, a factor λ should be introduced as done previously.

4.7
Simulations

In this section we evaluate the performance of the proposed THP-RS schemes using zero-forcing (ZF) filters and compare them with existing techniques. First, we consider a MISO BC channel with 4 transmit antennas and 4 users. The inputs follow a Gaussian distribution with variance $\sigma_s^2 = 1$. We also consider additive white Gaussian noise and flat fading Rayleigh channels scenario, where all the users experience the same noise variance. The ASR was calculated using a total of 100 error matrices for each estimated channel. Then the ESR was obtained averaging over 100 independent channel estimates. The precoder for the common message was obtained using a singular value decomposition (SVD) of the channel matrix ($\mathbf{H} = \mathbf{USV}$), i.e., $\mathbf{p}_c = \mathbf{v}_1$. A percentage of the power from the private precoders has been assigned to the common precoder. The power assigned to the common precoder was found through exhaustive search, while the remaining power was uniformly allocated across the private precoders.

Figs. 4.3 and 4.4 illustrate the results for the precoding algorithms with perfect and imperfect CSIT, respectively. We consider a power loss factor of $\lambda = 0.75$ for the THP structures. For imperfect CSIT we used a fixed error with zero mean and $\mathbb{E}\left[\tilde{\mathbf{h}}_{i,*}\tilde{\mathbf{h}}_i\right] = 0.05$. The results show that the proposed THP-RS schemes outperform previously reported THP and linear schemes. RS-based schemes only offer a small gain over standard schemes with perfect CSIT, as illustrated in Fig. 4.3, whereas those gains are substantial in the presence of imperfect CSIT, which corroborates the sum-rate results in the literature for linearly precoded RS schemes[3]. The results also show that the ZF-DPC approximation obtains the highest sum-rate, as expected, followed by THP and linear schemes. Specifically among RS-based schemes, the RS-ZF-DPC [65] obtains the best result followed by dTHP-RS, cTHP-RS and linearly precoded RS. Note that for the ZF-DPC implemented here, we considered uniform power allocation among the streams. The performance advantage of dTHP structures over cTHP ones is explained by the error covariance matrix previously presented, and by the use of more complex receive filters at the users, whereas cTHP only employs filters at the transmitter which translates into lower complexity [7]. The curves obtained for imperfect CSIT exhibit saturation due to the fact that the MUI scales with the SNR [23, 69]. This is

---

[3]Recall however that simulation results hold only for sum-rates, under uniform power allocation among private streams and with users experiencing similar channel strengths. If we allow optimization of the power across private streams, or choose a weighted sum-rate or experience user channel strength disparity, RS-based schemes can provide larger gains, as detailed in [21].

expected for THP schemes due to error propagation associated with imperfect CSIT.
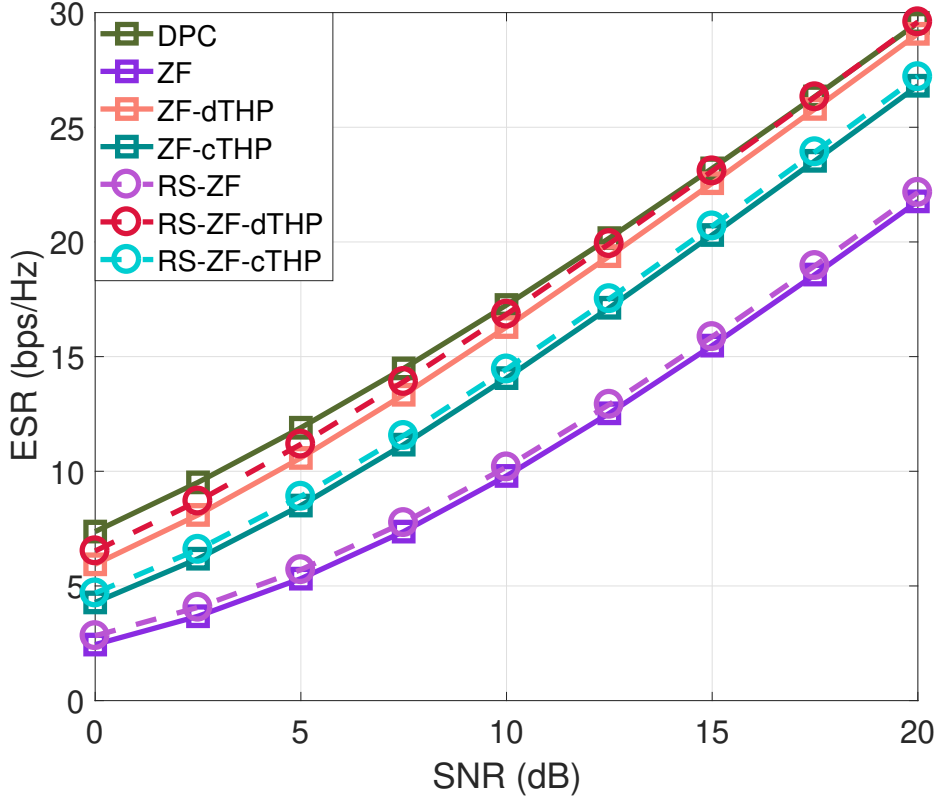
Figure 4.3: Ergodic sum-rate performance of RS systems considering perfect CSIT with $N_t = 4$ and $K = 4$.

In the next example for the MISO deployment, we consider the sum-rate performance for different error variances using SNR = 18 dB, as illustrated in Fig. 4.5. The results show that RS increases robustness for all error variances. In particular, the proposed RS-dTHP scheme achieves the highest sum-rate, followed by RS-cTHP and linearly precoded RS. The sum rates achieved by RS-dTHP can be up to 8% higher than RS-cTHP, whereas they can be up to 65% higher than those achieved by non RS-based schemes. This highlights the robustness of RS schemes against imperfect CSIT for a wide range of scenarios.

In the last example, we consider that the variance of the error scales with the SNR $\left(\sigma_e^2 = 0.8 E_{tr}^{-\alpha}\right)$. The curves obtained in Fig. 4.6 have been computed with $\alpha = 0.6$. The results indicate that RS-THP schemes are more robust than standard THP schemes and achieve higher sum rates than linear schemes. It can be noticed that the slope achieved by RS-based schemes is significantly higher than that associated with non RS-type approaches, which corroborates the robustness shown in Fig. 4.5 and the superiority of RS in terms of DoF [23, 70].

Figure 4.4: Ergodic sum-rate performance of RS systems considering imperfect CSIT with $N_t = 4$, $K = 4$, and $\sigma_e^2 = 0.05$.

Let us now consider the BC of MIMO system with a BS equipped 12 transmit antennas serving six users, each one equipped with two receive antennas. Let us consider RS with several ZF precoding schemes under perfect CSIT. Fig. 4.7 summarizes the sum-rate performance achieved. Note that the multiple antennas at the UE allow us to implement the common combiners and enhance the common rate. In contrast, for the private rate of the ZF techniques each receive antenna may be treated as a separate single-antenna user. The inclusion of the terms RS and MMSEc in the legend denote that the schemes employ RS with an MMSE combiner. Conventional precoding schemes omit these terms. Note that each stream transmitted provides a gain from ZF-THP over the conventional ZF precoder, which results in a substantial ESR gain. Although the major contribution of RS is to cope with CSIT uncertainties, Fig. 4.7 shows that the RS with the MMSEc combiner at the receiver provides a consistent gain of at least one bit/Hz for all the schemes examined. Therefore, RS-THP is a promising strategy even under perfect CSIT assumption. The benefits of RS are greater under imperfect CSIT, as shown in the following simulations.

In the second example, we explore an imperfect CSIT scenario where
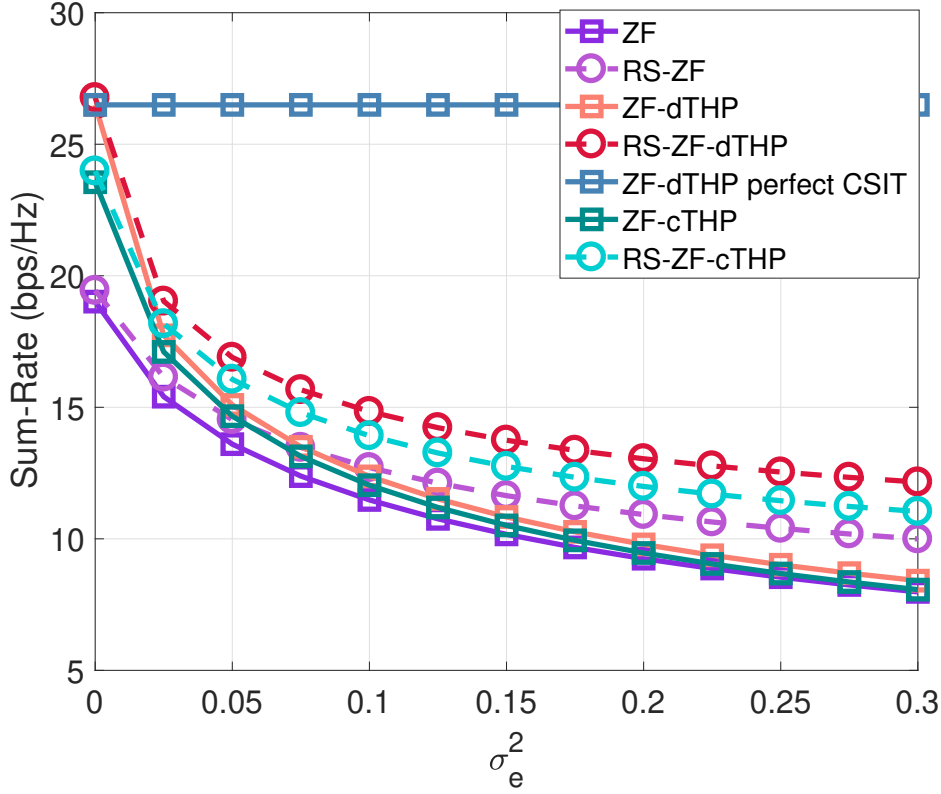
Figure 4.5: Sum-rate performance versus channel error variance at a SNR of 18 dB with $N_t = 4$ and $K = 4$.

we consider that each coefficient of $\tilde{\mathbf{H}}$ follows a Gaussian distribution with zero mean and variance equal to $\sigma_{e_i}^2 = 0.05$. Fig. 4.8 shows the sum-rate performance obtained by the ZF-cTHP and the ZF-dTHP structures, whereas Fig. 4.9 shows the MMSE-cTHP and MMSE-dTHP structures. From Fig. 4.8 we notice that all dTHP schemes outperform those using the cTHP architecture. However, the dTHP scheme requires more complex receivers. Fig. 4.9 shows that MMSE-THP achieves better performance than that of ZF-THP for all the combiners employed, as expected especially for SNR values below 15 dB. This gain comes from the reduced interference due to the MMSE precoders, which results in a reduction of the power loss. The results show that RS-THP attains better performance than other schemes under CSIT uncertainties. The common combiners implemented at the receiver further increase the RS-THP performance, while MMSEc is the best combiner.

In the third example, we assess the common rate attained by the combiners. The parameters remains the same as in the previous experiment. From Fig. 4.10 we can see that the common combiners greatly increase the performance of the common rate when compared to conventional RS. Note that linear precoders without combiners achieve a higher common rate than non-
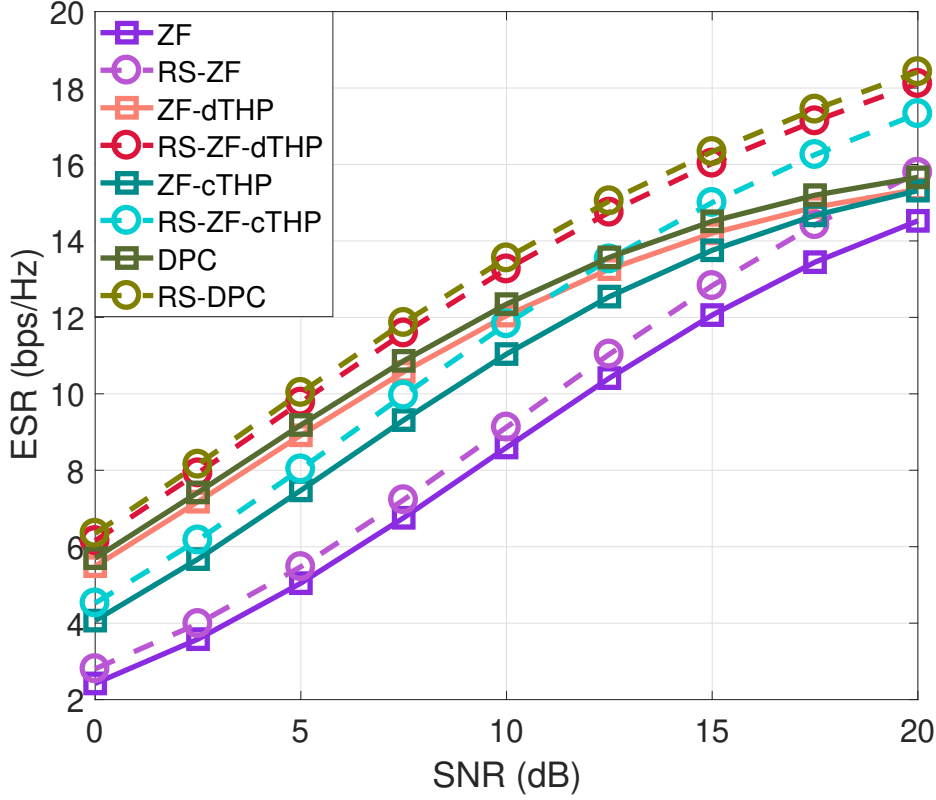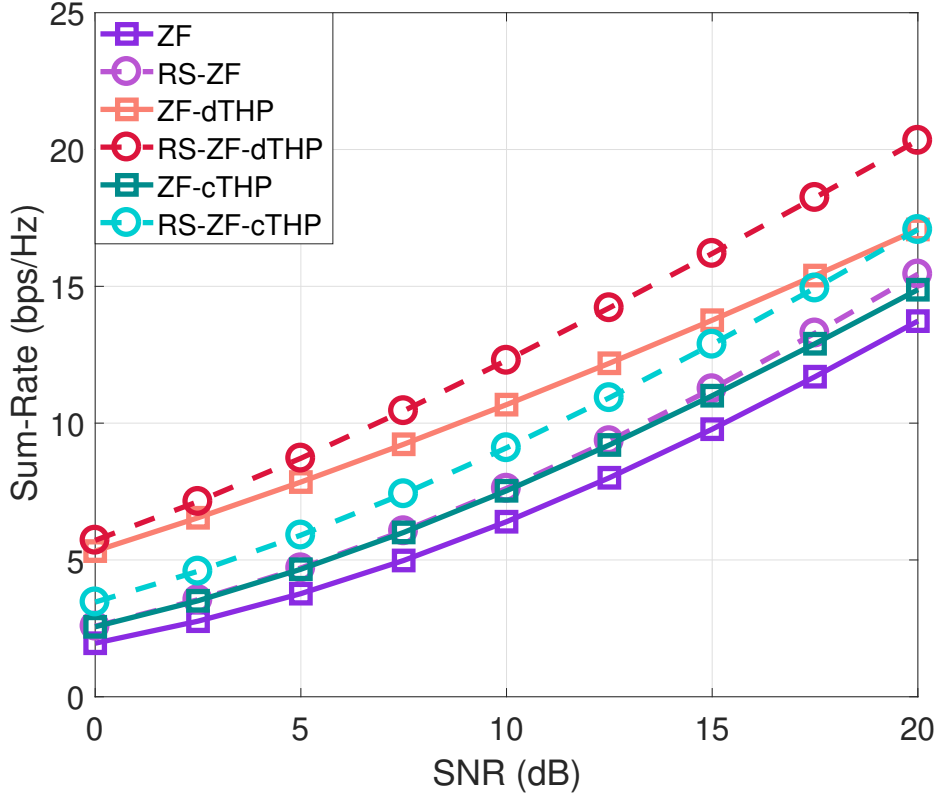
Figure 4.6: Ergodic sum-rate performance of RS systems considering imperfect CSIT with $N_t = 4$, $K = 4$ and $\sigma_e^2 = 0.8E_{tr}^{-0.6}$.

linear ones since they saturate faster and allocate more power to the common stream in order to deal with CSIT uncertainties.

In the fourth example, we consider that the SNR is fixed at 20dB. Table 4.4 summarizes the ESR performance of the ZF-based schemes at different levels of σ_e^2. Remark that the ZF-cTHP obtains a gain of approximately 11 bps/Hz at $\sigma_{e_i}^2 = 0.05$ when compared to the conventional ZF technique. However, as shown in Table 4.4, this gain decays as the variance of the error increases, reducing the gap between the ZF-THP schemes and linear ZF precoder. On the other hand, Fig. 4.11 presents the ESR obtained by the MMSE-based schemes. The quality of the CSIT estimate, i.e., $\sigma_{e_i}^2$, varies in $[0.02, 0.1]$. The MMSE-dTHP structures perform better than their corresponding MMSE-cTHP structures. From the results we can conclude that the RS-MMSE-dTHP-MMSEc scheme is the most robust strategy among the proposed ones. As expected, multiple antennas at the receiver increase the robustness of the system since the combiners allow the receivers to process multiple copies of the common symbol. Moreover, the robustness increases with the number of antennas at the receiver, i.e., the performance degrades less than conventional approaches even when the variance of the error increases.
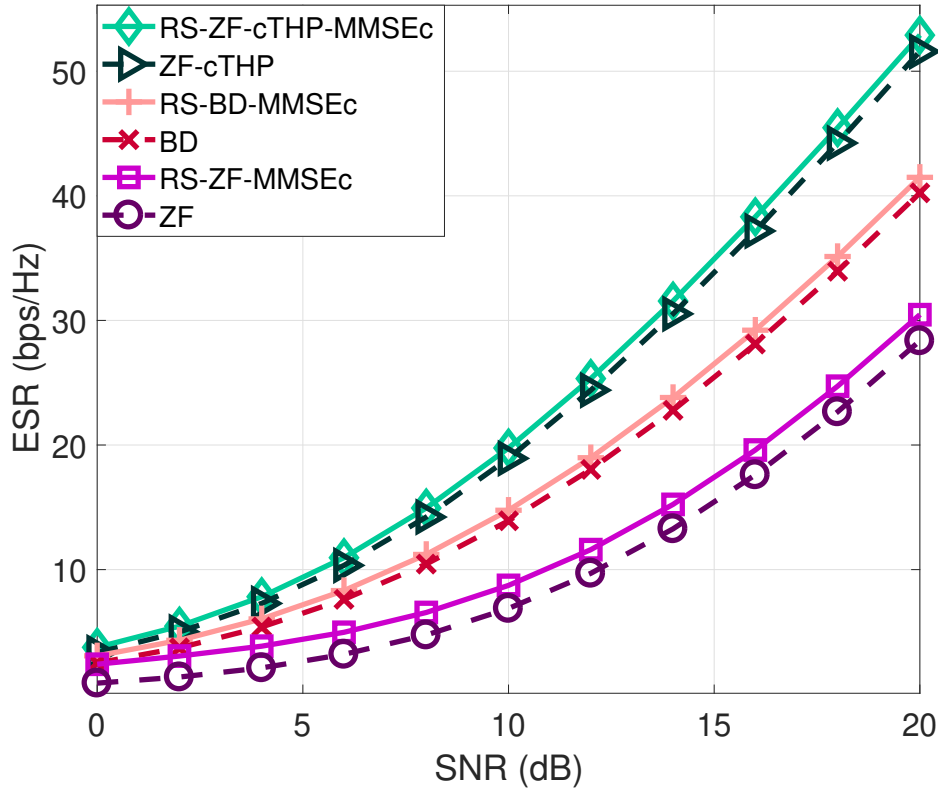
Figure 4.7: Sum-Rate Performance of ZF-based precoding schemes with Perfect CSIT, $N_t = 12$, $K = 6$, and $N_k = 2$.

Table 4.4: ESR performance of ZF-based schemes under different $\sigma_{e_i}^2$

Scheme	Error Variance		
	$\sigma_{e_i}^2 = 0.05$	$\sigma_{e_i}^2 = 0.1$	$\sigma_{e_i}^2 = 0.2$
ZF	9.88	6.56	3.90
ZF-cTHP	21.62	15.43	9.84
ZF-dTHP	28.21	21.45	14.78
RS-ZF-MMSEc	14.22	11.55	9.30
RS-ZF-cTHP-MMSEc	25.16	19.39	14.18
RS-ZF-dTHP-MMSEc	30.60	24.32	18.06

In Fig. 4.12, the power allocated by each technique to the common stream is shown. We can see that the power allocated to the common stream increases as the variance of the error in the channel estimate gets higher.
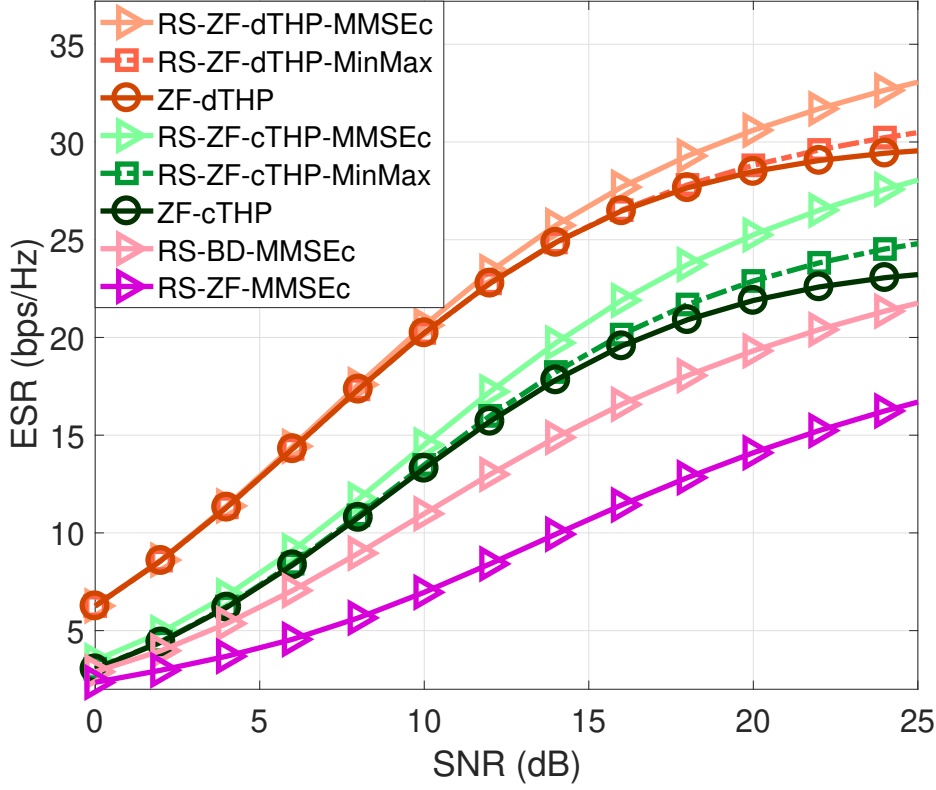
Figure 4.8: Sum-Rate Performance of ZF-based precoding schemes under imperfect CSIT with $N_t = 12$, $K = 6$, $N_k = 2$ and $\sigma_e^2 = 0.05$.

Linear precoders allocate more power to the common stream than non-linear techniques in order to deal with CSIT uncertainties since they saturate faster.

In the next example, we take into account that the quality of the CSIT improves as the SNR increases. We consider that each coefficient of $\tilde{\mathbf{H}}$ has a variance that scales as $\sigma_{e_i}^2 = 0.95(E_{tr})^{-0.6}$, which is inversely proportional to the SNR since the variance of the noise is fixed. Fig. 4.13 shows the results of the proposed strategies. Note that the curves in Fig. 4.13 show no saturation due the improvement in the CSIT quality.

We then consider the proposed RS-THP with the MB scheme. The term MB in the legends represents the number of branches employed in the simulation. We employ up to four branches with both the ZF-cTHP and ZF-dTHP structures. First, power allocation of the common stream is carried out. Once the power allocation is performed, multiple THP branches are explored in order to select the branch that leads to the best performance. Fig. 4.14 shows the result of the ZF-cTHP scheme. As expected, the best performance is obtained by the RS scheme with ZF-cTHP, four branches and the MMSEc combiner, denoted as RS-ZF-cTHP-MMSEc. On the other hand,
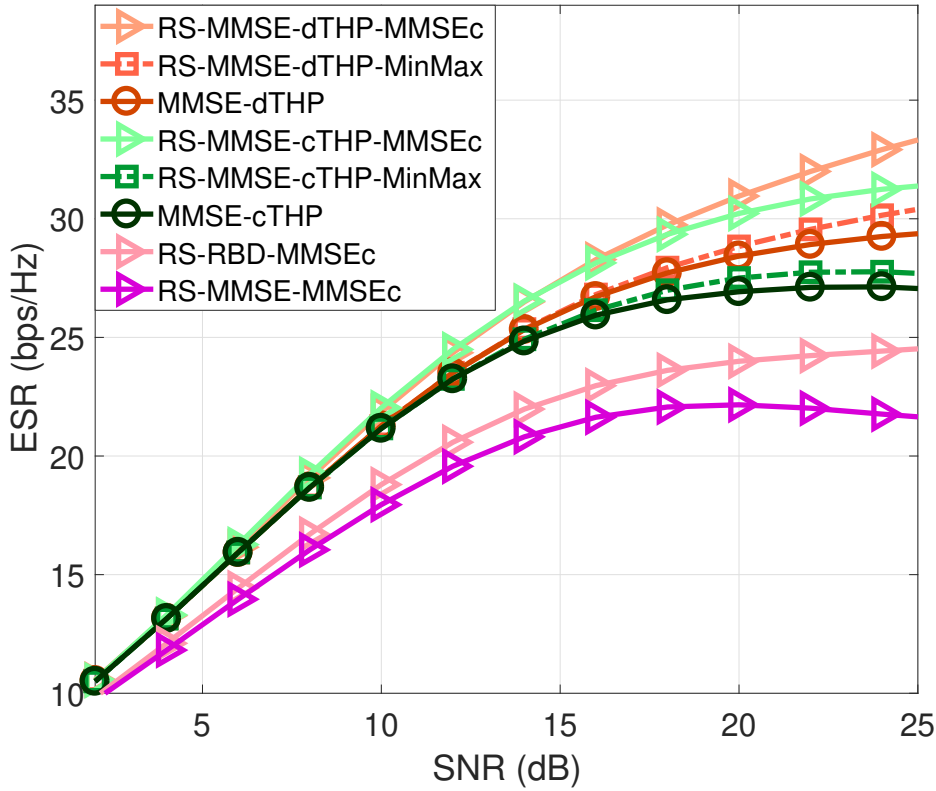
Figure 4.9: Sum-Rate Performance of MMSE-based precoding schemes under imperfect CSIT with $N_t = 12$, $K = 6$, $N_k = 2$ and $\sigma_e^2 = 0.05$.

Fig. 4.15 summarizes the results for the ZF-dTHP structure. Once again the best performance is obtained by the RS scheme with four branches of a ZF-dTHP precoder with an MMSE stream combiner, denoted as RS-ZF-dTHP-MMSEc.

In the last example, we asses the performance of the MMSE-THP precoder with MB. Once again, four branches were used to obtain the results shown in Fig. 4.16. The RS-MMSEc-cTHP-MMSEc with four braches attains the best performance. As expected, the MB technique improves the results obtained since it considers four different symbol orderings.

4.8
Summary

In this chapter THP-RS schemes have been proposed. Two different structures have been considered, namely the RS-cTHP and the RS-dTHP. Moreover, the SINR and sum-rate expressions have been derived to evaluate the performance of the proposed strategies with perfect and imperfect CSIT. We have also examined the sum-rate performance of ZF-DPC with and without
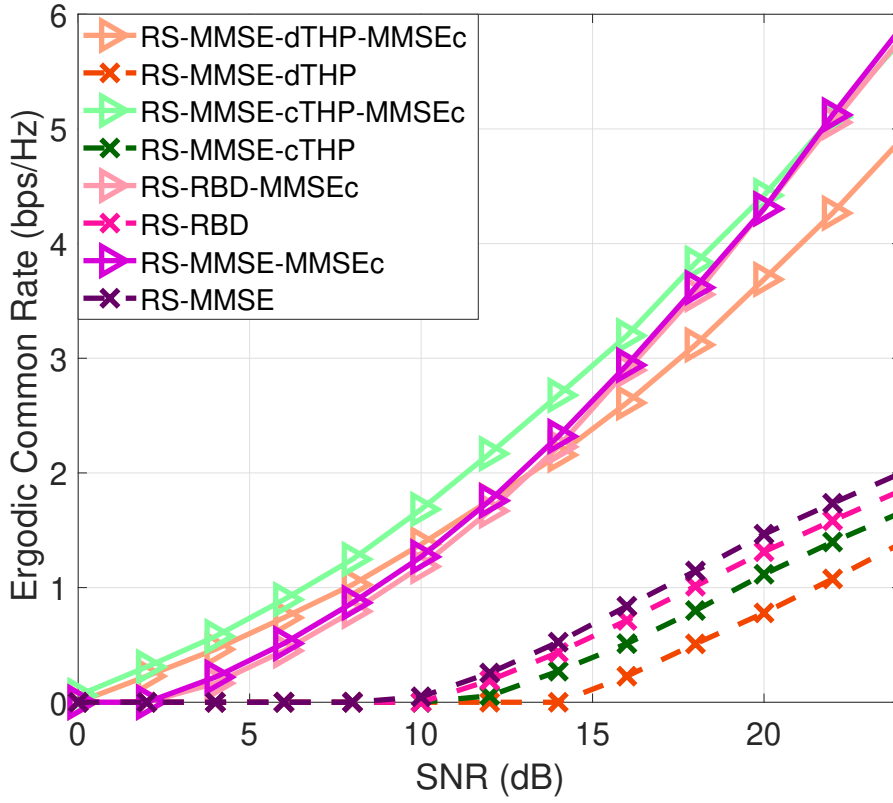
Figure 4.10: Common Rate Performance of MMSE-based schemes under imperfect CSIT with $N_t = 12$, $K = 6$, $N_k = 2$ and $\sigma^2_{e_i} = 0.05$.

RS for perfect and imperfect CSIT. We also evaluate the performance of a MIMO system employing RS and non-linear precoders with common combiners at the receivers. Simulation results have shown that the proposed RS-THP schemes can achieve higher sum rates than those of existing THP and linear schemes, and are more robust against imperfect CSIT than standard THP schemes. The common and private rates can be further enhanced by adopting the MB technique.
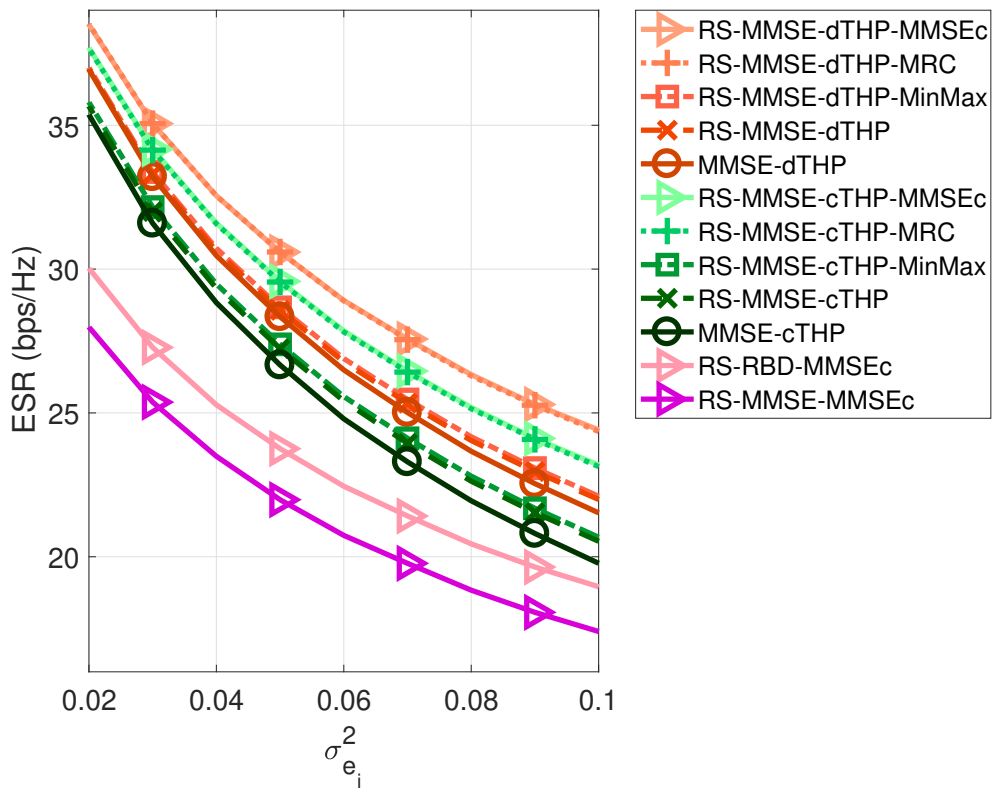
Figure 4.11: Sum-Rate Performance vs Error Variance at a SNR of 20 dB with $N_t = 12$, $K = 6$ and $N_k = 2$.

Figure 4.12: Power allocated to the common stream vs Error Variance at a SNR of 20 dB with $N_t = 12$, $K = 6$ and $N_k = 2$
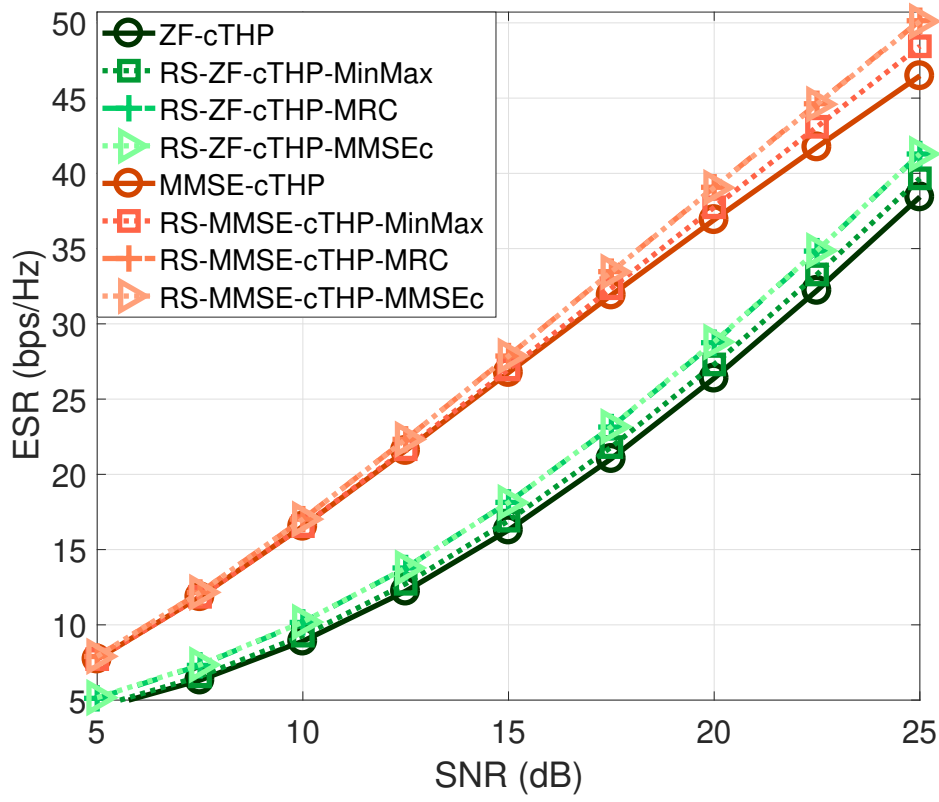
Figure 4.13: Sum-Rate Performance under imperfect CSIT with $N_t = 12$, $K = 6$, $N_k = 2$ and $\sigma_{e_i}^2 = 0.95(E_{tr})^{-0.6}$.
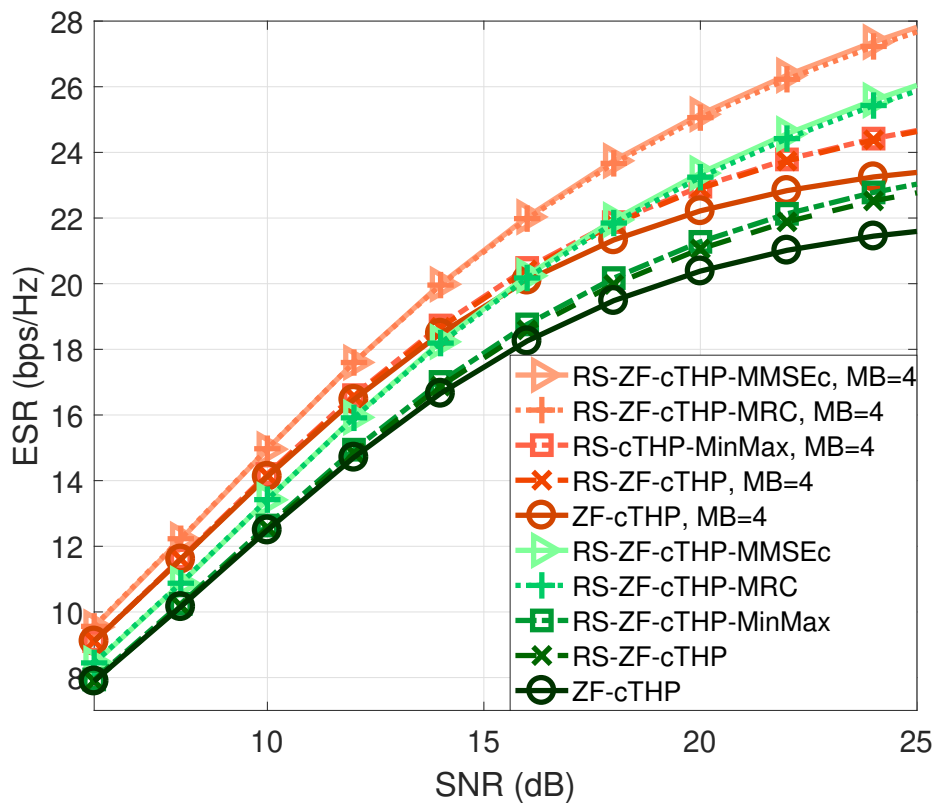
Figure 4.14: Sum-Rate Performance of the ZF-cTHP schemes considering 4 branches, $N_t = 12$, $K = 6$, $N_k = 2$, and $\sigma_{e_i}^2 = 0.06$.
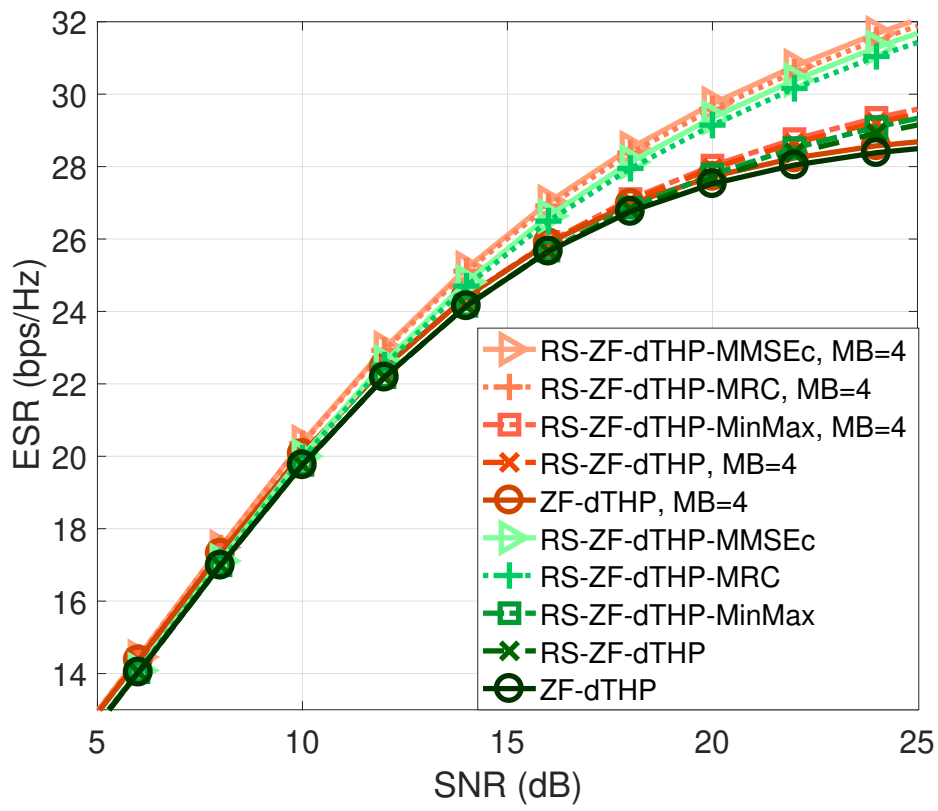
Figure 4.15: Sum-Rate Performance of the ZF-dTHP schemes considering 4 branches, $N_t = 12$, $K = 6$, $N_k = 2$, and $\sigma_{e_i}^2 = 0.06$.
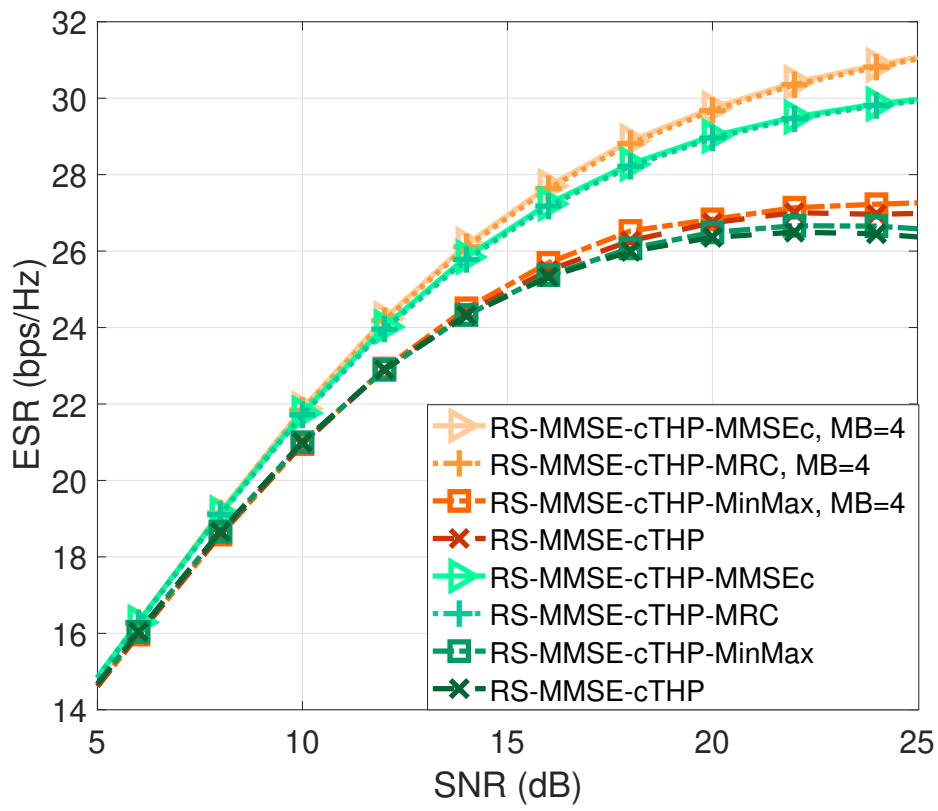
Figure 4.16: Sum-Rate Performance of the MMSE-cTHP schemes considering 4 branches, $N_t = 12$, $K = 6$, $N_k = 2$, and $\sigma_{e_i}^2 = 0.06$.

5
Adaptive and Robust Power Allocation Techniques

The overall performance of MU-MIMO systems depends on the design of several parameters, such as the precoder and the power allocation. In this sense, optimizing these parameters is a mandatory task to enhance the performance of wireless communications systems and better manage the available resources. The optimal solution, known as dirty paper coding (DPC), can be computed by solving an optimization problem involving a set of discrete and continuous variables. In general, this is an extremely complex task and leads to an increase in computational complexity, which in turn translates into a waste of time and resources. Therefore, suboptimal techniques are employed to guarantee the feasibility of the system. Such techniques can be obtained by relaxing or reformulating the original optimization problem, leading to practical solutions.

The power allocation problem becomes non-convex in a MU-MIMO scenario due to the MUI, which requires an exhaustive search over the entire space of possible values to find the optimal. Indeed, the power allocation problem is an NP-hard problem [71, 72], and the optimal is found at the expense of an exponential growth in computational complexity. Therefore suboptimal approaches that jointly optimize the precoder and the power allocation were developed. In [73], a MU-MIMO scenario where the users are equipped with single-antenna terminals is analyzed. In [74], the previous work is extended to consider UE with multiple antennas. Both approaches require the formulation and solution of geometric programming (GP) which is computationally demanding. In [75, 76], the optimal power allocation is found through monotonic optimization whereas in [77] convex optimization is used. Both techniques are computationally costly and require a large number of iterations. The connection between SINR and weighted sum rate (WSR) has been explored in [78]. Due to the complexity of the previous approaches, in [79, 80] local optima have been studied, reducing the complexity.

The power allocation strategy plays even a more critical role in RS systems because it significantly impacts their performance and robustness against imperfect CSIT. However, the design of a power allocation strategy for RS is more challenging since the common symbol is superimposed to the vector of symbols. If the power of the common and private streams is

not assigned correctly, the overall performance is dramatically degraded and other approaches such as NOMA and SDMA could perform better. So far in this thesis, an exhaustive search has been implemented to find the best power coefficient for the common stream. However, this greatly increases the amount of time devoted for transmit processing. Moreover, most works rely on the augmented WMMSE [21, 23, 81], which is an extension of the WMMSE proposed in [82], to perform the power allocation task. This approach requires also an alternating optimization, which increases the computational complexity. It turns out that power allocation is not only a challenging task, but also a crucial problem that needs to be solved.

In this chapter, we introduce adaptive and robust power allocation techniques to reduce the computational complexity of optimal techniques and to increase the robustness of the system against CSIT imperfections. Two of the proposed algorithms, referred here as adaptive power allocation (APA) and robust APA (APA-R), are first designed for conventional SDMA systems. Both algorithms employ the mean square error between the symbols and the received signal as the objective function. Then, a stochastic gradient descent algorithm is devised to reach its minimum value. The other two algorithms are specifically designed for RS systems. First, a linear transformation is applied to the received signal to match the dimensions of the transmitted vector. Then, a minimization of the MMSE is formulated and a stochastic gradient descent algorithm is developed in a similar fashion to the development of the previous algorithms. Since the focus of this chapter is to present power allocation techniques, we consider for simplicity that the communication systems employs linear precoders, such as the MF and the ZF precoders.

The rest of this chapter is organized as follows. In Section 5.1 the system model is described. Then, in Section 5.2, the adaptive power allocation algorithm is presented and in Section 5.3 a robust version of this algorithm is introduced. An adaptive power allocation for RS systems is derived in Section 5.4, whereas a robust version of this algorithm is described in 5.5. Section 5.7 depicts the simulations results obtained by the proposed algorithms. Finally, Section 5.8 summarizes this chapter.

5.1
System Model

Let us consider an RS MU-MIMO system architecture where the BS is equipped with N_t antennas and the kth UE is equipped with N_k antennas. The message of one user is split into a common message and a private message, similar to previous chapters. The vector $\mathbf{s}^{(\mathrm{RS})} = [s_c, \mathbf{s}_p]^{\mathrm{T}}$ contains

the information transmitted to all users, where $s_c \in \mathbb{C}^{N_k}$ is common symbol and $\mathbf{s}_p = \left[\mathbf{s}_1^{\mathrm{T}}, \mathbf{s}_2^{\mathrm{T}}, \cdots, \mathbf{s}_K^{\mathrm{T}}\right]^{\mathrm{T}}$ contains the private symbols of all users. The transmitted vector can be expressed as follows:

$$
\begin{aligned}
\mathbf{x}^{(\mathrm{RS})} =& \mathbf{P}^{(\mathrm{RS})}\mathbf{A}^{(\mathrm{RS})}\mathbf{s}^{(\mathrm{RS})} = \mathbf{P}^{(\mathrm{RS})}\mathrm{diag}\left(\mathbf{a}^{(\mathrm{RS})}\right)\mathbf{s}^{(\mathrm{RS})} \\
=& a_c s_c \mathbf{p}_c + \sum_{m=1}^{M} a_m s_m \mathbf{p}_m.
\end{aligned}
\tag{5-1}
$$

The power loading matrix $\mathbf{A}^{(\mathrm{RS})} \in \mathbb{R}^{M+1 \times M+1}$ contains the weights that allocate the power to each data stream. The system is subject to transmit power constraint given by $\mathbb{E}\left[\mathbf{x}^{(\mathrm{RS})}\right] \leq E_{tr}$, where $\mathbf{x}^{(\mathrm{RS})} \in \mathbb{C}^{N_t}$ is the transmitted vector and E_{tr} denotes the total available power. The model established lead us to the following received signal:

$$
\mathbf{y} = \mathbf{HP}^{(\mathrm{RS})}\mathrm{diag}\left(\mathbf{a}^{(\mathrm{RS})}\right)\mathbf{s}^{(\mathrm{RS})} + \mathbf{n},
\tag{5-2}
$$

where $\mathbf{n} \in \mathbb{C}^{N_r}$ represents the uncorrelated noise vector, which follows a complex normal distribution, i.e., $\mathbf{n} \sim \mathcal{CN}\left(\mathbf{0}, \sigma_n^2\mathbf{I}\right)$. From (5-2) we can obtain the received signal per user, which is given by

$$
\mathbf{y}_k = a_c s_c \mathbf{H}_k \mathbf{p}_c + \mathbf{H}_k \sum_{i \in \mathcal{M}_k} a_i^{(k)} s_i^{(k)} \mathbf{p}_i^{(k)} + \mathbf{H}_k \sum_{\substack{l=1 \\ l \neq k}}^{K} \sum_{j \in \mathcal{M}_l} a_j^{(l)} s_j^{(l)} \mathbf{p}_j^{(l)} + \mathbf{n}_k
\tag{5-3}
$$

Considering a conventional MU-MIMO architecture, no message is split and a_c is set to zero. Then, the model is described by

$$
\mathbf{y} = \mathbf{HP}\mathrm{diag}\left(\mathbf{a}\right)\mathbf{s} + \mathbf{n},
\tag{5-4}
$$

where the received signal at the kth user is given by

$$
\mathbf{y}_k = \mathbf{H}_k \sum_{i \in \mathcal{M}_k} a_i^{(k)} s_i^{(k)} \mathbf{p}_i^{(k)} + \mathbf{H}_k \sum_{\substack{l=1 \\ l \neq k}}^{K} \sum_{j \in \mathcal{M}_l} a_j^{(l)} s_j^{(l)} \mathbf{p}_j^{(l)} + \mathbf{n}_k
\tag{5-5}
$$

5.2
Adaptive Power Allocation

Let us first consider the conventional MU-MIMO model described by (5-4) and (5-5). Assuming knowledge of the precoder which remains fixed during the transmission of a packet and also considering perfect CSIT, the problem is to find suitable values for the coefficients $a_i \ \forall \ i = 1, 2, \cdots, N_r$ to enhance the overall performance of the system. For this purpose let us consider the minimum mean square error (MMSE) between the transmitted signal and the estimated signal at the receiver as the objective function. Then, we have

$$\min_{\mathbf{a}} \mathbb{E}\left[\varepsilon\right]$$

$$\text{s.t.} \quad \text{tr}\left(\mathbf{P}\text{diag}\left(\mathbf{a}\odot\mathbf{a}\right)\mathbf{P}^{H}\right) = \frac{E_{tr}}{\sigma_{s}^{2}}, \tag{5-6}$$

where the error is defined as $\varepsilon = \|\mathbf{s}_p - \mathbf{y}\|^2$. Evaluating the error we get

$$\begin{aligned}
\varepsilon =& \|\mathbf{s}_p - \mathbf{HP}\text{diag}\left(\mathbf{a}\right)\mathbf{s}_p - \mathbf{n}\|^2 \\
=& \mathbf{s}_p^H \mathbf{s}_p - \mathbf{s}^H \mathbf{HP}\text{diag}\left(\mathbf{a}\right)\mathbf{s}_p + \mathbf{s}_p^H \text{diag}\left(\mathbf{a}\right)\mathbf{P}^H\mathbf{H}^H\mathbf{HP}\text{diag}\left(\mathbf{a}\right)\mathbf{s}_p \\
& - \mathbf{s}_p^H \mathbf{n} - \mathbf{s}_p^H \text{diag}\left(\mathbf{a}\right)\mathbf{P}^H\mathbf{H}^H\mathbf{s}_p + \mathbf{s}_p^H \text{diag}\left(\mathbf{a}\right)\mathbf{P}^H\mathbf{H}^H\mathbf{n} - \mathbf{n}^H\mathbf{s}_p \\
& + \mathbf{n}^H \mathbf{HP}\text{diag}\left(\mathbf{a}\right)\mathbf{s}_p + \mathbf{n}^H\mathbf{n}. \tag{5-7}
\end{aligned}$$

Remark that equation (5-7) is a scalar. Thus we can apply the trace operator over the right-hand side of the equation while preserving the equality. By applying the property $\text{tr}\left(\mathbf{C}+\mathbf{D}\right) = \text{tr}\left(\mathbf{C}\right) + \text{tr}\left(\mathbf{D}\right)$, where $\mathbf{C}$ and $\mathbf{D}$ are two general matrices with the same dimension, we obtain

$$\begin{aligned}
\varepsilon =& \text{tr}\left(\mathbf{s}_p^H\mathbf{s}_p\right) - \text{tr}\left(\mathbf{s}_p^H\mathbf{HP}\text{diag}\left(\mathbf{a}\right)\mathbf{s}_p\right) + \text{tr}\left(\mathbf{s}_p^H\text{diag}\left(\mathbf{a}\right)\mathbf{P}^H\mathbf{H}^H\mathbf{HP}\text{diag}\left(\mathbf{a}\right)\mathbf{s}_p\right) \\
& - \text{tr}\left(\mathbf{s}_p^H\mathbf{n}\right) - \text{tr}\left(\mathbf{s}_p^H\text{diag}\left(\mathbf{a}\right)\mathbf{P}^H\mathbf{H}^H\mathbf{s}_p\right) + \text{tr}\left(\mathbf{s}_p^H\text{diag}\left(\mathbf{a}\right)\mathbf{P}^H\mathbf{H}^H\mathbf{n}\right) \\
& - \text{tr}\left(\mathbf{n}^H\mathbf{s}_p\right) + \text{tr}\left(\mathbf{n}^H\mathbf{HP}\text{diag}\left(\mathbf{a}\right)\mathbf{s}_p\right) + \text{tr}\left(\mathbf{n}^H\mathbf{n}\right). \tag{5-8}
\end{aligned}$$

Taking the expected value of (5-8) leads us to

$$\begin{aligned}
\mathbb{E}\left[\varepsilon\right] =& \text{tr}\left(\mathbf{R_s}\right) - \text{tr}\left(\mathbf{HP}\text{diag}\left(\mathbf{a}\right)\mathbf{R_s}\right) + \text{tr}\left(\text{diag}\left(\mathbf{a}\right)\mathbf{P}^H\mathbf{H}^H\mathbf{HP}\text{diag}\left(\mathbf{a}\right)\mathbf{R_s}\right) \\
& - \text{tr}\left(\text{diag}\left(\mathbf{a}\right)\mathbf{P}^H\mathbf{H}^H\mathbf{R_s}\right) + \text{tr}\left(\mathbf{R_n}\right), \\
=& N_r\sigma_s^2 - \sigma_s^2\text{tr}\left(\mathbf{HP}\text{diag}\left(\mathbf{a}\right)\right) + \sigma_s^2\text{tr}\left(\text{diag}\left(\mathbf{a}\right)\mathbf{P}^H\mathbf{H}^H\mathbf{HP}\text{diag}\left(\mathbf{a}\right)\right) \\
& - \sigma_s^2\text{tr}\left(\text{diag}\left(\mathbf{a}\right)\mathbf{P}^H\mathbf{H}^H\right) + N_r\sigma_n^2, \tag{5-9}
\end{aligned}$$

where the elements of the input vector are assumed uncorrelated. By taking the derivative of (5-9) with respect to power loading matrix $\mathbf{A}$ and using the equality $\frac{\partial \text{tr}(\mathbf{CD})}{\partial \mathbf{C}} = \mathbf{D}\odot\mathbf{I}$, where $\mathbf{C}$ is a diagonal matrix the operator $\odot$ is the Hadamard product, we obtain

$$\begin{aligned}
\frac{\partial \mathbb{E}\left[\varepsilon\right]}{\partial \mathbf{A}} =& 2\sigma_s^2\left(\mathbf{P}^H\mathbf{H}^H\mathbf{HP}\text{diag}\left(\mathbf{a}\right)\right)\odot\mathbf{I} - \sigma_s^2\left(\mathbf{P}^H\mathbf{H}^H\right)\odot\mathbf{I} - \sigma_s^2\left(\mathbf{HP}\right)\odot\mathbf{I} \\
=& 2\sigma_s^2\left(\mathbf{P}^H\mathbf{H}^H\mathbf{HP}\text{diag}\left(\mathbf{a}\right)\right)\odot\mathbf{I} - 2\sigma_s^2\Re\left\{\left(\mathbf{HP}\right)\odot\mathbf{I}\right\} \tag{5-10}
\end{aligned}$$

Employing a stochastic gradient descent approach we obtain the following

update equation:

$$
\begin{aligned}
\mathbf{a}\left[i\right] =&\mathbf{a}\left[i-1\right]-\mu\frac{\partial\mathbb{E}\left[\varepsilon\right]}{\partial\mathbf{A}}\\
=&\mathbf{a}\left[i-1\right]-\mu\sigma_s^2\left(\left(\mathbf{P}^H\mathbf{H}^H\mathbf{H}\mathbf{P}\mathrm{diag}\left(\mathbf{a}\left[i-1\right]\right)\right)\odot\mathbf{I}-\Re\left\{\left(\mathbf{H}\mathbf{P}\right)\odot\mathbf{I}\right\}\right),
\end{aligned}
$$
(5-11)

where μ is the step size that governs the learning rate of the adaptive algorithm. After each iteration the coefficients are properly scaled employing a power scaling factor β to satisfy the transmit power constraint. Fig. 5.1 shows the curves of (5-6) for three different linear precoders where only two streams are being transmitted. Fig. 5.2 expands the previous graphic to consider the MMSE precoder with three data streams. In both cases the function is convex. Algorithm 2 summarizes the proposed algorithm.
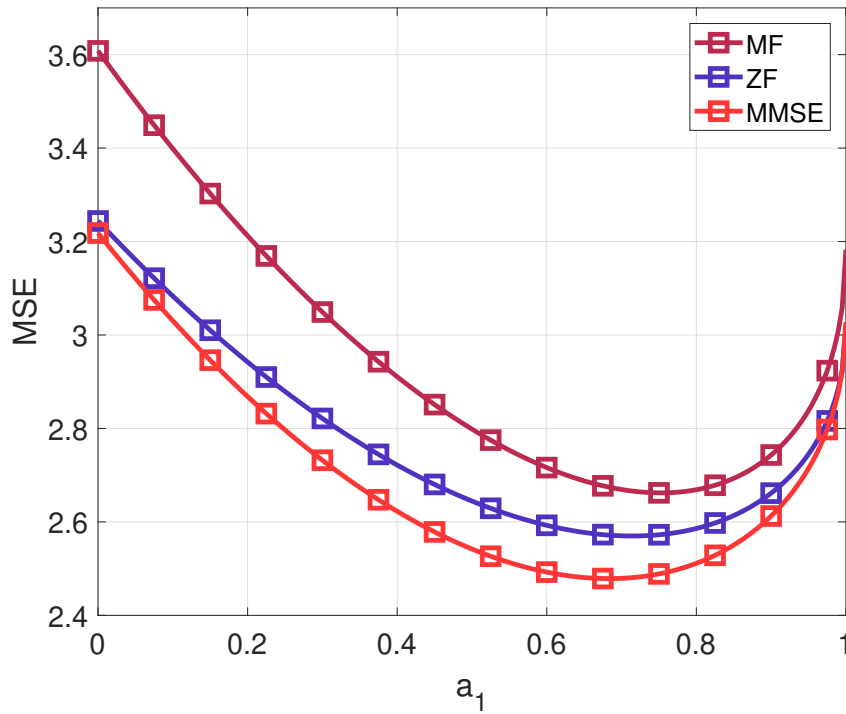
Figure 5.1: Objective function: MSE with two streams
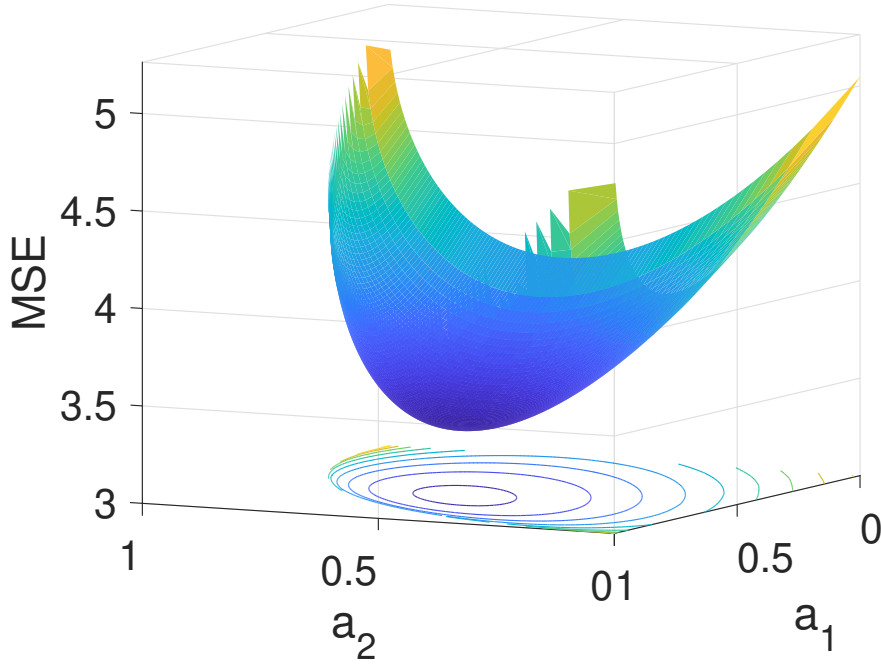
Figure 5.2: Objective function: MSE with three streams

Algorithm 2: MMSE Adaptive Power allocation

---

1 given $\mathbf{H}, \mathbf{P}$ and μ;

2 $\mathbf{a}\left[1\right] = \mathbf{0}$;

3 **for** $i = 2$ **to** I_t **do**

4 $\quad \frac{\mathbb{E}[\varepsilon]}{\partial \mathbf{A}} = 2\sigma_s^2 \left(\mathbf{P}^H \mathbf{H}^H \mathbf{H} \mathbf{P} \text{diag}\left(\mathbf{a}\left[i-1\right]\right)\right) \odot \mathbf{I} - 2\sigma_s^2 \Re\left\{(\mathbf{H}\mathbf{P}) \odot \mathbf{I}\right\}$;

5 $\quad \mathbf{a}\left[i\right] = \mathbf{a}\left[i-1\right] - \mu\frac{\partial \mathbb{E}[\varepsilon]}{\partial \mathbf{A}}$;

6 $\quad$ **if** $\text{tr}\left(\text{diag}\left(\mathbf{a}\left[i\right] \odot \mathbf{a}\left[i\right]\right)\right) \neq 1$ **then**

7 $\quad\quad \beta = \sqrt{\frac{1}{\text{tr}(\text{diag}(\mathbf{a}[i] \odot \mathbf{a}[i]))}}$;

8 $\quad\quad \mathbf{a}\left[i\right] = \beta\mathbf{a}\left[i\right]$;

9 $\quad$ **end**

10 **end**

Closed-Form Power Allocation

A closed-form power allocation solution can be obtained by equating (5-10) to zero, which leads us to

$$\underbrace{\left(\mathbf{P}^H \mathbf{H}^H \mathbf{H} \mathbf{P} \text{diag}\left(\mathbf{a}\right)\right) \odot \mathbf{I}}_{\text{I}} = \underbrace{\Re\left\{(\mathbf{H}\mathbf{P}) \odot \mathbf{I}\right\}}_{\text{II}} \qquad (5\text{-}12)$$

The matrix on the left-hand side of the last equation can be expanded as

$$\text{diag} \begin{bmatrix} a_1 \sum_{i=1}^{N_r} |\mathbf{h}_{i,*}\mathbf{p}_1|^2 + a_2 \sum_{j=1}^{N_r} \mathbf{p}_1^H \mathbf{h}_{j,*}^H \mathbf{h}_{j,*}\mathbf{p}_2 + \cdots + a_{N_r} \sum_{q=1}^{N_r} \mathbf{p}_1^H \mathbf{h}_{q,*}^H \mathbf{h}_{q,*}\mathbf{p}_{N_r} \\ a_1 \sum_{i=1}^{N_r} \mathbf{p}_2^H \mathbf{h}_{i,*}^H \mathbf{h}_{i,*}\mathbf{p}_1 + a_2 \sum_{j=1}^{N_r} |\mathbf{h}_{j,*}\mathbf{p}_2|^2 + \cdots + a_{N_r} \sum_{q=1}^{N_r} \mathbf{p}_2^H \mathbf{h}_{q,*}^H \mathbf{h}_{q,*}\mathbf{p}_{N_r} \\ \vdots \\ a_1 \sum_{i=1}^{N_r} \mathbf{p}_{N_r}^H \mathbf{h}_{i,*}^H \mathbf{h}_{i,*}\mathbf{p}_1 + a_2 \sum_{j=1}^{N_r} \mathbf{p}_{N_r}^H \mathbf{h}_{j,*}^H \mathbf{h}_{j,*}\mathbf{p}_2 + \cdots + a_{N_r} \sum_{q=1}^{N_r} |\mathbf{h}_{q,*}\mathbf{p}_{N_r}|^2 \end{bmatrix}. \tag{5-13}$$

The diagonal of matrix (5-13) can be rewritten as a vector as follows:

$$\mathrm{I} = \mathbf{Ja}, \tag{5-14}$$

where we introduced the auxiliary matrix $\mathbf{J}$, such that each element of the matrix is defined by

$$j_{i,j} = \sum_{q=1}^{N_r} \mathbf{p}_i^H \mathbf{h}_{q,*}^H \mathbf{h}_{q,*} \mathbf{p}_j. \tag{5-15}$$

Then, the main diagonal of the right-hand side of (5-12) can be expressed by

$$\mathbf{c} = \begin{bmatrix} \mathbf{h}_{1,*}\mathbf{p}_1 \\ \mathbf{h}_{2,*}\mathbf{p}_2 \\ \vdots \\ \mathbf{h}_{N_r,*}\mathbf{p}_{N_r} \end{bmatrix} \tag{5-16}$$

We found that

$$\mathbf{Ja} = \mathbf{c}. \tag{5-17}$$

Thus, the power loading matrix can be obtained by computing the following:

$$\mathbf{a} = \mathbf{J}^{-1}\mathbf{c}. \tag{5-18}$$

5.3
Robust Power Allocation

The techniques presented in the previous section assume perfect CSIT knowledge. However, this assumption is rather optimistic, as mentioned in Chapter 2. Hence, in this section an adaptive power allocation technique that takes into account CSIT imperfections is developed. Let us consider the square of the error function given by

$$\begin{aligned} \varepsilon = &\|\mathbf{s}_p - \left(\hat{\mathbf{H}} + \tilde{\mathbf{H}}\right)\mathbf{P}\text{diag}\left(\mathbf{a}\right)\mathbf{s}_p - \mathbf{n}\|^2, \\ = &\|\mathbf{s}_p - \hat{\mathbf{H}}\mathbf{P}\text{diag}\left(\mathbf{a}\right)\mathbf{s}_p - \tilde{\mathbf{H}}\mathbf{P}\text{diag}\left(\mathbf{a}\right)\mathbf{s}_p - \mathbf{n}\|^2. \end{aligned} \tag{5-19}$$

By expanding the terms, we have

$$
\begin{aligned}
\varepsilon = & \left(\mathbf{s}_p - \left(\hat{\mathbf{H}} + \tilde{\mathbf{H}} \right) \mathbf{P} \mathrm{diag} \left(\mathbf{a} \right) \mathbf{s}_p - \mathbf{n} \right)^H \left(\mathbf{s}_p - \left(\hat{\mathbf{H}} + \tilde{\mathbf{H}} \right) \mathbf{P} \mathrm{diag} \left(\mathbf{a} \right) \mathbf{s}_p - \mathbf{n} \right) \\
= & \mathbf{s}_p^H \mathbf{s}_p - \mathbf{s}_p^H \hat{\mathbf{H}} \mathbf{P} \mathrm{diag} \left(\mathbf{a} \right) \mathbf{s}_p + \mathbf{s}_p^H \mathrm{diag} \left(\mathbf{a} \right) \mathbf{P}^H \hat{\mathbf{H}}^H \hat{\mathbf{H}} \mathbf{P} \mathrm{diag} \left(\mathbf{a} \right) \mathbf{s}_p \\
& + \mathbf{s}_p^H \mathrm{diag} \left(\mathbf{a} \right) \mathbf{P}^H \hat{\mathbf{H}}^H \mathbf{s}_p + \mathbf{n}^H \mathbf{n} - \mathbf{s}_p^H \tilde{\mathbf{H}} \mathbf{P} \mathrm{diag} \left(\mathbf{a} \right) \mathbf{s}_p - \mathbf{s}_p^H \mathbf{n} \\
& + \mathbf{s}_p^H \mathrm{diag} \left(\mathbf{a} \right) \mathbf{P}^H \tilde{\mathbf{H}}^H \tilde{\mathbf{H}} \mathbf{P} \mathrm{diag} \left(\mathbf{a} \right) \mathbf{s}_p - \mathbf{s}_p^H \mathrm{diag} \left(\mathbf{a} \right) \mathbf{P}^H \tilde{\mathbf{H}}^H \mathbf{s}_p \\
& + \mathbf{s}_p^H \mathrm{diag} \left(\mathbf{a} \right) \mathbf{P}^H \hat{\mathbf{H}}^H \tilde{\mathbf{H}} \mathbf{P} \mathrm{diag} \left(\mathbf{a} \right) \mathbf{s}_p + \mathbf{s}_p^H \mathrm{diag} \left(\mathbf{a} \right) \mathbf{P}^H \tilde{\mathbf{H}}^H \hat{\mathbf{H}} \mathbf{P} \mathrm{diag} \left(\mathbf{a} \right) \mathbf{s}_p \\
& + \mathbf{s}_p^H \mathrm{diag} \left(\mathbf{a} \right) \hat{\mathbf{H}}^H \mathbf{P}^H \mathbf{n} + \mathbf{s}_p^H \mathrm{diag} \left(\mathbf{a} \right) \tilde{\mathbf{H}}^H \mathbf{P}^H \mathbf{n} - \mathbf{n}^H \mathbf{s}_p \\
& + \mathbf{n}^H \hat{\mathbf{H}} \mathbf{P} \mathrm{diag} \left(\mathbf{a} \right) \mathbf{s}_p + \mathbf{n}^H \tilde{\mathbf{H}} \mathbf{P} \mathrm{diag} \left(\mathbf{a} \right) \mathbf{s}_p .
\end{aligned}
\tag{5-20}
$$

Including the trace operator over the right-hand side and rearranging terms we get

$$
\begin{aligned}
\varepsilon = & \mathrm{tr} \left(\mathbf{s}_p \mathbf{s}_p^H \right) - \mathrm{tr} \left(\hat{\mathbf{H}} \mathbf{P} \mathrm{diag} \left(\mathbf{a} \right) \mathbf{s}_p \mathbf{s}_p^H \right) + \mathrm{tr} \left(\mathrm{diag} \left(\mathbf{a} \right) \mathbf{P}^H \hat{\mathbf{H}}^H \hat{\mathbf{H}} \mathbf{P} \mathrm{diag} \left(\mathbf{a} \right) \mathbf{s}_p \mathbf{s}_p^H \right) \\
& + \mathrm{tr} \left(\mathrm{diag} \left(\mathbf{a} \right) \mathbf{P}^H \hat{\mathbf{H}}^H \mathbf{s}_p \mathbf{s}_p^H \right) + \mathrm{tr} \left(\mathbf{n} \mathbf{n}^H \right) - \mathrm{tr} \left(\tilde{\mathbf{H}} \mathbf{P} \mathrm{diag} \left(\mathbf{a} \right) \mathbf{s}_p \mathbf{s}_p^H \right) \\
& + \mathrm{tr} \left(\mathrm{diag} \left(\mathbf{a} \right) \mathbf{P}^H \tilde{\mathbf{H}}^H \tilde{\mathbf{H}} \mathbf{P} \mathrm{diag} \left(\mathbf{a} \right) \mathbf{s}_p \mathbf{s}_p^H \right) - \mathrm{tr} \left(\mathrm{diag} \left(\mathbf{a} \right) \mathbf{P}^H \tilde{\mathbf{H}}^H \mathbf{s}_p \mathbf{s}_p^H \right) \\
& + \mathrm{tr} \left(\mathrm{diag} \left(\mathbf{a} \right) \mathbf{P}^H \hat{\mathbf{H}}^H \tilde{\mathbf{H}} \mathbf{P} \mathrm{diag} \left(\mathbf{a} \right) \mathbf{s}_p \mathbf{s}_p^H \right) - \mathrm{tr} \left(\mathbf{n} \mathbf{s}_p^H \right) \\
& + \mathrm{tr} \left(\mathrm{diag} \left(\mathbf{a} \right) \hat{\mathbf{H}}^H \mathbf{P}^H \mathbf{n} \mathbf{s}_p^H \right) + \mathrm{tr} \left(\mathrm{diag} \left(\mathbf{a} \right) \tilde{\mathbf{H}}^H \mathbf{P}^H \mathbf{n} \mathbf{s}_p^H \right) - \mathrm{tr} \left(\mathbf{s}_p \mathbf{n}^H \right) \\
& + \mathrm{tr} \left(\hat{\mathbf{H}} \mathbf{P} \mathrm{diag} \left(\mathbf{a} \right) \mathbf{s}_p \mathbf{n}^H \right) + \mathrm{tr} \left(\tilde{\mathbf{H}} \mathbf{P} \mathrm{diag} \left(\mathbf{a} \right) \mathbf{s}_p \mathbf{n}^H \right) \\
& + \mathrm{tr} \left(\mathrm{diag} \left(\mathbf{a} \right) \mathbf{P}^H \tilde{\mathbf{H}}^H \hat{\mathbf{H}} \mathbf{P} \mathrm{diag} \left(\mathbf{a} \right) \mathbf{s}_p \mathbf{s}_p^H \right) .
\end{aligned}
\tag{5-21}
$$

Taking the expected value we get

$$
\begin{aligned}
\mathbb{E}_{\mathbf{s}|\mathbf{H}} \left[\varepsilon \,|\, \mathbf{H} \right] = & \mathrm{tr} \left(\mathbf{R_s} \right) - \mathrm{tr} \left(\hat{\mathbf{H}} \mathbf{P} \mathrm{diag} \left(\mathbf{a} \right) \mathbf{R_s} \right) + \mathrm{tr} \left(\mathbf{R_n} \right) - \mathrm{tr} \left(\tilde{\mathbf{H}} \mathbf{P} \mathrm{diag} \left(\mathbf{a} \right) \mathbf{R_s} \right) \\
& - \mathrm{tr} \left(\mathrm{diag} \left(\mathbf{a} \right) \mathbf{P}^H \hat{\mathbf{H}}^H \mathbf{R_s} \right) + \mathrm{tr} \left(\mathrm{diag} \left(\mathbf{a} \right) \mathbf{P}^H \hat{\mathbf{H}}^H \hat{\mathbf{H}} \mathbf{P} \mathrm{diag} \left(\mathbf{a} \right) \mathbf{R_s} \right) \\
& + \mathrm{tr} \left(\mathrm{diag} \left(\mathbf{a} \right) \mathbf{P}^H \tilde{\mathbf{H}}^H \tilde{\mathbf{H}} \mathbf{P} \mathrm{diag} \left(\mathbf{a} \right) \mathbf{R_s} \right) - \mathrm{tr} \left(\mathrm{diag} \left(\mathbf{a} \right) \mathbf{P}^H \tilde{\mathbf{H}}^H \mathbf{R_s} \right) \\
& + \mathrm{tr} \left(\mathrm{diag} \left(\mathbf{a} \right) \mathbf{P}^H \hat{\mathbf{H}}^H \tilde{\mathbf{H}} \mathbf{P} \mathrm{diag} \left(\mathbf{a} \right) \mathbf{R_s} \right) \\
& + \mathrm{tr} \left(\mathrm{diag} \left(\mathbf{a} \right) \mathbf{P}^H \tilde{\mathbf{H}}^H \hat{\mathbf{H}} \mathbf{P} \mathrm{diag} \left(\mathbf{a} \right) \mathbf{R_s} \right)
\end{aligned}
$$

$$
\tag{5-22}
$$

Note that the system has only access to $\hat{\mathbf{H}}$. Moreover, the entries of $\tilde{\mathbf{H}}$ are independent from the elements in $\hat{\mathbf{H}}$. Then, taking the expected value with

respect to $\tilde{\mathbf{H}}$, we obtain

$$
\begin{aligned}
\mathbb{E}_{\tilde{\mathbf{H}}}\left[\varepsilon|\hat{\mathbf{H}}\right] =& \operatorname{tr}\left(\mathbf{R_s}\right) - \operatorname{tr}\left(\hat{\mathbf{H}}\mathbf{P}\operatorname{diag}\left(\mathbf{a}\right)\mathbf{R_s}\right) + \operatorname{tr}\left(\operatorname{diag}\left(\mathbf{a}\right)\mathbf{P}^H\hat{\mathbf{H}}^H\hat{\mathbf{H}}\mathbf{P}\operatorname{diag}\left(\mathbf{a}\right)\mathbf{R_s}\right) \\
& - \operatorname{tr}\left(\operatorname{diag}\left(\mathbf{a}\right)\mathbf{P}^H\hat{\mathbf{H}}\mathbf{R_s}\right) + \operatorname{tr}\left(\mathbf{R_n}\right) - \operatorname{tr}\left(\mathbb{E}\left[\tilde{\mathbf{H}}^H\right]\mathbf{P}\operatorname{diag}\left(\mathbf{a}\right)\mathbf{R_s}\right) \\
& + \operatorname{tr}\left(\operatorname{diag}\left(\mathbf{a}\right)\mathbf{P}^H\mathbb{E}\left[\tilde{\mathbf{H}}^H\tilde{\mathbf{H}}\right]\mathbf{P}\operatorname{diag}\left(\mathbf{a}\right)\mathbf{R_s}\right) \\
& - \operatorname{tr}\left(\operatorname{diag}\left(\mathbf{a}\right)\mathbf{P}^H\mathbb{E}\left[\tilde{\mathbf{H}}^H\right]\mathbf{R_s}\right) \\
& + \operatorname{tr}\left(\operatorname{diag}\left(\mathbf{a}\right)\mathbf{P}^H\hat{\mathbf{H}}^H\mathbb{E}\left[\tilde{\mathbf{H}}\right]\mathbf{P}\operatorname{diag}\left(\mathbf{a}\right)\mathbf{R_s}\right) \\
& + \operatorname{tr}\left(\operatorname{diag}\left(\mathbf{a}\right)\mathbf{P}^H\mathbb{E}\left[\tilde{\mathbf{H}}^H\tilde{\mathbf{H}}\right]\mathbf{P}\operatorname{diag}\left(\mathbf{a}\right)\mathbf{R_s}\right).
\end{aligned} \tag{5-23}
$$

Let us consider that $\tilde{\mathbf{h}}_k$ is a random vector with zero mean and independent from $\tilde{\mathbf{h}}_j$ with $j \neq k$. By simplifying (5-23), we arrive at

$$
\begin{aligned}
\mathbb{E}_{\tilde{\mathbf{H}}}\left[\varepsilon|\hat{\mathbf{H}}\right] =& \operatorname{tr}\left(\mathbf{R_s}\right) - \operatorname{tr}\left(\hat{\mathbf{H}}\mathbf{P}\operatorname{diag}\left(\mathbf{a}\right)\mathbf{R_s}\right) + \operatorname{tr}\left(\operatorname{diag}\left(\mathbf{a}\right)\mathbf{P}^H\hat{\mathbf{H}}^H\hat{\mathbf{H}}\mathbf{P}\operatorname{diag}\left(\mathbf{a}\right)\mathbf{R_s}\right) \\
& - \operatorname{tr}\left(\operatorname{diag}\left(\mathbf{a}\right)\mathbf{P}^H\hat{\mathbf{H}}\mathbf{R_s}\right) + \operatorname{tr}\left(\mathbf{R_n}\right) \\
& + \operatorname{tr}\left(\operatorname{diag}\left(\mathbf{a}\right)\mathbf{P}^H\mathbf{\Xi}\mathbf{P}\operatorname{diag}\left(\mathbf{a}\right)\mathbf{R_s}\right),
\end{aligned} \tag{5-24}
$$

where the diagonal error matrix $\mathbf{\Xi}$ is defined by

$$
\mathbf{\Xi} = \mathbb{E}\left[\tilde{\mathbf{H}}^H\tilde{\mathbf{H}}\right] = \begin{bmatrix} \sigma_{e,1}^2 & 0 & \cdots & 0 \\ 0 & \sigma_{e,2}^2 & \cdots & 0 \\ \vdots & \vdots & \ddots & \vdots \\ 0 & 0 & \cdots & \sigma_{e,N_t}^2 \end{bmatrix}. \tag{5-25}
$$

Without loss of generality, we consider that $\sigma_e^2 = \sigma_{e,i}^2 = \sigma_{e,j}^2 \ \forall i, j$. Furthermore, we consider that each coefficient of $\tilde{\mathbf{H}}$ has a variance equal to $\sigma_{e_i}^2$. Then, $\sigma_e^2 = N_r\sigma_{e_i}^2$, which lead us to

$$
\mathbf{\Xi} = N_r \begin{bmatrix} \sigma_{e_i}^2 & 0 & \cdots & 0 \\ 0 & \sigma_{e_i}^2 & \cdots & 0 \\ \vdots & \vdots & \ddots & \vdots \\ 0 & 0 & \cdots & \sigma_{e_i}^2 \end{bmatrix}. \tag{5-26}
$$

By taking the derivative of (5-24), we obtain

$$
\begin{aligned}
\frac{\partial\mathbb{E}_{\tilde{\mathbf{H}}}\left[\varepsilon|\hat{\mathbf{H}}\right]}{\mathbf{A}} =& 2\sigma_s^2\left(\mathbf{P}^H\hat{\mathbf{H}}^H\hat{\mathbf{H}}\mathbf{P}\operatorname{diag}\left(\mathbf{a}\right)\right)\odot\mathbf{I} - 2\sigma_s^2\Re\left(\left(\check{\mathbf{H}}\mathbf{P}\right)\odot\mathbf{I}\right) \\
& + 2\sigma_s^2\left(\mathbf{P}^H\mathbf{\Xi}\mathbf{P}\operatorname{diag}\left(\mathbf{a}\right)\right)\odot\mathbf{I}
\end{aligned} \tag{5-27}
$$

From (5-27) we get the gradient descent recursion

$$
\begin{aligned}
\mathbf{a}\left[i\right] = &\mathbf{a}\left[i-1\right] - \mu\sigma_s^2 \left(\left(\mathbf{P}^H \hat{\mathbf{H}}^H \hat{\mathbf{H}} \mathbf{P} \mathrm{diag}\left(\mathbf{a}\left[i-1\right]\right) \right) \odot \mathbf{I} - \Re\left(\left(\check{\mathbf{H}} \mathbf{P} \right) \odot \mathbf{I} \right) \right) \\
&- \mu\sigma_s^2 N_r \left(\left(\mathbf{P}^H \mathbf{\Xi} \mathbf{P} \mathrm{diag}\left(\mathbf{a}\left[i-1\right]\right) \right) \odot \mathbf{I} \right)
\end{aligned}
\tag{5-28}
$$

The statistical information of the CSIT imperfection is included into the recursion of the power allocation coefficients, increasing the robustness against CSIT uncertainties. The proposed technique aims at maximizing the ASR given a channel estimate $\hat{\mathbf{H}}$, since the instantaneous rate is not achievable.

Algorithm 3: MMSE Robust Adaptive Power allocation

---

1 given $\hat{\mathbf{H}}$, $\mathbf{P}$, $\mathbf{\Xi}$ and μ;

2 $\mathbf{a}\left[1\right] = \mathbf{0}$;

3 **for** $i = 2$ **to** I_t **do**

4 $\quad \frac{\partial \mathbb{E}_{\check{\mathbf{H}}}\left[\varepsilon|\hat{\mathbf{H}}\right]}{\mathbf{A}} = 2\sigma_s^2 \left(\mathbf{P}^H \hat{\mathbf{H}}^H \hat{\mathbf{H}} \mathbf{P} \mathrm{diag}\left(\mathbf{a}\right) \right) \odot \mathbf{I} - 2\sigma_s^2 \Re\left(\left(\hat{\mathbf{H}} \mathbf{P} \right) \odot \mathbf{I} \right)$

$\quad \quad + 2\sigma_s^2 \left(\mathbf{P}^H \mathbf{\Xi} \mathbf{P} \mathrm{diag}\left(\mathbf{a}\right) \right) \odot \mathbf{I}$;

5 $\quad \mathbf{a}\left[i\right] = \mathbf{a}\left[i-1\right] - \mu\frac{\partial \mathbb{E}_{\check{\mathbf{H}}}\left[\varepsilon|\hat{\mathbf{H}}\right]}{\partial \mathbf{A}}$;

6 $\quad$ **if** $\mathrm{tr}\left(\mathrm{diag}\left(\mathbf{a}\left[i\right] \odot \mathbf{a}\left[i\right]\right)\right) \neq 1$ **then**

7 $\quad \quad \beta = \sqrt{\frac{1}{\mathrm{tr}(\mathrm{diag}(\mathbf{a}[i]\odot\mathbf{a}[i]))}}$;

8 $\quad \quad \mathbf{a}\left[i\right] = \beta\mathbf{a}\left[i\right]$;

9 $\quad$ **end**

10 **end**

5.4
Suboptimal Power Allocation for RS

Let us now employ the model established in (5-3) Furthermore, let us define $a_c^2 = \delta E_{tr}$ and also consider the vector $\mathbf{y}' = \mathbf{T}\mathbf{y}^{(\mathrm{RS})}$, where $\mathbf{T}$ is a transformation matrix given by

$$
\mathbf{T} = \begin{bmatrix} 1 & 1 & \cdots & 1 \\ 1 & 0 & \cdots & 0 \\ 0 & 1 & \cdots & 0 \\ \vdots & \vdots & \ddots & \vdots \\ 0 & 0 & \cdots & 1 \end{bmatrix}.
\tag{5-29}
$$

It follows that

$$\mathbf{y}' = \begin{bmatrix} y_c \\ y_1 \\ y_2 \\ \vdots \\ y_M \end{bmatrix} = \begin{bmatrix} \sum_{i=1}^{M} y_i \\ y_1 \\ y_2 \\ \vdots \\ y_M \end{bmatrix}, \tag{5-30}$$

where

$$y_i = a_c s_c \mathbf{h}_{i,*}\mathbf{p}_c + \sum_{j=1}^{M} a_j s_j \mathbf{h}_{i,*}\mathbf{p}_j + n_i. \tag{5-31}$$

Let us define the objective function as

$$\min_{\mathbf{a}} \mathbb{E}\left[\|\mathbf{s}^{(\mathrm{RS})} - \mathbf{y}'\|^2\right]$$

$$\text{s.t.} \quad \mathrm{tr}\left(\mathbf{P}^{(\mathrm{RS})}\mathrm{diag}\left(\mathbf{a}^{(\mathrm{RS})} \odot \mathbf{a}^{(\mathrm{RS})}\right)\mathbf{P}^{(\mathrm{RS})^H}\right) = E_{tr} \tag{5-32}$$

The mean square error is

$$\begin{aligned}
\mathbb{E}\left[\varepsilon\right] &= \mathbb{E}\left[\left(\mathbf{s}^{(\mathrm{RS})} - \mathbf{y}'\right)^H \left(\mathbf{s}^{(\mathrm{RS})} - \mathbf{y}'\right)\right] \\
&= \mathbb{E}\left[\mathbf{s}^{(\mathrm{RS})^H}\mathbf{s}^{(\mathrm{RS})}\right] - \mathbb{E}\left[\mathbf{s}^{(\mathrm{RS})^H}\mathbf{y}'\right] - \mathbb{E}\left[\mathbf{y}'^H\mathbf{s}^{(\mathrm{RS})}\right] + \mathbb{E}\left[\mathbf{y}'^H\mathbf{y}'\right]. \tag{5-33}
\end{aligned}$$

The first term of (5-33) is expressed by

$$\begin{aligned}
\mathbb{E}\left[\mathbf{s}^{(\mathrm{RS})^H}\mathbf{s}^{(\mathrm{RS})}\right] &= \mathbb{E}\left[s_c^* s_c\right] + \mathbb{E}\left[s_1^* s_1\right] \cdots + \mathbb{E}\left[s_M^* s_M\right], \\
&= (M+1)\sigma_s^2. \tag{5-34}
\end{aligned}$$

The second expected value of (5-33) requires the computation of the following term:

$$\begin{aligned}
\mathbf{s}^{(\mathrm{RS})}\mathbf{y}' &= s_c^* y_c + s_1^* y_1 + \cdots + s_M^* y_M, \\
&= s_c^*\left(a_c s_c \sum_{l=1}^{M} \mathbf{h}_{l,*}\mathbf{p}_c + \sum_{l=1}^{M} \mathbf{h}_{l,*} \sum_{j=1}^{M} a_j s_j \mathbf{p}_j + \sum_{l=1}^{M} n_l\right) \\
&\quad + s_1^*\left(a_c s_c \mathbf{h}_{1,*}\mathbf{p}_c + \sum_{l=1}^{M} a_l s_l \mathbf{h}_{1,*}\mathbf{p}_l + n_1\right) + \cdots \\
&\quad + s_M^*\left(a_c s_c \mathbf{h}_{M,*}\mathbf{p}_c + \sum_{l=1}^{M} a_l s_l \mathbf{h}_{M,*}\mathbf{p}_l + n_M\right). \tag{5-35}
\end{aligned}$$

By taking the expected value and expanding the terms in the last equation,

we have

$$
\mathbb{E}\left[\mathbf{s}^{(\mathrm{RS})^H}\mathbf{y}'\right] = a_c\mathbb{E}\left[s_c^*s_c\right]\sum_{l=1}^{M}\mathbf{h}_{l,*}\mathbf{p}_c + \sum_{l=1}^{M}\mathbf{h}_{l,*}\sum_{j=1}^{M}a_j\mathbb{E}\left[s_c^*s_j\right]\mathbf{p}_j + \sum_{l=1}^{M}\mathbb{E}\left[s_c^*n_l\right]
$$
$$
+ a_c\mathbb{E}\left[s_1^*s_c\right]\mathbf{h}_{1,*}\mathbf{p}_c + \sum_{l=1}^{M}a_l\mathbb{E}\left[s_1^*s_l\right]\mathbf{h}_{1,*}\mathbf{p}_l + \mathbb{E}\left[s_1^*n_1\right] + \cdots
$$
$$
+ a_c\mathbb{E}\left[s_M^*s_c\right]\mathbf{h}_{M,*}\mathbf{p}_c + \sum_{l=1}^{M}a_l\mathbb{E}\left[s_M^*s_l\right]\mathbf{h}_{M,*}\mathbf{p}_l + \mathbb{E}\left[s_M^*n_1\right]. \tag{5-36}
$$

Since the symbols are uncorrelated, equation (5-36) is reduced to

$$
\mathbb{E}\left[\mathbf{s}^{(\mathrm{RS})^H}\mathbf{y}'\right] = a_c\sum_{j=1}^{M}\mathbf{h}_{j,*}\mathbf{p}_c + \sigma_s^2\left(\sum_{l=1}^{M}a_l\mathbf{h}_{l,*}\mathbf{p}_l\right). \tag{5-37}
$$

The third term of (5-33) can be computed in a similar way as the second term, which lead us to

$$
\mathbb{E}\left[\mathbf{y}'^H\mathbf{s}^{(\mathrm{RS})}\right] = a_c\sum_{j=1}^{M}\left(\mathbf{h}_{l,*}\mathbf{p}_c\right)^* + \sigma_s^2\left(\sum_{l=1}^{M}a_l\left(\mathbf{h}_{l,*}\mathbf{p}_l\right)^*\right). \tag{5-38}
$$

For the last term we need to evaluate the following expression:

$$
\mathbf{y}'^H\mathbf{y}' = y_c^*y_c + y_1^*y_1 + \cdots + y_M^*y_M,
$$
$$
= \left(\sum_{l=1}^{M}y_l^*\right)\left(\sum_{j=1}^{M}y_j\right) + \sum_{i=1}^{M}y_i^*y_i. \tag{5-39}
$$

Taking the expected value on the last equation results in

$$
\mathbb{E}\left[\mathbf{y}'^H\mathbf{y}'\right] = \sum_{l=1}^{M}\sum_{j=1}^{M}\mathbb{E}\left[y_l^*y_j\right] + \sum_{i=1}^{M}\mathbb{E}\left[y_i^*y_i\right],
$$
$$
= \sum_{\substack{l=1 \\ }}^{M}\sum_{\substack{j=1 \\ j\neq l}}^{M}\mathbb{E}\left[y_l^*y_j\right] + 2\sum_{i=1}^{M}\mathbb{E}\left[y_i^*y_i\right]. \tag{5-40}
$$

We know that

$$
\mathbb{E}\left[y_i^*y_i\right] = a_c^2|\mathbf{h}_{i,*}\mathbf{p}_c|^2 + \sum_{l=1}^{M}a_l^2|\mathbf{h}_{i,*}\mathbf{p}_l|^2 + \sigma_n^2. \tag{5-41}
$$

Additionally, we have

$$
\mathbb{E}\left[y_i^*y_j\right] = \left(a_cs_c\mathbf{h}_{i,*}\mathbf{p}_c + \sum_{q=1}^{M}a_qs_q\mathbf{h}_{i,*}\mathbf{p}_q + n_i\right)^*\left(a_cs_c\mathbf{h}_{j,*}\mathbf{p}_c + \sum_{l=1}^{M}a_ls_l\mathbf{h}_{j,*}\mathbf{p}_l + n_j\right),
$$
$$
= a_c^2\left(\mathbf{h}_{i,*}\mathbf{p}_c\right)^*\left(\mathbf{h}_{j,*}\mathbf{p}_c\right) + \sum_{l=1}^{M}a_l^2\left(\mathbf{h}_{i,*}\mathbf{p}_l\right)^*\left(\mathbf{h}_{j,*}\mathbf{p}_l\right), \tag{5-42}
$$

for all $i \neq j$. Employing (5-41) and (5-42) we can compute the following quantities:

$$\sum_{i=1}^{M} \mathbb{E}\left[y_i^* y_i\right] = \sum_{l=1}^{M} a_c^2 |\mathbf{h}_{l,*}\mathbf{p}_c|^2 + \sum_{i=1}^{M}\sum_{j=1}^{M} a_j^2 |\mathbf{h}_{i,*}\mathbf{p}_j|^2 + M\sigma_n^2, \qquad (5\text{-}43)$$

$$\sum_{l=1}^{M}\sum_{\substack{j=1 \\ j\neq l}}^{M} \mathbb{E}\left[y_l^* y_j\right]$$

$$= \sum_{l=1}^{M}\sum_{\substack{j=1 \\ j\neq l}}^{M} a_c^2 \left(\mathbf{h}_{l,*}\mathbf{p}_c\right)^* \left(\mathbf{h}_{j,*}\mathbf{p}_c\right) + 2\sum_{i=1}^{M-1}\sum_{q=i+1}^{M}\sum_{r=1}^{M} a_r^2 \Re\left[\left(\mathbf{h}_{i,*}\mathbf{p}_r\right)^* \left(\mathbf{h}_{q,*}\mathbf{p}_r\right)\right].$$

$$(5\text{-}44)$$

Substituting (5-34),(5-37), (5-38) and (5-44) in (5-33) we get the mean square error which is given by

$$\mathbb{E}\left[\varepsilon\right] = (M+1)\sigma_s^2 - 2a_c\sigma_s^2 \sum_{j=1}^{M} \Re\left[\mathbf{h}_{j,*}\mathbf{p}_c\right] - 2\sum_{l=1}^{M} a_l\sigma_s^2 \Re\left[\mathbf{h}_{l,*}\mathbf{p}_l\right]$$

$$+ 2\left(\sum_{l=1}^{M} a_c^2 |\mathbf{h}_{l,*}\mathbf{p}_c|^2 + \sum_{i=1}^{M}\sum_{j=1}^{M} a_j^2 |\mathbf{h}_{i,*}\mathbf{p}_j|^2 + M\sigma_n^2\right)$$

$$+ \sum_{l=1}^{M}\sum_{\substack{j=1 \\ j\neq l}}^{M} a_c^2 \left(\mathbf{h}_{l,*}\mathbf{p}_c\right)^* \left(\mathbf{h}_{j,*}\mathbf{p}_c\right) + 2\sum_{i=1}^{M-1}\sum_{q=i+1}^{M}\sum_{r=1}^{M} a_r^2 \Re\left[\left(\mathbf{h}_{i,*}\mathbf{p}_r\right)^* \left(\mathbf{h}_{q,*}\mathbf{p}_r\right)\right].$$

$$(5\text{-}45)$$

Taking the derivative with respect to $\mathbf{a}^{(\mathrm{RS})}$ we get

$$\frac{\partial \mathbb{E}\left[\varepsilon\right]}{\partial a_c} = 4a_c \sum_{i=1}^{M} |\mathbf{h}_{i,*}\mathbf{p}_c|^2 + \sum_{l=1}^{M}\sum_{\substack{j=1 \\ j\neq l}}^{M} 2a_c \left(\mathbf{h}_{l,*}\mathbf{p}_c\right)^* \left(\mathbf{h}_{j,*}\mathbf{p}_c\right) - 2\sum_{q=1}^{M} \Re\left[\mathbf{h}_{q,*}\mathbf{p}_c\right],$$

$$(5\text{-}46)$$

$$\frac{\partial \mathbb{E}\left[\varepsilon\right]}{\partial a_i} = 4a_i \sum_{j=1}^{M} |\mathbf{h}_{j,*}\mathbf{p}_i|^2 + 4a_i \sum_{r=1}^{M-1}\sum_{q=r+1}^{M} \Re\left[\left(\mathbf{h}_{r,*}\mathbf{p}_i\right)^* \left(\mathbf{h}_{q,*}\mathbf{p}_i\right)\right] - 2a_i \Re\left[\mathbf{h}_{i,*}\mathbf{p}_i\right].$$

$$(5\text{-}47)$$

The power allocation coefficients are adapted using (5-46) and (5-47) in the following recursion:

$$a_c\left[t+1\right] = a_c\left[t\right] - \mu\frac{\partial \mathbb{E}\left[\varepsilon\right]}{\partial a_c}$$

$$a_i\left[t+1\right] = a_i\left[t\right] - \mu\frac{\partial \mathbb{E}\left[\varepsilon\right]}{\partial a_i}. \qquad (5\text{-}48)$$

At each iteration, the power constraint is analyzed. Then, the coefficients are properly scaled with a power scaling factor if the power restriction is not met.

5.5
Robust RS-APA

Let us now consider a robust strategy for an imperfect CSIT environment. Then, (5-31) is rewritten as

$$
y_i = a_c s_c \left(\hat{\mathbf{h}}_{i,*} + \tilde{\mathbf{h}}_{i,*} \right) \mathbf{p}_c + \sum_{j=1}^{M} a_j s_j \left(\hat{\mathbf{h}}_{i,*} + \tilde{\mathbf{h}}_{i,*} \right) \mathbf{p}_j + n_i. \tag{5-49}
$$

The mean square error is described by (5-33). The first term of that equation remains the same and is given by (5-34). For the second term we need to evaluate (5-37). However, the CSIT uncertainty leads to

$$
y_c = \sum_{i=1}^{M} a_c s_c \left(\hat{\mathbf{h}}_{i,*} + \tilde{\mathbf{h}}_{i,*} \right) \mathbf{p}_c + \sum_{l=1}^{M} \sum_{j=1}^{M} a_j s_j \left(\hat{\mathbf{h}}_{l,*} + \tilde{\mathbf{h}}_{l,*} \right) \mathbf{p}_j + \sum_{q=1}^{M} n_q. \tag{5-50}
$$

By evaluating the expected value of the different terms in (5-37) we get the following quantities:

$$
\mathbb{E}\left[s_i^* y_i \right] = a_i \sigma_s^2 \left(\hat{\mathbf{h}}_{i,*} + \tilde{\mathbf{h}}_{i,*} \right) \mathbf{p}_i, \tag{5-51}
$$

$$
\mathbb{E}\left[s_c^* y_c \right] = a_c \sigma_s^2 \sum_{i=1}^{M} \left(\hat{\mathbf{h}}_{i,*} + \tilde{\mathbf{h}}_{i,*} \right) \mathbf{p}_c, \tag{5-52}
$$

$$
\mathbb{E}\left[s_i^* y_i | \hat{\mathbf{H}} \right] = a_i \sigma_s^2 \hat{\mathbf{h}}_{i,*} \mathbf{p}_i, \tag{5-53}
$$

$$
\mathbb{E}\left[s_c^* y_c | \hat{\mathbf{H}} \right] = a_c \sigma_s^2 \sum_{i=1}^{M} \hat{\mathbf{h}}_{i,*} \mathbf{p}_c. \tag{5-54}
$$

These expressions allow us to compute the second term in (5-33), which is expressed by

$$
\mathbb{E}\left[\mathbf{s}^{(\text{RS})^H} \mathbf{y}' | \hat{\mathbf{H}} \right] = a_c \sigma_s^2 \sum_{i=1}^{M} \hat{\mathbf{h}}_{i,*} \mathbf{p}_c + \sigma_s^2 \sum_{j=1}^{M} a_j \hat{\mathbf{h}}_{j,*} \mathbf{p}_j. \tag{5-55}
$$

The third term can be calculated in a similar manner and is given by

$$
\mathbb{E}\left[\mathbf{y}'^H \mathbf{s}^{(\text{RS})} | \hat{\mathbf{H}} \right] = a_c \sigma_s^2 \sum_{i=1}^{M} \left(\hat{\mathbf{h}}_{i,*} \mathbf{p}_c \right)^* + \sigma_s^2 \sum_{j=1}^{M} a_j \left(\hat{\mathbf{h}}_{j,*} \mathbf{p}_j \right)^*. \tag{5-56}
$$

The last term of equation (5-33) requires the computation of several quantities.

Let us first consider the following expected value:

$$
\begin{aligned}
\mathbb{E}\left[y_i^* y_i\right] =& a_c^2 |\left(\hat{\mathbf{h}}_{i,*} + \tilde{\mathbf{h}}_{i,*}\right)\mathbf{p}_c|^2 + \sum_{j=1}^{M} a_j^2 |\left(\hat{\mathbf{h}}_{i,*} + \tilde{\mathbf{h}}_{i,*}\right)\mathbf{p}_j|^2 + \sigma_n^2 \\
=& a_c^2 \left(|\hat{\mathbf{h}}_{i,*}\mathbf{p}_c|^2 + 2\Re\left[\left(\hat{\mathbf{h}}_{i,*}\mathbf{p}_c\right)^*\left(\tilde{\mathbf{h}}_{i,*}\mathbf{p}_c\right)\right] + |\tilde{\mathbf{h}}_{i,*}\mathbf{p}_c|^2\right) \\
&+ \sum_{j=1}^{M} a_j^2 \left(|\hat{\mathbf{h}}_{i,*}\mathbf{p}_j|^2 + 2\Re\left[\left(\hat{\mathbf{h}}_{i,*}\mathbf{p}_j\right)^*\left(\tilde{\mathbf{h}}_{i,*}\mathbf{p}_j\right)\right] + |\tilde{\mathbf{h}}_{i,*}\mathbf{p}_j|^2\right) + \sigma_n^2.
\end{aligned}
\tag{5-57}
$$

Assuming that the entries of $\tilde{\mathbf{h}}_{i,*}$ $\forall i$ are uncorrelated with zero mean lead us to

$$
\begin{aligned}
\mathbb{E}\left[y_i^* y_i | \hat{\mathbf{H}}\right] =& a_c^2 |\hat{\mathbf{h}}_{i,*}\mathbf{p}_c|^2 + a_c^2 \mathbb{E}\left[|\tilde{\mathbf{h}}_{i,*}\mathbf{p}_c|^2\right] + \sum_{j=1}^{M} a_j^2 |\hat{\mathbf{h}}_{i,*}\mathbf{p}_j|^2 \\
& \sum_{l=1}^{M} a_l^2 \mathbb{E}\left[|\tilde{\mathbf{h}}_{i,*}\mathbf{p}_l|^2\right] + \sigma_n^2.
\end{aligned}
\tag{5-58}
$$

Note that

$$
\begin{aligned}
\mathbb{E}\left[|\tilde{\mathbf{h}}_{i,*}\mathbf{p}_l|^2\right] =& |p_1^{(l)}|^2 \mathbb{E}\left[\tilde{h}_{i,1}^* \tilde{h}_{i,1}\right] + |p_2^{(l)}|^2 \mathbb{E}\left[\tilde{h}_{i,2}^* \tilde{h}_{i,2}\right] + \cdots + |p_{N_t}^{(l)}|^2 \mathbb{E}\left[\tilde{h}_{i,N_t}^* \tilde{h}_{i,N_t}\right], \\
=& |p_1^{(l)}|^2 \sigma_{e_i}^2 + |p_2^{(l)}|^2 \sigma_{e_i}^2 + \cdots |p_{N_t}^{(l)}|^2 \sigma_{e_i}^2 \\
=& \sigma_{e_i}^2 \|\mathbf{p}_l\|^2,
\end{aligned}
\tag{5-59}
$$

and

$$
\begin{aligned}
\mathbb{E}\left[|\tilde{\mathbf{h}}_{i,*}\mathbf{p}_c|^2\right] =& |p_1^{(c)}|^2 \mathbb{E}\left[\tilde{h}_{i,1}^* \tilde{h}_{i,1}\right] + |p_2^{(c)}|^2 \mathbb{E}\left[\tilde{h}_{i,2}^* \tilde{h}_{i,2}\right] + \cdots + |p_{N_t}^{(c)}|^2 \mathbb{E}\left[\tilde{h}_{i,N_t}^* \tilde{h}_{i,N_t}\right], \\
=& |p_1^{(c)}|^2 \sigma_{e_i}^2 + |p_2^{(c)}|^2 \sigma_{e_i}^2 + \cdots |p_{N_t}^{(c)}|^2 \sigma_{e_i}^2 \\
=& \sigma_{e_i}^2 \|\mathbf{p}_c\|^2.
\end{aligned}
\tag{5-60}
$$

Then, (5-58) turns into

$$
\mathbb{E}\left[y_i^* y_i | \hat{\mathbf{H}}\right] = a_c^2 \left(|\hat{\mathbf{h}}_{i,*}\mathbf{p}_c|^2 + \frac{\sigma_e^2}{N_r}\|\mathbf{p}_c\|^2\right) + \sum_{j=1}^{K} a_j^2 \left(|\hat{\mathbf{h}}_{i,*}\mathbf{p}_j|^2 + \frac{\sigma_e^2}{N_r}\|\mathbf{p}_j\|^2\right) + \sigma_n^2.
\tag{5-61}
$$

Let us now evaluate the expected value of $y_i^* y_j$ when $i \neq j$, which results in

$$
\begin{aligned}
\mathbb{E}\left[y_i^* y_j\right] =& a_c^2 \left(\hat{\mathbf{h}}_{i,*}\mathbf{p}_c + \tilde{\mathbf{h}}_{i,*}\mathbf{p}_c\right)^* \left(\hat{\mathbf{h}}_{j,*}\mathbf{p}_c + \tilde{\mathbf{h}}_{j,*}\mathbf{p}_c\right) \\
&+ \sum_{l=1}^{M} a_l^2 \left(\hat{\mathbf{h}}_{i,*}\mathbf{p}_l + \tilde{\mathbf{h}}_{i,*}\mathbf{p}_l\right)^* \left(\hat{\mathbf{h}}_{j,*}\mathbf{p}_l + \tilde{\mathbf{h}}_{j,*}\mathbf{p}_l\right), \\
=& a_c^2 \left(\hat{\mathbf{h}}_{i,*}\mathbf{p}_c\right)^* \left(\hat{\mathbf{h}}_{j,*}\mathbf{p}_c\right) + a_c^2 \left(\hat{\mathbf{h}}_{i,*}\mathbf{p}_c\right)^* \left(\tilde{\mathbf{h}}_{j,*}\mathbf{p}_c\right) \\
&+ a_c^2 \left(\tilde{\mathbf{h}}_{i,*}\mathbf{p}_c\right)^* \left(\hat{\mathbf{h}}_{j,*}\mathbf{p}_c\right) + a_c^2 \left(\tilde{\mathbf{h}}_{i,*}\mathbf{p}_c\right)^* \left(\tilde{\mathbf{h}}_{j,*}\mathbf{p}_c\right) \\
&+ \sum_{l=1}^{M} a_l^2 \left(\hat{\mathbf{h}}_{i,*}\mathbf{p}_l\right)^* \left(\hat{\mathbf{h}}_{j,*}\mathbf{p}_l\right) + \sum_{q=1}^{M} a_q^2 \left(\hat{\mathbf{h}}_{i,*}\mathbf{p}_q\right)^* \left(\tilde{\mathbf{h}}_{j,*}\mathbf{p}_q\right) \\
&+ \sum_{r=1}^{M} a_r^2 \left(\tilde{\mathbf{h}}_{i,*}\mathbf{p}_r\right)^* \left(\hat{\mathbf{h}}_{j,*}\mathbf{p}_r\right) + \sum_{t=1}^{M} a_t^2 \left(\tilde{\mathbf{h}}_{i,*}\mathbf{p}_t\right)^* \left(\tilde{\mathbf{h}}_{j,*}\mathbf{p}_t\right). \quad (5\text{-}62)
\end{aligned}
$$

Remark that the channel imperfections for a given channel estimate are not known. Thus, we have

$$
\mathbb{E}\left[y_i^* y_j | \hat{\mathbf{H}}\right] = a_c^2 \left(\hat{\mathbf{h}}_{i,*}\mathbf{p}_c\right)^* \left(\hat{\mathbf{h}}_{j,*}\mathbf{p}_c\right) + \sum_{l=1}^{M} a_l^2 \left(\hat{\mathbf{h}}_{i,*}\mathbf{p}_l\right)^* \left(\hat{\mathbf{h}}_{j,*}\mathbf{p}_l\right). \quad (5\text{-}63)
$$

Equation (5-61) and (5-63) lead us to the following expressions:

$$
\begin{aligned}
\sum_{i=1}^{M} \mathbb{E}\left[y_i^* y_i | \hat{\mathbf{H}}\right] =& \sum_{j=1}^{M} a_j^2 \left(\sum_{l=1}^{M} |\hat{\mathbf{h}}_{l,*}\mathbf{p}_j|^2 + \frac{M\sigma_e^2}{N_r} \|\mathbf{p}_j\|^2\right) + M\sigma_n^2 \\
&+ a_c^2 \left(\sum_{i=1}^{M} |\hat{\mathbf{h}}_{i,*}\mathbf{p}_c|^2 + \frac{M\sigma_e^2}{N_r} \|\mathbf{p}_c\|^2\right). \quad (5\text{-}64)
\end{aligned}
$$

$$
\begin{aligned}
\sum_{l=1}^{M} \sum_{\substack{j=1 \\ j \neq l}}^{M} \mathbb{E}\left[y_l^* y_j | \hat{\mathbf{H}}\right] =& 2 \sum_{i=1}^{M-1} \sum_{q=i+1}^{M} \sum_{r=1}^{M} a_r^2 \Re\left[\left(\hat{\mathbf{h}}_{i,*}\mathbf{p}_r\right)^* \left(\hat{\mathbf{h}}_{q,*}\mathbf{p}_r\right)\right] \\
&+ \sum_{l=1}^{M} \sum_{\substack{j=1 \\ j \neq l}}^{M} a_c^2 \left(\hat{\mathbf{h}}_{l,*}\mathbf{p}_c\right)^* \left(\hat{\mathbf{h}}_{j,*}\mathbf{p}_c\right). \quad (5\text{-}65)
\end{aligned}
$$

With (5-55), (5-56) , (5-64) and (5-65) we can calculate the MSE, which

is given by

$$
\begin{aligned}
\mathbb{E}\left[\varepsilon|\hat{\mathbf{H}}\right] =& \sigma_s^2\left(M+1\right) - 2a_c\sigma_s^2\sum_{i=1}^{M}\Re\left\{\hat{\mathbf{h}}_{i,*}\mathbf{p}_c\right\} - 2\sigma_s^2\sum_{j=1}^{M}a_j^2\Re\left\{\hat{\mathbf{h}}_{j,*}\mathbf{p}_j\right\} \\
&+ 2\sum_{j=1}^{M}a_j^2\left(\sum_{l=1}^{M}|\hat{\mathbf{h}}_{l,*}\mathbf{p}_j|^2 + \frac{M\sigma_e^2}{N_r}\|\mathbf{p}_j\|^2\right) + 2M\sigma_n^2 \\
&+ 2a_c^2\left(\sum_{i=1}^{M}|\hat{\mathbf{h}}_{i,*}\mathbf{p}_c|^2 + \frac{M\sigma_e^2}{N_r}\|\mathbf{p}_c\|^2\right) \\
&+ 2\sum_{i=1}^{M-1}\sum_{q=i+1}^{M}\sum_{r=1}^{M}a_r^2\Re\left[\left(\hat{\mathbf{h}}_{i,*}\mathbf{p}_r\right)^*\left(\hat{\mathbf{h}}_{q,*}\mathbf{p}_r\right)\right] \\
&+ \sum_{l=1}^{M}\sum_{\substack{j=1\\j\neq l}}^{M}a_c^2\left(\hat{\mathbf{h}}_{l,*}\mathbf{p}_c\right)^*\left(\hat{\mathbf{h}}_{j,*}\mathbf{p}_c\right)
\end{aligned}
\tag{5-66}
$$

Taking the derivative with respect to $\mathbf{a}$ we obtain

$$
\begin{aligned}
\frac{\partial\mathbb{E}\left[\varepsilon|\hat{\mathbf{H}}\right]}{\partial a_c} =& -2\sigma_s^2\sum_{i=1}^{M}\Re\left\{\hat{\mathbf{h}}_{i,*}\mathbf{p}_c\right\} + 4a_c\left(\sum_{i=1}^{M}|\hat{\mathbf{h}}_{i,*}\mathbf{p}_c|^2 + \frac{M\sigma_e^2}{N_r}\|\mathbf{p}_c\|^2\right) \\
&+ 2\sum_{l=1}^{M}\sum_{\substack{j=1\\j\neq l}}^{M}a_c\left(\hat{\mathbf{h}}_{l,*}\mathbf{p}_c\right)^*\left(\hat{\mathbf{h}}_{j,*}\mathbf{p}_c\right),
\end{aligned}
\tag{5-67}
$$

$$
\begin{aligned}
\frac{\partial\mathbb{E}\left[\varepsilon|\hat{\mathbf{H}}\right]}{\partial a_i} =& -2\sigma_s^2\Re\left\{\hat{\mathbf{h}}_{i,*}\mathbf{p}_i\right\} + 4a_i\left(\sum_{l=1}^{M}|\hat{\mathbf{h}}_{l,*}\mathbf{p}_i|^2 + \frac{M\sigma_e^2}{N_r}\|\mathbf{p}_i\|^2\right) \\
&+ 4a_i\sum_{l=1}^{M-1}\sum_{q=l+1}^{M}\Re\left[\left(\hat{\mathbf{h}}_{l,*}\mathbf{p}_i\right)^*\left(\hat{\mathbf{h}}_{q,*}\mathbf{p}_i\right)\right].
\end{aligned}
\tag{5-68}
$$

Then, the coefficients are adapted using the following equations:

$$
a_c\left[t+1\right] = a_c\left[t\right] - \mu\frac{\partial\mathbb{E}\left[|\varepsilon|^2|\hat{\mathbf{H}}^{\mathrm{T}}\right]}{\partial a_c},
$$

$$
a_i\left[t+1\right] = a_i\left[t\right] - \mu\frac{\partial\mathbb{E}\left[|\varepsilon|^2|\hat{\mathbf{H}}^{\mathrm{T}}\right]}{\partial a_i}.
\tag{5-69}
$$

5.6
Computational Complexity

The optimal power allocation for the conventional SDMA system requires the exhaustive search over $\mathbf{A}$ with a fine grid. Given a system with 12 streams and a grid step of 0.001, the exhaustive search would require the evaluation of 5 005 000 different power allocation matrices for each channel realization. In

contrast, the adaptive approaches presented require only the computation of around 30 iterations. Furthermore, the complexity of the exhaustive search for an RS system is even higher since the search is perform over $\mathbf{A}^{(\mathrm{RS})}$, which additionally contains the power allocated to the common stream. Table 5.1 summarizes the computational complexity of the proposed algorithms employing the big $\mathcal{O}$ notation. In Table 5.1, I_o denotes the number of points of the grid given a step size, I_w refers to the number of iterations of the alternating procedure and I_a denotes the number of iterations for the adaptive algorithms. It is worth noting that $I_o >> I_a$. Moreover, the inner iterations employed in the WSR are much more demanding than the iterations of the adaptive algorithms. Fig 5.3 shows the computational complexity in terms of FLOPS assuming that $N_t = N_r = n$. The step of the grid was set to 0.01 for the ES and the number of iterations to 30 for the APA and APA-R approaches.

Table 5.1: Computational complexity of the power allocation algorithms.

Technique	$\mathcal{O}$
SDMA-ES	$\mathcal{O}\left(N_t I_o^2 M^3\right)$
WSR	$\mathcal{O}\left(I_w N_t M^2\right)$
APA	$\mathcal{O}\left(I_a N_t M^2\right)$
APA-R	$\mathcal{O}\left(I_a N_t M^2\right)$
RS-ES	$\mathcal{O}\left(N_t I_o^2 (M+1)^3\right)$
RS-APA	$\mathcal{O}\left(I_a N_t (M+1)^2\right)$
RS-APA-R	$\mathcal{O}\left(I_a N_t (M+1)^2\right)$

5.7 Simulations

In this section, the performance of the proposed power allocation techniques is assessed and compared with conventional approaches. We consider a MIMO system where the BS is equipped with four antennas and transmits data to two users, each one equipped with two antennas. The inputs are statistically independent and follow a Gaussian distribution. A flat fading Rayleigh channel, which remains fixed during the transmission of a packet, is considered. Moreover, we assume additive white Gaussian noise with zero mean and unit variance. It follows that the SNR varies with E_{tr}.
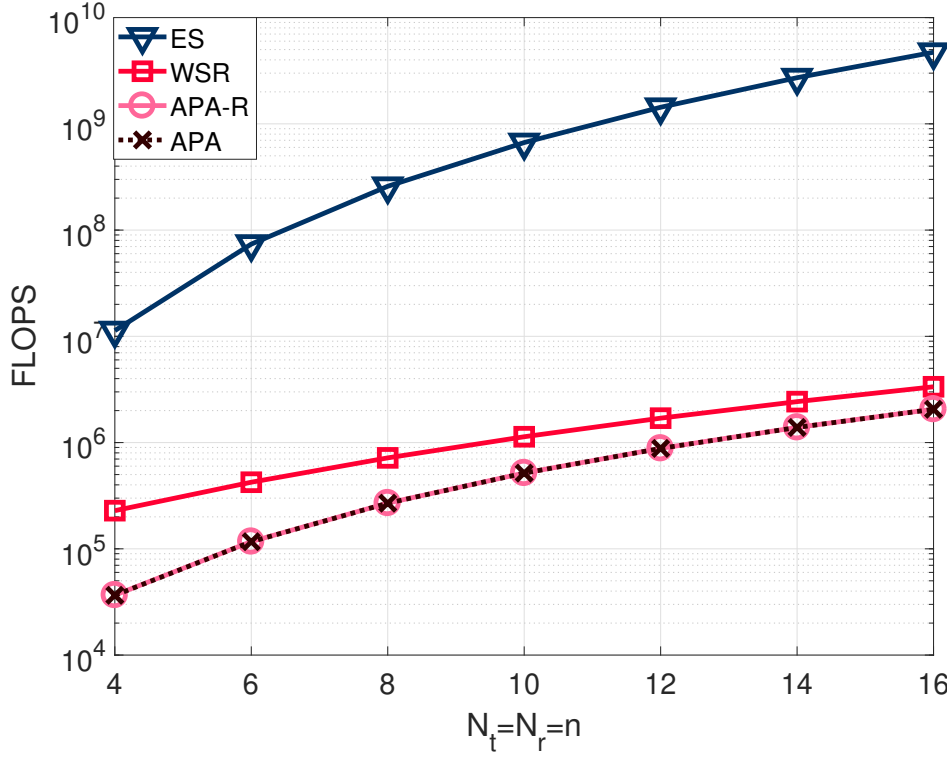
Figure 5.3: Computational complexity in terms of FLOPS for a MU-MIMO system with $N_t = N_r = n$.

First, let us analyse the learning curves of the adaptive algorithms. Fig 5.4 shows the mean square deviation (MSD) obtained with three different linear precoders, namely the MF, the ZF and the MMSE precoders. The MSD is computed between the coefficients obtained by employing the first adaptive power allocation scheme proposed and the optimum coefficients that solve (5-6). This value was obtained through exhaustive search with a step of 0.005. The learning curves were obtained by averaging over 1000 independent Monte Carlo simulations. The step of the adaptive algorithm was set to 0.01 for all precoders. The adaptive algorithm reaches its steady state with about 30 iterations, which corresponds to a fast convergence as compared to the competing WSR approach.

Let us consider an example based on a perfect CSIT scenario with a ZF precoder. Fig. 5.5 shows the performance of different power allocations. The ESR was obtained by averaging 10000 channel realizations. The optimal performance has been obtained employing exhaustive search with a step equal to $0.005 E_{tr}$. The step size of the adaptive algorithms was set to 0.01 and a total of 20 iterations were performed. Note that the adaptive allocation, termed APA, reaches a close-to-optimal performance, but with a much lower
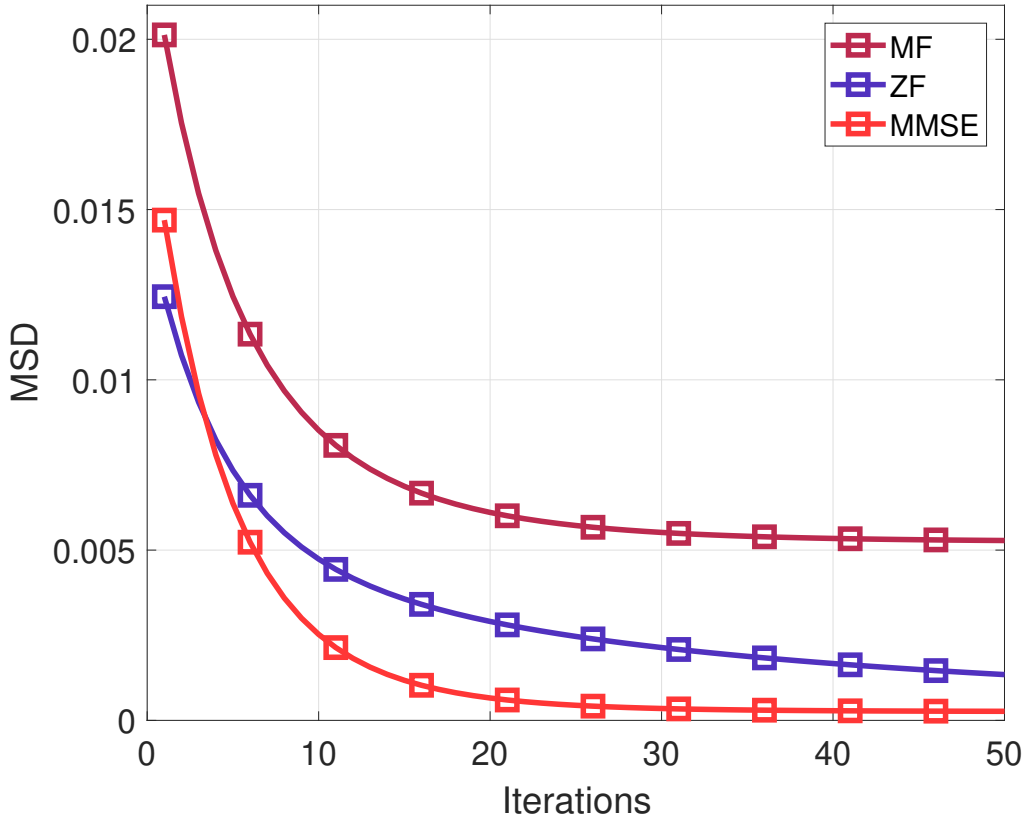
Figure 5.4: Learning curves of the adaptive power allocation techniques.

computational complexity.

For the next experiment, we consider an imperfect CSIT scenario with $\sigma_e^2 = 0.1$. The ASR was obtained by averaging 100 channel error realizations, whereas ESR was obtained by averaging 100 independent channels. Fig. 5.6 shows the performance obtained employing different power allocation techniques with a ZF precoder. As expected, the best performance is attained with the exhaustive search, i.e., ES. However, the very high computational complexity of the ES approach makes it impractical. Moreover, the time spent increases exponentially with the number of users. The proposed strategies not only increase the performance of the system when compared to UPA but also maintain the computational complexity low, which is very important for real communication systems. We can notice that the robust APA-R approach performs better than the APA algorithm at the expense of a slight increase in computational complexity, which is justified based on the improved performance of APA-R over APA. In addition, the proposed APA and APA-R algorithms significantly outperform the uniform power allocation, i.e., UPA, and the random power allocation, denoted as Random, strategies.
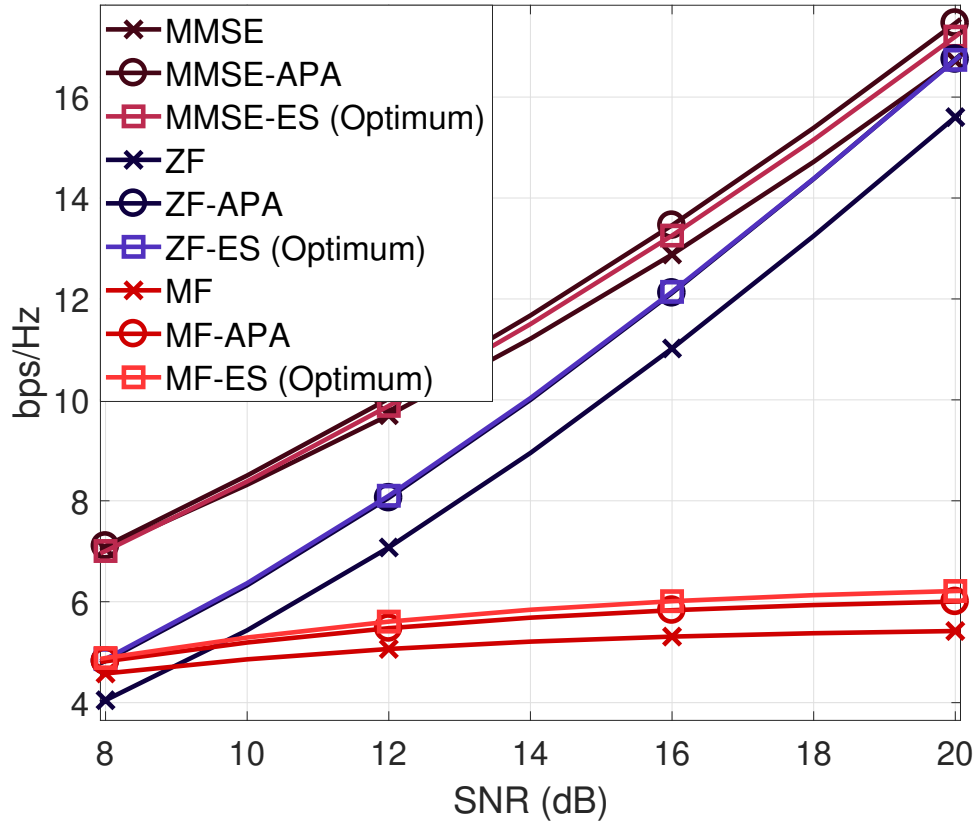
Figure 5.5: Sum-rate performance with perfect CSIT

Fig. 5.7 shows the results obtained with an MMSE precoder. For this example, the parameters of the previous simulation example remain the same. Once again the proposed APA and APA-R algorithms achieve better performance than the existing ES and Random algorithms.

In the next example an RS-MIMO system is considered. The proposed adaptive algorithms are compared against a combination of ES, uniform and random power allocation algorithms. The first fixes a random power allocation for the private streams and then an exhaustive search is carried out to find the best power allocation for the common stream. The second scheme considers that the power is uniformly distributed among private streams and then performs an exhaustive search to find the optimum value for a_c. Fig. 5.8 shows the performance obtained with a MF. Although the exhaustive search obtains the best performance, it also requires a great amount of resources in terms of computational complexity.

In the last example, the ZF precoder has been considered. Fig. 5.9 shows the results obtained. The algorithms that perform exhaustive search, which are termed as RS-ZF-ES+Random and RS-ZF-ES-UPA, have the best
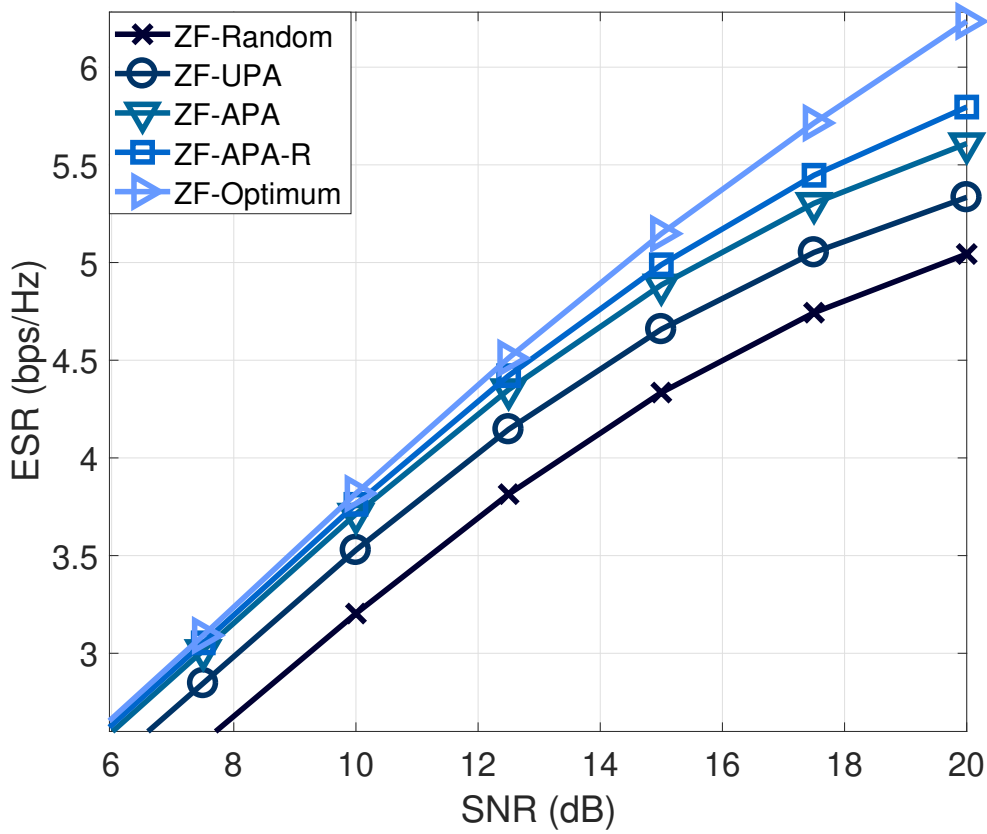
Figure 5.6: Sum-rate performance of ZF precoding scheme, $N_t = 4$, $N_k = 2$, $K = 2$, and $\sigma_e^2 = 0.1$.

performance. However, the adaptive algorithms obtain a consistent gain when compared to the conventional ZF algorithm.

5.8
Summary

In this chapter, several adaptive power allocation techniques have been developed for conventional MIMO system and for RS-MIMO architectures. Differently to optimal power allocation often employed for RS-based systems that are computationally very costly, the proposed APA and APA-R algorithms are characterised by a low computational complexity, being suitable for practical systems. Simulation results have shown that the proposed adaptive power allocation algorithms, namely APA and APA-R, perform better than the conventional UPA and are not very far from the performance of exhaustive search power allocation algorithms. Furthermore, the proposed robust techniques, i.e., APA-R, increase the robustness of the system against CSIT imperfections.
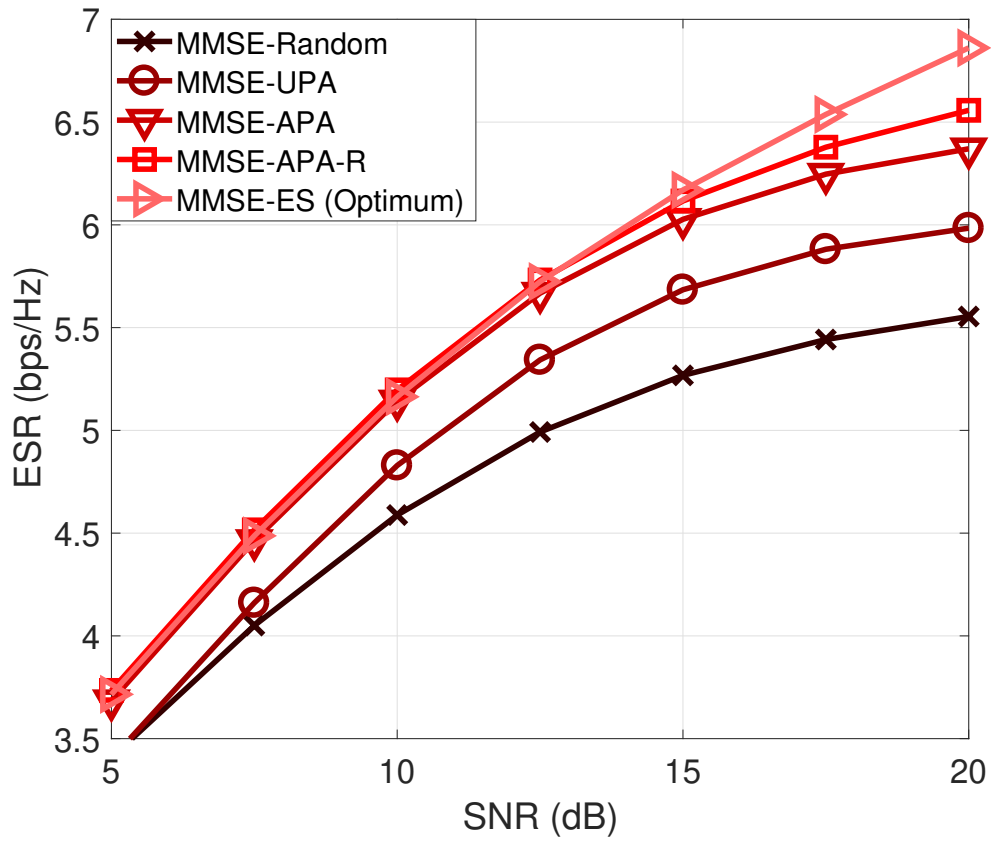
Figure 5.7: Sum-rate performance of MMSE precoding scheme, $N_t = 4$, $N_k = 2$, $K = 2$, and $\sigma_e^2 = 0.1$.
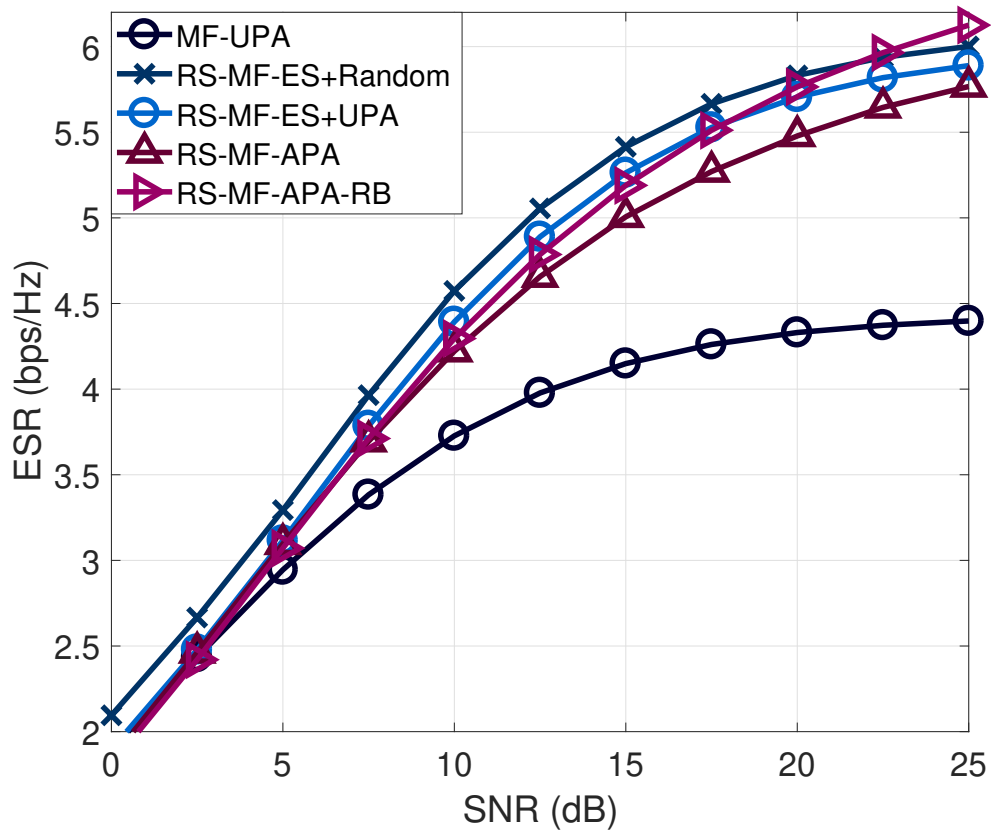
Figure 5.8: Sum-rate performance of RS-ZF precoding scheme, $N_t = 4$, $N_k = 2$, $K = 2$, and $\sigma_e^2 = 0.1$.
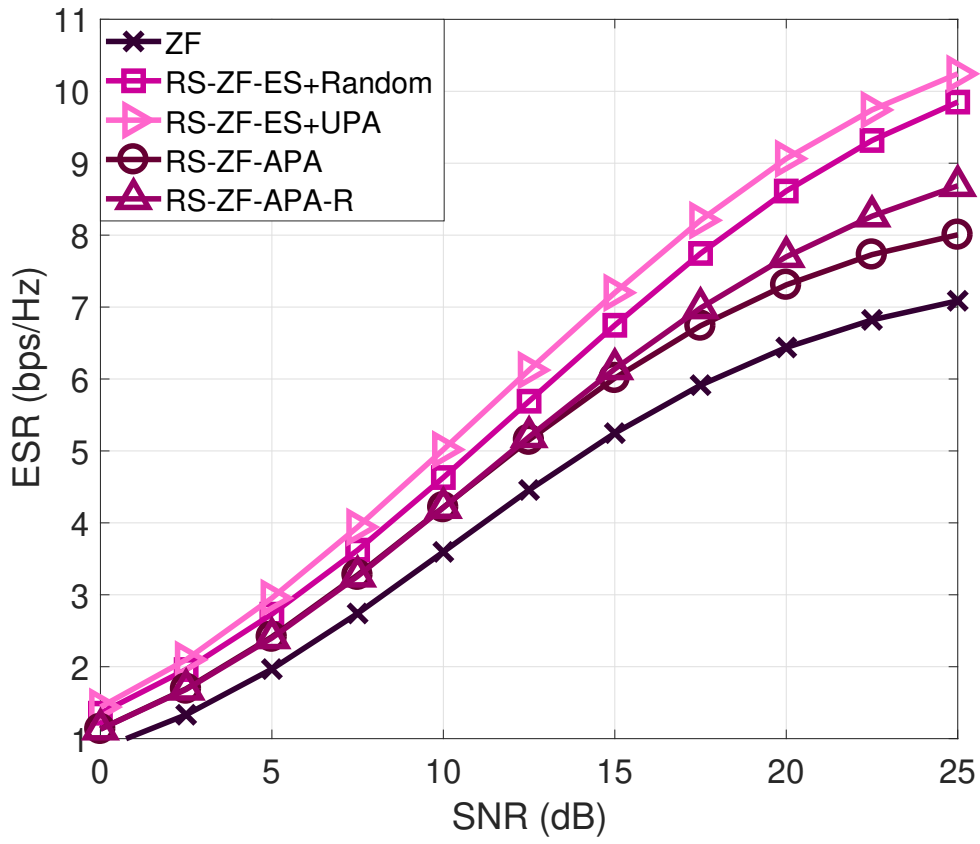
Figure 5.9: Sum-rate performance of RS-MMSE precoding scheme, $N_t = 4$, $N_k = 2$, $K = 2$, and $\sigma_e^2 = 0.1$.

6
Conclusions and Future Work

The quality of the CSIT plays a fundamental role in the performance of wireless communications systems. Most signal processing techniques are developed under the assumption that perfect CSIT is available. However, this assumption does not hold in real applications neither for FDD nor for TDD systems, due to the inherent uncertainty of the estimation process. In this context, the development of alternative techniques capable of dealing with CSIT imperfections is mandatory. In these circumstances, RS has become an attractive solution due to its natural robustness against CSIT uncertainties. However, the performance of the common rate of an RS system is bounded by the worst user and depends on an appropriate power allocation scheme, which can be computational demanding. Moreover, RS has been predominantly considered in the literature with channel inversion-type linear precoders. Motivated by these facts, this thesis developed techniques to further enhance the rate obtained by RS. This final chapter summarizes the thesis and includes a brief discussion about possible future works.

Interestingly, most works related to RS considered MISO system deployments. However, it is well known that users equipped with multiple antennas can further enhance the benefits of the common rate of RS systems. Since multiple copies of the common symbol are available at each user, stream combiners can be implemented at the receivers improving the overall performance. In this work, three different stream combiners have been proposed to take advantage of the multiple antennas at the receivers, namely the Min-Max, MRC and MMSE combiners. The simplest approach is the Min-Max criterion, but it also leads to the smallest common rate improvement. The MMSE stream combiner obtains the best performance but it requires knowledge of the covariance matrix of the received vector as additional information. Analytical expressions to describe the SINR of the proposed combiners were derived. Simulations results have shown that the proposed stream combiners obtain a consistent gain when compared to traditional RS schemes. Recall that an appropriate power allocation strategy is mandatory to obtain the benefits of RS.

It is well known that non-linear precoders obtain a better performance than their linear counterparts. Thus, another way to improve the performance

of RS systems is to implement non linear precoders at the transmitter. In this thesis two different THP precoders were proposed, one based on linear ZF transmit filters and the other inspired by linear MMSE transmit filters. Furthermore, for each one of the precoding algorithms two different deployments were considered, the centralized THP and the decentralized THP. A statistical analysis of the proposed strategies has been carried out, which led us to analytical expressions to describe the SINR. Simulation results have shown that non linear precoders increase the sum rate performance by up to 30%. We should also take into account that the symbol order directly affects the performance of THP algorithms. In this sense a symbol ordering technique for the proposed RS-THP schemes based on the MB technique has been developed. This technique further improves the sum rate performance obtained by RS-THP at the expense of additional computational complexity since multiple transmit patterns are created and evaluated. Simulation results have shown that even few branches results in a consistent improvement.

The benefits of the stream combiners and non linear precoders require an appropriate power allocation. This task usually relies on solving complex optimization problems, which result in high computational complexity. To avoid this issue, adaptive power allocations techniques, which are characterized for its low complexity, have been proposed. First, two adaptive power allocation for conventional SDMA have been proposed. The first approach is based on stochastic gradient techniques and performs power allocation adaptively with reduced computational costs. The second technique constitutes a robust implementation which aims to deal with CSIT imperfections based on the worst-case optimization applied to the MSE objective function. Simulation results have shown that the developed techniques attain better sum rate than conventional approaches under imperfect CSIT scenarios. Inspired by this result, two adaptive power allocation techniques for RS systems have been proposed. These algorithms greatly reduce the computational complexity when compared to an exhaustive search or to the alternating optimization procedure. Furthermore, they are more adequate for practical large-scale systems.

Although the proposed techniques are an improvement for RS systems, more complex RS architectures may lead to even higher sum rates. However, this will require the transmission of multiple common streams. Since more layers of common streams are included the receiver would need to implement SIC several times. This would increase the complexity of the receivers. One of the major disadvantages of this multilayer approach is that error propagation may become a critical factor. In this sense, there is still a lot of aspects that need to be further investigated and optimized in order to implement

a multilayer RS scheme.

Receivers with multiple antennas could allow the transmission of multiple common streams without the need for implementing SIC several times. This could reduce the error propagation problem but will require the development of novel detection techniques. Power allocation should be implemented carefully in order the obtain the expected benefits.

RS schemes could also be extended to other wireless architectures such as cell-free MIMO systems. The use of low-resolution signal processing techniques with quantization to few bits in RS systems also remain unexplored. It is also important to investigate other metrics which can be important for different deployments and system requirements. For instance, the proposed techniques could be evaluated considering a fairness or a specific QoS approach. The BER performance is another metric that can be investigated in conjunction with channel coding techniques. Furthermore, modulation schemes with finite alphabets should be also explored for both downlink and uplink settings.

To summarize, RS schemes constitute a brand new research topic with the capability of outperforming SDMA and NOMA-based wireless systems. In this regard, there is still a lot of work in terms of algorithmic development, theoretical bounds and practical deployments that needs to be carried out in this research field. We can conclude that RS is a promising multiple-access technology for future wireless communications systems.

Bibliography

[1] Cisco. (2020). *Cisco Annual Internet Report (2018-2023).* [Online], Available: https://www.cisco.com/c/en/us/solutions/collateral/executiveperspectives/annual-internet-report/white-paper-c11-741490.html.

[2] Ericsson. (2019). *Ericsson Mobility Report November 2019.* [Online], Available: https://iotbusinessnews.com/download/white-papers/ERICSSON-mobility-report-november-2019.pdf.

[3] A. Ramírez-Arroyo, P. H. Zapata-Cano, Á. Palomares-Caballero, J. Carmona-Murillo, F. Luna-Valero, and J. F. Valenzuela-Valdés. Multi-layer network optimization for 5G & 6G. *IEEE Access*, 8:204295–204308, 2020.

[4] Q. C. Li, H. Niu, A. T. Papathanassiou, and G. Wu. 5G network capacity: Key elements and technologies. *IEEE Vehicular Technology Magazine*, 9(1):71–78, March 2014.

[5] M. Joham, W. Utschick, and J. A. Nossek. Linear transmit processing in MIMO communications systems. *IEEE Transactions on Signal Processing*, 53(8):2700–2712, August 2005.

[6] Q. H. Spencer, A. L. Swindlehurst, and M. Haardt. Zero-forcing methods for downlink spatial multiplexing in multiuser MIMO channels. *IEEE Transactions on Signal Processing*, 52(2):461–471, February 2004.

[7] K. Zu, R. C. de Lamare, and M. Haardt. Multi-branch Tomlinson-Harashima precoding design for MU-MIMO systems: Theory and algorithms. *IEEE Transactions on Communications*, 62(3):939–951, March 2014.

[8] B. Clerckx, H. Joudeh, C. Hao, M. Dai, and B. Rassouli. Rate splitting for MIMO wireless networks: a promising PHY-layer strategy for LTE evolution. *IEEE Communications Magazine*, 54(5):98–105, May 2016.

[9] D. Tse and P. Viswanath. *Fundamentals of Wireless Communications.* Cambridge University Press, 2005.

[10] S. Yang, M. Kobayashi, D. Gesbert, and X. Yi. Degrees of freedom of time correlated MISO broadcast channel with delayed CSIT. *IEEE Transactions on Information Theory*, 59(1):315–328, January 2013.

[11] E. Telatar. Capacity of multi-antenna Gaussian channels. *European Transactions on Telecommunications*, 10(6):585–596, November 1999.

[12] Q. Li, G. Li, W. Lee, M. Lee, D. Mazzarese, B. Clerckx, Z. LiQ. Li, G. Li, W. Lee, M. Lee, D. Mazzarese, B. Clerckx, and Z. Li. MIMO techniques in WiMAX and LTE: a feature overview. *IEEE Communications Magazine*, 48(5):86–9–2, May 2010.

[13] V. Jones and H. Sampath. Emerging technologies for WLAN. *IEEE Communications Magazine*, 53(3):141–149, March 2015.

[14] L. Lu, G. Li, A. Swindlehurst, A. Ashikhmin, and R Zhanh. An overview of massive MIMO: Benefits and challenges. *IEEE Journal of Selected Topics in Signal Processing*, 8(5):742–758, October 2014.

[15] A. J. Viterbi. *CDMA: principles of spread spectrum communication.*, volume 122. Addison-Wesley Reading, 1995.

[16] L. Dai, B. Wang, Y. Yuan, S. Han, C. I, and Z. Wang. Non-orthogonal multiple access for 5G: solutions, challenges, opportunities, and future research trends. *IEEE Communications Magazine*, 53(9):74–81, September 2015.

[17] Y. Saito, Y. Kishiyama, A. Benjebbour, T. Nakamura, A. Li, and K. Higuchi. Non-orthogonal multiple access (NOMA) for cellular future radio access. *2013 IEEE 77th Vehicular Technology Conference (VTC Spring)*, 2013.

[18] H. Nikopour and H. Baligh. Sparse code multiple access. *2013 IEEE 24th Annual International Symposium on Personal, Indoor, and Mobile Radio Communications (PIMRC)*, 2013.

[19] Z. Ding, Y. Liu, J. Choi, Q. Sun, M. Elkashlan, C. I, and H. V. Poor. Application of non-orthogonal multiple access in LTE and 5G networks. *IEEE Communications Magazine*, 55(2):185–191, February 2017.

[20] Te Han and K. Kobayashi. A new achievable rate region for the interference channel. *IEEE Transactions on Information Theory*, 27(1):49–60, 1981.

[21] Y. Mao, B. Clerckx, and V.O.K. Li. Rate-splitting multiple access for downlink communication systems: Bridging, generalizing and outperforming SDMA and NOMA. *EURASIP Journal on Wireless Communications and Networking*, 2018(1):133, May 2018.

[22] B. Clerckx, Y. Mao, R. Schober, and H. V. Poor. Rate-splitting unifying SDMA, OMA, NOMA, and multicasting in MISO broadcast channel: A simple two-user rate analysis. *IEEE Wireless Communications Letters*, 9(3):349–353, March 2020.

[23] H. Joudeh and B. Clerckx. Sum-rate maximization for linearly precoded downlink multiuser MISO systems with partial CSIT: A rate-splitting approach. *IEEE Transactions on Communications*, 64(11):4847–4861, November 2016.

[24] C. Hao, Y. Wu, and B. Clerckx. Rate analysis of two-receiver MISO broadcast channel with finite rate feedback: A rate-splitting approach. *IEEE Transactions on Communications*, 63(9):3232–3246, September 2015.

[25] H. Joudeh and B. Clerckx. Rate-splitting for max-min fair multigroup multicast beamforming in overloaded systems. *IEEE Transactions on Wireless Communications*, 16(11):7276–7289, November 2017.

[26] H. Joudeh and B. Clerckx. Robust transmission in downlink multiuser MISO systems: A rate-splitting approach. *IEEE Transactions on Signal Processing*, 64(23):6227–6242, December 2016.

[27] M. Dai, B. Clerckx, D. Gesbert, and G. Caire. A rate splitting strategy for massive MIMO with imperfect CSIT. *IEEE Transactions on Wireless Communications*, 15(7):4611–4624, July 2016.

[28] C. Hao and B. Clerckx. MISO networks with imperfect CSIT: A topological rate-splitting approach. *IEEE Transactions on CommunicationsIEEE Transactions on Communications*, 65(5):2164–2179, May 2017.

[29] G. Lu, L. Li, H. Tian, and F. Qian. MMSE-based precoding for rate splitting systems with finite feedback. *IEEE Communications Letters*, 22(3):642–645, March 2018.

[30] O. Kolawole, A. Panazafeironoulos, and T. Ratnarajah. A rate-splitting strategy for multi-user millimeter-wave systems with imperfect CSI. *2018 IEEE 19th International Workshop on Signal Processing Advances in Wireless Communications (SPAWC)*, June 2018.

[31] Lai-U Choi and R. D. Murch. A transmit preprocessing technique for multiuser MIMO systems using a decomposition approach. *IEEE Transactions on Wireless Communications*, 3(1):1558–2248, January 2004.

[32] M. Vu and A. Paulraj. MIMO wireless linear precoding. *IEEE Signal Processing Magazine*, 24(5):86–105, September 2007.

[33] R. Esmailzadeh and M. Nakagawa. Pre-RAKE diversity combination for direct sequence spread spectrum mobile communications systems. *IEICE Transactions Communications*, E76-B(8):1008–1015, August 1993.

[34] W. Zhang, R. C. de Lamare, C. Pan, M. Chen, J. Dai, B. Wu, and X. Bao. Widely linear precoding for large-scale MIMO with IQI: Algorithms and performance analysis. *IEEE Transactions on Wireless Communications*, 16(5):3298–3312, 2017.

[35] K. Zu, R. C. de Lamare, and M. Haardt. Generalized design of low-complexity block diagonalization type precoding algorithms for multiuser MIMO systems. *IEEE Transactions on Communications*, 61(10):4232–4242, October 2013.

[36] V. Stankovic and M. Haardt. Generalized design of multi-user MIMO precoding matrices. *IEEE Transactions on Wireless Communications*, 7(3):953–961, March 2008.

[37] H. Sung, S. . Lee, and I. Lee. Generalized channel inversion methods for multiuser MIMO systems. *IEEE Transactions on Communications*, 57(11):3489–3499, November 2009.

[38] M. Tomlinson. New automatic equaliser employing modulo arithmetic. *Electronics Letters*, 7(5):138–139, March 1971.

[39] H. Harashima and H. Miyakawa. Matched-transmission technique for channels with intersymbol interference. *IEEE Transactions on Communications*, 20(4):774–780, Aug 1972.

[40] R. F. H. Fischer, C. Windpassinger, A. Lampe, and J. B. Huber. Space-time transmission using Tomlinson-Harashima precoding. In *2002 ITG Conf. on Source and Channel Coding*, pages 139–147, 2002.

[41] C. Windpassinger, R. F. H. Fischer, T. Vencel, and J. B. Huber. Precoding in multiantenna and multiuser communications. *IEEE Transactions on Wireless Communications*, 3(4):1305–1316, July 2004.

[42] E. Debels and M. Moeneclaey. SNR maximization and modulo loss reduction for Tomlinson-Harashima precoding. *EURASIP Journal on Wireless Communications and Networking*, 2018(257), 2018.

[43] L. Zhang, Y. Cai, R. C. de Lamare, and M. Zhao. Robust multibranch Tomlinson-Harashima precoding design in amplify-and-forward MIMO relay systems. *IEEE Transactions on Communications*, 62(10):3476–3490, Oct 2014.

[44] A. R. Flores, B. Clerckx, and R. C. de Lamare. Tomlinson-harashima precoded rate-splitting for multiuser multiple-antenna systems. In *2018 15th International Symposium on Wireless Communication Systems (ISWCS)*, pages 1–6, Lisbon, August 2018.

[45] D. P. Palomar and J. R. Fonollosa. Practical algorithms for a family of waterfilling solutions. *IEEE Transactions on Signal Processing*, 53(2):686–695, February 2005.

[46] Y. Cheng, S. Li, J. Zhang, F. Roemer, B. Song, M. Haardt, Y. Zhou, and M. Dong. An efficient transmission strategy for the multicarrier multiuser MIMO downlink. *IEEE Transactions on Vehicular Technology*, 63(2):628–642, February 2014.

[47] E. Matskani, N. D. Sidiropoulos, Z. Luo, L. TassiulasE. Matskani, N. D. Sidiropoulos, Z. Luo, and L. Tassiulas. Convex approximation techniques for joint multiuser downlink beamforming and admission control. *IEEE Transactions on Wireless Communications*, 7(7):2682–2693, July 2008.

[48] S. Boyd and L. Vandenberghe. *Convex Optimization.* Cambridge Univ. Press., Cambridge, U.K., 2004.

[49] E. Bjornson and E. Jorswieck. *Optimal Resource Allocation in Coordinated Multi-Cell Systems.*, volume 9. Now, 2014.

[50] G.D. Golden. Detection algorithm and initial laboratory results using V-BLAST space-time communication architecture. *Electronics Letters*, 35:14–16(2), January 1999.

[51] M. Mohammad and R. M. Buehrer. The effects of ordering criteria in linear successive interference cancellation in CDMA systems. *IEEE Transactions on Wireless Communications*, 7(11):4128–4132, November 2008.

[52] A. Zanella, M. Chiani, and M. Z. Win. MMSE reception and successive interference cancellation for MIMO systems with high spectral efficiency. *IEEE Transactions on Wireless Communications*, 4(3):1244–1253, May 2005.

[53] R. C. De Lamare, R. Sampaio-Neto, and A. Hjorungnes. Joint iterative interference cancellation and parameter estimation for CDMA systems. *IEEE Communications Letters*, 11(12):916–918, 2007.

[54] R. C. De Lamare and R. Sampaio-Neto. Minimum mean-squared error iterative successive parallel arbitrated decision feedback detectors for DS-CDMA systems. *IEEE Transactions on Communications*, 56(5):778–789, May 2008.

[55] P. Li, R. C. de Lamare, and R. Fa. Multiple feedback successive interference cancellation detection for multiuser MIMO systems. *IEEE Transactions on Wireless Communications*, 10(8):2434–2439, 2011.

[56] P. Li and R. C. De Lamare. Adaptive decision-feedback detection with constellation constraints for MIMO systems. *IEEE Transactions on Vehicular Technology*, 61(2):853–859, 2012.

[57] R. C. de Lamare. Adaptive and iterative multi-branch MMSE decision feedback detection algorithms for multi-antenna systems. *IEEE Transactions on Wireless Communications*, 12(10):5294–5308, 2013.

[58] A. G. D. Uchoa, C. T. Healy, and R. C. de Lamare. Iterative detection and decoding algorithms for MIMO systems in block-fading channels using LDPC codes. *IEEE Transactions on Vehicular Technology*, 65(4):2735–2741, 2016.

[59] M. Biguesh and A. B. Gershman. Training-based MIMO channel estimation: a study of estimator tradeoffs and optimal training signals. *IEEE Transactions on Signal Processing*, 54(3):884–893, March 2006.

[60] S. M. Kay. *Fundamentals of Statistical Signal Processing: Estimation Theory*. Prentice-Hall, 1993.

[61] H. Joudeh. *A Rate-Splitting Approach to Multiple-Antenna Broadcasting*. PhD thesis, Imperial College London, 2016.

[62] K. Kusume, M. Joham, W. Utschick, and G. Bauch. Cholesky factorization with symmetric permutation applied to detecting and precoding

spatially multiplexed data streams. *IEEE Transactions on Signal Processing*, 55(6):3089–3103, June 2007.

[63] K. Zu, R. C. de Lamare, and M. Haardt. Multi-branch Tomlinson-Harashima precoding design for MU-MIMO systems: Theory and algorithms. *IEEE Transactions on Communications*, 62(3):939–951, March 2014.

[64] L. Sung and M.R. McKay. Tomlinson-Harashima precoding for multiuser MIMO systems with quantized CSI feedback and user scheduling. *IEEE Transactions on Signal Processing*, 62(16):4077 – 4090, July 2014.

[65] G. Caire and S. Shamai. On the achievable throughput of a multiantenna Gaussian broadcast channel. *IEEE Transactions on Information Theory*, 49(7):1691–1706, July 2003.

[66] A. A. Ahmad, J. Kakar, H. Dahrouj, A. Chaaban, K. Shen, A. Sezgin, T. Y. Al-Naffouri, and M. Alouini. Rate splitting and common message decoding for MIMO C-RAN systems. In *2019 IEEE 20th International Workshop on Signal Processing Advances in Wireless Communications (SPAWC)*, 2019.

[67] A. R. Flores, R. C. De Lamare, and B. Clerckx. Linear precoding and stream combining for rate splitting in multiuser MIMO systems. *IEEE Communications Letters*, 24(4):890–894, January 2020.

[68] G. Golub and C. Van Loan. *Matrix Computations*. The Johns Hopkins University Press, 1996.

[69] A. Gholami Davoodi and S. A. Jafar. Aligned image sets under channel uncertainty: Settling conjectures on the collapse of degrees of freedom under finite precision CSIT. *IEEE Transactions on Information Theory*, 62(10):5603–5618, October 2016.

[70] E. Piovano and B. Clerckx. Optimal DoF region of the K-User MISO BC with partial CSIT. *IEEE Communications Letters*, 21(11):2368–2371, November 2017.

[71] Z. Luo and S. Zhang. Dynamic spectrum management: Complexity and duality. *IEEE Journal of Selected Topics in Signal Processing*, 2(1):57–73, February 2008.

[72] Y. Liu, Y. Dai, and Z. Luo. Coordinated beamforming for MISO interference channel: Complexity analysis and efficient algorithms. *IEEE Transactions on Signal Processing*, 59(3):1142–1157, March 2011.

[73] M. Schubert and H. Boche. Solution of the multiuser downlink beamforming problem with individual SINR constraints. *IEEE Transactions on Vehicular Technology*, 53(1):18–28, January 2004.

[74] M. Codreanu, A. Tolli, M. Juntti, and M. Latva-aho. Joint design of Tx-Rx beamformers in MIMO downlink channel. *IEEE Transactions on Signal Processing*, 55(9):4639–4655, September 2007.

[75] E. Björnson, G. Zheng, M. Bengtsson, and B. Ottersten. Robust monotonic optimization framework for multicell MISO systems. *IEEE Transactions on Signal Processing*, 60(5):2508–2523, May 2012.

[76] W. Utschick and J. Brehmer. Monotonic optimization framework for coordinated beamforming in multicell networks. *IEEE Transactions on Signal Processing*, 60(4):1899–1909, April 2012.

[77] M. T. Palhares, R. C. de Lamare, A. R. Flores, and L. T. N. Landau. Seleção de pontos de acesso, pré-codificação MMSE e alocação de potência iterativa para sistemas de múltiplas antenas livres de células. In *2020 XXXVIII Simposio Brasileiro de Telecomunicações e Processamento de Sinais (SBrT)*, pages 1–6, Brasil, November 2020.

[78] C. W. Tan, M. Chiang, and R. Srikant. Maximizing sum rate and minimizing MSE on multiuser downlink: Optimality, fast algorithms and equivalence via max-min SINR. *IEEE Transactions on Signal Processing*, 59(12):6127–6143, December 2011.

[79] Q. Shi, M. Razaviyayn, Z. Luo, and C. He. An iteratively weighted MMSE approach to distributed sum-utility maximization for a MIMO interfering broadcast channel. *IEEE Trans. Signal Process.*, 59(9):4331–4340, September 2011.

[80] E. Bjornson, N. Jalden, M. Bengtsson, and B. Ottersten. Optimality properties, distributed strategies, and measurement-based evaluation of coordinated multicell OFDMA transmission. *IEEE Transactions on Signal Processing*, 59(12):6086–6101, December 2011.

[81] Y. Mao and B. Clerckx. Beyond dirty paper coding for multi-antenna broadcast channel with partial CSIT: A rate-splitting approach. *IEEE Transactions on Communications*, 68(11):6775–6791, November 2020.

[82] S. S. Christensen, R. Agarwal, E. De Carvalho, and J. M. Cioffi. Weighted sum-rate maximization using weighted MMSE for MIMO-BC beamform-

ing design. *IEEE Transactions on Wireless Communications*, 7(12):4792–4799, December 2008.